ABSTRACT

GUPTA, ANURADHA. Composites from Natural Fibers: Hemp Fiber Reinforced Composites from 3D Orthogonal Woven Preforms and their Potential Applications in the US. (Under the direction of Dr. Abdel-Fattah M. Seyam).

Natural fibers reinforcements are a prevalent option for applications in composite manufacturing. There is significant ongoing research in the field of natural fiber reinforced composites, which mainly aims at reducing the overall carbon footprint. Natural fiber composites have great potential as the focus of many industries is shifting from synthetic fibers that are commonly used in manufacturing composites today like glass, carbon, and aramid to more sustainable natural fibers. Some of the major issues with synthetic fibers are high-energy consumption during production and non-degradability. Similarly, polymer resins like epoxy and vinyl ester, which are most commonly used in high-performance composites, are petroleum based. With the reserve of petroleum depleting, alternative sustainable fibers and resins are the substitutes.

The applications of natural fibers are growing in the field of engineering and technology due to its favorable properties like biodegradability, sustainability, high strength, and corrosion resistance. Due to these benefits, synthetic fibers and resins from hazardous chemicals are being substituted with natural fibers and resins. As a result, the term “Green composites” or “bio-composites” have emerged, which is a blend of the intrinsic properties of fiber and matrix derived from natural resources.

Hemp has proven to be one of the strong contenders for the replacement. Hemp-based composites help reduce the carbon footprint of the end composite and enhanced energy recovery at the end of their lifecycle. Hemp fibers are used as reinforcement in composites due to high specific strength and high specific Young’s modules. Moreover, hemp fibers possess a much higher vibration dampening capacity, higher fiber yield, pest resistant and drought resistance. All these properties make it an excellent candidate for composite reinforcement.

The objectives of this research are to explain the importance of hemp-fiber reinforced composites, highlighting the potential application. 3D Orthogonal Woven fabrics incorporate through-thickness reinforcement and can exhibit remarkable inter-laminar properties that aid damage suppression prevent delamination and delay crack propagation. A comprehensive study

on the performance of hemp/vinyl ester composites in terms of their structural parameters was performed. Composite panels were manufactured using a 3D orthogonal weaving (3DOW) technology and Vacuum Assisted Resin Transfer Molding (VARTM) process. A range of 3DOW composites was tested for its tensile and compression strength and impact resistance to understanding their failure mechanisms in terms of their structural parameters. A thorough analysis of the effect of weave design, the contribution of Z-binders and thickness was investigated, and the study concluded that the number of Y-layers had the most significant effect on the mechanical strength.

An additional goal of this work is to identify potential markets of hemp-based experimental composites based on their performance characteristics. Hemp newly gained agricultural crop status is gaining momentum in the United States and will further strengthen high-performance composite applications of industrial hemp.

Composites from Natural Fibers: Hemp Fiber Reinforced Composites from 3D Orthogonal Woven Preforms and their Potential Applications in the US

by
Anuradha Gupta

A dissertation submitted to the Graduate Faculty of
North Carolina State University
in partial fulfillment of the
requirements for the Degree of
Doctor of Philosophy

Textile Technology Management

Raleigh, North Carolina

2019

APPROVED BY:

_____	_____
Dr. Abdel-Fattah Mohamed Seyam Chair of Advisory Committee	Dr. A. Blanton Godfrey
_____	_____
Dr. Kristin A. Thoney- Barletta	Dr. Thomas W. Theyson

DEDICATION

I would like to dedicate my Ph.D. to my partner and guide, Rahul Vallabh, for always believing in me. He provided much needed motivation throughout my research and beyond. His suggestions and viewpoints always helped me to think beyond my realm. Thank you for stepping in every single time, even without asking, for Vivaan and me. Without his help and understanding, this journey would not have been this smooth. His presence in every step of the way gave me strength and much needed time for my research.

I would also like to thank my parents Mrs. Kaushalya Gupta and Mr. Kailash Prasad Gupta for believing in me. My ever supporting in-laws Mrs. Sanyukta and Mr. Ajit Sah for showering their blessing, love, and support throughout this journey. To my brother and sister-in-law, Nitesh and Poonam, for always loving me and giving me "Aarav". Big shout out to my inspirations, Dr. Parineeta and my little sister, Sneha, who taught me to fight all odds to achieve your dreams and to never give up. I love you all so much.

Special thanks to my friends Betsy, Sangeeta, Dolly, and Ashish, who has stood for me against all odds and always believed in me in every step of my way.

And last but certainly not the least, my son Vivaan, for being such a good kid. You are the one who gives me hope and strength that life is beautiful.

BIOGRAPHY

Anuradha Gupta was born in Cooch Behar, a small town to her maternal grandmother in West Bengal. She was raised in Cuttack, Orissa (India), where she has spent most of her academic life. She is the second of three children to Mr. Kailash Prasad Gupta and Mrs. Kaushalya Gupta. In 1998, she finished her schooling from New Stewart School and started Ravenshaw Junior college for her 11^{th} and 12^{th}. In 2000. She gained admission to one of the oldest (1868) and most prestigious universities in the India, Ravenshaw University where Anuradha graduated with her undergraduate degree in Accounting. Her love for numbers gave her the boost to do a double Master degree in Finance and Marketing from Ravenshaw University (2005) and Indian Business Academy, Bangalore (2009). Following her graduation in 2009, she worked as Business Analyst (Risk Management) at Tata Consultancy with one of the most reputed German investment bank.

In 2012, she got married to Rahul Vallabh and moved to the Raleigh, United States of America to start a new life. After gaining a management degree, her next goal was to go for an advanced degree in a specific field and choose textiles to be her next avenue. The year 2014 was eventful for her were in spring 2014 she started her doctoral journey from NCSU and in summer welcomed her son, Vivaan. Anuradha, during her doctoral degree, also taught an undergraduate lab and mentored many students. After her degree, she aims at working in an industry where she can apply her textile knowledge and management expertise.

.

ACKNOWLEDGEMENTS

I would like to express my sincere gratitude to everyone who helped me in achieving this milestone. To my advisor, Dr. Seyam, for his support, understanding, and motivation throughout my Ph.D. To my mentor and committee member, Dr. Godfrey, for his every word of encouragement and inspiration which helped me identify my real potential. I would also like to extend my sincere thanks to Dr. Bourham, Dr. Thoney, and Dr. Theyson for being an integral part of my committee. I'm grateful to Ashland Inc. for donating the Vinyl ester resin.

Special thanks to Tri, for coming to my rescue every single time and providing me the much-needed help with everything. To Jeff Krauss for all his lab support.

I would also like to thank all my friends and colleagues, Hadir Eldeeb, Ruth Adikorley, Shan Shan Li and Mohamad Midani for all their support and encouragement. To Margaret and Divya, thank you for assistance and taking time out of your busy schedules to help me with my research. To my family away from home, Shriti, Alok Anubha, and Raj, for their trust and valuable friendship.

To one of my closest friend and colleague, Betsy Claunch. Thank you for all your love and support. You are the best aunt to Vivaan. You will always be part of my family.

And last but certainly not the least, my husband, Rahul Vallabh, for making my life so easy and smooth. I owe this research to you.

TABLE OF CONTENTS

LIST OF FIGURES

LIST OF TABLES

CHAPTER 1 - INTRODUCTION

1.1. Composites

Composites are found in our day to day life in various forms like doors and window panels, construction materials, automobiles, aerospace, etc. The most primitive of all is the use of mud/clay and straw/gravel, which acts as a binder, to form bricks as construction material. Concrete, also an example of composites, is the most used man-made material in the world. Another example is plywood where multiple layers of wood are glued together in different angles with an adhesive and yield better properties than natural wood. Composites are defined as a combination of two or more materials which have different and better mechanical, physical and chemical properties than the individual components used.

Due to increasing demand for stiffer and stronger material in various applications like transportation, construction, sports and leisure, electronics, etc., composites have gained popularity over the past few decades (Chou, T. W., 1993; Hull & Clyne, 1996). Figure 1.3 lists the comparison between composites and metals. Composites prove to be a better substitute for metals and as a result, has encouraged to assimilate high-performance fibers and natural fibers as reinforcement. Also, with increasing environmental concerns, green or bio-composites is also gaining popularity. Green composites are composites where both matrix and reinforcement are biodegradable. Natural fibers are used as reinforcement whereas biopolymers are used as a matrix (Zini & Scandola, 2011). This, in turn, has also promoted green supply chains, which is responsible for converting all the aspects like purchasing, designing, manufacturing, marketing, and distribution and reverse logistics more eco-friendly (Ghobakhloo, Tang, Zulkifli, & Ariffin, 2013).

1.2. Fiber reinforced composites

A composite is a heterogeneous combination of two or more materials, reinforcement, and matrix, to give a resultant material which has completely different and superior chemical, physical and mechanical properties. The advantages of composites are high strength and stiffness along with low density, which contributes to different applications, improve productivity and lower cost. The reinforcement provides mechanical properties and load-bearing capacity to the

composites. The type and quantity of reinforcement determine the final properties of the composite. The matrix, on the other hand, acts as a binder and provides physical form and dimension to the composite. This helps to transfer the load or stress applied in the direction of the reinforcement and protects against environmental effects. The properties of the resultant composite are based on the polymer used, fiber surface and manufacturing processes engaged.

1.3. Types of composite

Composites can be broadly classified into two groups namely types of fibers used and types of matrix used (Hull & Clyne, 1996; Mallick, 1993) as shown in Figure 1.1. Continuous fibers used in composites possess the best mechanical properties. High-performance fibers like Kevlar, HDPE, glass, carbon, aramid, etc. are usually mixed to get desired composites. They have exceptional high longitudinal specific stiffness (three times than that of conventional alloys) and high specific strength which is twice than that of metal alloys (Deve & McCullough, 1995). Since these high-performance fibers are expensive, its application is limited to a few applications where performance is given more priority than cost.

Short fiber reinforced composites impart certain benefits like low strength and stiffness and therefore are used in interiors of automobiles and aerospace, constructions, etc.(De, S. K., & White, 1996; Mallick, 1993). Short fiber composites are reinforced with staple fibers or lignocellulose fibers and undergo less wear and tear during processing and are very flexible and cheaper than continuous fibers reinforced composites (Herrera-Franco & Valadez-González, 2005).

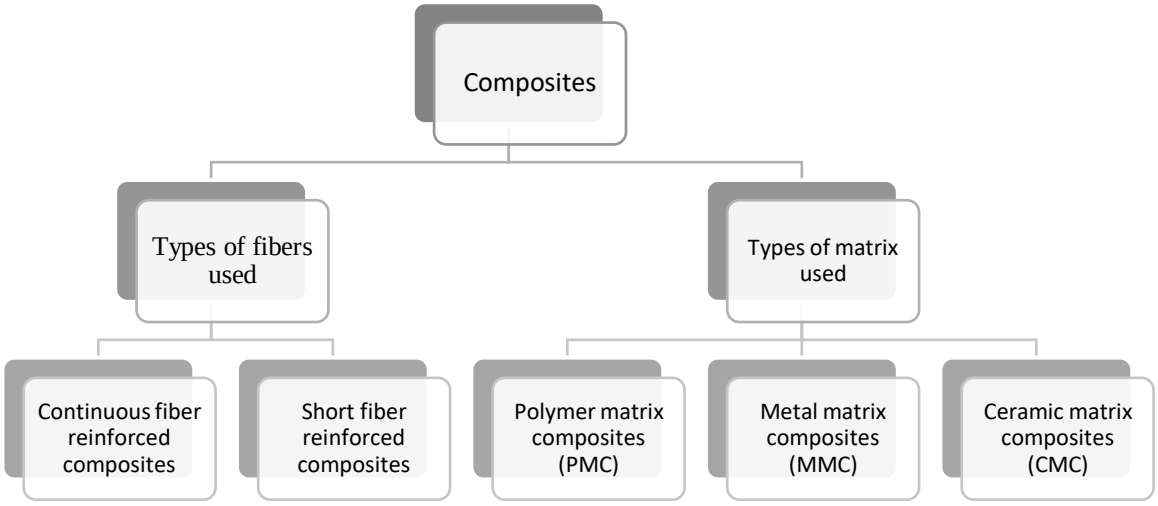

Figure 1.1. Classification of composites on basis of fibers and matrix used (Hull & Clyne, 1996; Mallick, 1993).

Polymer matrix composites otherwise known as fiber reinforced polymers or plastics are the most common type of composites as they are machine friendly and moldable (Matthews, de FL, 1999). In this type of composite, large molecules of polymers, which act as structural units, are continuously coupled with covalent chemical bonds. These materials use polymer-based resin like epoxy, vinyl ester, etc. as the matrix, and a variety of fibers such as glass, carbon, aramid and natural fiber as the reinforcement. PMCs are further divided into thermoset and thermoplastic polymers. In the case of thermoset polymer are low viscosity resins where the molecules are chemically cross-linked using covalent bonds in the form of a network and are irreversible after curing. Examples of thermosetting resins that are widely used are polyester, epoxy resin, phenol formaldehyde, and vinyl esters. Thermoplastics, on the other hand, are high viscous resins that can be processed above the melting temperature for additional processing. Examples are Polypropylene (PP), polyethylene (PE), polystyrene (PS), and PVC (polyvinyl chloride). The advantages and disadvantages of thermoset and thermoplastic polymer are outlined in table 1.1.

Table 1.1. Advantages and disadvantages of thermosets and thermoplastics (Vigo, T. L., and Kinzig, 1992).

Property	Thermosets	Thermoplastics
Preparation	Complex	Simple
Processing cycle	Long	Short to long
Processing temperature	Low to moderate	High
Processing pressure	Low to moderate	High
Fabrication cost	High	Low
Environmental durability	Good	Unidentified
Fiber impregnation	Easy	Difficult
Solvent resistance	Excellent	Poor to good
Damage tolerance	Poor to excellent	Fair to good
Melt viscosity	Very low	High

PMCs are cheaper and are less dense than metal or ceramic composites and can be fabricated easily (Matthews, de FL, 1999). Also, they have strong resistance towards atmospheric and other types of corrosion and are a bad conductor of electrical current (Vinay, Govindaraju, & Banakar, 2014). Metal matrix composites, on the other hand, are composed of two parts namely metal or alloy and other material which can be fiber or metal. They are mostly used in automotive and aircraft parts because of high stiffness and high strength to density ratio, fire resistance, hydrophobic nature and are a good conductor of electricity and temperature. In the automotive industry, a metal such as aluminum is used as the matrix, and reinforces it with advanced ceramic fibers such as silicon carbide or boron nitride. These composites use ceramic, glass or carbon as matrix and reinforced with short fibers or whiskers. They are used in very high-temperature settings and have high fracture toughness and less fragile compared to ceramics. The list of the matrix is illustrated in table 1.2.

Table 1.2. Types of matrix and reinforcement used in composites (Cardarelli, 2001).

Category	Matrix used	Reinforcement used
PMCs	Thermoplastics (PPS, PES)	Fibers (carbon fibers or wires) Laminates (glass and aluminum sheets)
	Thermosets (epoxy, Vinyl)	Fibers (glass, carbon) Laminates (glass and aluminum sheets, honeycomb)
MMCs	Metals	Fibers (Silicon Carbide, boron, carbon monofilaments, whiskers) Particulates, flakes (ceramic, hard metal)
	Alloys	Fibers (Silicon Carbide, boron, carbon monofilaments, whiskers) Particulates, flakes (ceramic, hard metal)
CMCs	Ceramic	Fiber (carbon mono-filaments, whiskers) Metals fibers, cut wires, whiskers, particulates or flakes
	Glass or glass ceramic	Particulates

1.4. Composites vs. Metals

Unlike metal, composites have many advantages delineated below in table 1.3 which makes a composite better choice for applications like automobile, aerospace, construction, etc. Apart from fulfilling diverse design requirements with significant weight savings, composites have a better strength-to-weight ratio.

Table 1.3. Comparison between composites and metals (Campbell, 2010; Chandramohan & Marimuthu,2011; Vigo, T.L.&Kinzig,1992).

- Better tensile strength around four to six times greater than that of steel or aluminum.
- High specific strength and stiffness.
- Higher impact properties.
- Better damage endurance like impact resistance, fracture resistance, abrasion resistance.
- Better protection from corrosion and requires less maintenance.
- The poor transmitter of vibration, less wear, and tear than metals and less noisy during processing.
- Composites are more flexible than metals and can be designed accordingly to meet performance needs and complex design requirements.
- Composites have reduced lifecycle cost and component cost like less fabrication cost, lower scrappage cost compared to metals.
- Composite parts have fewer joints/fasteners and minimal plies which provides simplification and integrated design compared to conventional metallic parts.

1.5. Factors affecting composite performance

Composites are formed by mixing an appropriate amount of matrix and reinforcement. However, while manufacturing composites, there is a list of factors which directly affect composite performance. The ingredients, reinforcement, and matrix must have very strong bonding to give the resultant composite appropriate strength and stiffness. In the case where the flow of matrix is not uniform or the preform sheet is irregular, the weak spot will appear. In that case, load distribution in the composite will not be uniform and crack/fracture might appear. Fiber orientation is also important as strength and stiffness are dependent on how the fibers are placed. A small fluctuation in angle during lay up or a push during resin penetration can greatly affect the stiffness. Hoa, 2009 found out that a change in angle from 0° to 10°, can lower the stiffness by almost 30%.

The role of resin is to uphold the fibers as straight as possible to prevent bulking. This will also determine the adhesive and stiffness properties of the resin system thereby improving

performance of the composite. The compression properties of natural fiber composite (flax, bamboo, and coir) was compared with that of glass fiber composites and found out that glass fiber composites are superior to natural fibers.

One other important factor which directly influences composite performance is fiber volume fraction (FVF), which is defined as the ratio of fiber volume to the total volume of the composite.

A composite strength and stiffness are based on the amount of fiber used, choosing the right amount of fiber, also known as critical fiber volume fraction, is of utmost significance. In other words, critical fiber volume is the fiber volume fraction at which the properties of composites start to improve. However, it is important to note that even though the quantity of fiber enhances composite strength, there should be some spacing between the fibers. Typically, reinforcement should be around 68%-70% by volume to give composite its optimum strength (Hoa, 2009; Campbell, 2010). Also, this will vary with the type of fiber used i.e., short or continuous fibers as shown in figure 1.2. It is important to note that uniform fiber distribution is a vital consideration especially when the strength of the composite is the priority.

One way to form composites is to lay the fibers a unidirectional layer so that the resin flow is uniform. However, there will always be an area which has more concentration of resin. These areas act as the site for cracks or breakage and is always a good idea to keep this area to a minimum. Another factor which can cause cracks is the time for the resin to harden. In the case of thermoset, it is called curing whereas for thermoplastic it is called solidification. During composite manufacturing, the resin should not be very viscous to allow it to penetrate in the fiber and should be cured or solidified enough for reinforcement to occur. This will reduce defects or voids, which might also occur due to separation between layers or due to low pressure in the resin during curing.

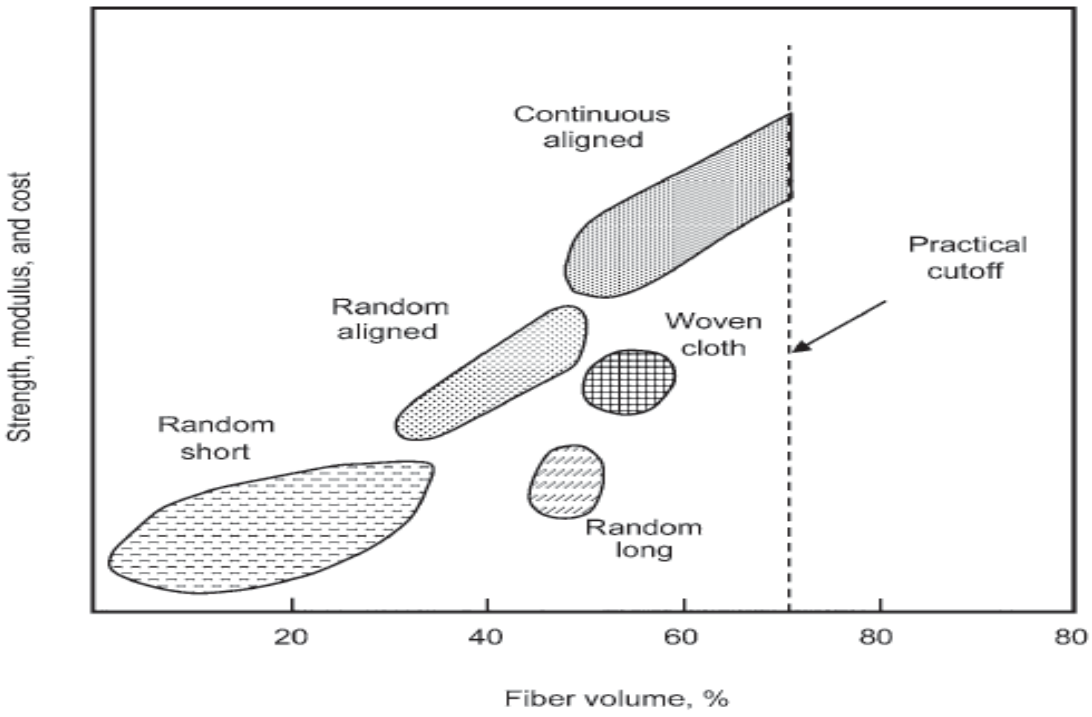

Figure 1.2. Influence of fiber type and quantity on composite performance (Campbell, 2010).

Shear load slides adjacent layers of fibers over each other and resin plays a major role in transferring the stresses across the composites uniformly. For a composite, in order to perform well under shear loads, the resin must exhibit two important characteristics namely good mechanical properties and high adhesion to the reinforcement fiber. However, two kinds of shear, in-plane and inter-laminar shear strength of a composite designates the overall strength of composites. In-plane shear explains the bonding between each lamina and layer whereas inter-laminar shear is for multilayer composites. The combination of tensile strength, compression and shear are called flexural load. This can be explained better in terms of multilayer composite i.e. when the load is applied to the upper surface, it undergoes compression, and the lower face is in tension, the upper face in compression, and the central portion of the material experiences shear.

1.6. Natural fiber composites

In the past decade, research and engineering have shifted from synthetic reinforcements like glass, aramid and carbon fibers to more environmentally friendly natural material. The shift is due to the environmental awareness and stringent regulations imposed towards waste management regulations by the governing bodies. One of such laws recently imposed by European Unions is End to Life Vehicles (ELV) (Holbery & Houston, 2006). This law restricted the automotive manufacturers to produce vehicles which are 95% recyclable by 2015. As a result, the use of natural reinforcements along with biodegradable matrix is gaining importance. The fibers like glass, carbon, and aramid are being replaced by natural fibers. Likewise, thermoplastic resins like polypropylene, polyolefin, polyethylene, polyurethane, polyamide, etc. are replaced by plants based polymeric matrix like cellulosic and starch plastic, soybean-based and corn-based polymer resins, etc. Notably, apart from the fact that natural fibers are derived from renewable sources which are more sustainable, they are typically low cost (if available in abundance and the predicted cost increase of disposing synthetic materials), and possess competitive mechanical properties compared to synthetic fibers. All of these qualities help to strengthen the case for bio-based composites as engineering materials.

Despite making significant research progress in over past two decades, natural fiber reinforced composites (NFRC) have only found application successfully only in a few areas like automotive industry (both for interior and exterior components), construction, and consumer goods including sporting goods. There are many untapped markets where natural fiber composites can make a substantial footprint. Most of the NFRC advancement is made in the European Union, particularly Germany and France.

1.7. 3D Weaving technology

Textile manufacturing processes are sub-divided into four broad categories namely weaving, braiding, knitting and non-woven. However, this section focuses on the two broad segments on weaving namely, 2D weaving and 3D weaving. In the traditional 2D weaving, two sets of yarns namely warp and weft (filling) are interlaced perpendicular to form a 2D fabric. 3D weaving technology is fairly new technology compared to the traditional 2D-weaving. The 3D weaving process is defined by Khokar as “the action of interlacing a grid-like multiple-layer

warp with the sets of vertical and horizontal wefts (Khokar, 1996). A similar concept using 3D orthogonal weaving was developed at the Wilson College of Textiles, NC State University in the 1990s. Instead of just two sets of yarns (warp and weft) in 2D weaving, there are three sets of yarns namely weft (X-yarns), warp (Y-yarns) and binders (Z-yarns) interlaced together. The interlacing of these three sets of yarns produces fabric (preforms) that have better potential for improving the mechanical properties due to its fiber orientation. Since warp and weft yarns are laid straight, it forms crimpless preform except for the crimp from Z-binders. The preform from 3D weaving is protected from delamination as the fabric comes out from the weaving machine, ready for the next step (mostly infusion). There is no need for layering to create a 3D part because a single fabric provides the full 3D reinforcement. There is no restriction in terms of thickness and the Z to Y ratio to the fabric. Since the Z-yarns are inserted through the heddle eye, the proportion of Z-yarns can be changed just by removing the Z-yarns from the heddle.

There are several types of woven fabrics that are commercially available; they could be classified according to their weaving technique as shown in Figure 1.3. For this research, the focus is on 3D orthogonal weaving (3DOW) which is discussed in the details.

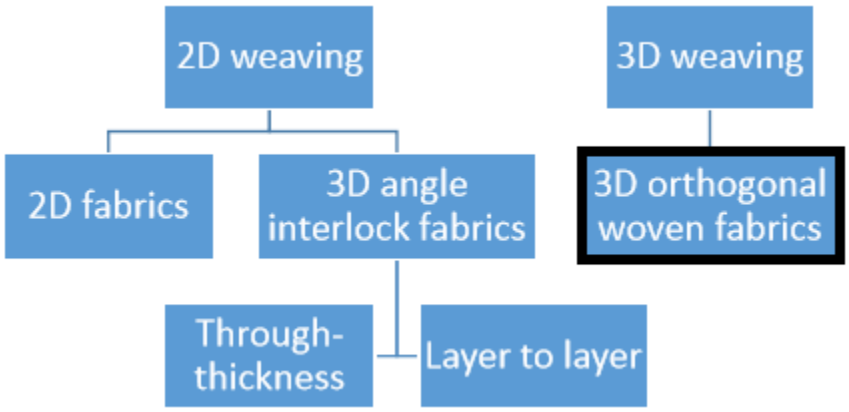

Figure 1.3. Classification of woven fabrics (F. Stig, n.d.).

3DOW is produced in the 3D weaving loom developed and patented in 1992 by Mohamed and Zhang (5,085,252, 1992). The architecture of the 3DOW preform consists of three sets of yarns namely warp (Y-yarn), the weft of filling (X-yarn) and binder (Z-yarn) as

illustrated in Figure 1.4. The Z-yarns runs through-thickness direction in the preform, binding or stitching multiple layers together.

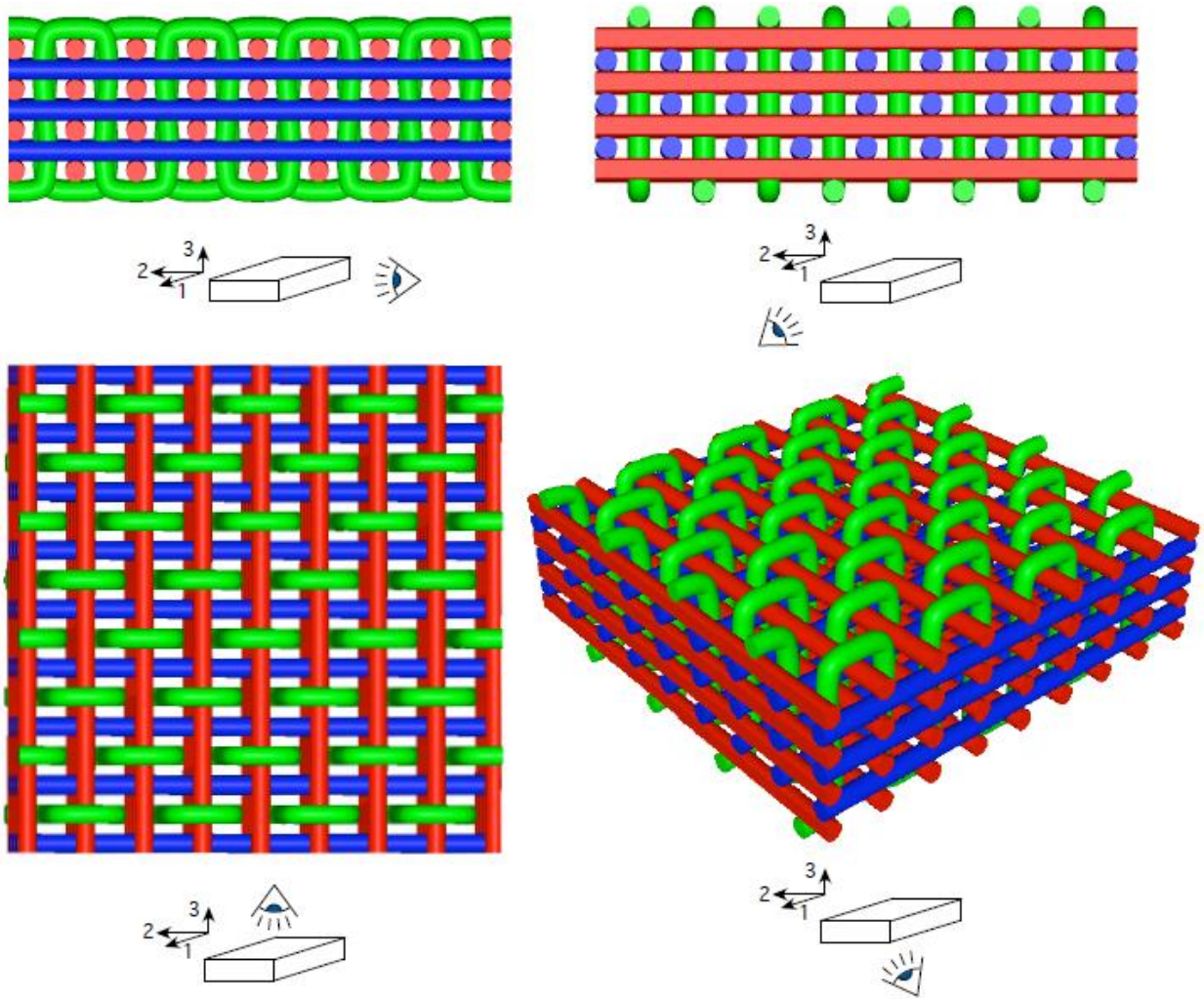

Figure 1.4. 3D orthogonal woven fabric from different view angles (F. Stig, n.d.).

The Y-yarns and Z-yarns are fed through the warp direction whereas weft yarns are inserted through the rapier. Warp and weft yarns are orthogonal to each other and are laid straight in alternate layers. Z-binder yarns run through the heddle eye controlled by harnesses, which move the Z-yarns up and down along the Y-direction stitching all the layers into one fabric as shown in Figure 1.5, giving structural integrity to the preform.

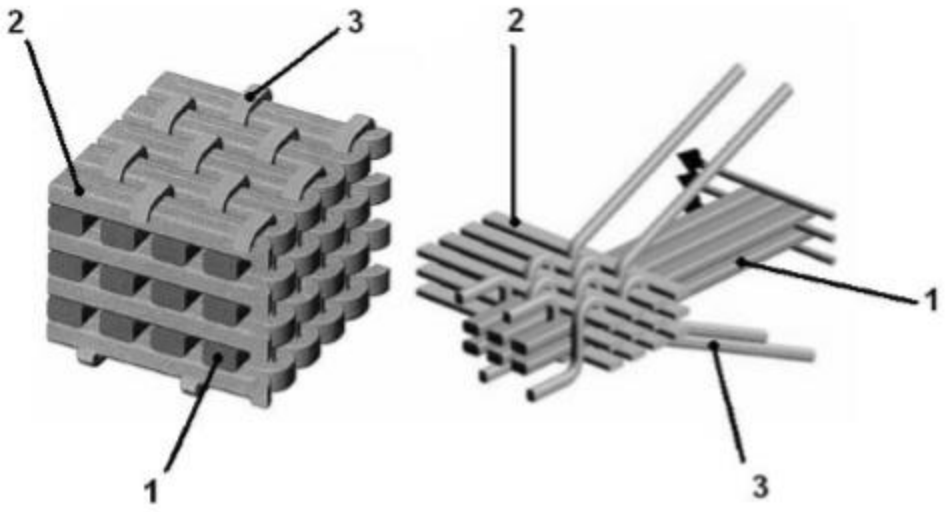

Figure 1.5. Schematic of 3DOW: 1. warp, 2. weft, 3. Z-binders (Mohamed, et al, 2001).

The 3DOW preform tightness can be determined by pick density so there is flexibility in terms of compactness of the structure. The number of weft layer is always one layers more than the warp layers. In this case, there is multiple pick insertion simultaneously in the shed created by the warp yarns, which remain stationary. Reinforcement properties, matrix properties, and fabric architecture heavily contribute to the mechanical properties of the 3D woven composites. Additionally, fiber volume fraction (FVF) and thickness, which is controlled by the number of layers and yarns' linear densities, of composite panel play a vital role in determining the structural and mechanical properties of the composite.

CHAPTER 2 - LITERATURE REVIEW

2.1. Natural fiber composites

The importance of natural fiber in the composite is gaining momentum in the current materials engineering market. As a result of the increasing acceptance of biomaterial boost the desire to replace synthetic fiber (like glass, carbon, aramid) with sustainable natural fiber. There has been a lot of work published to improve the shortcomings of natural fibers. Natural fibers demonstrate many expedient characteristics like low density which contributes to the lightweight composite material with relatively higher specific strength and stiffness. Additionally, renewable source of natural fiber and ease of processing with less hazardous manufacturing are major merits of using natural fibers in composites. This, in turn, helps in reducing petroleum dependency in composite manufacturing (Francucci, Manthey, Cardona, & Aravinthan, 2014; Khot et al., 2001).

Another advancement in the area of natural fiber composite is the development of bio-composites to replace polymeric resin with plant-based resin. Bio-composites are different from natural-fiber composite as the former use plant-based reinforcement and resin whereas the latter are formed by natural reinforcement. Bio-composites are mainly advantageous in areas with low load bearing applications and are biodegradable and/or renewable resources (Khot et al., 2001). This will, in turn, reduce the carbon footprint considering the life cycle of the composites at the disposal stage (Joshi, Drzal, Mohanty, & Arora, 2004).

The comparative performance of the bio-composites is lower than the composites from synthetic materials due to the drawbacks or inconsistencies inherent to the natural fiber. A few downsides of using natural fiber in the composite is due to the hydrophilic nature. Natural fiber tends to absorb water which can result in swelling of the fiber which lowers the dimensional stability and mechanical properties of their composites. This deterioration of the physical and chemical properties are reflected in the composites as water presence makes the interfacial bonding between fiber and matrix weak. The performance of composites is negatively affected by moisture absorption which can be curtailed by chemical and physical treatments. These surface modification methods help to improve interfacial bonding of fiber and matrix which is extensively discussed by Bledzki and Gassan (Bledzki & Gassan, 1999). Chemical modification

introduces the reactive group and removes lignin, hemicellulose, and wax from the fiber surface for better compatibility of reinforcement and matrix. A typical specific strength and stiffness could be attained with better bonding that is very brittle in nature with easy crack propagation through the matrix and fiber. The effectiveness of stress and load transfer from matrix to fiber could be condensed with a weaker interface (Faruk, Bledzki, Fink, & Sain, 2012).

As nanocomposites are the future trend, not much research is dedicated to deriving nanofibers and whiskers using bast fibers. Natural fibers like sisal, jute, hemp, flax and kenaf are good replacement because of high specific properties stiffness (Mike & Brady, 2008), impact resistance (Sydenstricker, Mochnaz, & Amico, 2003), flexibility (Manikandan Nair, Diwan, & Thomas, 1996) and modulus (Eichhorn et al., 2001).

Although, in terms of flexural modulus, glass fiber composites perform significantly better than treated and untreated natural fiber composites. Apart from these benefits, natural fibers are biodegradable and renewable, low cost, low density, low weight, low contributor of carbon dioxide to the environment and abundance availability, see Figure 2.1.

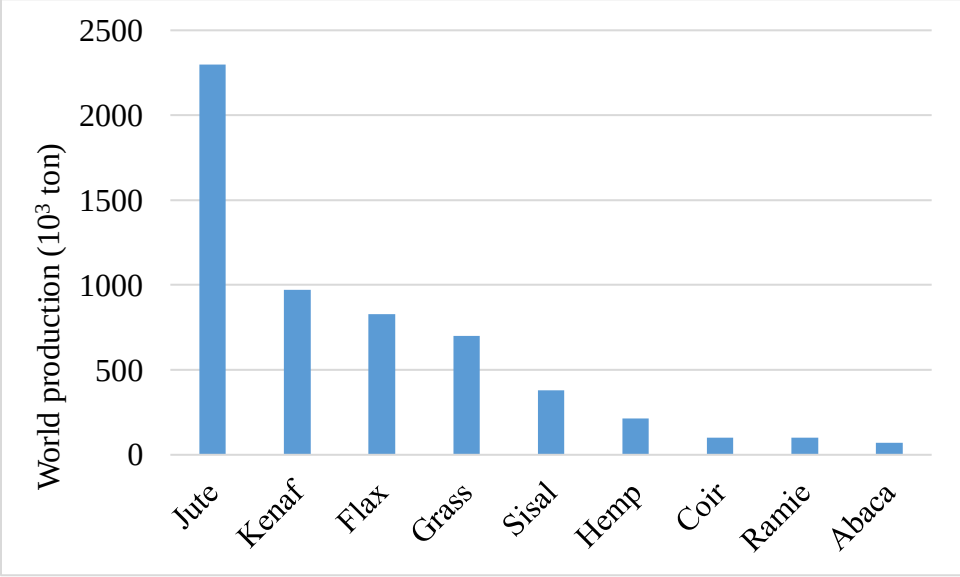

Figure 2.1. World production of different natural fibers (Faruk et al., 2012).

But natural fibers being hydrophilic in nature provides poor adhesion or bonding with hydrophobic matrices. Sgriccia et al. found out that natural fibers, both treated and untreated,

absorbs considerably more water than glass fibers (Sgriccia, Hawley, & Misra, 2008). Water absorption can cause deformation, low adhesion, and results in low strength composites. Natural fibers are also not compatible with thermosets, which have high curing time, as they have very low degradation temperature which is less than 200°C (Sgriccia et al., 2008). This particularly restricts the applications of composites to low temperature. Besides, there are also other variations in mechanical and physical properties, lower elongation, and handling of fibers and cultivation conditions which greatly differs owing to different sources. The challenge is to produce quality fibers to be used for various applications by using better cultivation methods using genetic engineering.

However, these impediments can be curtailed to some extent by various fiber treatments like alkali and saline treatments. The two popular methods to compare treated and untreated natural fibers and their composites are X-ray photoelectron spectroscopy (XPS) and Fourier transform infrared spectroscopy (FTIR) (Sgriccia et al., 2008). Ouajai and Shanks (2005) studied the effect of alkali treatments on hemp fibers and found that pectin and hemicelluloses, which give a waxy layer to the fiber surface, were removed by the treatment. George, Sreekala, and Thomas (2001), used bleached Kraft pulp fibers and compared with untreated ones and found out that bleached fibers are more hydrophilic in nature and have a higher oxygen to carbon (O/C) ratio (George et al., 2001). However, Dash et al. studied jute/polyester composites in outdoor weathering conditions and found that bleached fiber composites absorbed less water than the untreated composites (Dash BN, Rana AK, Mishra HK, Nayak SK, 2000).

There are other ways to decrease hydrophilicity of natural fibers chemically by esterification and etherification (Baiardo, Frisoni, Scandola, & Licciardello, 2002; Baiardo, Zini, & Scandola, 2004; Frisoni et al., 2001; Zini, Scandola, & Gatenholm, 2003), silane treatment (Arbelaiz, Fernández, Ramos, & Mondragon, 2006; Bledzki & Gassan, 1999; Tran, Graiver, & Narayan, 2006), plasma or corona treatment (Belgacem & Gandini, 2005; Bledzki & Gassan, 1999; Gassan & Gutowski, 2000) and polymer matrix modifications (R. Karnani, M. Krishnan, 1997; Wu, 2009). Another proven method to improve mechanical properties by chemical modification is by altering polar hydroxyls with polar groups. For any of these modifications, it is important to keep in mind that any reaction should be restricted to surface level in order to protect the mechanical property of fibers.

In order to produce uniform and optimized fibers for specific sectors like automotive, construction, etc., improved treatment methods should be adopted (Craig MC, 2005). Since natural fibers are prone to water absorption, suitable low-cost coating and encapsulation methods like acetylation of the hydroxyl groups present in the fiber should be developed to reduce its hydrophilicity. This will minimize fiber swelling and water absorption rate and also improve matrix-matrix bonding (Bledzki & Gassan, 1999; John & Thomas, 2008; a. K. Mohanty, Misra, & Drzal, 2001, 2002; Netravali & Chabba, 2003)

The advantages and disadvantages of using natural fibers in composites are listed in Table 2.1. However, the disadvantages can be curtailed to some extent by pretreatments and chemical treatments (Scarponi & Messano, 2015).

Table 2.1. Advantages and disadvantages of using natural fiber in composites.

Adavantages	Disadvantages
• Biodegradable • Low density and high specific strength and stiffness • Less expensive if produced in abundance • Low hazardous processing & manufacturing • Increased flexibility • Renewable resource	• Hydrophillic nature causing swelling of fibers • Poor interfacial bonding • Low temperature processing • Higher variability of fiber properties

However, there are other advantages of using natural fiber composites over other synthetic or metal composites.

- The density of the products is drastically reduced (~30%) as compared to conventional metallic composites.
- The products from natural fibers are low in weight and consume less energy and as a result, they are less hazardous to the environment.
- Natural fiber composites are more compatible with bio-polymers which results in bio-composites.
- The manufacturing of natural fiber composites is safer than glass or metal composites, which emits dangerous airborne particles.

2.2. Types of natural fibers

Natural fibers can be classified into six categories namely bast fibers, leaf fibers, Fruit fibers, seed fibers, grass fibers, straw fibers and wood fibers (Anandjiwala & Blouw, 2007). The classification of natural fiber is represented in Figure 2.2.

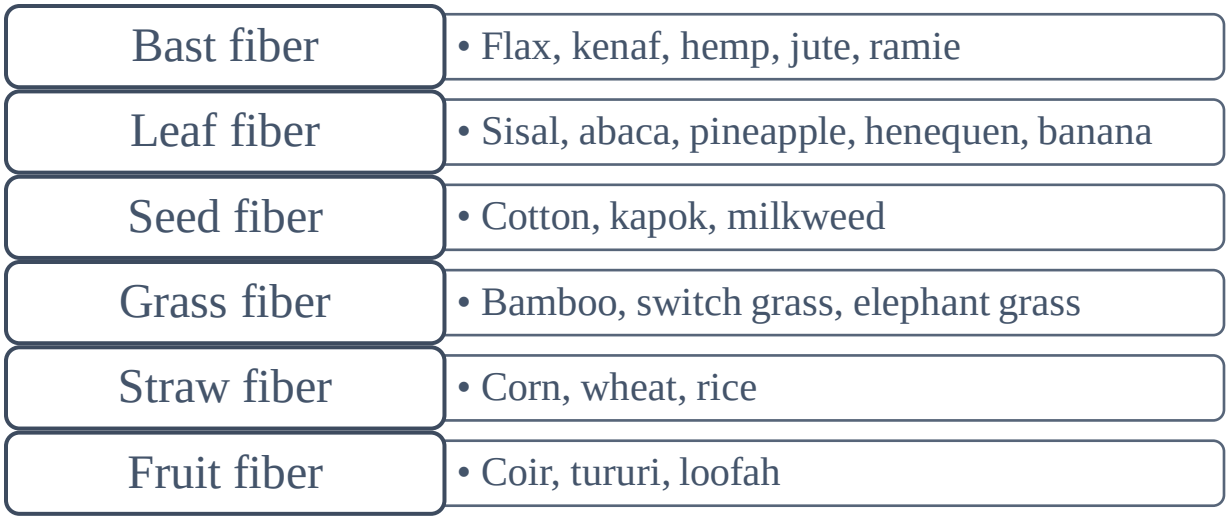

Figure 2.2. Classification of natural fiber from plants for reinforcing in composites (Anandjiwala & Blouw, 2007).

The first five types of fibers are grouped as non-wood fibers. Natural fibers can also be broadly classified as plant-based, which are rich in polysaccharides and animal-based fiber like silk, wool, and feathers are made up of proteins (Zini & Scandola, 2011). Bast fiber is most popular and most copiously used fiber in composites. Although the density and tensile strength of all the bast fibers is lower than glass fiber, some varieties of hemp and flax are comparable with glass fiber due to its elastic modulus and specific modulus due to low density, as shown in Table 2.2. Due to its hydrophilic nature, the composite formation becomes challenging. However, this can be altered by various pretreatments which control the moisture absorption rate. All the properties of bast fibers differ due to chemical constituent and internal fiber structure like fiber origin, maturity time of plant, fiber separation processes, soil type, and weather conditions, retting process, etc.

Table 2.2. Comparison of physical properties of natural fiber.

Fiber	Density (g/cm^3)	Elongation (%)	Young's modulus (Gpa)	Tensile strength (MPa)	Specific tensile strength (MPa cm^3/g)	Water absorption (%)
E-glass	2.5	2.5	70	2000-3500	800-1400	-
Aramid	1.4	3.3-3.7	63-67	3000-3150	2140-2250	-
Carbon	1.4	1.4-1.8	230-240	4000	2860	-
Flax	1.5	1.2-3.2	27-80	345-1500	230-1000	7
Cotton	1.5-1.6	3.0-10.0	5.5-12.6	287-800	190-530	8 to 25
Jute	1.3-1.5	1.5-1.8	10 to 55	393-800	300-610	12
Hemp	1.5	1.6	70	550-900	370-600	8
Sisal	1.3-1.5	2.0-2.5	9.4-28	511-635	390-490	11
Ramie	1.5	2.0-3.8	44-128	400-938	270-620	12 to 17
Coir	1.2	15-30		131-220	110-180	10
Soft wood kraft	1.5	-	40	1000	670	-
Chicken feathers	0.89	-	3 to 10	100-200	112-220	-
Silkworm silk	1.3-1.4	15	1.5	-	-	-

2.3. Morphology of natural fiber

Plant fibers are tubular structures where the central lumen, which is responsible for water uptake, is surrounded by primary and secondary cell wall (Figure 5, Tsoumis, 1991). These cell walls are made up of cellulose microfibrils embedded in a hemicellulose and lignin matrix, which vary in composition depending on the fiber type as depicted in Figure 2.3.

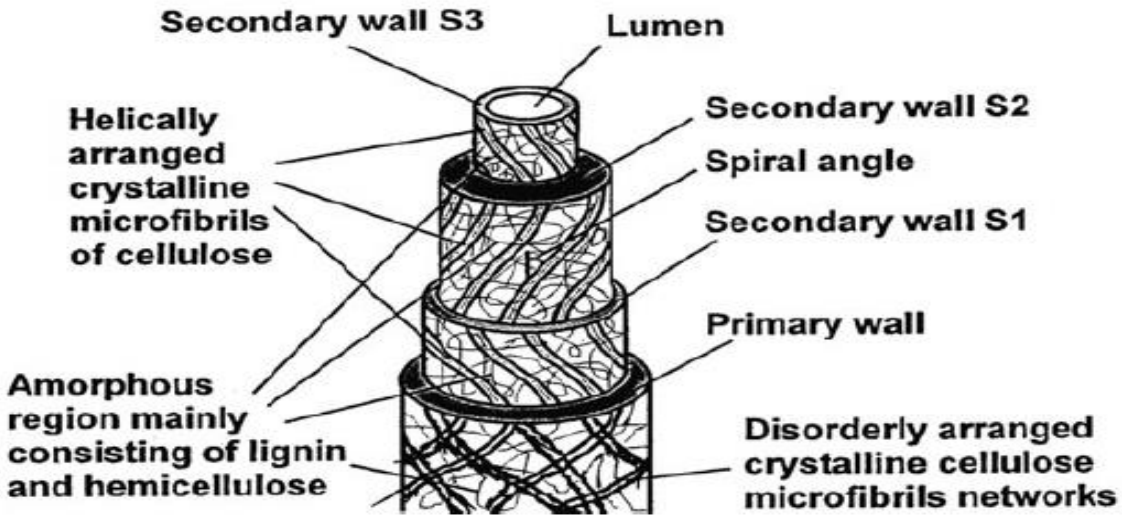

Figure 2.3. Structural constituents of the natural fiber plant cell (Rong, Zhang, Liu, Yang, & Zeng, 2001).

These microfibrils have a diameter of about 10 – 30 mm and have cellulose molecules in form of chain that provide mechanical strength to the fiber. Figure 2.4 shows the arrangement of fibrils, microfibrils, and cellulose in the cell walls of plant fiber. The most efficient cellulose fibers are those with high cellulose content coupled with a low micro-fibril angle (angle between cellulose microfibrils and fiber axis) is in the range of 7°to l2° to the fiber axis (Barnett & Bonham, 2004).

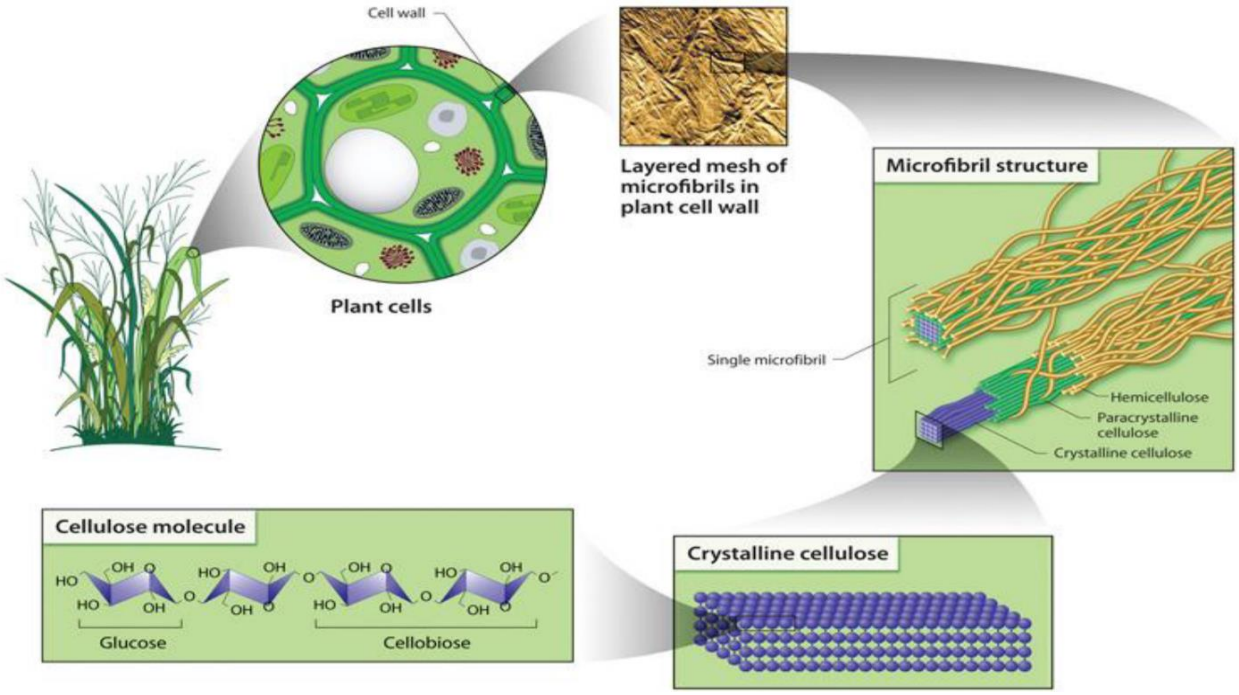

Figure 2.4. Arrangement of microfibrils and cellulose in a plant cell (Siqueira, Bras, & Dufresne, 2010).

Natural fibers primarily have components namely cellulose, hemicellulose, pectin, and lignin. The ratio of the individual component varies with different types of fibers which directly depends on growing and harvesting conditions and methods as shown in Figure 2.5.

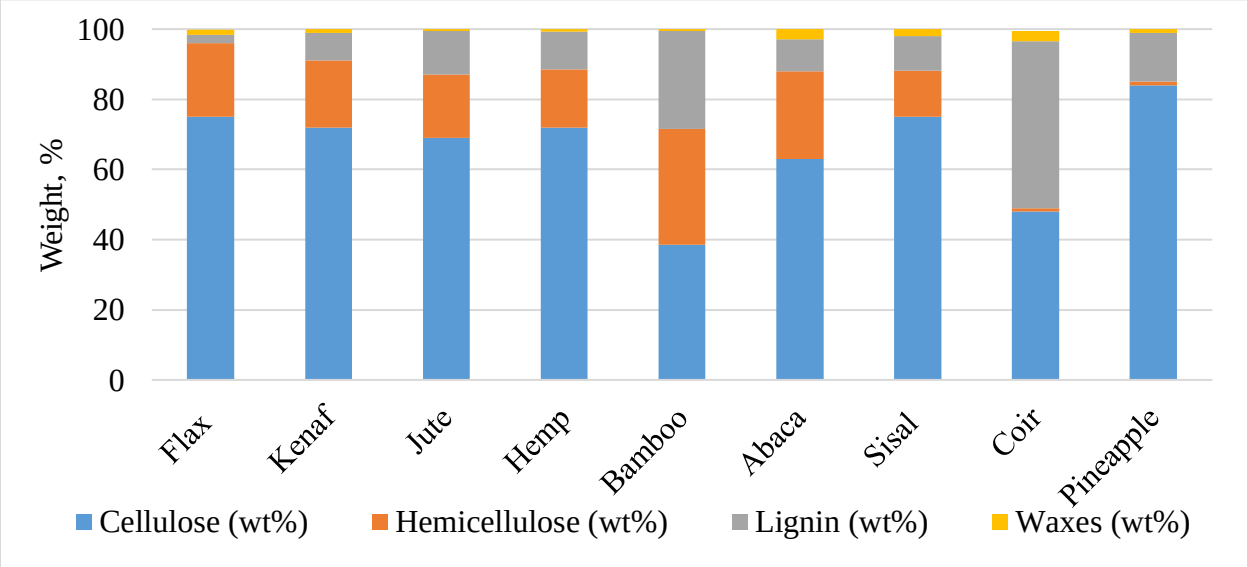

Figure 2.5. Chemical composition of natural fibers (O. Faruk et al., 2012).

Cellulose is a semi-crystalline polysaccharide and is the component which is responsible for the hydrophilic nature of natural fibers. The hydrophilic nature greatly influences the mechanical strength of the composites. For example, a composite made from coir fibers would have much greater moisture content than would a composite made from flax or kenaf fibers. Hemicellulose is amorphous polysaccharide with a lower molecular weight compared to cellulose. The amorphous nature of hemicelluloses results in it be in partially soluble in water and alkaline solutions. The hemicellulose is responsible for moisture absorption, bio and thermal degradation in a natural fiber. Pectin is a polysaccharide like cellulose and hemicellulose and is responsible for binding the fibers together. Lignin is an amorphous polymer and has a negligible presence in fibers percentage-wise. They are mainly responsible for aromatics and thermal stability and has little effect on water absorption although they are accountable for UV degradation. Figure 2.6 shows the structural representation of fiber composition.

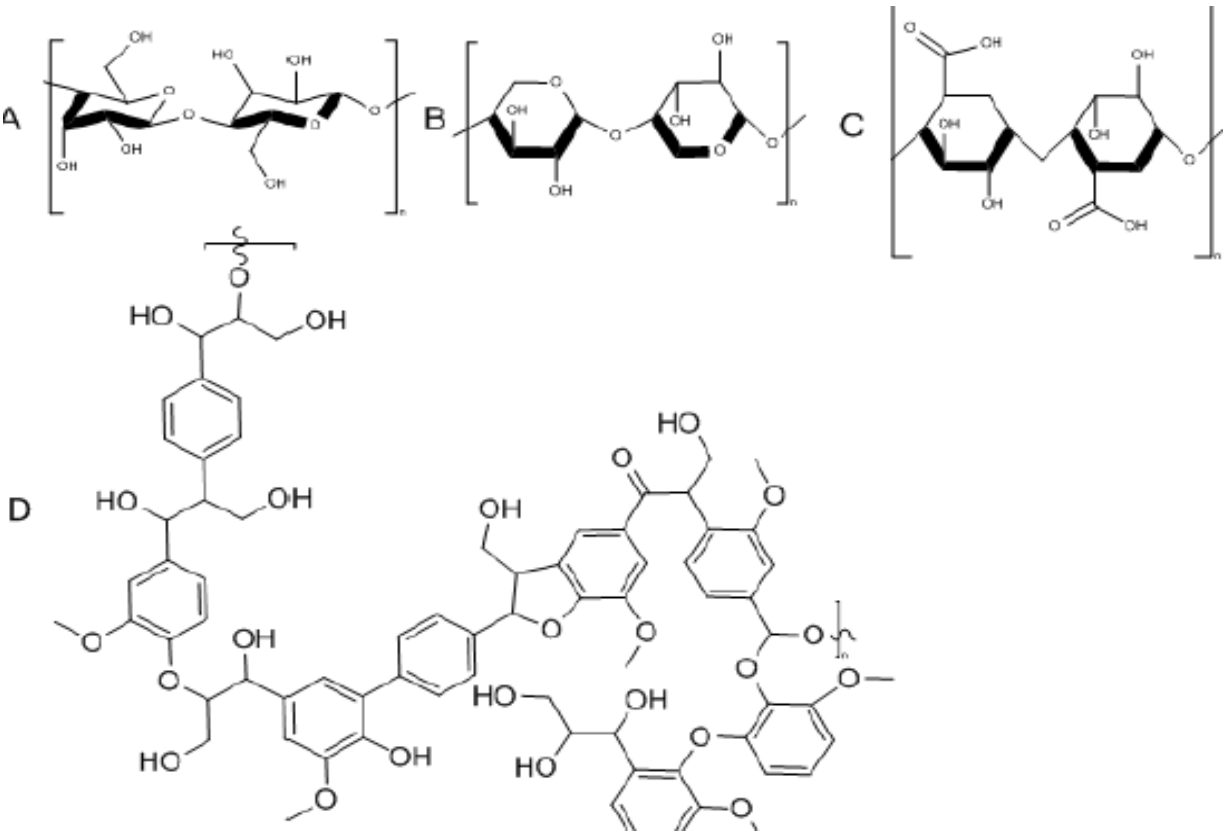

Figure 2.6. Structural representation of (A) cellulose, (B) hemicellulose, (C) pectin, and (D) lignin (Odian, 2004).

2.4. Criteria for selecting natural fiber

Natural fibers differ in their mechanical, physical and chemical properties and therefore selecting right fiber as reinforcement is very crucial. This will ultimately affect the functionality of the composites and the subsequent manufacturing processes. There are various criteria in selecting the reinforcement which are addressed in the sections below.

Density - Density is one of the important criteria is selecting natural fiber as it determines the weight of the composites. This is particularly important in an automotive application where low weight contributes towards reduced energy consumption and thereby supports sustainability. In this context, natural fibers are comparable with any synthetic fibers like glass, carbon, and aramid, where values of specific tensile strength and specific modulus of elasticity are considered important. Specific tensile strength and specific modulus of elasticity is the ratio between the mechanical properties (tensile strength and modulus of elasticity) and fiber density. The lower the value of density, the higher will be the specific values and thereby more favored to be used in composites.

Aspect ratio - The fiber length to diameter ratio is known as the aspect ratio. Continuous filaments are stronger and stiffer than short fibers and have a higher aspect ratio than short fibers (Lewin, 2006). Short or discontinuous fibers (length > 100 x diameter) are used for bulk production as it is easier to fabricate complex parts and are isotropic in nature (Lewin, 2006). Continuous fiber composites (from woven cloth and helical winding) have preferred orientation and single layers of different orientations are stacked together to attain desired strength and stiffness (Campbell, 2010). Discontinuous fibers like chopped fibers and random mat have random orientation. High strength composites are produced with small diameter fibers as there are fewer surface defects, more flexibility but are costly to produce. However, it is important to note that if the fiber aspect ratio is too high, the fibers may get intertwined during processing and result in poor composite mechanical strength, due to poor dispersion (De, S. K., & White, 1996). The problem with high-performance synthetic fibers is that they are brittle and tends to break during processing whereas cellulosic/natural fibers are more flexible (Lee, 1991). Hence, it is important to know fiber length and fiber length distribution to predict reinforcement strength.

Thermal conductivity - Thermal conductivity is an important criterion when it comes to industrial applications, especially in the automotive industry. In the case of natural fibers, the hollow tubular structure is responsible for thermal and acoustic insulation. Agoudjil et al. (2011), compared the values of thermal conductivity of date palm, coir, hemp and sisal and found out that hemp has the highest thermal conductivity followed by date palm, sisal, and coir. This makes natural fiber a good substitute for interiors in the automotive industry.

Chemical composition of the fiber - Cellulose, hemicellulose, and lignin are three major components of the cell wall of plant fiber. Different fibers have a different composition (Faruk et al., 2012; Madsen, 2004) depending on the molecular composition and structure, which in turn determines mechanical, chemical and water absorption properties of the fiber. The more the cellulose content in the fiber, the less is the water absorption capacity of the fiber, hence making natural fiber a feasible alternative in the automotive sector.

Availability and cost of raw material - One of the reasons for selecting natural fiber over any synthetic fiber is abundant accessibility of natural fiber. However, the availability differs from type to type, region to region and different period of time. Also, the cost factor is important in this respect. The cost tends to fluctuate from time to time and therefore necessary steps should be taken to ensure that bulk quantity is purchased in advance for uninterrupted production. Even though the cost of natural fiber is comparatively less than glass or carbon, but there is intense competition within the varieties of natural fibers in terms of cost as illustrated in Figure 2.7. It clearly explains that date palm is much cheaper than other varieties depicted in the figure.

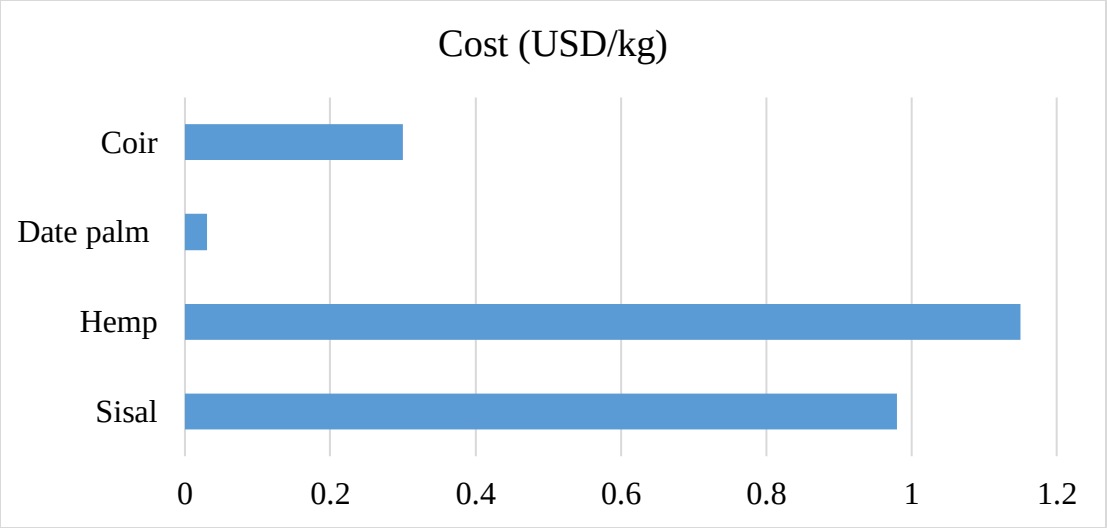

Figure 2.7. Cost comparison of different natural fibers used in automotive industries (AL-Oqla & Sapuan, 2014).

It is worth mentioning that government support is also an integral part. For example, hemp cultivation and application were prohibited in the United States due to a law passed a few decades back due to its relationship with marijuana (*Cannabis Sativa*). Both have toxic ingredient tetrahydrocannabinol (THC) which can be extracted to make psychoactive drugs. But the biggest difference is the amount of THC in industrial hemp. An industrial plant has a THC content of 0.3%. So, the availability and cost are influenced as it not readily available.

Mechanical properties of natural fiber - The value of elasticity, tensile strength, and elongation to break are mechanical properties important in the selection of the suitable reinforcing fibers in automotive applications. However, natural fibers have low mechanical properties but specific values like specific modulus of elasticity and specific tensile strength are comparable to the glass fiber. It is important to develop optimum reinforcements to obtain the desired mechanical properties. This is particularly important in hybrid bio-composites, in which there is a chance to manipulate biodegradable properties. This can be accomplished by right blend ratio of bast and leaf fibers (popularly known as engineered natural fibers), which gives right stiffness and toughness (K. A. Mohanty, Drzal, & Misra, 2002).

The specific modulus of elasticity with respect to cost ratio is a critical factor in natural fiber selection. The more is the value of the ratio, the more desirable is the fiber type in most applications. (AL-Oqla & Sapuan, 2014).

2.5. Applications of natural composites

Composite materials are used in various sectors namely automotive, heavy truck, aerospace, civil infrastructure, marine, and durable goods. The main purpose of using composites instead of metal are durability, strength, lightweight that qualify them for a wide range of applications. There has been a tremendous development in the applications of polymer-matrix composites (PMCs). The bifurcation of composites usage is shown in Figure 2.8, which depicts sector-wise distribution. However, the advent of natural fiber composites gives a whole new dimension to the market as they are eco-friendly and easily available. For example, asbestos used in automotive brakes and clutch linings are being replaced by aramid fiber composites and synthetic fiber used in seats in automobiles are switched by recyclable coconut fibers.

PMCs are gaining popularity due to the availability of multiple fiber types and advantages like easy processing, high specific strength and a wide variety of usage. Fiber-reinforced composites often aim to improve the strength and stiffness to weight ratios. These properties will reduce the weight of the components produced by the fibers and therefore fibers used for composite materials will have high strength, high flexibility and it is most widely used for textiles and other major fields. PMCs are used in helicopter rotor blades, circuit boards, pipes and tanks, conveyor belts, tennis rackets, rockets and missiles, marine applications, etc. Around three decades ago, aramid fibers in the form of Kevlar revolutionized the composite market. Since these are lightest, strongest and most impact resistant, they are used in bulletproof vests.

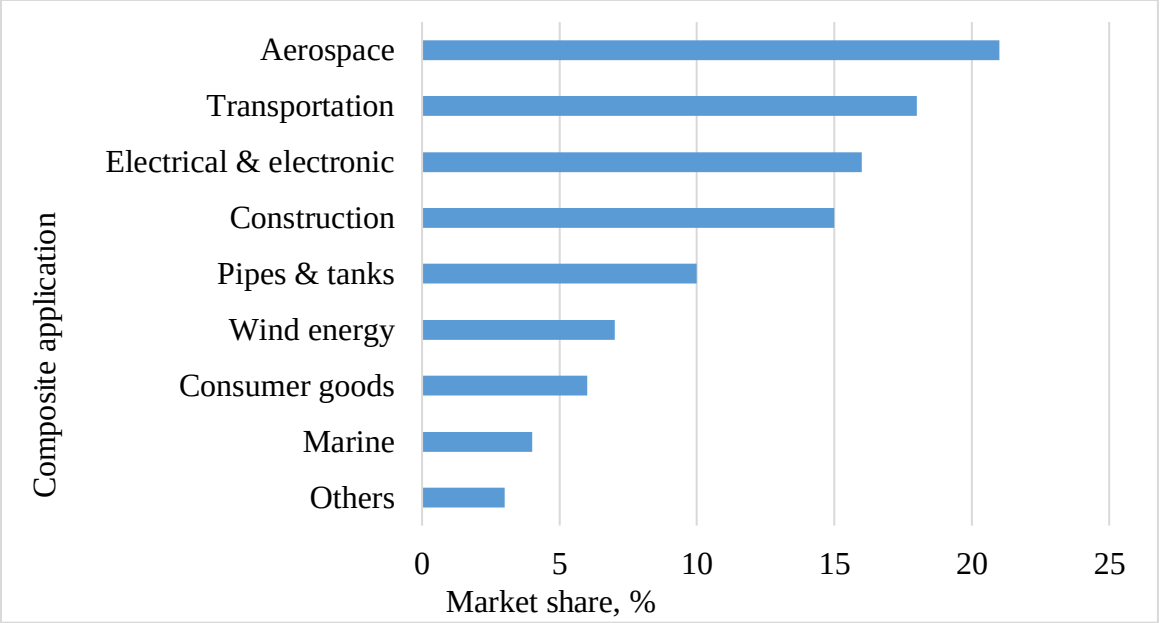

Figure 2.8. Sector-wise distribution of the composite market (Zini & Scandola, 2011).

Other applications were composites are being employed for fluid transport and storage are pipes, tanks and vessels applications. Glass reinforced epoxy (GRE), which has been used for both low and high-pressure applications with a wide variety of fluids, including hydrocarbons are being utilized. They are chemical and high-temperature resistance for a particular fluid depending on the type of resin and hardener used. Glass reinforced epoxy tubes are largely insusceptible to chemicals like hydrogen sulfide and carbon dioxide but not to water, which poses a major danger.

Advanced composites in aircraft and helicopters are around 20 – 30 % lighter compared to conventional metals. They are used in fairings, landing gears, engine cowls, rudder, fin boxes, doors, floor boards, etc. where metallic and non-metallic materials are combined to develop an advanced composite (Prasad & Ramakrishnan, 2000). The Advanced Light Helicopter (ALH) which is made up of around 60% composite structure is a good example of PMCs application. However, the most recent one in the field of aircraft is the use of hemp fibers in rotorcraft interiors instead of glass fibers which prove that hemp is comparable in terms of strength, weight, and cost. Hemp being an example of natural fiber, is biodegradable and has a low environmental impact but characteristics like durability, fire retardant, and hydrophilic nature

should also be factored in when used in aeronautics. (Van Vuure, Baets, Wouters, & Hendrickx, 2015). There are a lot of modern applications of natural fiber composites, especially flax and hemp as shown in Figure 2.9.

Figure 2.9. Natural fiber composites used in various areas (Tambyrajah, D., 2015).

The automotive industry is one of the sectors where composites, both polymer-based and natural fiber-based, are used extensively. Nowadays, composites from synthetic fibers are replaced with natural fiber composites due to the regulations being imposed on the manufacturing firm. It started decades back in 1941 when Henry Ford used hemp-based plastic in the body of an automotive (Figure 2.10). Replacing metal with hemp significantly reduced its weight and increased impact strength without denting.

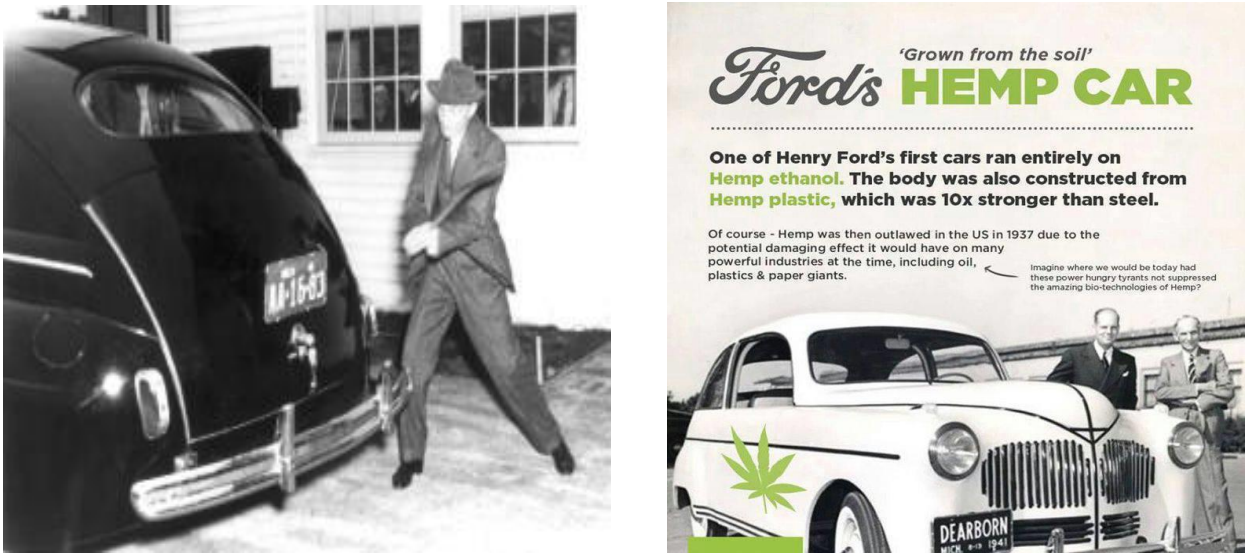

Figure 2.10. Henry Ford demonstrating car made from hemp fiber.

However, natural fiber composites are now replacing many interiors as well as exterior parts of an automobile as shown in Figure 2.11. The list of interiors and exterior parts are delineated in Table 2.3. Bruce Michael Dietzen of Florida got inspired by Henry Ford's idea of the green car and has come up with his own version of the green car. The car on the right is made from three plies of woven hemp which makes it lighter than fiberglass and 10 times more dent-resistant than steel.

Figure 2.11. Use of natural fibers in Mercedes Benz E-class components (Elliott-Sink, 2005) and car from woven hemp fabric (right).

Porsche revolutionized the sports cars market by launching a GTS Clubsport model of a sports car in 2019 which was made out of natural fiber body parts, see Figure 2.12. Hemp and flax fiber reinforced composites were used to manufacture driver and co-driver doors and rear wing replacing previously used carbon fiber. The main advantages of using natural fiber are its low density and high specific stiffness which make lighter composites giving a better fuel efficiency. These natural fibers have many commonalities with carbon fiber and allowed the vehicle a lighter weight of 2910 pounds. These natural fibers have many commonalities with carbon fiber and allowed the vehicle to be lighter. The motivation for using natural fiber in a sports car was to further improve drivability with faster lap times and usage of sustainable material.

Figure 2.12. Porsche 718 GT4 sports car made from natural-fiber (hemp & flax) composites.

Table 2.3. Example of interior and exterior automotive parts from natural fiber (B. Singh, A. Verma, 1998; A. K. Mohanty, Misra, & Drzal, 2005).

Parts	Vehicle parts	Material used
Interior	Glove box	wood/cotton fiber molded, flax/sisal
	Door panels	Flax/sisal with thermoset resin
	Seat coverings	Leather/wool backing
	Seat surface/backrest	Coconut fiber/natural rubber
	Trunk panel	Cotton fiber
	Trunk floor	Cotton with PP/PET fibers
	Insulation	Cotton fiber
Exterior	Floor panels	Flax mat with polypropylene

2.6. Bio composites

As described earlier, bio-composites otherwise known as green composites are composites in which both matrix and reinforcement are derived from natural resources. Like other composites, bio-composites is a blend of the intrinsic properties of fiber and matrix and also depends on fiber volume ratio, the aspect ratio of fibers and the bonding of fiber and matrix interface (Manson, 2001). However, it is important to note that bio-degradable materials are different from bio-based material. Bio-based materials are those which are derived from environmentally friendly sources whereas biodegradable are those materials, which at the end of life are compostable. In the case of bio-composites, even though the fiber is from natural components and is biodegradable, bio-based polymers can either be biodegradable either completely or partially or can be non-bio-degradable (which contribute to landfill). This is illustrated in Figure 2.13. Even though biodegradability is a much sought-after property but in some applications, as long-lasting construction application, durability is of utmost importance.

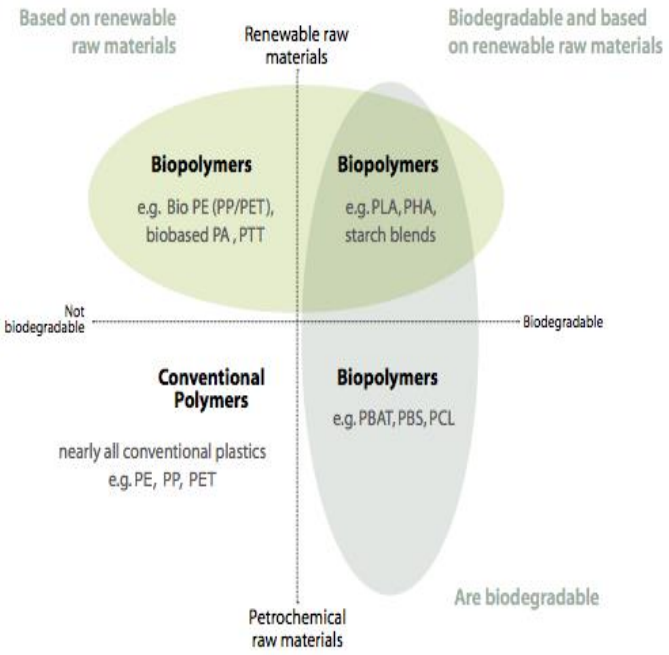

PE	Polyethylene
PP	Polypropylene
PET	Polyethyleneterephtalate
PA	Polyamides
PTT	Polytrimethylene terephthalate
PLA	Polylactic acid
PHA	Polyhydroxyalcanoate
PBAT	Polybutylene adipateco terephtalate
PBS	Polybutylene succinate
PCL	Polycaprolactone

Figure 2.13. Examples of oil-based, partially and completely bio-based polymers (Pathak, Sneha, & Mathew, 2016).

Thermosetting green composites are prepared from natural oils like soybean, castor, linseed, etc. and can act as a substitute of petrochemical resins like unsaturated polyesters, vinyl esters, and epoxy resins (Khot et al., 2001). The advantages of natural oils are that they are cheap, abundantly available and renewable. They are based on triglycerides of fatty acids, and they can be polymerized when chemical functionalities are added on their active sites (double bonds, allylic carbons, ester groups, and carbons alpha to the ester group). Epoxidation, ring opening reaction with halo acids or alcohols, ozonolysis, and hydration are some of the methods used to formulate unsaturated plant oils (Khot et al., 2001). In the case of thermoplastic green composites, PLA form is the most studied and is derived from starch fermentation. However, there is a maximum limit of fiber volume % (50%w/w).

2.7. Hemp-fiber reinforced composites

Natural fibers can be either derived from plant or animals. Fibers from plant source are composed of cellulose and therefore are stronger and stiffer than animal fibers, which mainly contain proteins. Plant fibers can further be derived from leaf, bast, fruit, seed, wood, straw or grass. Hemp is an example of bast fiber with high cellulose content. It is a renewable resource and most widely used in composites for natural fiber reinforcement, after sisal (Shahzad, 2012).

It has the highest Young's modulus and aspect ratios (only flax is comparable) among other natural fiber like sisal, bamboo, and kenaf, which makes it a good fit for fiber reinforced composites. Hemp is gaining popularity among the agricultural community because of higher fiber yields, pest resistant and drought resistance and high strength.

Like much other natural fibers, hemp also has major cellulose percentage as compared to hemicellulose, pectin or lignin. Hemp is a tall plant can grow as tall as 5 meters with a diameter about 60 mm in just 12 weeks. The hollow pith of the stem is surrounded by a wood core called xylem. The bast layer which is the outer most layer of bark covering xylem has components layers of cambium, cortex and epidermis as shown in Figure 2.14.

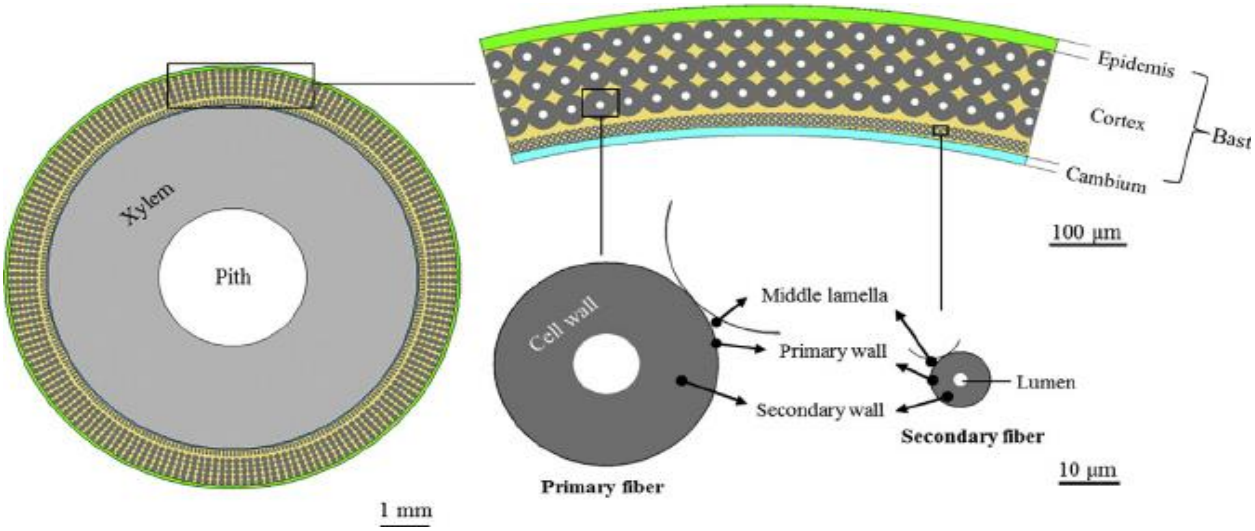

Figure 2.14. Schematic diagram of a transverse section of hemp stem showing the organization and morphology of a single fiber (Liu, et. al., 2015).

Hurd, which forms 75% of the stem volume provides stiffness to the plant. The bast fiber of the bark gives tensile and flexural strength and the outer epidermis makes the plant pest proof. Hemp fibers have high strength and stiffness makes it the most extensively used reinforcements after sisal, which has exponentially increased the world production of hemp globally. Hemp fiber has higher tenacity than flax (about 20% higher) but has a lower elongation (Malkapuram & Kumar, 2008). Hemp fiber has a massive influence on the environment compared to glass fiber, which depletes the ecological balance. Power consumption, toxic gas

emission and biochemical oxygen demand (BOD) by 1 kg of hemp fiber is significantly less than 1 kg of glass fiber as found by Mougin, G., 2006.

In Hemp fiber, cellulose is the main constituent which makes up to 70%-75% while hemicellulose is roughly around 18%-22%. Other compositions are Lignin (4%-6%), pectin (1%) and other waxes (0.8%). However, the composition differs in every publication. Hemp fiber properties are strongly influenced by many factors, particularly chemical constituent composition, which differs from region to region. The factors that may affect the fiber quality are location, climatic conditions, soil type, harvesting process, fiber extraction, processes and transportation, and storage conditions. All these will dictate the properties of the end product. The high variation could also be due to inheriting nature of the material, handling of the fiber during processing and fabrication, resin infusion techniques and testing. There is a very close resemblance between the hemp and flax in terms of their chemical composition and mechanical strength as pointed out by Seile and Belakova (Seile et al., 2014).

Hemp fiber composites in the exterior body of the car were first used by Henry Ford in 1941 (Figure 2.10). The impact resistance of the car was claimed to be ten times higher than the conventional metal panels. Nevertheless, the concept was never commercialized due to economic limitation and the increasing popularity of glass fiber. But the scenario has changed as the attractiveness of natural fiber has gained momentum in recent time as well as growing demand from government agencies to safeguard the environment. Hemp is one of the sustainable options for high-performance composite applications. Many studies have suggested that hemp is suitable for using it as a reinforcement in the composite in terms of behavior, mechanical and physical properties, and chemical structure. Choosing bio-polymer as a matrix of the composite, hemp could be used as a component of bio-composite.

The mechanical properties of hemp are comparable to glass (Shahzad, 2011). Mechanical properties of untreated hemp fiber infused unsaturated polyester composites were studied and found that tensile and flexural strength and modulus, except impact strength, of hemp, is at par with glass composites as depicted in Table 2.4.

Table 2.4. Mechanical properties of untreated hemp fiber reinforced unsaturated polyester composites compared to glass composites.

Fiber	Fiber fraction wt. /vol (%)	Tensile strength (MPa)	Tensile modulus (GPa)	Flexural strength (MPa)	Flexural modulus (GPa)	Impact strength (kJ/m^2)
Hemp	35.0	60.2	1.7	112.9	6.4	14.2
Hemp	36.0	-	-	110.0	7.5	13.0
Hemp	30.0	38.0	6.0	100.0	6.5	20.0
Hemp	20.0	33.0	1.4	54.0	5.0	4.8
Glass (CSM)	7.0	-	-	108.0	5.6	34.0
Glass (CSM)	20.0	73.4	7.9	233.8	9.3	80.4

Surface treatment of hemp fiber is essential to reduce the hydrophilic nature and to have a better interfacial bonding between resin and reinforcement. Mutje et al. observed that due to irregular surface morphology, hemp fibers have a weak interaction with PP, which was almost about 50% of that of glass-PP composites at 40 % fiber volume fraction. By using maleated polypropylene (MAPP) about 4% of PP matrix with a range of 20-40% reinforcement, enhanced the mechanical properties. The tensile stress of hemp strand composites is comparable to glass fiber as shown in Figure 2.14 which might have the potential to replace glass fiber.

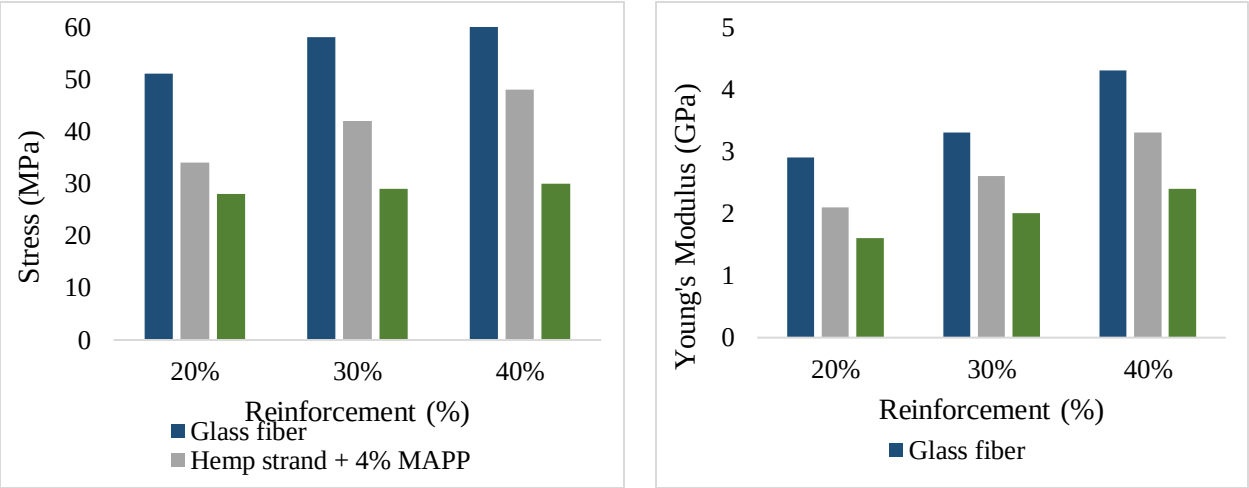

Figure 2.15. Comparison of hemp strand and glass fiber with MAPP (Mutje et al., 2007).

Wambua et al. and Zampaloni compared the mechanical properties of natural fiber/PP composites and found the potential of hemp to replace glass fibers. Wambua used natural fibers like kenaf, coir, sisal, hemp and jute fibers at 40% fiber volume fraction. Hemp fiber composites

show the best mechanical properties including tensile strength and modulus and flexural strength and modulus, all of which are comparable to glass fiber composites.

However, the Charpy impact strength was much lower than glass as shown in Figure 2.16. Conversely, when the specific modulus of various fibers are compared, kenaf was found to be more effective than hemp, flax, and E-glass as shown in Figure 2.17 (Zampaloni, 2007). The density of natural fiber is lower than glass which leads to the fact that the specific properties of natural fibers such as hemp, kenaf, jute, flax, and sisal have comparable strength/weight ratios with composite from synthetic reinforcements (Mohanty et al., 2000).

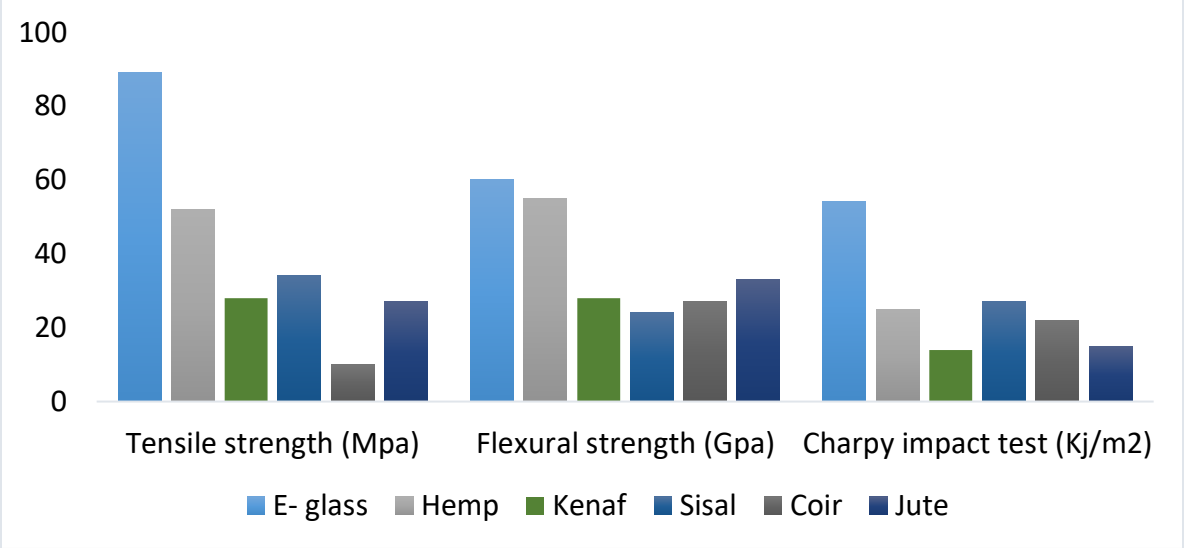

Figure 2.16. Comparison of flexural/ Tensile strength and Charpy impact of natural fiber composites (Wambua et al.,).

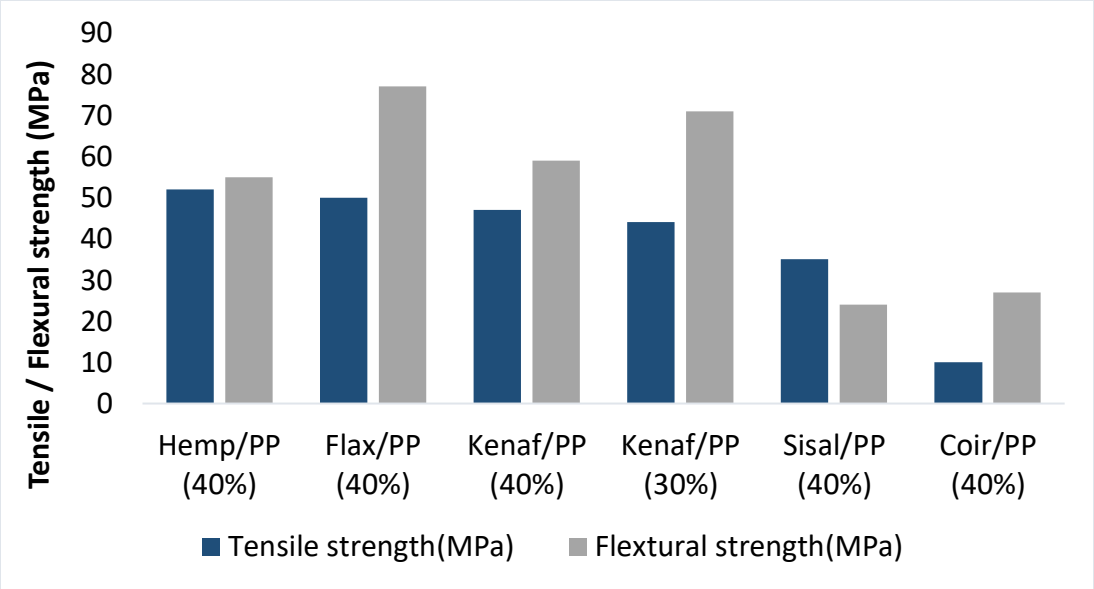

Figure 2.17. Comparison of flexural/ Tensile strength of natural fiber composites with PLA (Zampaloni, 2007).

Zampaloni also found that specific modulus and modulus of composites from natural fibers per cost was superior to their counter parts from glass fibers. High specific modulus materials are used where minimum structural weight is required like aerospace.

Aziz and Ansell (2004) studied the mechanical properties of natural fiber to understand the effect of alkali treatment. The composites were developed from hemp and kenaf-fiber reinforced with polyester and compared the results of untreated and alkali treatment. The composites from alkali treatment exhibited superior flexural strength and flexural modulus values compared to untreated fiber composites. The improvement in properties was observed for short, long, and random mat fibers. The flexural stiffness of alkali treated composites was comparable to the glass fiber. However, it is worth noting that natural fiber used is in fiber mat form stacked in multiple layers and then compression molded. 3D orthogonal fabric will provide a better structure and will also eliminate the possibility of delamination. Even though resin impregnation might be challenging, the mechanical properties might be more promising.

Richardson and Zhang observed the effects of nonwoven hemp on mechanical properties of phenolic. Presence of non-woven hemp in phenolic increased the flexural strength and modulus in phenolic along with impact toughness. The study concludes that non-woven hemp is

tougher and stronger mechanically than the phenolic matrix and thereby increases the mechanical properties overall. Another factor which contributes to the enhanced mechanical properties is that non-woven hemp has the capability of reducing void or defect areas in the composite. However, it fails to explain the role of hemp in other kinds of resins and preform structures.

2.8. Chemical treatment of hemp

The alkalization treatment of fibers helps in improving the chemical bonding between the resin and fiber positively affecting the mechanical properties of the composites. Impact strength (Izod impact) shows that hemp laminate has the highest impact strength compared to E-glass as illustrated in Figure 2.18 (Samuel, Agbo, & Adekanye, 2012).

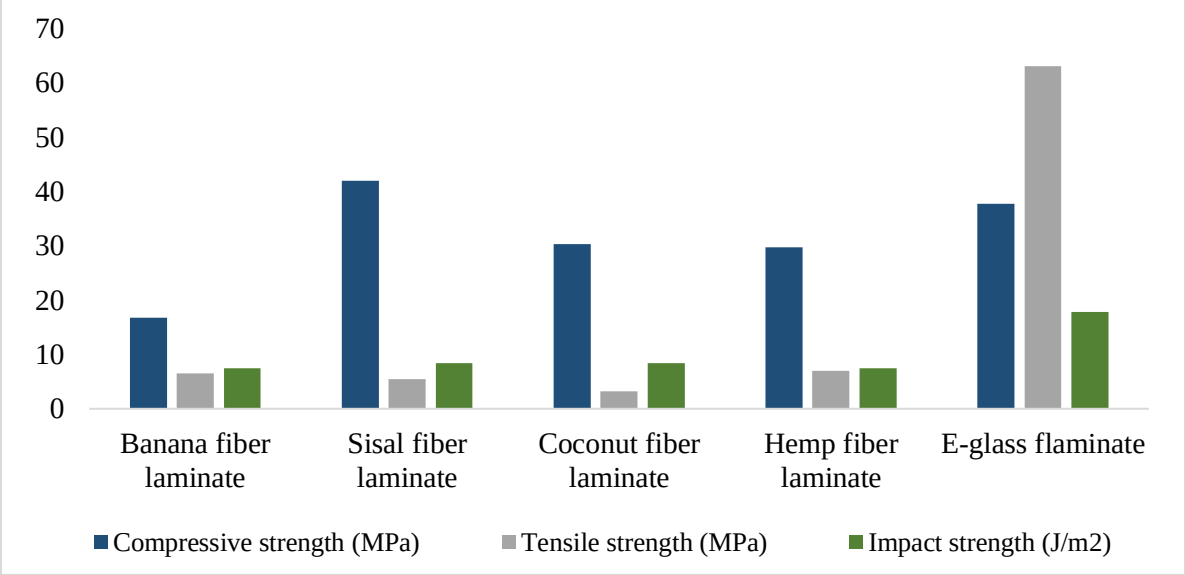

Figure 2.18. Impact strength of alkalized treatment of natural fiber reinforced laminate samples (Samuel et al., 2012).

Surface treatment like alkaline treatment with sodium hydroxide has been used to improve interfacial adhesion between reinforcement and matrix. Successful removal of lignin, hemicellulose and other non-cellulose from fiber surface using alkali treatment dictates the short and long-term compatibility of natural fibers with a polymer matrix. All these chemical constituents of the natural fiber are sensitive to ultraviolet (UV) radiation and moisture which prevents bonding. These are also responsible for strength, thermal and biological degradation.

(O. Faruk et al., 2014). Out of the various surface treatments methods, the most feasible surface treatment is alkali treatment using sodium hydroxide (NaOH) (Islam, Pickering, & Foreman, 2010). Kenaf fiber treated with NaOH to produce kenaf fiber reinforced PLA composites using film stacking reported a 34% increase of flexural strength, 69% increase of flexural modulus and a 50% increase of impact strength (IS) compared to the composites with untreated kenaf fiber (Huda et al, 2006). Sawpan, Pickering, and Fernyhough, 2011, found Young's modulus and impact strength of short hemp fiber reinforced PLA composites were found to be increased with increased fiber content (10–30 wt.%). PLA can best reinforce with 30 % fiber content. Tensile properties and impact strength of the composites were increased further with fiber treatments (e.g. alkali and silane) which could be due to improved fiber/matrix adhesion and increased Both tensile and flexural strength of Kenaf–PP composites is comparable to 40% by weight flax and hemp polypropylene. The tensile strength is higher and the flexural strength is almost doubled when compared against the coir and sisal. Kenaf fiber shows a higher modulus/cost and a higher specific modulus than sisal, coir, hemp, flax, and E-glass.

However, there are many challenges which comes naturally with natural fibers specifically such as lack of interfacial bonding between reinforcement and resin which directly affects the overall composite performance. Another major issue is with hemp is the hydrophilic nature where the rate is high (8 – 10%) which affects the fiber-matrix bonding (Dhakal, Zhang, & Richardson, 2007). Dhakal et al. studied hemp fibers infused with unsaturated polyester to form HFRUPE (hemp fiber reinforced unsaturated polyester) composites and found that there is a direct relationship of fiber volume fraction and temperature on water absorption. However, when the water temperature is increased, the moisture saturation time (MST) is greatly reduced. The rate of water absorption and the maximum water uptake increases for all HFRUPE composites samples as the fiber volume fraction increases.

CHAPTER 3 - RESEARCH OBJECTIVES

The growing market of hemp in the US is a boost in research areas. By the end of 2018, about 40 states in the US have legalized the growing of hemp. One of the biggest moves by lawmakers in December 2018 came as the Agriculture Improvement Act or the Farm Bill which was signed into law for immediate effect. According to the new law, industrial hemp or *Cannabis sativa L,* and its derivatives was removed from the Controlled Substance Act. More specifically, all plant products that contain less than 0.3 % of the psychoactive drug, Tetrahydrocannabinol (THC), have been made legal. This provides a huge scope of industrial hemp research.

The high negative environmental impact caused by synthetic unsustainable composite materials made with petroleum-based polymeric resins and synthetic fibers (glass, carbon, aramid) has encouraged the development of sustainable natural-fiber reinforced composites to replace those materials predominately in non-structural applications and reduce the carbon footprint overall. Due to increasing pressure from various environmental agencies, the use of conventional fibers and resins from a hazardous chemical used in production need to be substituted with more eco-friendly alternatives. Green composites channelize its application in different sectors like automobile, consumer's goods, electrical and electronics, construction, etc. Composites from natural fiber reinforcement offer a sustainable alternative to a wide range of the current composite market. In the current scenario, natural fiber composite finds usage in the automotive industry both internal and external parts including doors and trunk. With the enforcement of the End of Life Vehicle (ELV) and Waste Electrical and Electronic equipment (WEEE), industries will adopt more green composites in manufacturing.

The production of synthetic fibers like glass, carbon, and aramid have high energy consumption as well as major degradable issues. Similarly, polymer resins like epoxy and vinyl ester, which are mostly used in high-performance composites are petroleum based, which are struggling to tackle the depleting quantities. However, the biodegradability of any thermoset resin is a major issue, even though it is from a plant-based resource. As a result, this research aims at only replacing synthetic reinforcement with natural-fiber reinforcement.

This research will familiarize the development of 100% hemp-fiber reinforced composites using 3D orthogonal weaving (3DOW) to form preforms. This work will aim at producing different 3D woven fabric structure and testing mechanical performance. Due to the versatility of 3DOW, different types of woven structures can be produced by altering any of its structural parameters. Any change in warp and filling or weft yarn pattern, Z to Y ratio, weave factors, and yarn linear density produces a new woven structure. The use of 3D orthogonal weaving technology instead of the traditional 2D weaving or loose webs, which most of the previous research focused on, will be advantageous. This novel process of producing woven fabrics from 3D technology has many advantages like crimpless interlacing of yarns, which has positive effects on composite performance. 3D weaving technology has increased the capacity to withstand multidirectional stress and eliminate delamination. There is also no restriction in terms of a number of layers or thickness of the fabric. Moreover, the 3D woven fabric is produced by the use of multilayer warp yarns with simultaneous weft yarn insertion all at the same time. All these advantages of 3D weaving contribute to the overall enhancement of the mechanical properties of composites.

In order to understand the effect of moisture in the natural fiber composite, a few samples from the woven preforms were desiccated before resin infusion. In addition to it, a few samples were mercerized to comprehend chemical treatment effect on the final composites' performance. The treated and untreated samples were tested for tensile test, impact test (Tup and Charpy) and compression test. The test results were compared to the test results of glass fiber composite from 3DOW. The aim is to show that green composite has a great potential to substitute conventional glass fiber in various areas including automotive, construction, consumer goods, etc.

The first objective of the research is to produce 3D orthogonal woven structure to form preforms from 100% hemp yarns. Since the main goal of this research is to produce composite made from natural fiber and explore the benefit of hemp in different applications. Secondly, the hemp composites will be tested for their performance characteristics (tensile strength, impact resistance, and compression strength) and compared to those glass fiber composite of similar construction and specifications to prove the possibility of future use of hemp as a substitute for glass fiber. Lastly, this research will also concentrate on understanding and predicting the market

potential of hemp reinforced composites for the US market assuming government legalizing industrial hemp in most of the states.

CHAPTER 4 - EXPERIMENTAL WORK

This section covers the experimental plan of work used in the research to accomplish the objectives. Different hemp yarns were sourced, converted to 3DOW preforms of different architectures, which in turn treated with vinyl ester resin system. The experimental composites were tested and evaluated for their performance characteristics using testing equipment available at the Composite Core Facility in the Wilson College of Textiles. The details of the experimental procedures followed are addressed in the following sections.

4.1. Materials

The materials used in this research is subdivided into two categories. The first category is the hemp fiber and the second category is the resin type.

4.1.1. Fiber

The composite group at NC State Wilson College of Textiles has been working in composites from natural fibers for 10 years for the reason addressed in the Introduction and Literature Review Chapters. Research work completed includes composites from 3DOW preforms from Cotton and resin generated from vinyl ester (80%) and soy-based resin (20%) composites from Tururi fiber sacks and vinyl ester resin. The group is currently conducting research that deals with composites from 3DOW made of flax and hemp fibers. The focus of this research is composites from 3DOW preforms made from hemp yarns. The yarns used for reinforcement is 100% hemp sourced from Hemp traders, California. The US market has a tremendous demand for hemp products and currently, many states have legalized the use of industrial hemp. By creating a natural composite using 100% hemp fiber supplements composite development that can be tailored to industry-specific applications. Hemp fiber also has a high specific modulus and find its application in areas where minimum structural weight is required. The Y-yarn (warp), X-yarn (weft), and Z-yarn have different linear density and specification was used in this research. The details of the yarns are shown in Table 4.1.

Table 4.1. Warp, weft and Z-yarns specifications.

Yarn	Linear density (denier)	Yarn details
X - yarn	1500	long fiber half dry spun yarns
Y - yarn	1059	short fiber open-end yarns
Z - yarn	250	long fiber wet spun semi-bleached

The single yarn diameter was calculated using the following equation based on the yarn (denier), a packing factor of the yarn, and the fiber density. Fiber density is average taken from literature.

$$d(cm) = \frac{4 * Nd}{9000\pi\phi\rho_f * 1000} * 100$$

d = diameter of yarn (cm)

N_d = Yarn number (denier)

ϕ = Yarn packing factor

ρ_f = Fiber density (kg/m^3)

The average diameters of the single yarns are reported in table 4.2 based on the equation and average packing factor of approximately 0.65 and fiber density of approximately 1480 kg/m^3. The calculation is shown in Appendix 1.

Table 4.2. Calculation of single yarn diameter of warp, weft, and Z-yarn.

Yarn	Denier of single yarns	Packing Factor (spun yarn)	Fiber density kg/m^3	Single yarn diameter, cm	Denier after doubling
X - yarn	1500	0.65	1480	0.0469	3000
Y - yarn	1059	0.65	1480	0.0395	3177
Z - yarn	250	0.65	1480	0.0192	250

The yarns were doubled without any twist in order to increase the thickness of the yarns. X-yarns were doubled using two sets of yarns whereas y-yarns were doubled using three pair of yarns.

4.1.2. Resin

The matrix used to produce the 3D orthogonal woven composites in this research was an epoxy-based Vinyl ester resin, The DERAKANE® 8084, which was generously donated by Ashland LLC, Ohio. It is compatible with hemp fiber preforms and Vinyl ester resin was selected based on its performance and cost. Vinyl ester has a higher modulus and tensile strength than polyester resins and it is cost-effective than epoxy resins along with comparable modulus and tensile strength as epoxy. Epoxidised vinyl ester resin is a hybrid form of polyester resin which is toughened with epoxy molecules to enhance the performance. Vinyl ester resin has better vibrational load resistance since they are more tolerant of stretching as compared to polyester resins and as a result, demonstrate less stress cracking and better impact resistance. One of the benefits of using vinyl ester is that it cures at room temperature without the need of any additional processing.

Vinyl ester is typically used when high longevity, thermal permanency and high corrosion is a priority. It can be used in various areas like piping, chemical storage tanks, home appliances and marine applications in which corrosion resistance is required. Furthermore, styrene content in the vinyl ester is low as compared to polyester resin making it less harmful in nature. The unsaturated bonds of the vinyl ester oligomers copolymerize with the co-monomer to form a similar cross-linked network to the curing reactions of unsaturated polyesters. Vinyl esters have reactive double bonds at the ends of the chains only thereby creating more controlled crosslink density which in turn enhances corrosion resistance. The ester groups, present in the terminal sites, contribute to the chemical resistance are the most vulnerable part of the resin since they are subject to hydrolysis. Therefore, the damage is only restricted to these terminal sites leaving the majority of the backbone of the molecule unaffected.

The Vinylester resin has good interfacial adhesion with the fibers, due to the OH groups present in the epoxy-based vinyl ester which increases the interfacial bonding between the reinforcement and matrix to improve the overall strength of the composite. In the cross-linking

stage, vinyl ester converts into gel form and helps all the double bonds to react at the end of the curing process. This helps in a uniform glass transition (Tg) throughout the composite panel. Typical properties of the DERAKANE® 8084 epoxy based and elastomer modified Vinylester resin are listed in Table 4.3, while the typical properties of the post-cured resin are listed in Table 4.4.

Table 4.3. Typical liquid resin properties of Derakane® 8084 (Ashland chemicals, 2006).

Property	**Value**
Density, 25 °C	1.02 g/mL
Dynamic Viscosity, 25 °C	360 mPa·s (cP)
Kinematic Viscosity	350 CST
Styrene Content	40%
Shelf Life, Dark, 25 C °6 months	6 months

Table 4.4. Typical properties of post-cured Derakane® 8084 resin clear casting (Ashland chemicals, 2006).

Property	**Value**	**Test Method**
Tensile Strength	76 Mpa	ASTM D -638 / ISO 527
Tensile Modulus	2.9 Gpa	ASTM D -638 / ISO 527
Tensile Elongation, Yield	8-10 %	ASTM D -638 / ISO 527
Flexural Strength	130 Mpa	ASTM D - 790 / ISO 178
Flexural Modulus	3.3 Gpa	ASTM D - 790 / ISO 178
Density	1.14 g/cm^3	ASTM D - 792 / ISO 1183
Volume Shrinkage	8.2%	
Heat Distortion Temperature	82°C	ASTM D - 648 Method A / ISO 75
Glass Transition Temperature, Tg2	115°C	ASTM D - 3419 / ISO 11359-2
IZOD Impact (unnotched)	480 J/m	ASTM D - 256
Barcol	30	ASTM D - 2583 / EN59

Vinyl ester is a four-part resin system including vinyl ester, and MEKP, CoNap, and DMA as curing agents which acts as initiator, promoter, and accelerator, respectively. The gelation time of the resin system can be controlled by changing the proportion of these curing agents. Gelation time is the time interval where the resin system converts from a liquid state to a solid material with the highly cross-linked polymer. At this stage, polymer cross-linking is in its early stage and any disturbance in the gel state might negatively impact the final product. The aim of this stage is to infiltrate the resin inside the reinforcement by wetting it at the fiber level during consolidation.

Gel time is an important parameter in deciding the resin for the composite. The viscosity of the resin determines the gel time. During infusion, polymers present in the resin change from liquid to gel state before solidifying. If the complete transition is too quick, the resin does not saturate the fabric completely which results in low resin penetration. Similarly, if the resin has a long gel time, it slows down the whole process by increasing the production time. So, it is very important to choose an optimum gel time for maximum efficiency to consolidate the composite panel. Table 4.5 lists the typical gelation times of Derakane® 8084 at different temperatures and the corresponding amount of MEKP-925H (initiator), Cobalt Naphtenate-6% (promoter) and DMA (accelerator). DMA was not used as a component of the resin system as it speeds up the chemical reaction which results in curing the resin during degassing. After multiple attempts, the decision to discontinue DMA was made without compromising the integrity of the resin system. The temperature where the resin infusion process takes place is almost 24°C, and the time required to degas the resin and complete a resin infusion cycle was almost 45-60 minutes. The recommended proportion of component provided by Ashland LLC, is illustrated in Table 4.5 along with the highlighted proportion used in this research.

Table 4.5. Typical gel times for Derakane® 8084 Resin (Ashland chemicals, 2006).

Temperature	Auxiliary Curing Chemicals	Gel Time of Resin		
		15 ±5 Minutes	30 ±10 Minutes	60 ±15 Minutes
18^{0}C	MEKP (Initiator), wt.%	3.0	3.0	2.5
	CoNap6% (Promoter) , wt.%	0.6	0.4	0.4
	DMA (Accelerator) , wt.%	0.3	0.2	0.1
24^{0}C	MEKP (Initiator), wt.%	2.0	2.0	1.5
	CoNap6% (Promoter) , wt.%	0.5	0.4	0.3
	DMA (Accelerator) , wt.%	0.3	0.2	0.05
30^{0}C	MEKP (Initiator), wt.%	2.0	1.5	1.5
	CoNap6% (Promoter) , wt.%	0.3	0.3	0.3
	DMA (Accelerator) , wt.%	0.2	0.05	0.025

4.2. Design of experiment

Experimental plan was designed in order to achieve the research objectives. Experimental design A was structured to achieve the research objectives namely

1) To study the mechanical properties of the 3D orthogonal woven composites based on various parameters, namely thickness, weave pattern and Z to Y ratio,

2) To study the behavior of different architecture under a variety of mechanical tests like Tensile, Impact, and Compression and also corroborate the correlation between Tup and Charpy impact responses.

The main experimental design A was further subdivided into two categories, A1 and A2. The objective of the design of experiment A1 was to study the behavior of moisture on 3D orthogonal woven composites whereas A2 was designed to study the effect of chemical treatment on 3D orthogonal woven composites.

4.2.1. Design of experiment A

The experimental design was prudently structured in order to achieve the objectives of the research which was to understand how the architectural variables affect the tensile, impact and compression resistance of the composites from 3DOW preforms formed from hemp and compare the results with glass fiber composites with similar construction. There were three architectural variables that were altered in the research.

(1) Number of Y-yarn layers,

(2) Number of Z-yarn/Y-yarn ratio (referred to as Z to Y or Z:Y for short), and

(3) Weave structure.

The number of Y-yarn layers controls the thickness, which affects the overall composite architecture and resin impregnation. The ratio of Z to Y sequence was changed in order to study Z-yarns contribution to the overall structure. The design was carefully planned to systematically reduce the Z-yarns percentage from the maximum interlacement of 1:1 to half, which is 1:2 and then was further reduced to 1:3 ratio. The weave structures used in the experiment were plain, 2x2 warp rib and 3x3 warp rib to understand how the float length influence on the performance of the resultant composites. The design of the experiment is shown in table 4.6 with different variables.

Table 4.6. Design of Experiment A

Variables	**Values**	**Levels**
No. of layers	3,6,9	3
Z to Y sequence	1:1, 1:2, 1:3	3
Weaves	Plain ,2x2 warp rib, 3x3 warp rib	3
Total no. of runs	3x3x3	27

Pick density, which is a number of X-yarns /inch/layer, was calculated using the linear densities and number of layers of X-yarns and Y- yarns. The calculation was done based on balanced structure (the total denier/unit length of X-yarns = the total denier/unit width of Y-yarns) since balanced construction tends to have a better interlaminar performance than the

unbalanced ones (Ince, 2013). Table 4.7 demonstrates the pick density calculation for different layers. The details of the calculation are shown in Appendix 2. The weft insertion is two yarns per insertion

Table 4.7. Pick density calculation in terms of X & Y layers.

No. of layers (X)	No. of layers (Y)	Pick density (no. of X-yarns/inch/layer)	Pick density per insertion
4	3	5.14	10.28
7	6	5.88	11.76
10	9	6.17	12.34

4.2.2. Design of experiment A1

Additionally, the above design of the experiment was extended to two subcategories, A1 and A2, to understand the effect of moisture and alkali treatment respectively. In order to understand the optimal effect of moisture, the samples were dried to drive the moisture out. The samples were prepared keeping layers and Z to Y ratio constant and altering the weave to understand effect of weave on treated samples. A total of three samples were chosen to study the moisture effect as depicted in Table 4.8. Samples for the mechanical characterization were cut from the manufactured composite panels, dried at 122°F for 24 hours to ensure the removal of any induced moisture and immediately infused with resin.

Table 4.8. Effect of moisture on the mechanical properties - Experimental design A1.

Sample ID	Variables	Values	Levels
10M	No. of layers	6	1
11M	Z to Y sequence	1:1	1
12M	Weaves	Plain, 2x2 warp rib, 3x3 warp rib	3

4.2.3. Design of experiment A2

In order to understand the effect of chemical treatment, three samples were treated with Sodium hydroxide. The effect of chemical treatment was to improve fiber dispersion and induce strong bonding of matrix and reinforcement by increasing the number of reactive sites on the fiber surface. Previous research indicated that composites made out of chemically treated fibers have improved properties including better interfacial bonding, a decrease in moisture absorption and an increase in fiber crystallinity. It was important to maintain an optimum temperature during the treatment, which was 70°F ±2, as natural fiber cannot withstand high temperature. The similar set of samples was used as in case of the design of experiment A1 in order to compare untreated samples with desiccated and chemically treated samples. A total of three samples were chosen to study the chemical treatment effect and the mechanical properties of the composite as depicted in Table 4.9.

Alkali solution was prepared by dissolving Sodium Hydroxide (NaOH) in water at room temperature. The liquor ratio of 20:1 by weight was maintained. The samples of the 3DOW preforms were soaked in the alkali solution for 1 hour and were left untouched. After an hour, the samples were washed in room temperature water for multiple times to neutralize and remove all the excess solution from the samples. The samples were exposed to minimize distortion to maintain structural integrity. The samples were then washed in 1% acetic acid to remove any alkali solution left in the samples. After removing the excess solution, the samples were placed on a clean, dry towel to remove excess water dripping from the samples. The samples were then dried in an oven at 122°F for 24 hours and then immediately infused with the vinyl ester.

Table 4.9. Effect of chemical treatment on the mechanical properties - Experiment design A2.

Sample ID	**Variables**	**Values**	**Levels**
10C	No. of layers	6	1
11C	Z to Y sequence	1:1	1
12C	Weaves	Plain, 2x2 warp rib, 3x3 warp rib	3

4.3. Preforms Formation

Preforms were woven using 3D weaving machine, shown in Figure 4.2, which was donated by 3TEX Inc. and was available at the core composite facility in the Wilson College of Textiles, NC State University. The loom has two sets of creel (shown in Figure 4.1) to directly supply Y-yarns and Z-yarns. The Z-yarns packages were intentionally placed in the middle to have uniform tension throughout. The creel has the capacity to hold up to 1088 packages. For weft insertion, another small creel was used to hold the weft yarn packages at the insertion side. This 3D loom utilizes single rigid rapiers and inserts multiple X-yarns simultaneously depending on the number of Y-layers 3D weaving machine is illustrated in Figure 4.3. The unique rapier insertion mechanism results in a double insertion/shed of the X-yarns during each insertion cycle, and also results in a continuous X-yarn.

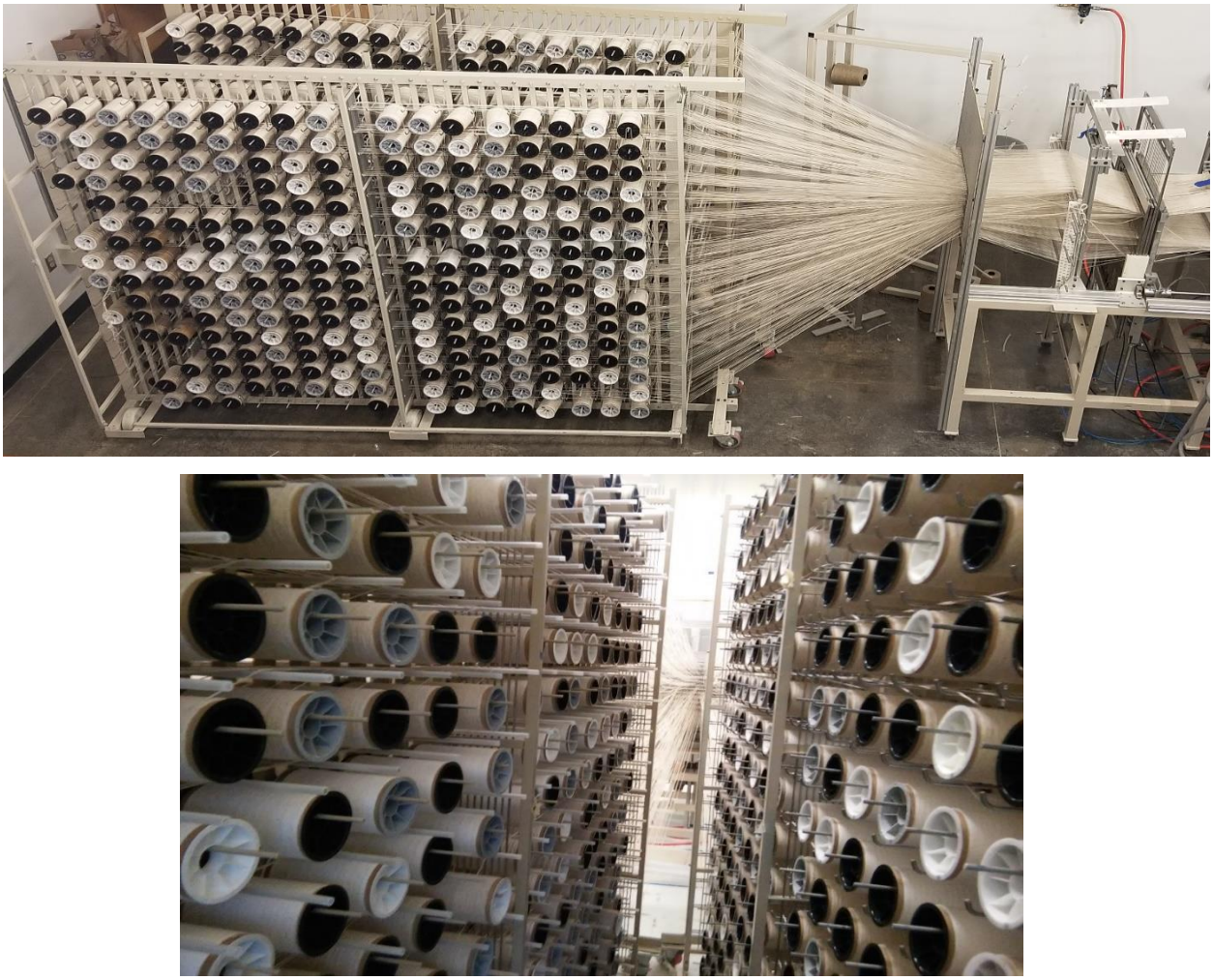

Figure 4.1. Creel with hemp yarn packages in the 3D machine NC State University

Figure 4.2. Weaving loom at Wilson College of Textiles, NC State University.

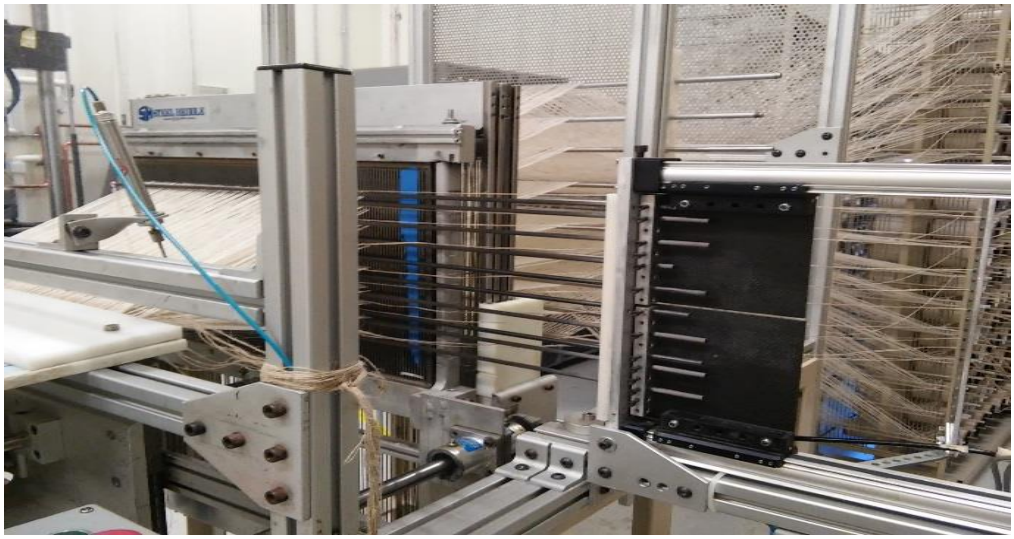

Figure 4.3. Rapier weft insertion in the 3D weaving loom.

Every warp layer consisted of 102 Y-yarns, which were spaced evenly using a reed with a dent density of 2.36 dents/cm (6 dents/inch), where each Y-yarn in a layer was placed in a dent. Correspondingly, the total number of Z-yarns were 102 for full Z-yarns interlacement in which the Z-yarns to Y-yarns ratio is 1:1, and in this case every Z-binders yarn end was threaded through an eye of a heddle wire attached in a harness. The width of the preform was about 40 cm. The loom includes four harnesses to be able to form the weaves required. In order to weave plain, 2x2 warp rib and 3x3 warp rib, all the harnesses were used due to the limited heddles in

each harness. 2x2 warp rib and 3x3 warp rib are similar to plain weave with longer floats. In order to create a different weave pattern, the software was coded individually. The machine comes with a very simple and easy to use software where the user feeds in two inputs namely X-yarn density and weave type. Figure 4.4 shows woven preform samples made by using 3D weaving loom.

Figure 4.4. Woven samples (preform) made from hemp yarns using the 3D loom.

4.4. Denting plan

The denting plan for this research was based on the Z to Y ratio in the weave. According to the experimental design, the amount of Z-yarn was reduced systematically in order to understand Z to Y ratio to the overall structure properties and integrity of the samples. Figure 4.5 below shows the schematic denting plan for 1:1, 1:2 and 1:3 ratio. For ratio, 1:1, there was one Z-yarn for every Y-yarn/layer as demonstrated in Figure 4.6. In the next step, alternate Z-yarns were removed to weave with a 1:2 ratio preform where there is one Z-yarn for every two Y-yarns/layer. Likewise, in a 1:3 ratio, there is one Z-yarn for every three y-yarns/layer. For every ratio, software coding was modified to weave the desired structure. For 1:3 sequence, all the Z-yarns were re-drawn through heddle wires and then methodically removed from heddle wire leaving one yarn intact out of three.

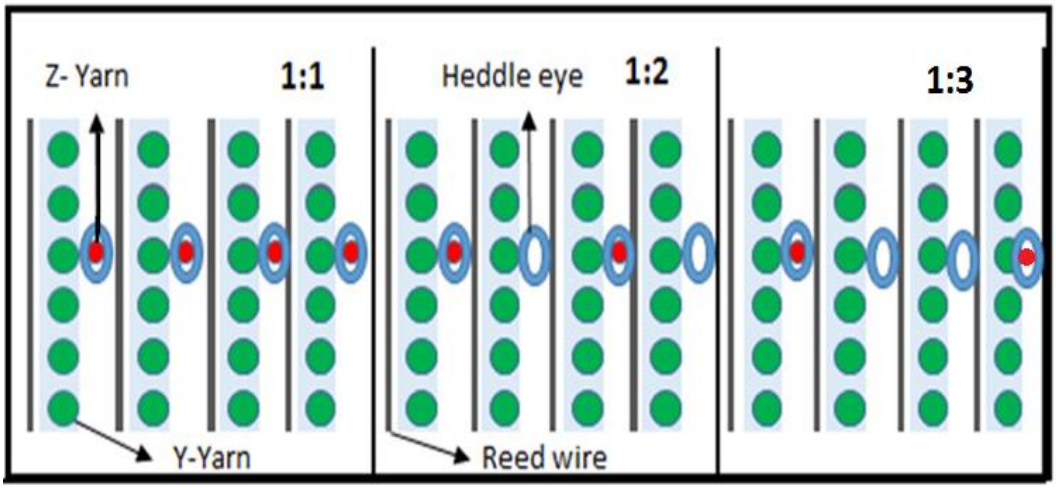

Figure 4.5. Denting plan for a six layers preform with various Z to Y ratios.

Figure 4.6. Weave showing 1:1 ratio in a 2x2 warp rib weave for a 9 layer preform

4.5. Fiber volume fraction (FVF) calculation

The fiber volume fraction is a vital element in composite engineering. FVF is calculated to determine the fiber contribution in the overall structure. While developing a composite, the fiber was impregnated with vinyl ester by using VARTM. Resin contribution to fiber ratio was calculated by the geometric organization of the fibers, as seen in the cross-section of the composite, in the overall structure which in turn determines the amount of resin permeability. The impregnation around the fibers is highly dependent on fiber orientation and compactness. The resin usually concentrates in the areas where there are gaps making it resin rich areas and

can be found throughout the structure. The fraction of fiber reinforcement is central to the overall mechanical properties transferred in the composite. The higher the fiber volume fraction typically results in better mechanical properties of the composites.

4.5.1. Theoretical FVF calculation

For fiber volume calculation of each of the yarns (X, Y, and Z) in the preform was calculated assuming the yarns have a circular cross-section. The equations below were used to calculate an individual set of yarns separately and added together to derive FVF of the sample. The nomenclature for FVF calculation is stated in Appendix 3. On the other hand, the matrix component volume fraction in a specific direction can be calculated by simply subtracting the sum of the yarns volume fractions in this direction from unity, assuming no voids in the structure.

4.5.2. Experimental Determination of FVF

For the experimental calculation, the volume of each sample was measured using a density kit available at the Composite Core Facility, Wilson College of Textiles, NCSU. The specimen (8mm x 8mm) were cut in order to fit the small beaker provided in the density kit. Five specimens from each sample were individually weighed and recorded in water and air to calculate average specific density for each sample and the average value was calculated. The weight of the preforms and composite panels was used to calculate the volume. The volume of the preform (V_f) was calculated using preform weight and density of hemp fiber (1.5 g/cm^3). Composite volume (V_c) was calculated using composite panel weight and average composite specimen weight. Fiber volume fraction was calculated using the formula below.

$$FVF = (\mathrm{Vf}/\mathrm{Vc})*100$$

4.5.3. Comparison between theoretical and experimental FVF calculation

The difference between theoretical and experimental FVF calculation is shown in Table 4.10. The inconsistency is because of the uneven nature of the preform formation during weaving.

Table 4.10. Theoretical and experimental FVF of samples (Experiment A).

Sample ID	No. of Y-layers	Weave	Ratio (Z to Y)	X-yarns density (picks/inch/layer)	Theoretical FVF	Experimental FVF
1	3	Plain	1:1	5.14	11.43	13.90
2	3	2x2 Warp rib	1:1	5.14	11.43	14.83
3	3	3x3 Warp rib	1:1	5.14	11.43	13.56
4	3	Plain	1:2	5.14	11.43	14.36
5	3	2x2 Warp rib	1:2	5.14	11.43	14.96
6	3	3x3 Warp rib	1:2	5.14	11.43	15.00
7	3	Plain	1:3	5.14	11.42	13.22
8	3	2x2 Warp rib	1:3	5.14	11.42	13.71
9	3	3x3 Warp rib	1:3	5.14	11.42	14.33
10	6	Plain	1:1	5.88	11.90	17.99
11	6	2x2 Warp rib	1:1	5.88	11.90	20.13
12	6	3x3 Warp rib	1:1	5.88	11.90	20.07
13	6	Plain	1:2	5.88	11.90	20.44
14	6	2x2 Warp rib	1:2	5.88	11.90	18.97
15	6	3x3 Warp rib	1:2	5.88	11.90	20.35
16	6	Plain	1:3	5.88	11.90	19.40
17	6	2x2 Warp rib	1:3	5.88	11.90	19.27
18	6	3x3 Warp rib	1:3	5.88	11.90	18.24
19	9	Plain	1:1	6.17	12.09	22.24
20	9	2x2 Warp rib	1:1	6.17	12.09	24.70
21	9	3x3 Warp rib	1:1	6.17	12.09	24.97
22	9	Plain	1:2	6.17	12.09	25.39
23	9	2x2 Warp rib	1:2	6.17	12.09	23.41
24	9	3x3 Warp rib	1:2	6.17	12.09	26.38
25	9	Plain	1:3	6.17	12.08	24.63
26	9	2x2 Warp rib	1:3	6.17	12.08	25.27
27	9	3x3 Warp rib	1:3	6.17	12.08	24.63

4.6. Resin Infusion

After weaving the 3D preforms, each preform was impregnated with vinyl ester resin using a vacuum assisted resin transfer molding technique (VARTM). The VARTM was performed using a VacMobiles® 20/2 vacuum system which is available at the composite core facility, Wilson College of Textiles, NCSU.

Each woven preform was cut into two halves for easy handling and quick uniform infusion. Each preform panel measured about 50 cm by 40 cm after cutting. The width of the preforms was selected as the resin flow direction as shown in Figure 4.7 and 4.8.
The preform was first placed on a release film for easy removal from the glass top table. Next peel ply (polyester fabric) was laid over the preform followed by the mesh fabric for uniform resin distribution across the length and thickness. Resin inlet and outlet tubes are placed and sealed lengthwise to make it airtight. The last layer of nylon bagging film was used to seal the entire set-up using double sided tacky tape. Once the assembly is complete, the resin outlet was connected to the vacuum pump, and the resin inlet was connected to pressure gauge, to check for any vacuum leakage, using an ultrasonic leak detector.

The different component of resin including DERAKANE® Epoxy Vinyl Ester Resins, Cobalt Naphthenate6% and Methyl Ethyl Ketone Peroxide (MEKP) were mixed together in a bucket covered with release film from the inside in the ratio mentioned in Table 4.5. The resin was mixed very carefully under the fume hood and then transferred and placed in the degassing chamber for about 20 minutes to remove all the bubbles and decrease the chance of injecting in the composites.

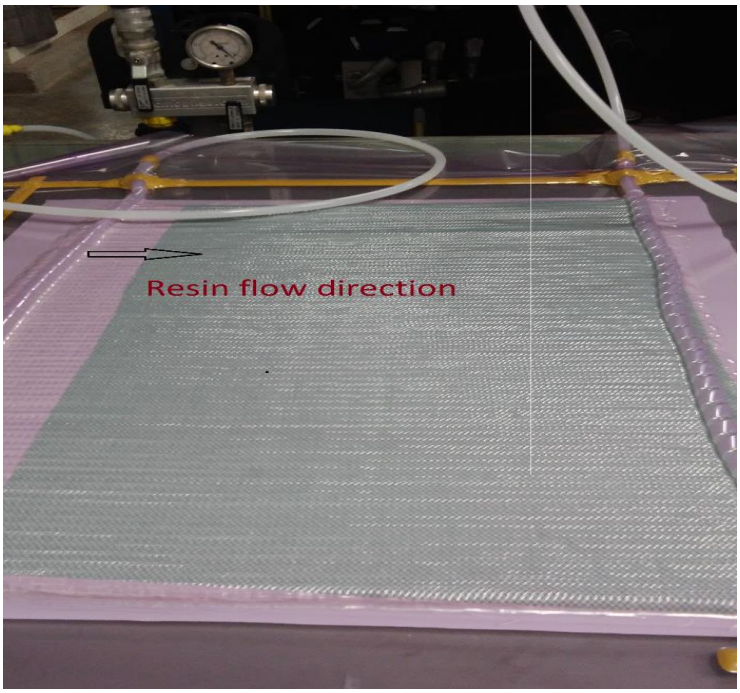

Figure 4.7. Before infusion (dry preform).

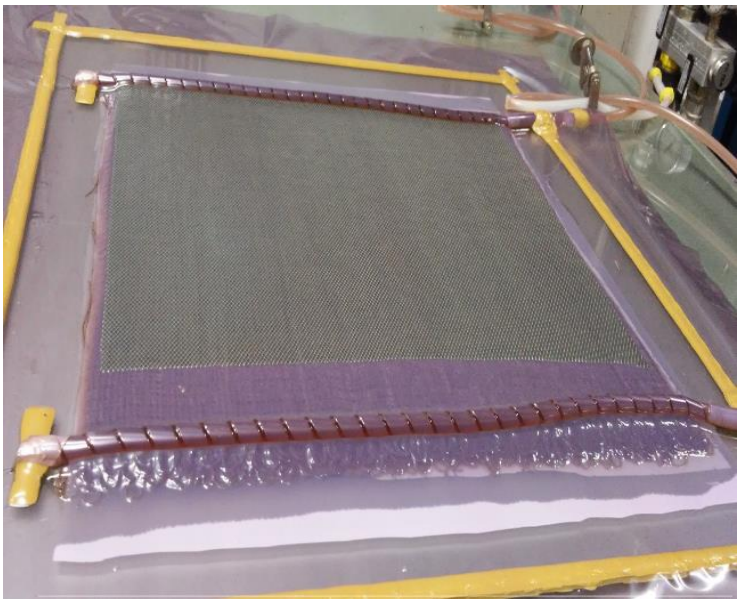

Figure 4.8. Preform after infusion.

4.7. Thickness

The thickness of the individual specimen from the 3DOW composite samples related to all the mechanical test was each measure five times to get an average thickness which is more representative of the overall thickness. The thickness was measured by using Vernier Caliper, shown below, available at the Composite Core Facility, Wilson College of Textiles.

4.8. Sampling

The sampling plan was developed to cut representative specimens from each panel. The test specimens conform to dimensions and geometry specified by ASTM standards. The main purpose of this plan was to have a better representation of the composite panel by testing at least 5 specimens for each test required by the ASTM standards. The average dimension of each sample panel was 46 cm x 36 cm. The layout is specifically designed to utilize the maximum available panel as shown in Figure 4.9. All the specimens were systematically marked for specimen identification as illustrated in Figure 4.10.

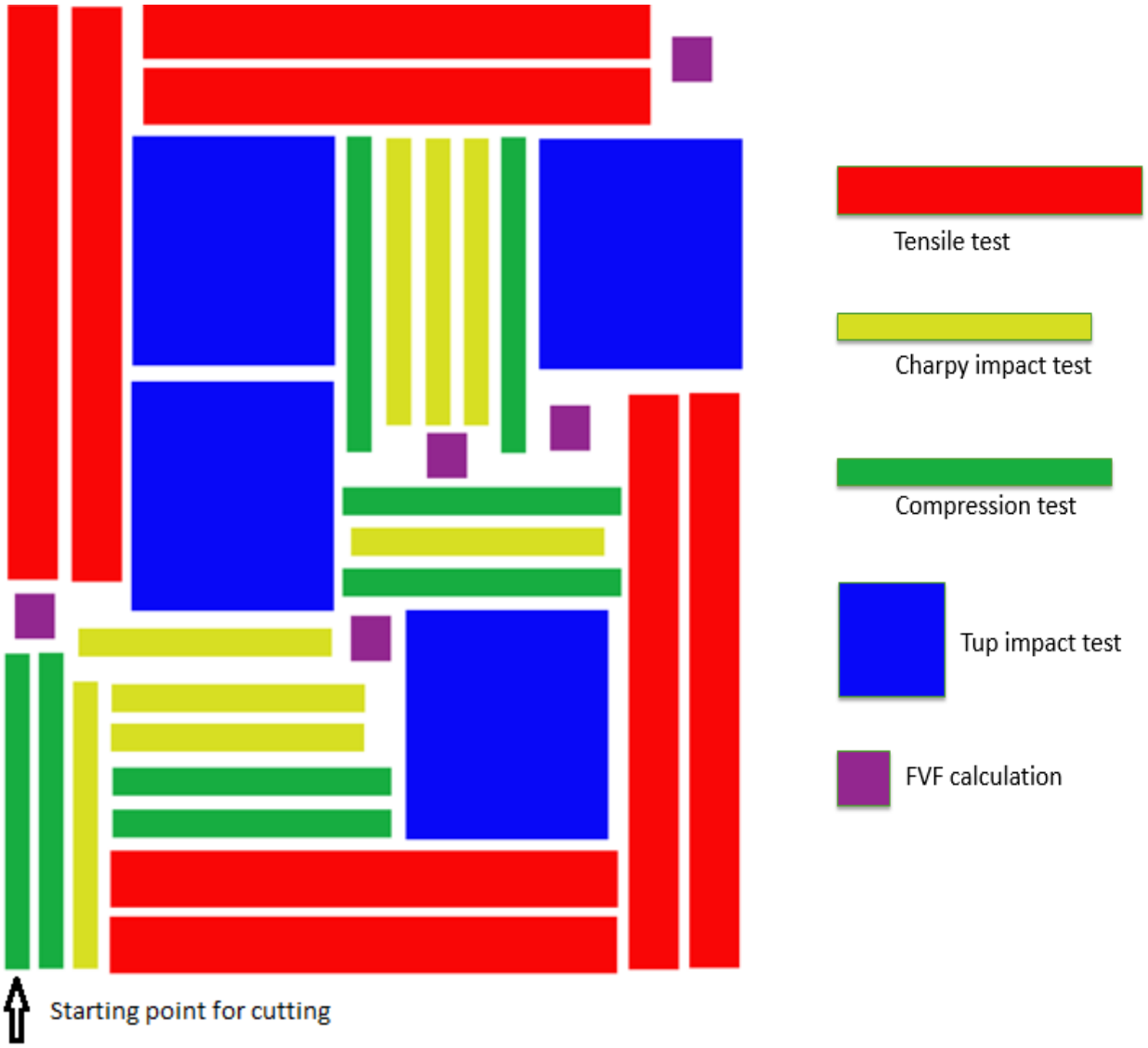

Figure 4.9. Cutting plan for non-treated samples.

(a)

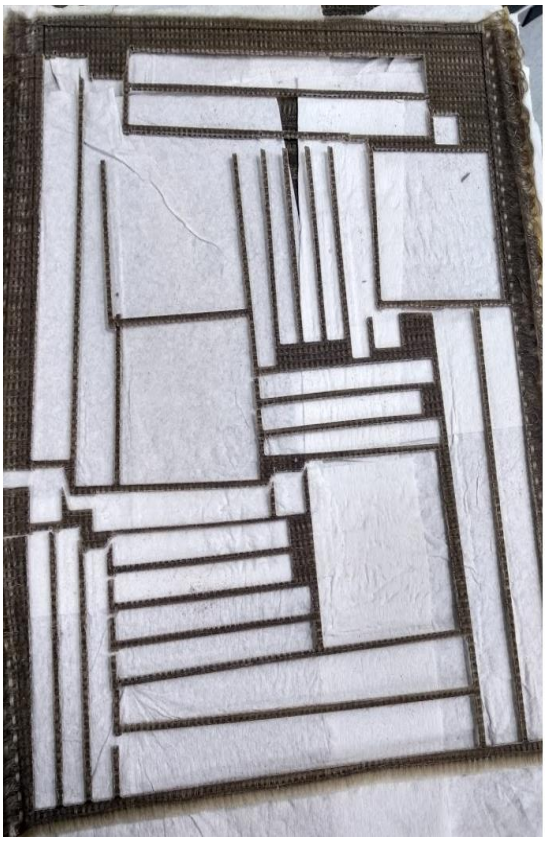

(b)

Figure 4.10. (a)After the samples cutting. (b) Leftover samples after specimens removal.

All non-treated specimens were cut using computerized waterjet cutting technology available at ADR Hydro-Cut, Inc., Morrisville, NC. The cutting plan was drawn using Adobe Illustrator and saved in DXf format to be used in the computerized machine. The waterjet cutting is very precise in nature and cut specimens exactly as specified. It has a very low coefficient of variation (less than 0.1%), and it doesn't cause any thermal induced damages or delamination to the composites, which are very common with the conventional CNC cutting.

However, the desiccated samples and chemical treated samples used a different cutting plan (shown in Figure 4.11) due to shrinkage of the preform during chemical treatment. The "X" mark on the image below is the starting point for cutting the panels.

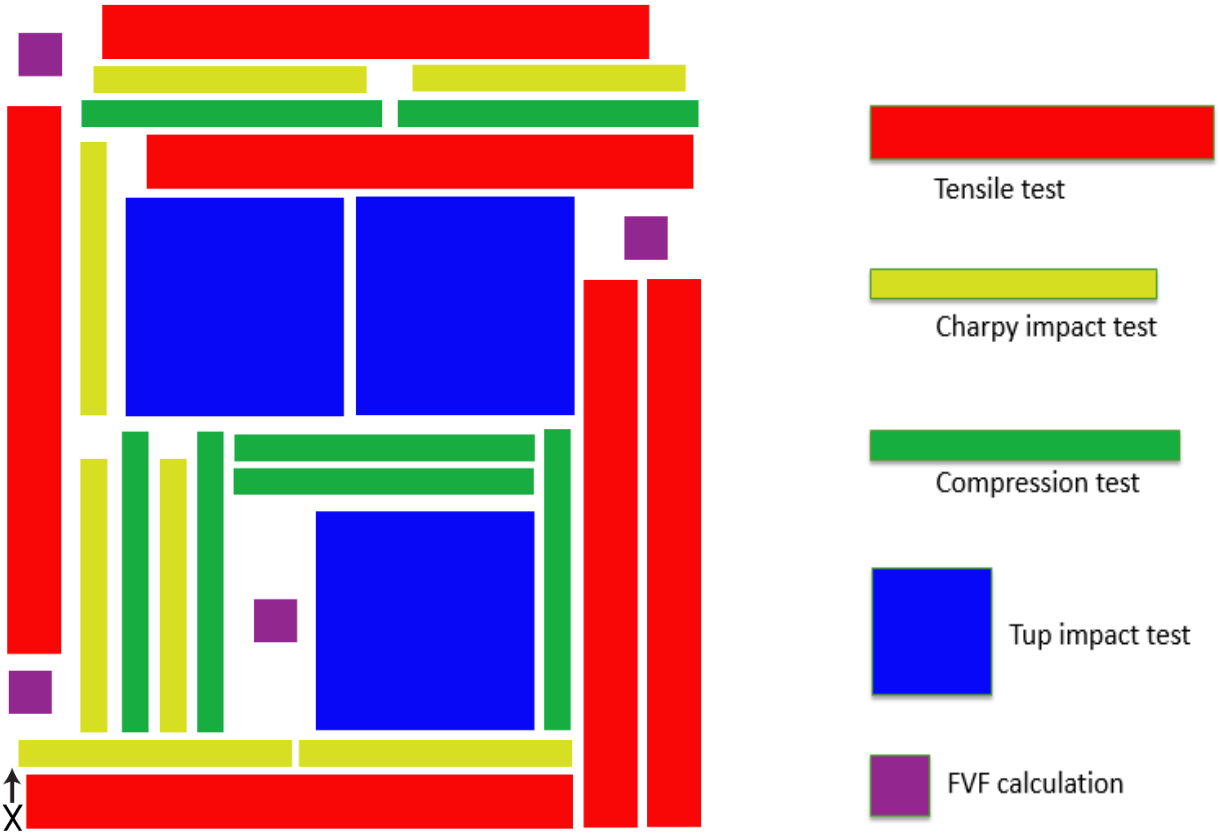

Figure 4.11. Cutting plan for desiccated and chemically treated samples.

4.9. Testing and Evaluation

In this research, various mechanical tests were conducted in order to determine the mechanical properties of composites. Tensile, Tup impact, Charpy and compression tests were conducted. The standard testing procedures along with the equipment being used are listed in Table 4.11. All equipment located in the composite core facility at the Wilson College of Textiles, NCSU.

Table 4.11. List of mechanical tests on final composite structures.

Test name	**Standard**	**Equipment**	**Figure reference**
Tensile strength Test	ASTM-D3039 Tensile Properties of Polymer Matrix Composite Materials	MTS Servo-hydraulic 370 load frame	4.12
Tup Impact Test	ASTM D3763: High-Speed Puncture Properties of Plastics Using Load and Displacement Sensors	Instron Drop Tower Impact CEAST 9350	4.13 (a)
Charpy Impact Test	ASTM D6110 Standard Test Method for Determining the Charpy Impact Resistance of Notched Specimens of Plastics	Instron Pendulum Impactor II	4.13 (b)
Compression Test	D6641 Standard Test Method for Compression Properties of Polymer Matrix Composite Materials Using a Combined Loading	MTS Servo-hydraulic 370 load frame	4.12

Figure 4.12. MTS Servo-hydraulic 370 load frame for tensile and compression test.

(a) (b)

Figure 4.13. Instron impact testing equipment, (a) drop tower impact CEAST 9350, and (b) pendulum impactor II.

4.9.1. Tensile test

MTS Servo-hydraulic 370 load frame was used, which is located at the Composite Core Facility, Wilson College of Textiles, NC State University, for testing the tensile properties of the composites. The tensile test was performed according to the ASTM D-3039, which is a standard test method for tensile properties of polymer matrix composite materials. As specified by ASTM, five specimens were tested from both warp and weft direction. The specimens were 250 mm x 25 mm (10 x 1 inch). The testing device has a 250 kN load capacity. In order to find the optimum grip pressure, grip length and gauge length, several trials were performed to make sure that the failure occurs within the gauge length area. The selected grip pressure was 2000 psi while the crosshead speed was 1 mm/min. The optimum grip length was 50 mm, and the gauge length was 152.4 mm. These parameters were optimum to restrain slippage and avoid crushing without the need for using end tabs. The test results of the tensile test both in warp and weft directions is illustrated in figure 4.14 and 4.15, respectively.

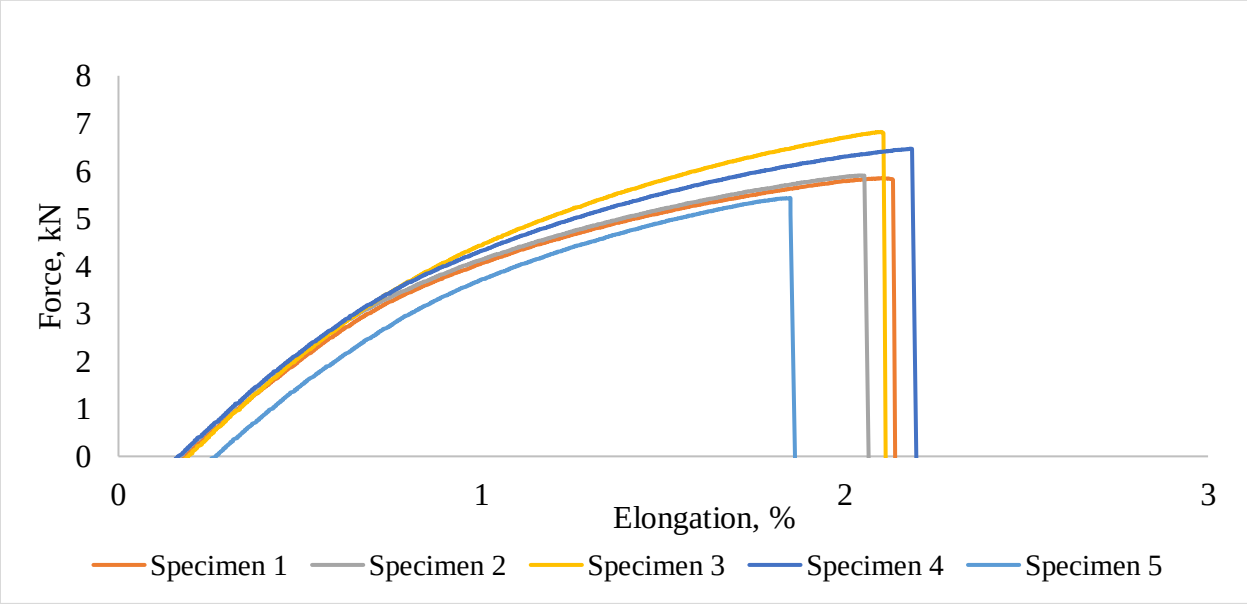

Figure 4.14. Typical graphs of the tensile test in the warp direction.

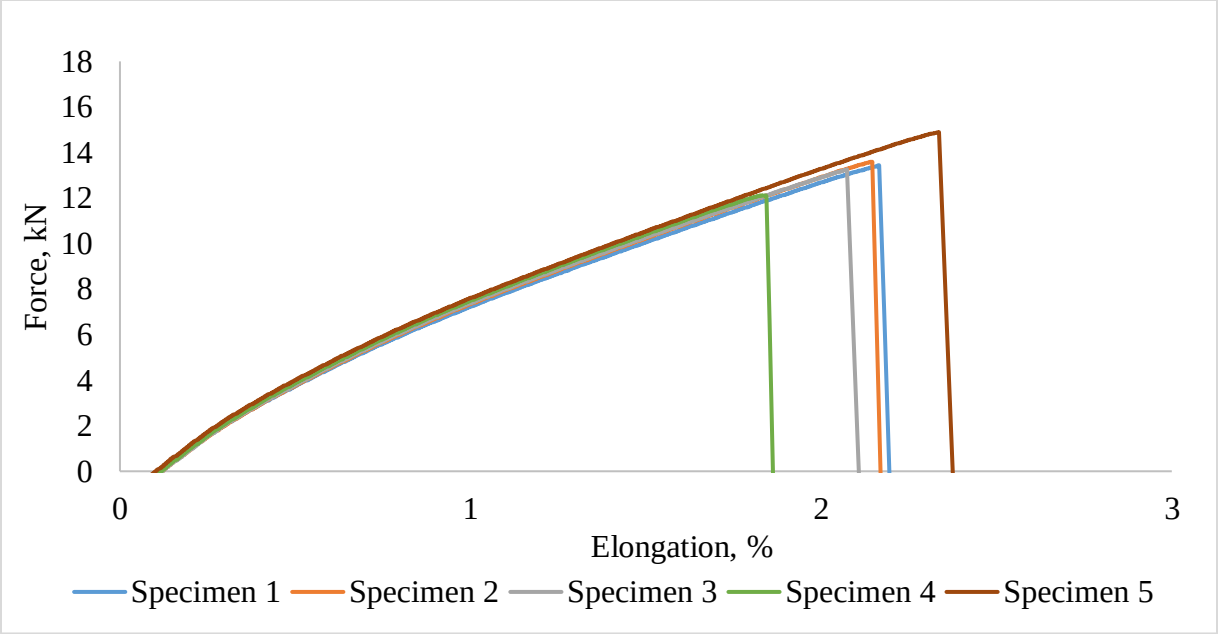

Figure 4.15. Typical graphs of the tensile test in the weft direction.

4.9.2. Tup impact test

Instron Drop Tower Impact CEAST 9350 was used for testing the Tup impact properties of the prepared composites specimens. The testing device is located at the Composite Core Facility, Wilson College of Textile, NC State University.

The Tup impact testing was performed according to ASTM D3763-15 Standard Test Method for High-Speed Puncture Properties of Plastics Using Load and Displacement Sensors. The selected specimen size was 101.6 mm x 101.6 mm. Preliminary trials were performed to determine the required energy level to achieve full puncture while maintaining an impact velocity of 4.4 m/s with a maximum 20% change. The trials were performed on the 9 layer sample, which is the strongest among all because of its thickness and pick density. No extra dead weights were used as the specimens are sensitive to very high energy impact.

The specimen is pneumatically clamped and then punched by the striker, which is connected to a piezoelectric transducer to measure the force exerted on the specimen in the direction of impact. The user interface delineates the force on the y-axis versus displacement curve on the x-axis. The total energy absorbed during the whole cycle is the total energy exerted to puncture the specimen and can be determined by calculating the area under the curve as

illustrated in Figure 4.16. The impact event is considered complete, once the force detected by the striker goes to zero, which indicates that full penetration is attained. The impact energy used initially for the trials ranged from 10J to 30J. However, after multiple attempts, a force of 49.7J was considered to be optimum, without any additional load.

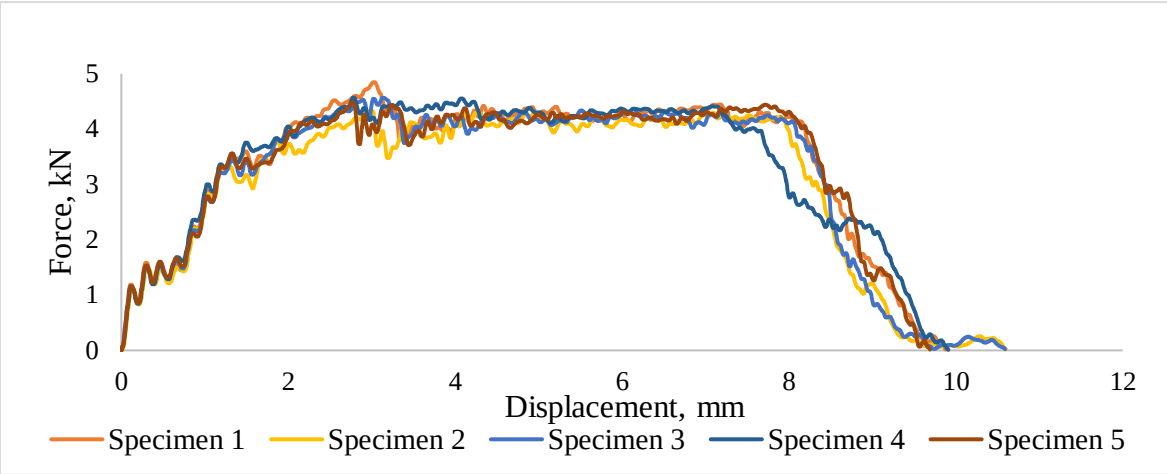

Figure 4.16. Typical graphs of Tup impact test.

4.9.3. Charpy impact test

Instron Pendulum Impactor II was used for testing the Charpy impact properties of the composites. Unlike Tup impact test which used 49.7J, Charpy test used low energy of 10.8J to impact the specimens. The testing device is located at the Composite Core Facility, College of Textile, NC State University. A modified version of ASTM D-6110 was followed for testing specimens for Charpy impact resistance. According to the standard, a notched specimen was recommended. However, the specimens used in this research were not notched as it would lower the impact resistance further. Impact resistance of five unnotched composite specimens was tested in both X- and Y- directions. The specimen size used was 127 mm in length and 12.7 mm in width. Several trials were performed in order to find the optimum striking energy. The selected striker energy was 10.8 J which was sufficient to completely break the specimen while maintaining the absorbed energy level less than 80% of the striker energy. The initial trials were performed on 9 layers, plain weave with maximum Z-binders (1:1 ratio).

4.9.4. Compression test

The MTS Servo-hydraulic 370 load frame was used for testing the compression properties of the composites. The test was performed according to the ASTM D-6641, which is a Standard Test Method for Compression Properties of Polymer Matrix Composite Materials Using a Combined Loading Compression (CLC) Test Fixture. This method of loading is a combination of shear and end loading. The CLC fixture consists of four steel blocks with specimen gripping surfaces coated with tungsten carbide, each pair being clamped together with four bolts as illustrated in Figure 4.17. The block measures 6” and has been designed to perfectly accommodate the 5.5" long tabbed or untabbed specimen exposing 0.5” gage length when assembled. Combined loading can be achieved by adjusting the bolt torque, the ratio of the end- to shear-loading of the specimen can be controlled. This provides sufficient shear loading to avoid crushing at the specimen ends and less clamping force than if the specimen was purely shear-loaded (lower clamping-induced stress concentrations). It is a relatively simple and inexpensive method of obtaining compression strength test results with fewer data scatter. The test results of the compression test both in warp and weft directions is illustrated in figure 4.18 and 4.19, respectively.

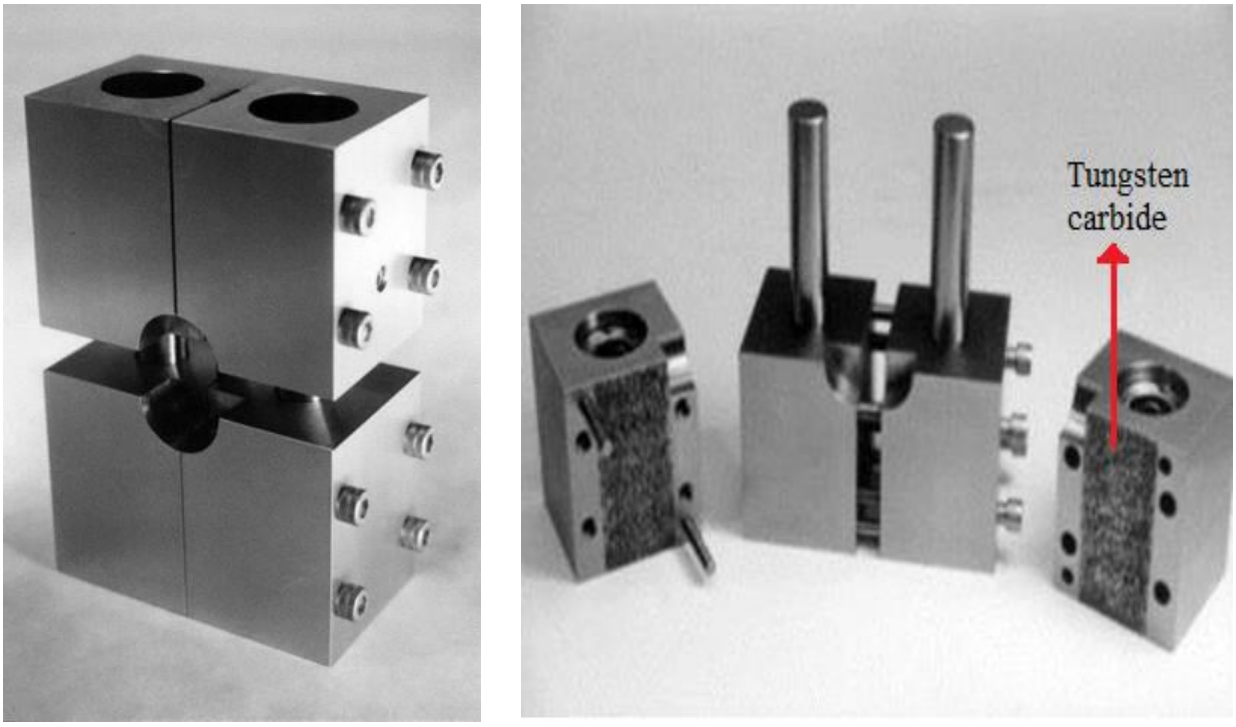

Figure 4.17. Fixtures used in Combined Loading Compression (CLC).

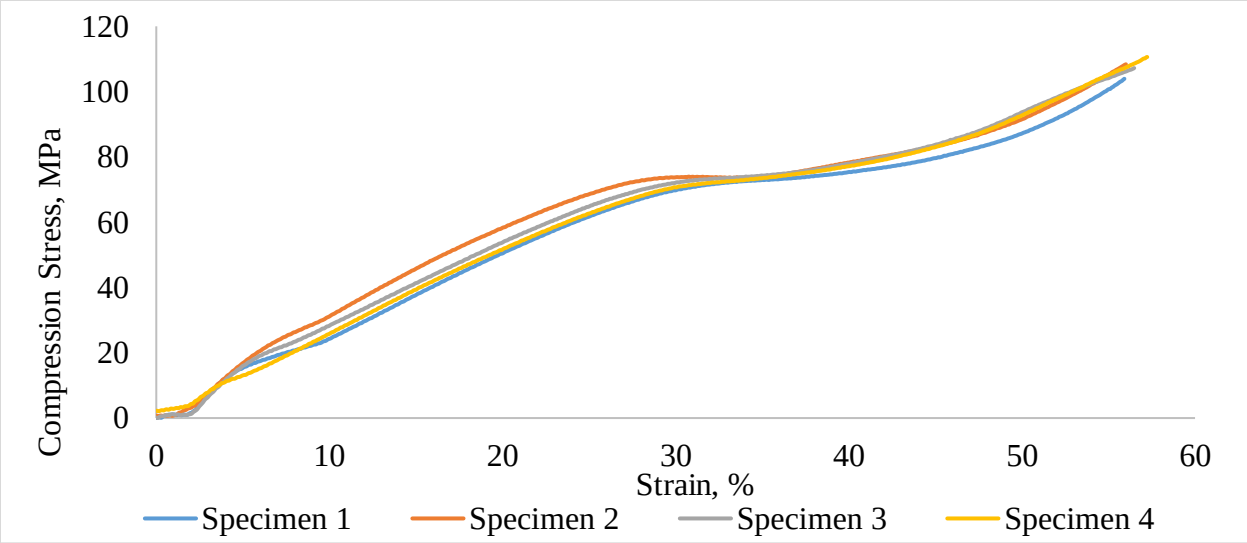

Figure 4.18. Typical graphs of Compression test in the warp direction.

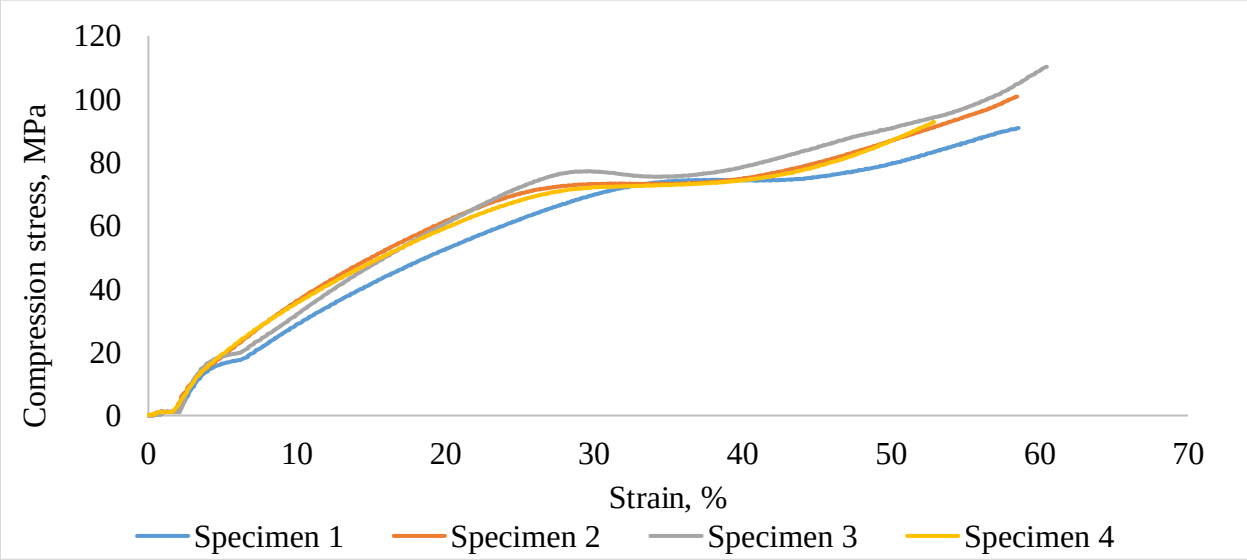

Figure 4.19. Typical graphs of Compression test in the weft direction.

4.10. Statistical analysis

In order to evaluate the effect of the structural parameters of the composites, data were analyzed using various statistical tools like ANOVA, regression, and Tukey HSD (Honestly Significant Difference). Statistical software tools like SAS and JMP were used for this purpose. The effect of all the independent structural parameters like thickness (determined by the number

of Y-layers), weave and ratio of Z-yarn in terms of Y-yarns were used to understand the effect of each of these variables. Thickness and stress were used for response (dependent) variable for tensile and compression whereas energy was used to understand impact resistance.

CHAPTER 5 - RESULTS AND DISCUSSION

This chapter discusses the result and findings of the experimental design. All the variables including weave, layers, and Z to Y ratio on the properties of the 3DOW composites are discussed in details. The effects of independent structural parameters on the different mechanical test, including tensile, impact and compression, is individually analyzed statistically. The factors like thickness, fiber volume fraction, preform areal density and composite areal density were taken into consideration while analyzing data. All the statistical analysis was done at a 95% confidence level.

5.1. Experiment A

In experiment A, factors like composite thickness (number of y-layers), weave design and the ratio between Z-yarns and Y-yarns were altered to understand the effect of each factor on tensile strength, compression strength and impact resistance. The pick density for different y-yarn layers is based on the balanced preforms in the X- and Y- directions. Table 5.1 gives details about all the samples used in Experiment A including sample ID, number of X- and Y- layers, weave, Z- to Y-yarn ratio. The nomenclature for all the statistical analysis is outlined in Appendix 4. X-yarn density in Table 5.1 represents rapier's double yarn insertion mechanism as two yarns are inserted per shed.

Table 5.1. Experiment A – Sample ID and variable parameters.

Sample ID	No. of Y-layers	No. of X-layers	Weave	Ratio (Z to Y)	X-yarns density (picks/inch/layer)
1	3	4	Plain	1:1	10.28
2	3	4	2x2 Warp rib	1:1	10.28
3	3	4	3x3 Warp rib	1:1	10.28
4	3	4	Plain	1:2	10.28
5	3	4	2x2 Warp rib	1:2	10.28
6	3	4	3x3 Warp rib	1:2	10.28
7	3	4	Plain	1:3	10.28
8	3	4	2x2 Warp rib	1:3	10.28
9	3	4	3x3 Warp rib	1:3	10.28
10	6	7	Plain	1:1	11.76
11	6	7	2x2 Warp rib	1:1	11.76
12	6	7	3x3 Warp rib	1:1	11.76
13	6	7	Plain	1:2	11.76
14	6	7	2x2 Warp rib	1:2	11.76
15	6	7	3x3 Warp rib	1:2	11.76
16	6	7	Plain	1:3	11.76
17	6	7	2x2 Warp rib	1:3	11.76
18	6	7	3x3 Warp rib	1:3	11.76
19	9	10	Plain	1:1	12.34
20	9	10	2x2 Warp rib	1:1	12.34
21	9	10	3x3 Warp rib	1:1	12.34
22	9	10	Plain	1:2	12.34
23	9	10	2x2 Warp rib	1:2	12.34
24	9	10	3x3 Warp rib	1:2	12.34
25	9	10	Plain	1:3	12.34
26	9	10	2x2 Warp rib	1:3	12.34
27	9	10	3x3 Warp rib	1:3	12.34

The value of the impact energy and tensile load was normalized by the cross-sectional area to give the design value, which is a concept used to design any parts from isotropic materials irrespective of their size. This will eliminate the need to test each sample with various dimensions and shapes. The same concept can be applied to 3DOW composites. However, there are some challenges in regards to 3DOW composite as it is anisotropic in nature due to the presence of the reinforcement in x- and y-directions only. The 3DOW composite is subject to variations throughout the formation process, which could pose major hurdles in configuring the design value. The building block of these hemp fiber composites is subject to variation. The

variation of hemp fiber properties, which are influenced by fiber length, thickness/diameter, environment (temperature, humidity, rain, etc.) are broad and uncontrollable. Additional variations result from the processing and handling of converting fiber to yarn. The variation could also come from the weaving process, infusion process as well as specimen cutting process. Examples of sources of variation include, thickness variation due to the presence of Z-yarn, which is more pronounced in preforms with a small number of layers, and as the number of layers increase, the effect of the Z-yarn crown diminishes. For example, the effect of Z-yarns is proportionally higher in 3 layers and keeps on decreasing as we increase the number of layers. During the infusion stage, resin saturation might not be very uniform which could lead to more variation. All these variations contributes to the challenges faced while working on the design plan of an anisotropic material such as 3DOW made from hemp.

However, this research troubleshoots some of these challenges by using different normalized methods, which will contribute to configuring the design value.

5.1.1. Tensile properties

Tensile properties of 3D orthogonal with different fiber volume fraction and different structural parameters including number of Y-yarns layers or thickness, through-thickness reinforcing fibers (Z-yarn) contribution and weave pattern were analyzed.
The tensile test is a destructive test, which is intended to measure the peak load, tensile modulus, tensile stress and tensile strain. The laser extensometer was used to check whether there is a difference between measuring the extension with and without the laser extensometer. It was found that there was no difference due to good specimen gripping by the jaws' pressure employed. A total of 133 (27x5-2 defective specimens) specimens from warp (Y-yarn) direction and 135 (27x5) specimens from weft (X-yarn) direction were analyzed using ANOVA and Tukey HSD to investigate the effect of the structural parameter on tensile properties. The results of the tensile test from samples 1 through 27 in warp (Y) direction are listed in Table 5.2. The weft (X) direction tensile data are shown in Table 5.3. The peak load was used to characterize the tensile behavior of the composite in this analysis.

Figure 5.1 shows specimens' images after tensile test with a typical tensile break in warp (Y-yarn) direction occurring at the gauge length. The results for the main effect of different

structural parameters on tensile properties of the composites were analyzed using a one-way ANOVA statistical analysis. The specimens were tested both in the warp (Y-yarn) direction and weft (X-yarn) direction as shown in Appendix 86. The samples were balanced structure indicating that the total linear density of fibers in the Y-direction/unit width is equal to the total linear density of fibers in the X-direction/unit length. However, the peak load of all the samples in the weft (X) direction was consistently higher than that in the warp (Y) direction. This was because X-yarn had higher yarn tenacity compared to Y-yarns, as shown in Appendix 83. Individual X- and Y-yarns were tested using USTER TENSORAPID® 4, available in physical testing lab at Wilson College of Textiles, NC State University.

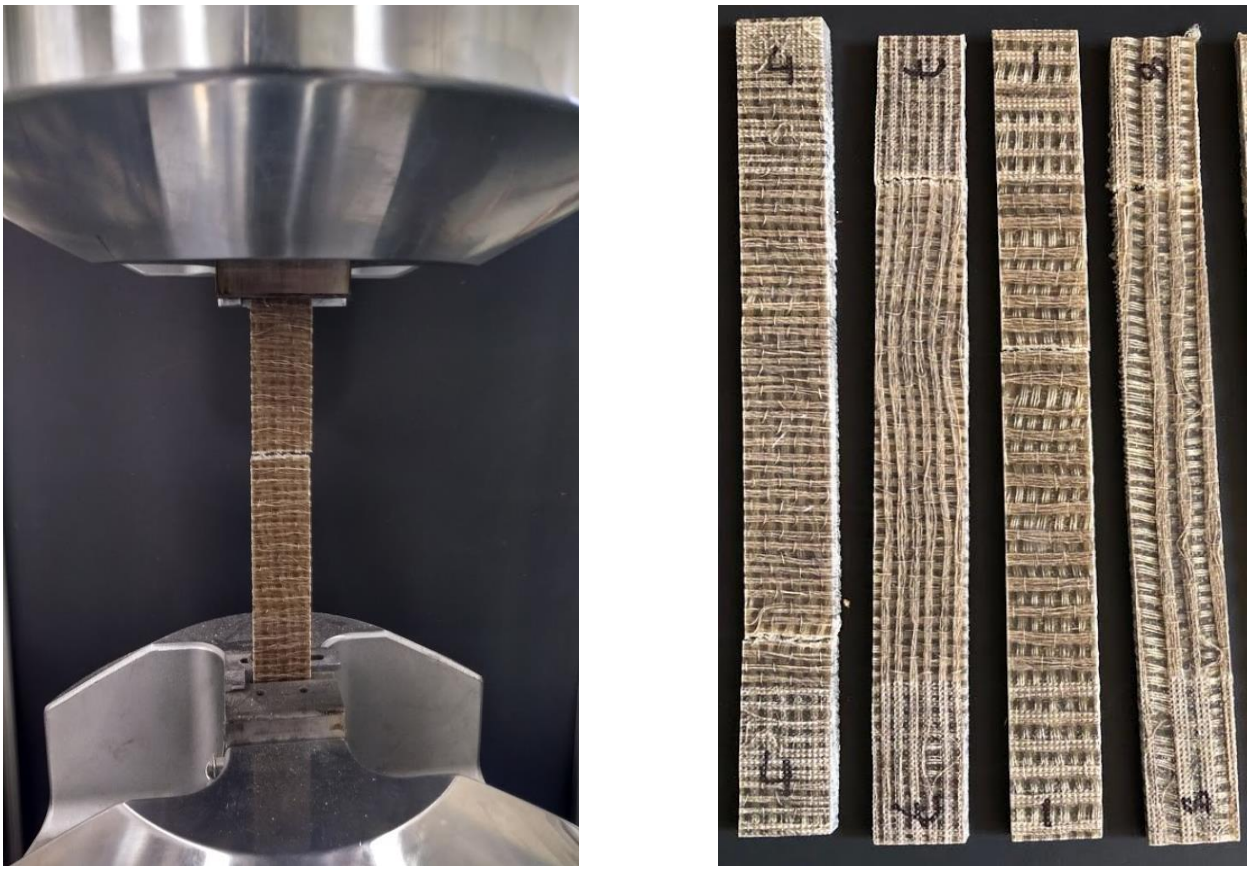

Figure 5.1 Typical tensile break at the gage length along with some tested specimens

Table 5.2. Average tensile data - warp direction.

Sample ID	Tensile specimen thickness, mm	MODULUS, GPa	CV, %	PEAK TENSILE STRESS, MPa	CV, %	FAILURE STRAIN, %	CV, %	PEAK LOAD, N	CV, %
1	2.79	2.22	6.70	26.36	2.52	2.42	9.01	1870.23	6.85
2	2.85	1.65	15.37	17.43	23.35	1.87	37.41	1257.58	21.84
3	2.86	2.33	23.51	23.37	13.58	1.68	21.08	1701.78	14.88
4	2.99	2.40	9.73	22.04	5.24	1.72	22.76	1672.42	3.28
5	3.22	2.57	12.30	21.48	7.73	1.53	18.77	1756.12	12.78
6	2.89	2.20	11.49	21.21	10.81	1.85	16.64	1558.99	12.33
7	2.92	2.84	8.39	23.41	17.09	1.29	28.14	1751.78	25.43
8	2.88	2.89	6.08	23.15	9.70	1.27	15.90	1690.28	7.50
9	2.85	2.27	5.21	20.65	5.56	1.42	15.69	1494.19	5.16
10	5.04	3.15	4.90	31.86	9.24	1.83	24.59	4074.29	8.35
11	5.08	3.10	9.37	33.91	8.88	1.90	9.95	4383.11	11.28
12	5.24	2.89	4.90	32.56	2.18	2.02	5.79	4331.32	2.27
13	4.80	2.62	3.00	27.43	3.32	2.43	12.55	3346.26	5.28
14	5.08	2.92	10.26	22.71	27.41	1.36	44.71	2912.42	25.03
15	4.96	2.54	10.24	23.16	10.60	1.58	18.31	2913.67	9.43
16	5.09	3.08	10.22	28.58	3.21	1.87	15.04	3692.01	3.10
17	5.05	3.43	3.83	30.19	3.63	1.79	12.27	3873.15	4.44
18	4.92	3.17	4.76	26.05	13.58	1.40	31.34	3256.73	14.70
19	7.18	2.95	6.48	34.55	5.75	2.38	12.65	6296.01	6.03
20	7.48	3.07	3.64	35.23	1.01	2.18	4.53	6690.14	1.89
21	7.63	2.82	7.58	29.90	14.14	1.68	28.67	5783.97	13.64
22	7.41	2.93	5.39	34.11	1.93	2.33	10.85	6423.50	3.46
23	7.20	3.13	2.45	31.82	11.35	2.04	19.48	5825.92	12.93
24	7.73	3.34	4.42	31.01	6.18	1.87	8.97	6093.07	9.03
25	7.53	3.62	2.54	30.78	2.30	1.71	7.38	5883.74	2.92
26	7.39	3.57	1.68	29.01	9.55	1.47	20.13	5443.39	8.99
27	7.67	3.29	7.95	28.98	6.44	1.84	10.67	5627.58	2.78

Table 5.3. Average tensile data - weft direction.

Sample ID	Tensile specimen thickness, mm	MODULUS, GPa	CV, %	PEAK TENSILE STRESS, MPa	CV, %	FAILURE STRAIN, %	CV, %	PEAK LOAD, N	CV, %
1	2.86	3.11	8.68	65.36	4.60	2.42	9.01	4740.36	3.16
2	2.92	2.49	11.26	57.52	10.97	2.88	10.35	4260.28	9.38
3	3.04	3.74	2.26	64.86	13.94	2.25	11.98	5053.07	21.87
4	2.96	3.61	7.93	67.72	6.36	2.38	7.83	5094.66	7.44
5	3.12	4.67	2.88	55.98	9.65	1.72	8.07	4442.15	11.57
6	2.90	3.98	13.96	57.06	7.78	1.97	11.59	4202.87	7.78
7	2.91	4.23	3.04	67.22	5.31	2.09	4.35	4956.65	9.40
8	2.91	4.38	2.82	58.51	11.48	1.81	12.37	4326.62	12.04
9	2.90	4.15	7.67	50.67	7.68	1.71	7.24	3730.55	8.53
10	5.09	4.57	1.49	76.14	7.57	2.24	8.58	9830.93	6.49
11	5.29	4.30	1.71	80.41	2.28	2.48	1.88	10800.55	2.28
12	5.53	4.31	5.03	71.11	14.86	2.19	17.84	9885.54	8.19
13	5.13	3.81	4.67	66.98	7.52	2.38	11.12	8735.48	8.20
14	5.03	5.09	6.84	36.77	12.32	1.10	13.83	4686.31	11.61
15	5.20	4.94	8.34	41.14	12.37	1.25	11.06	5436.31	12.87
16	5.09	4.67	4.16	69.42	8.83	2.11	12.36	8960.54	7.36
17	5.12	4.97	1.02	72.89	4.93	2.07	5.11	9478.66	4.98
18	5.20	5.02	4.66	53.83	5.51	1.54	6.48	7113.39	6.60
19	7.28	4.53	7.50	82.11	8.73	2.37	14.31	15188.19	9.18
20	7.55	4.34	6.96	76.98	8.07	2.35	11.41	14755.13	7.29
21	7.61	4.31	4.55	77.38	8.77	2.32	10.07	14941.55	8.73
22	7.41	4.39	7.82	81.13	4.25	2.41	10.08	15278.98	5.06
23	7.21	5.07	4.37	69.46	4.81	1.94	6.80	12720.87	5.51
24	7.48	5.38	8.12	48.73	17.53	1.31	19.90	9264.98	18.37
25	7.42	5.65	3.45	60.03	15.66	1.56	18.44	11320.72	16.25
26	7.45	5.09	3.04	71.14	8.07	2.01	9.43	13454.47	7.36
27	7.42	5.10	5.85	61.29	8.33	1.76	13.85	11547.89	8.02

5.1.1.1. Main Effect of number of layers on tensile properties

Figure 5.2 shows the effect of number of layers on the tensile peak load in the X- and Y-directions. The graph indicates a significant difference between the samples with different layers or thickness. This was also confirmed by the Tukey HSD for warp and weft directions in

Appendix 6 and 13, respectively. The 9 warp layers samples had the highest peak load in Y- and X-directions compared to 3 warp layers and 6 warp layers composite samples. This was due to the presence of a higher number of X- and Y-yarns in 9 warp layers compared to 3 or 6 warp layers. In 9 warp layers, more yarns contribute towards the tensile load. As the number of warp layers decreases, gradual decline in the tensile peak load is observed. Similarly, 6 warp layers of composite samples had higher tensile peak load compared to the 3 warp layers samples. The tensile load in the warp (Y) direction was lower than the weft (X) direction because the weft yarns collectively provide more tensile resistance that the warp yarns.

The tensile strain and tensile stress in Y- and X- directions are illustrated in Figure 5.3 and 5.4. The graph indicated no significant effect of number of layers on tensile strain and stress in both warp and weft direction as it can be seen from the error bars. While the effect of number of warp layers is not significant due to variability, the average tensile strain exhibited increase with number of layers. It was noticed that there is in plane yarn crimp (waviness) in the preforms and these could not be straightened during resin infusion. The tensile strain in the warp direction was highest in 9 layers samples followed by 6 layers and 3 layers which could be due to more waviness in 9 layers compared to 3 and 6 layers. However, in the case of weft direction, the highest tensile strain and stress was observed in 3 layers followed by 9 layers and 6 layers.

The tensile peak load in warp and weft directions was mainly influenced by the number of layers of y-yarns. ANOVA analysis in Appendix 5 illustrates that there was a significant difference between peak load as influenced by the number of layers (or thickness). The Tukey analysis, illustrated in Appendix 6, also aligns with ANOVA results showed a significant difference between the peak load of composites with 3 layers, 6 layers, and 9 layers. The results of the one-way ANOVA test were confirmed using a follow-up post hoc Tukey test. The statistical analysis results of ANOVA in warp and weft direction are illustrated in Appendices 5 and 12.

The peak load was normalized by several approaches, in order to segregate the effect of some dependent parameters from the analysis and to have a fair comparison between the samples irrespective of the thickness. This eliminates the effect of layers for the analysis. The peak load

was normalized in warp and weft direction, by using thickness as shown in Appendices 7 and 14, respectively, using Tukey multiple mean comparisons. In the case of warp direction, the peak load was normalized by the composite thickness, the normalized peak load showed a significant difference between composites with different layers. Apart from thickness, the fabric structure formation in 3D woven composites plays an integral part in determining the tensile strength including tensile stress and tensile strain. In order to mitigate the defect or at least keep the defects to a minimum, straight alignment of yarns was very important. However, in terms of the weft (X) direction, there was no significant difference between the 3 layers and 6 layers. A slight difference in the values could have emerged due to pre-existing formation defects. However, it was also deduced that 9 layer samples were significantly different from 3 layers and 6 layers which indicated that 9 layers sample comprises of more pre-existing defects as shown in Appendix 14.

To conclude, the tensile load of the composite samples due to changing the number of Y-yarn layers or thickness had a very significant effect on the tensile peak load in both warp and weft direction. The contribution of thickness in the overall structure in this research was very substantial compared to the contribution of Z-binders and weave pattern. However, it was observed that 9 layer samples have the highest peak load, tensile stress and tensile strain compared to 6 layers and 3 layers had the lowest values.

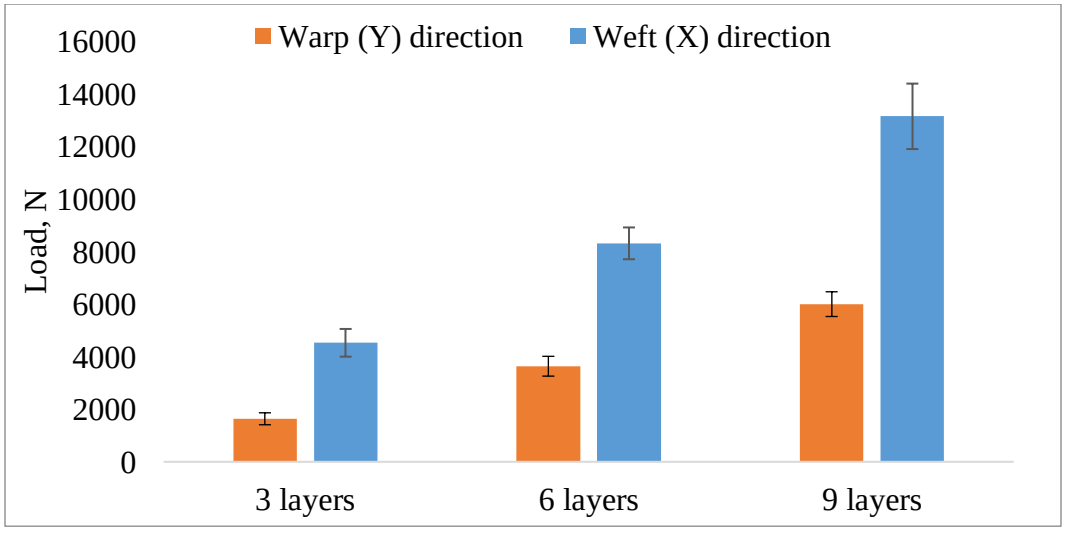

Figure 5.2. Main effects of layers on tensile load.

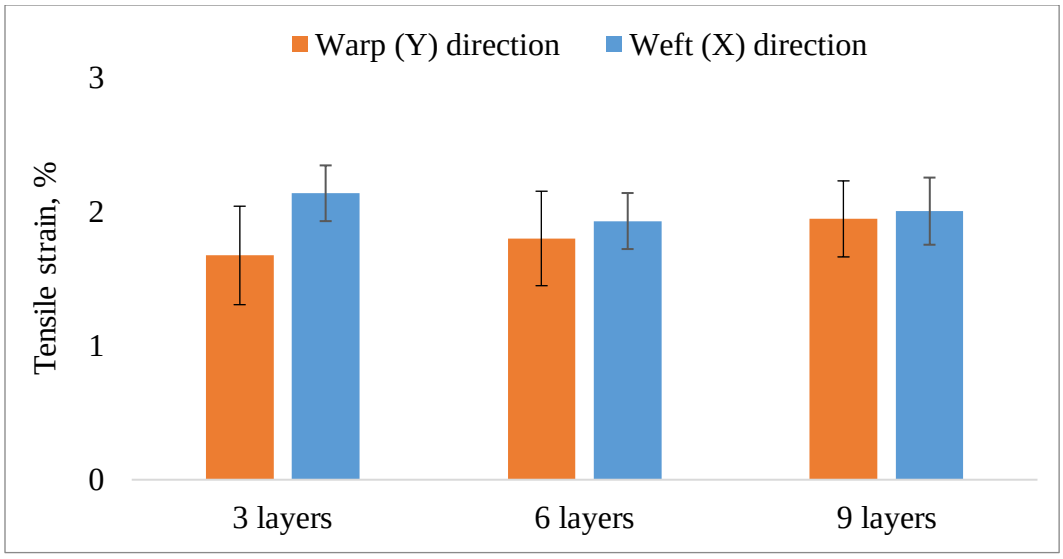

Figure 5.3. Main effects of layers on tensile strain.

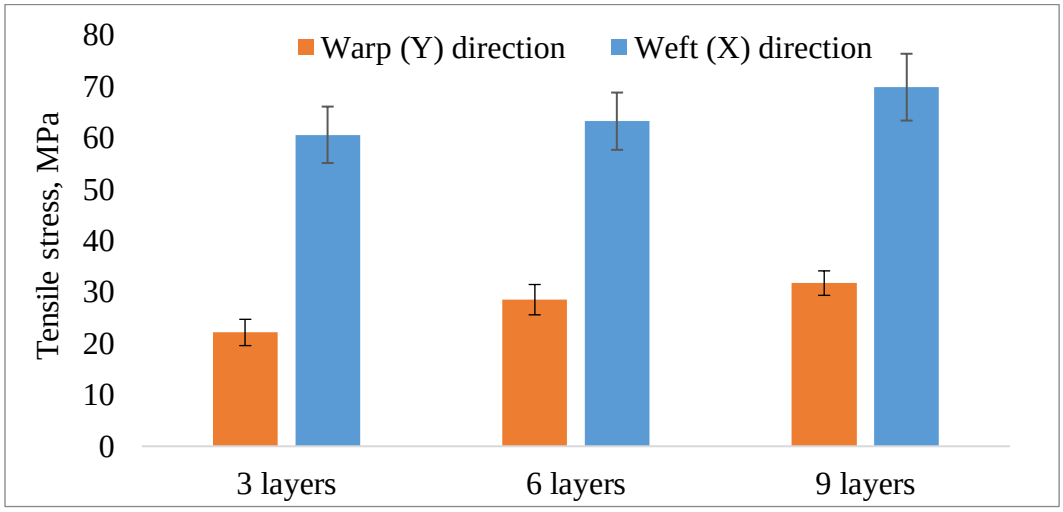

Figure 5.4. Main effects of layers on tensile stress.

5.1.1.2. Main Effect of weave on tensile properties

Figure 5.5 shows the effect of weave on the tensile peak load in the X- and Y- directions. The graph indicated that there was no significant difference between the samples with different weave pattern. This was also confirmed by the Tukey HSD test in Appendices 8 and 15 in warp and weft direction, respectively. While the difference is not statistically significant, plain weave showed the highest average peak load compared to 2x2 warp rib, followed by 3x3 warp rib which was true for both X- and Y- directions. This could be due to the fact that plain woven

structures are more compact with a less open spot for the resin to accumulate (and thus reduces formation of resin rich areas) compared to the 2x2 warp rib and 3x3 warp rib weave structure.

The tensile strain in Y- and X-directions as illustrated in Figure 5.6, indicated that there was no significant difference between the tensile strain of the samples in both warp and weft directions. Similar trend was seen for effect of weave on tensile stress indicated in Figure 5.7. The average tensile strain was highest in plain weave followed by 2x2 warp rib and 3x3 warp rib in both warp and weft direction. The tensile stress was slightly highest in plain weave followed by 2x2 warp rib and 3x3 warp rib in warp and weft direction.

The peak load was normalized by using thickness as shown in Appendices 9 and 16 for warp and weft direction respectively, using Tukey multiple mean comparisons. In the case of warp direction, the peak load was normalized by the composite thickness, the normalized peak load showed no significant difference between plain, 2x2 warp rib and 3x3 warp rib weave design. In case of weft (X) direction, there was no significant difference between 2x2 warp rib and 3x3 warp rib. However, it was also deduced that plain weave was significantly different from 2x2 warp rib and 3x3 wrap rib in weft direction as indicated in Appendix 16.

To conclude, the tensile load of the composite samples due to changing the weave pattern didn't have any significant effect on the tensile peak load in both warp and weft direction. The contribution of weave design in the overall structure in this research was very minimal compared to the contribution of layers. However, it was observed that plain weave had the highest peak load, tensile stress and tensile strain compared to 2x2 warp rib and 3x3 warp rib.

ANOVA analysis in Appendix 5 illustrates that there was no significant difference between the weave pattern namely plain, 2x2 warp rib and 3x3 warp rib. The Tukey analysis also acknowledges ANOVA results showing no significant difference between the weave patterns.

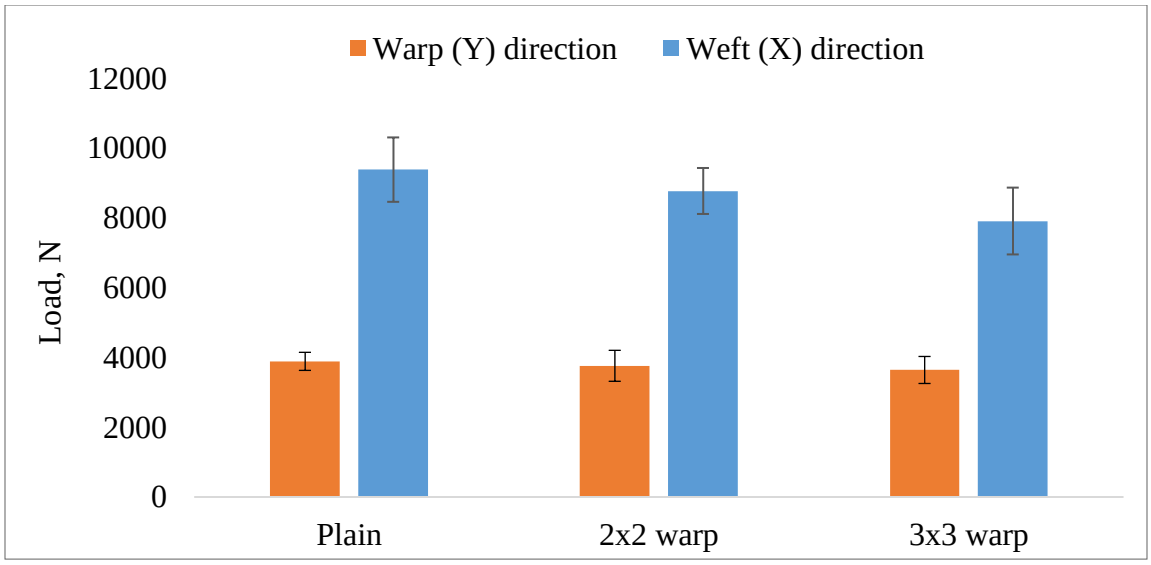

Figure 5.5. Main effects of weave on tensile load.

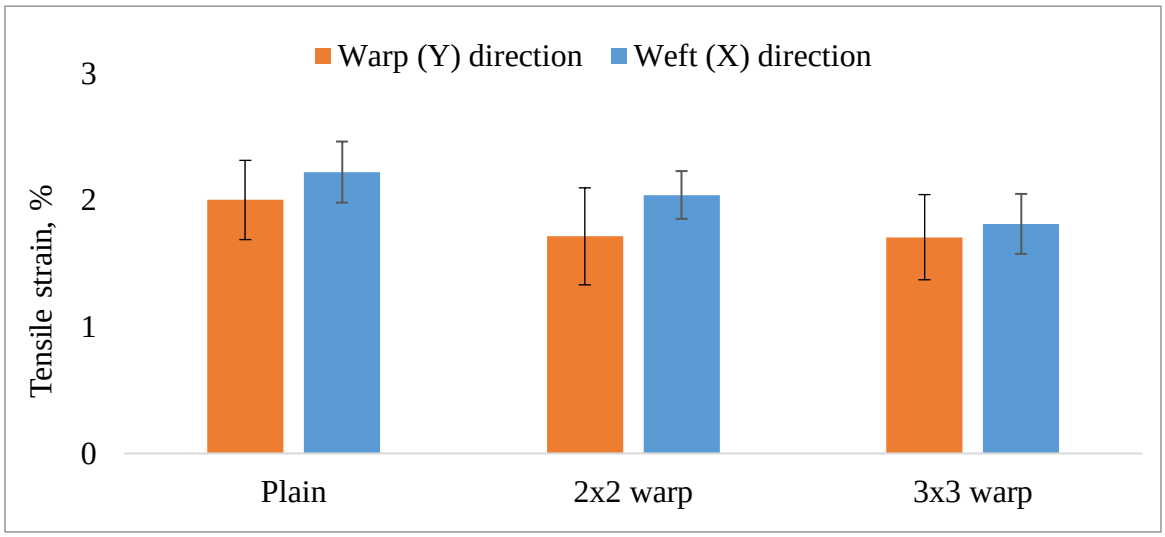

Figure 5.6. Main effects of weave on tensile strain.

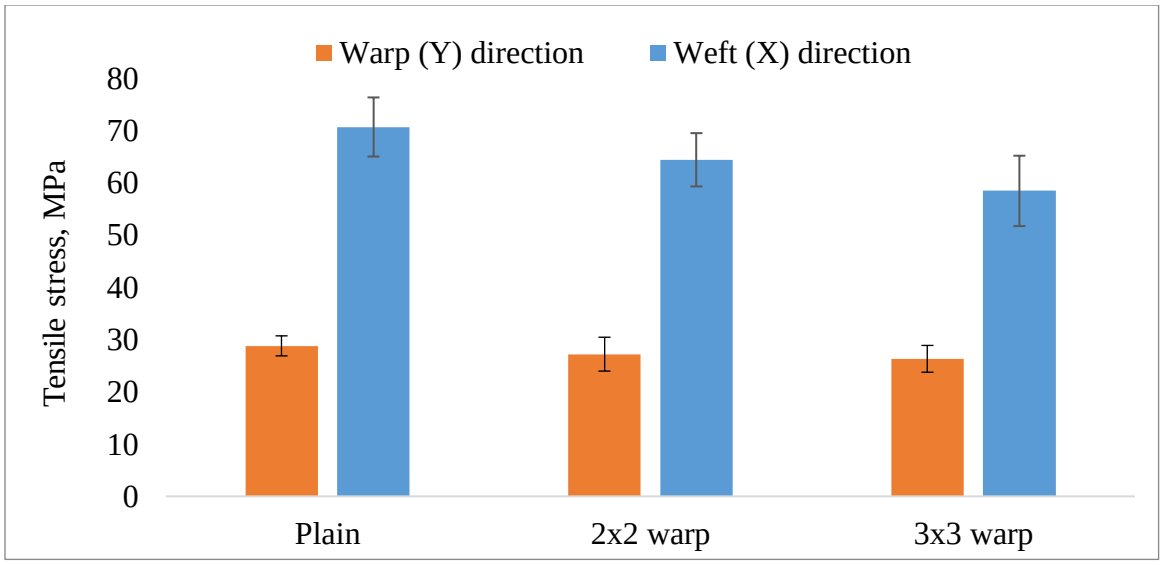

Figure 5.7. Main effects of weave on tensile stress.

5.1.1.3. Main Effect of Z to Y ratio on tensile properties

Figure 5.8 shows the effect of the Z to Y ratio on the tensile peak load in the X- and Y-directions, indicating there was no significant difference between the samples in warp (Y) direction and this was also confirmed by the ANOVA test in Y- and X-directions in Appendices 5 and 12. However, in terms of weft (X) direction, 1:1 ratio was not significantly different from 1:3 but 1:1 and 1:3 are significantly different from 1:2 ratio depicts highest tensile load both in warp and weft direction followed by 1:3 and 1:2, which is very typical given there are more Z-yarns contribution in 1:1 than the others. Ratio 1:2 was slightly lower than 1:3 in most cases. However, there was no significant difference between the two ratios in warp direction only. However, tensile load in the warp (Y) direction was lower than the weft (X) direction because the weft yarns collectively provided more tensile resistance than the warp yarns.

The tensile strain in Y- and X- directions illustrated in Figure 5.9, indicated that there was no significant difference between the tensile strain of the samples in both warp and weft direction. The tensile strain was higher in 1:1 ratio followed by 1:2 and 1:3 ratio in the warp direction. This trend was similar to tensile stress as illustrated in Figure 5.10. The decreasing trend was due to the consistent decrease in the number of Z-yarns from 1:1 to 1:2 and then 1:3. Even though the difference was not significant, the downward trend indicated that Z-binders

influence the tensile load. This trend is not consistent in the weft direction where we see 1:2 is slightly lower than 1:3. However, that wasn't true in case of tensile stress in X-direction, since changing the Z to Y ratio didn't have any significant effect in that case.

The peak load was normalized by using thickness as shown in Appendices 11 and 18. The Tukey HSD results for warp (Y) direction shows that 1:2 (indicated as 0.5) and 1:3 (indicated as 0.33) are not significantly different whereas 1:1 was significantly different than both 1:2 and 1:3.

To conclude, the tensile load of the composite samples due to changing the number of Z-binders didn't have any significant effect on the tensile peak load in both warp and weft direction. The effect of Z to Y ratio in the overall structure in this research was very minimal compared to that of the fiber volume contribution of X- and Y-yarns.

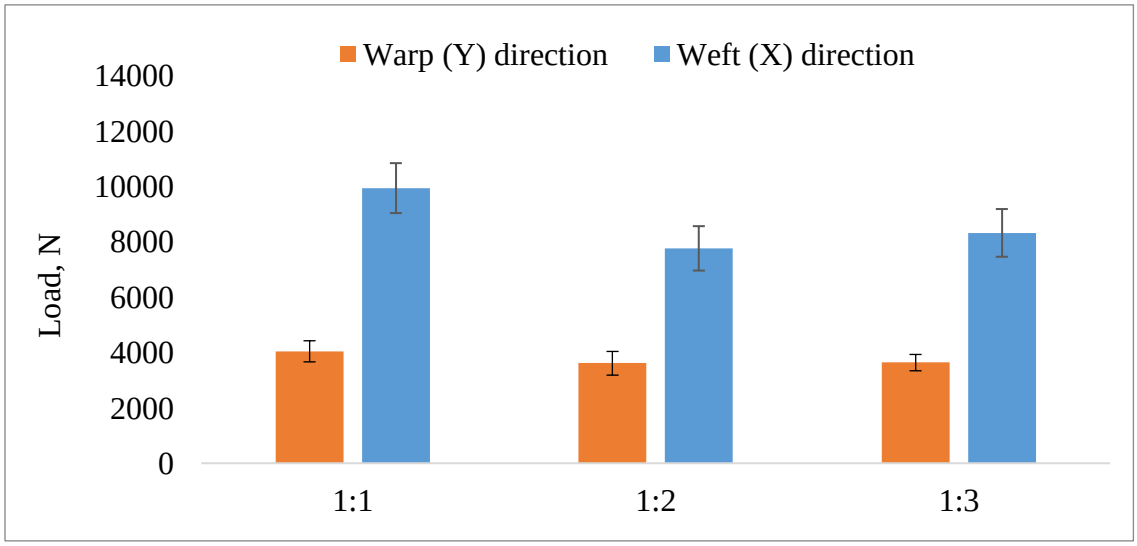

Figure 5.8. Main effects of Z to Y ratio on tensile load.

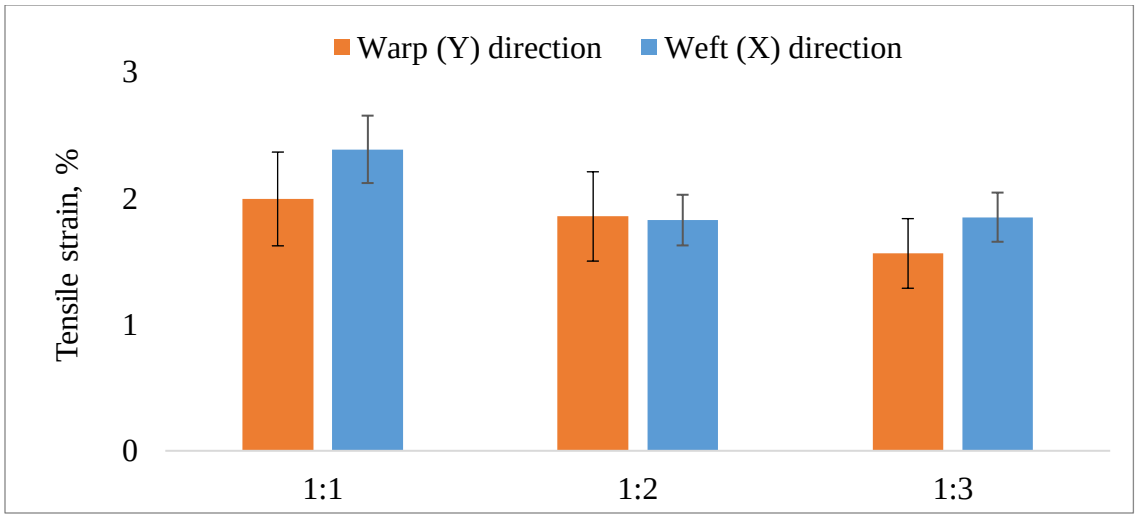

Figure 5.9. Main effects of Z to Y ratio on tensile strain.

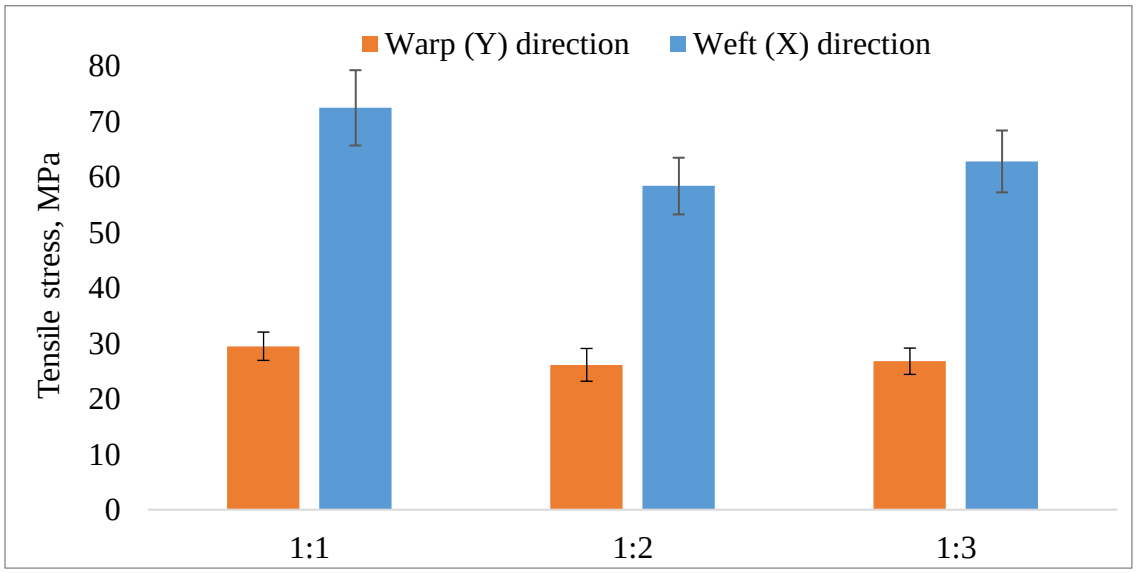

Figure 5.10. Main effect of Z to Y ratio on tensile stress.

5.1.1.4. Comparison of tensile properties of hemp composites with glass composites

As discussed earlier in the literature review, hemp-fiber reinforced (HFR) composites are comparable to glass-fiber reinforced (GFR) composites. The tensile properties of hemp and glass in terms of specific tensile stress and specific modulus as shown in Table 5.4. The glass composite data was obtained from Midani's dissertation (Midani, 2016) along with design of experiment in Appendix 89. Similar to the current research, Midani used 3D orthogonal weaving

and vinyl ester, giving it some similar properties for comparison. However, levels used for variables (number of Y-yarn layers, weave) were different. Z to Y ratio was not used for comparison as it does not have any significant effect. Tensile stress and modulus for glass and hemp were normalized using fiber density. The specific tensile stress of glass was found to be significantly higher compared to hemp specific tensile stress. However, specific modulus was found to be comparable.

Table 5.4. Comparison of tensile properties of hemp-fiber composites with glass-fiber composites.

		Warp			
Fiber	**Density, g/cm^3**	**Tensile stress, MPa**	**Modulus, GPa**	**Specific tensile stress, MPa cm^3/g**	**Specific modulus, GPa cm^3/g**
E-glass	2.54	338 - 488	13.5 - 26.4	133 - 192	5.3 - 10.4
Hemp	1.47	13-40	1.4 - 3.7	9 - 27.1	1 - 2.5
		Weft			
Fiber	**Density, g/cm^3**	**Tensile stress, MPa**	**Modulus, GPa**	**Specific tensile stress, MPa cm^3/g**	**Specific modulus, GPa cm^3/g**
E-glass	2.54	290 - 477	13 - 30	114 - 188	5.1 - 11.8
Hemp	1.47	30 - 91	2 - 6.1	20 - 62	1.4 - 4.1

5.1.1.5. Conclusion

The tensile properties of the finished composites panels was influenced by the structural characteristics of the 3D orthogonal woven preform including thickness or number of y-yarn layers. Weave and Z to Y ratio did not affect the tensile properties. The structural properties of the preform including weft density, weave, and a number of warp layers, affected the tensile properties in the two directions differently, thus highlighting the occurrence of a different physical phenomenon in the warp and weft directions, respectively. The warp direction properties was also influenced by the interactive effect of the weave and the number of warp layers. The specimen breaking mechanism was clean without any fiber pull-out as shown in figure 5.1.

5.1.2. Impact test – Tup and Charpy

All the 27 samples were exposed to two destructive impact test – Tup and Charpy. Tup is a high impact test whereas Charpy is a low impact test. ANOVA and Tukey HSD multiple means comparison was used to investigate how structural and process variables affect the impact properties of 3D orthogonal woven composites. A variety of independent structural variables along with dependent variables (mechanical and physical properties) were analyzed to understand the nature and extend on the overall structure.

5.1.2.1. Tup Impact - Result and discussion

Tup impact is also known as Dynatup, is a destructive test to measure the peak load at impact, peak impact energy, as well as the total energy required to penetrate the composite material by striking it with a drop weight at a specific testing condition. Tup impact test is independent of the test direction. The results of the Tup impact tests for samples 1 through 27 are listed in Table 5.5. Composite areal density is the average value from five individual impact specimens from a sample. Figure 5.11 and Appendix 84 shows a test specimen with a typical puncture from 3 different views. Total penetration energy of 135 (27 x 5) specimens from 27 composite panels were analyzed using ANOVA and Tukey HSD to investigate the effect of structural parameters on the impact energy of composite panels. The analysis was categorized by variable inputs and discussed individually. Appendix 87 shows test results of individual specimens sample-wise from Tup impact test.

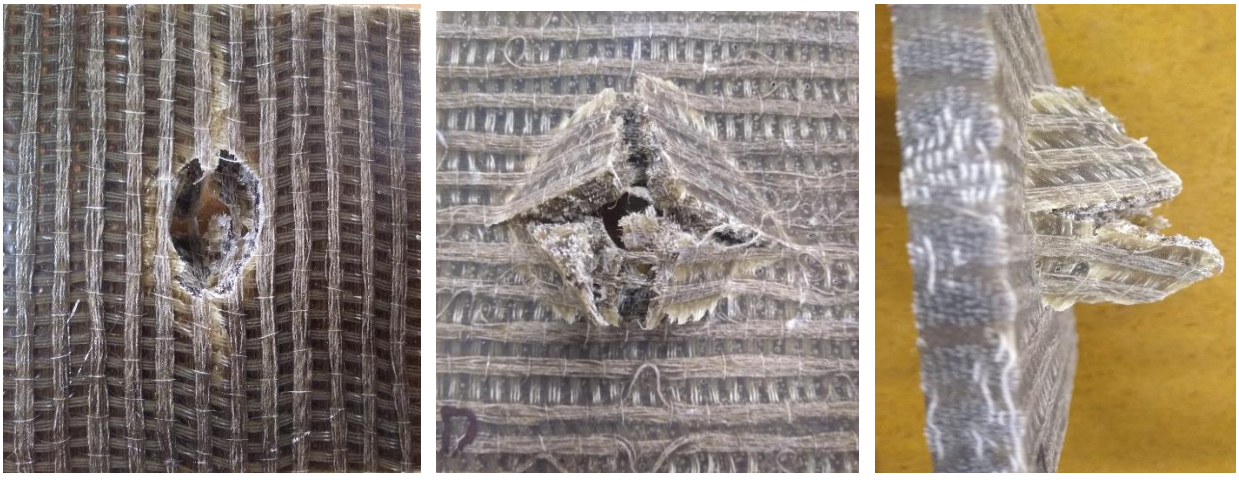

(a) (b) (c)

Figure 5.11 Tup impact specimen (a) Front view, (b) Back view, and (c) Side view

Table 5.5. Average Tup impact data.

ID	Composite areal density, g/m^2	Preform areal density, g/m^2	Composite thickness from profile, mm	Total energy, J	CV (%)	Total energy normalized by thickness (J/mm)	Total energy normalized by comp. areal density (kJ/g/mm^2)	Total energy normalized by Preform areal density (kJ/g/mm^2)
1	2920.6	888.8	2.8	5.4	47.3	2.0	1.9	6.1
2	2842.7	885.2	2.7	6.5	28.9	2.4	2.3	7.3
3	3066.1	868.8	2.9	5.1	32.1	1.8	1.7	5.9
4	3212.8	915.9	2.9	6.5	5.3	2.2	2.0	7.1
5	3226.3	915.7	3.0	6.1	4.2	2.1	1.9	6.7
6	3038.6	978.7	2.8	6.1	20.0	2.1	2.0	6.2
7	3266.3	855.4	2.9	3.8	43.5	1.3	1.1	4.4
8	2995.6	850.1	2.7	3.3	36.6	1.2	1.1	3.9
9	2855.9	1657.0	2.8	3.1	34.8	1.1	1.1	3.5
10	5674.2	1632.8	5.2	14.8	20.9	2.8	2.6	9.1
11	5936.9	1648.2	5.3	16.1	3.5	3.0	2.7	9.7
12	6013.8	1657.0	5.5	16.8	8.9	3.1	2.8	10.1
13	5632.8	1623.5	5.1	19.7	36.6	3.9	3.5	12.1
14	5462.1	1629.2	5.0	15.5	9.7	3.1	2.9	9.5
15	5709.2	1693.4	5.2	16.7	12.8	3.2	2.9	9.9
16	5609.3	1640.0	5.1	14.4	14.4	2.8	2.6	8.8
17	5763.9	1598.2	5.2	14.3	6.4	2.7	2.5	8.9
18	5609.3	1582.1	5.1	14.2	7.4	2.8	2.5	9.0
19	8031.2	2706.1	7.0	28.9	15.7	4.1	3.6	10.7
20	8803.8	2648.2	7.6	31.6	4.3	4.1	3.6	11.9
21	8736.8	2641.1	7.6	29.4	10.0	3.9	3.4	11.1
22	8481.4	2661.4	7.3	32.0	2.6	4.4	3.8	12.0
23	7979.6	2602.8	7.5	32.9	15.1	4.4	4.2	12.7
24	8359.2	2655.3	7.2	32.8	16.8	4.5	3.9	12.3
25	8788.5	2428.8	7.6	32.1	7.2	4.2	3.7	13.2
26	8561.1	2483.1	7.4	33.2	2.7	4.5	3.9	13.4
27	8499.6	2435.7	7.5	30.3	9.0	4.1	3.6	12.4

The test results of the tup impact were analyzed to investigate the effect of structural variables, including a number of layers (thickness), Z to Y ratio and weave design, on total energy. The analysis was based on the univariate analysis of variance, which was further confirmed by the Tukey test.

The statistical analysis output from ANOVA is shown in Appendix 19. Also, the graphs highlighting the main effect of each of the structural parameters are depicted in Figure 5.12 through 5.19.

In Figure 5.12(a), the total penetration energy significantly increased with increasing number of layers. However, the same trend was not followed by the weave design and Z to Y ratio illustrated in Figure 5.12 (b) and 5.13. The total penetration energy was not significantly different for plain, 2x2 warp rib and 3x3 warp rib, illustrated in Appendix 20. Similarly, decreasing the amount of Z to Y ratios from 1:1 to 1:2 did not significantly change total penetration energy as well as changing from 1:2 to 1:3 showed no significant change in total energy penetration. However, Tukey HSD results show a slightly different outcome. Unlike Tukey analysis where Z to Y ratio shows no significant difference, multivariate analysis shows that the 1:1, 1:2 and 1:3 ratio is significantly different with a p-value of 0.015. The Tukey HSD test which a multiple comparison tests, illustrated in Appendix 22, shows no significant difference between the Z to Y ratio as well as plain, 2x2 warp rib and 3x3 warp rib. Thus, it can be concluded that increasing the number of layers had the most significant effect on the total penetration energy and this was due to the increase in the number of fibers resisting the penetration.

Further, change in weave design was not as significant as increasing the number of Y-yarn layers or thickness (shown in Appendix 21), since the amount of fiber added to the structure by increasing the pick density was much less compared to the amount added by increasing extra number of layers. The only differentiating factor between the three weaves was the float which clearly does not contribute to the overall mechanical performance. Finally, changing the Z to Y ratio interlacing pattern, had divisive responses based on the ANOVA and Tukey tests results. Since ANOVA is more sensitive, it is capable of sensing every variation around mean which impacts the p-value. As per Tukey results, 1:2 has the highest mean as compared to 1:1 and 1:3, illustrated in Appendix 22. However, it has to be pointed out that the 1:1 ratio has the lowest mean. This was due to some 1:1 ratio samples that demonstrated low penetration energy due to poor structural integrity during preform formation.

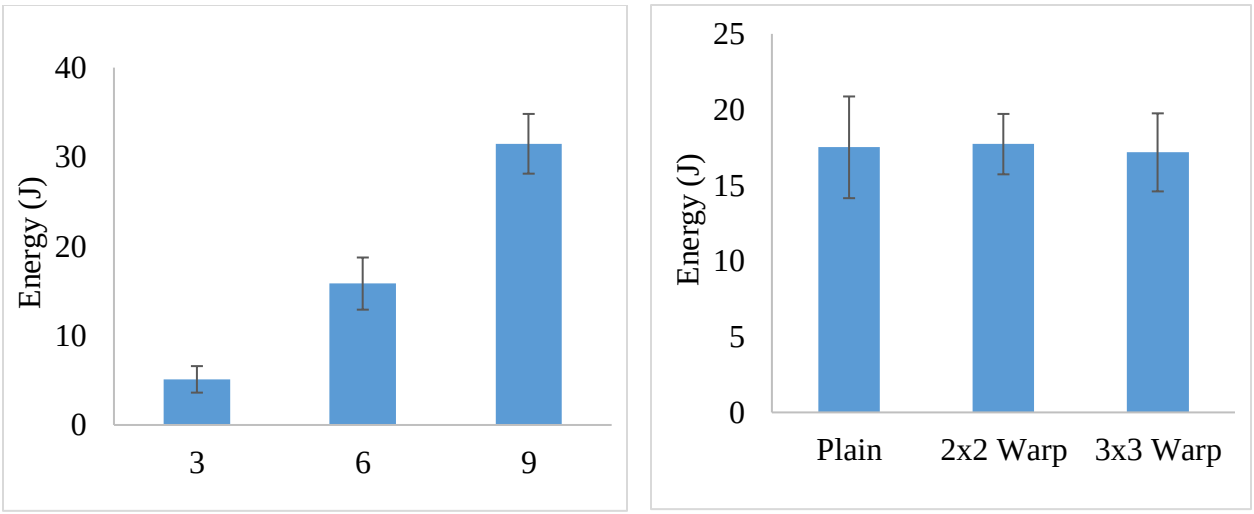

(a) (b)

Figure 5.12 (a) Main effect of number of layers on Tup impact energy, (b) Main effect of weave on Tup impact energy.

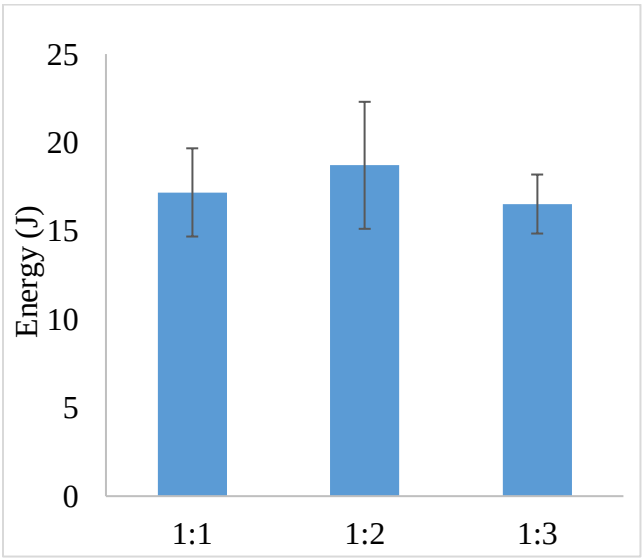

Figure 5.13. Main effect of Z to Y ratio on Tup impact energy.

The results of the total penetration energy were normalized using three different normalization approaches. First, total penetration energy was normalized by the composite thickness to eliminate the effect of the thickness from the analysis. This provides fair comparison

by nullifying the thickness effect. The results of the statistical analysis of the impact energy normalized by the composite thickness are shown in Figure 5.14 (a, b) and Figure 5.15.

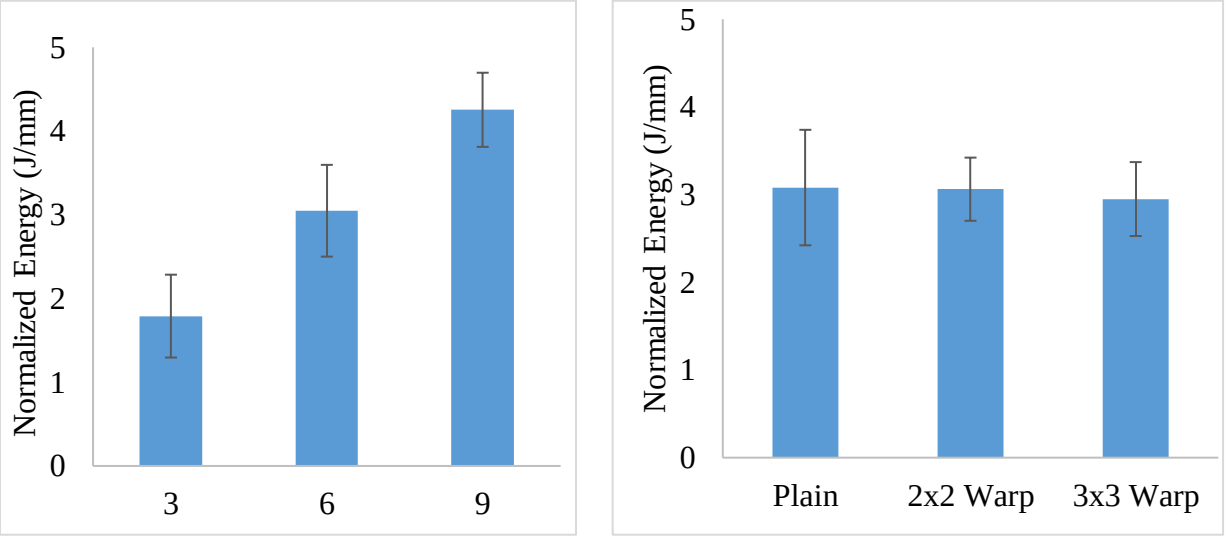

(a) (b)

Figure 5.14 (a) Main effect of number of layers on Tup impact energy normalized by composite thickness, (b) Main effect of weave on Tup impact energy normalized by composite thickness.

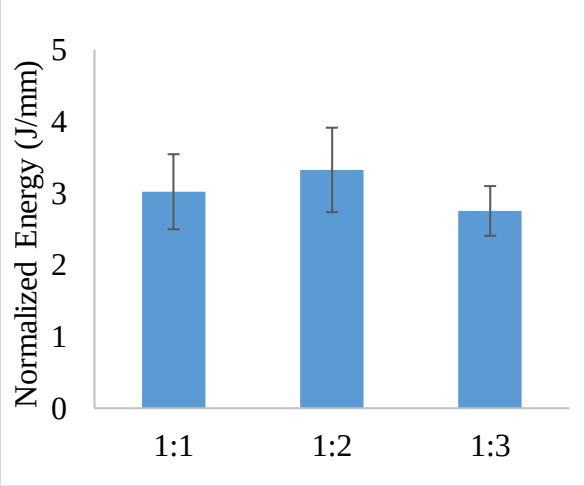

Figure 5.15. Main effect of Z to Y ratios on Tup impact energy normalized by composite thickness.

The second approach used was to normalize the total energy using composite areal density. This will help in comparing results from different samples. The graphs comparing the structural parameters are shown in Figure 5.16 (a, b) and Figure 5.17.

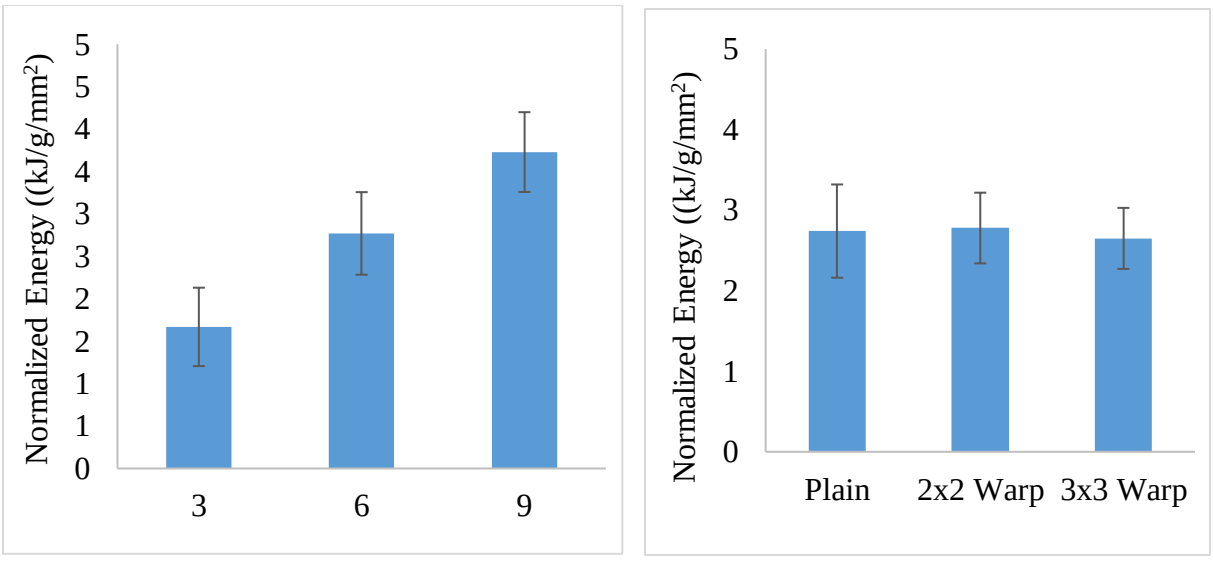

(a) (b)

Figure 5.16 (a) Main effect of number of layers on Tup impact energy normalized by composite areal density, (b) Main effect of weave on Tup impact energy normalized by composite areal density.

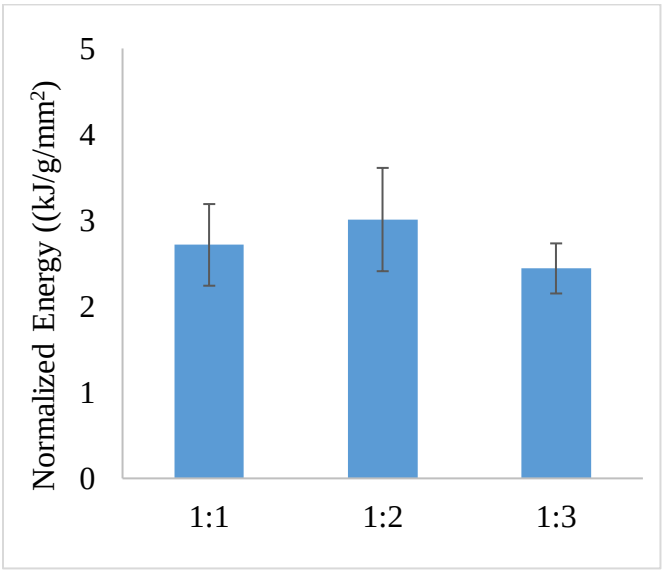

Figure 5.17. Main effect of Z to Y ratio on Tup impact energy normalized by composite areal density.

The third approach was normalized using preform areal density. The results of the impact energy normalized by the preform areal density are depicted in Figure 5.18 (a, b) and Figure 5.19.

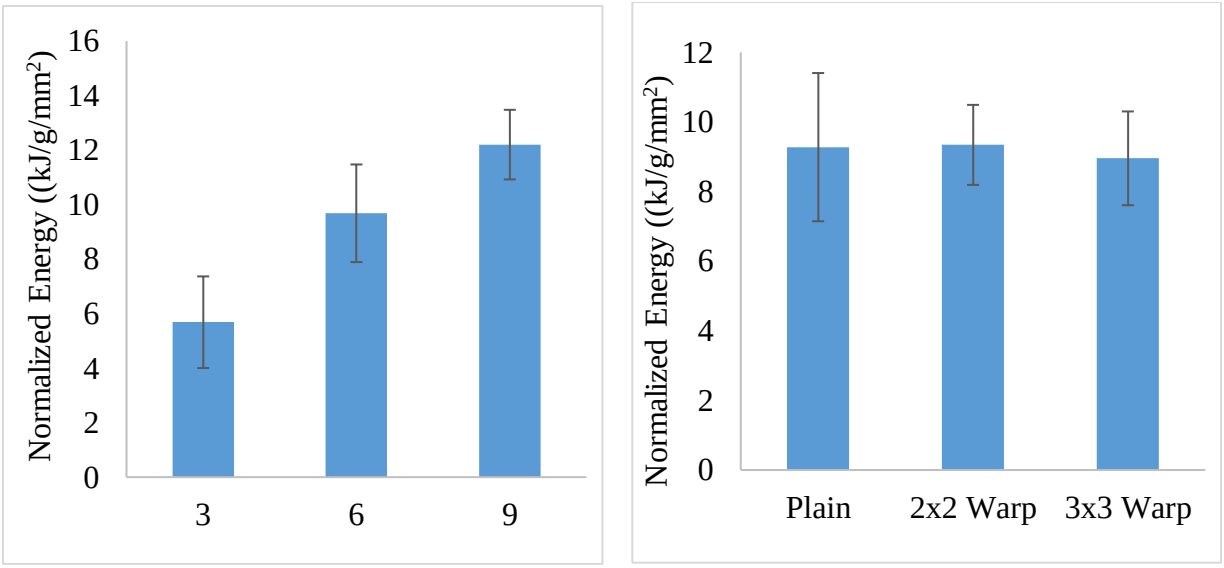

(a) (b)

Figure 5.18 (a) Main effect of number of layers on Tup impact energy normalized by preform areal density, (b) Main effect of weave on Tup impact energy normalized by preform areal density.

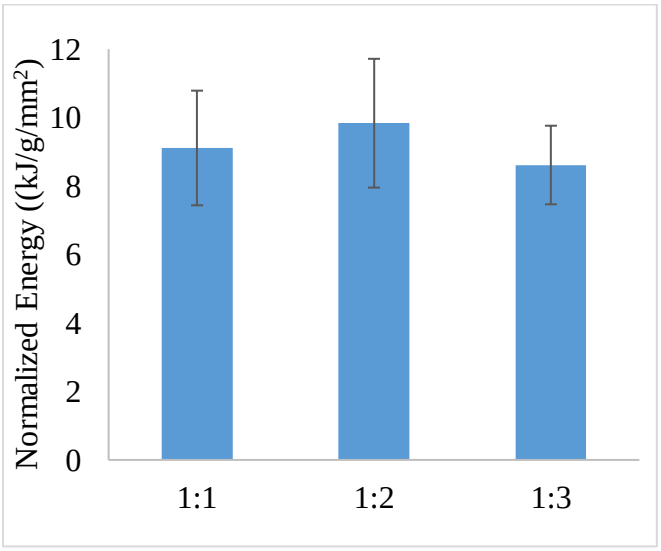

Figure 5.19. Main effect of Z to Y ratio on Tup impact energy normalized by preform areal density.

Appendix 24 shows the main effect of increasing the number of Y-yarn layers on the total energy normalized by the composite thickness, increasing the number of layers increased the normalized energy. Appendix 23 shows the main effect of the structural parameters on the normalized energy value. The results from a non-normalized value where the penetration energy

is compared are similar to the energy normalized by thickness. The layers were significantly different and are the main factor, which influences composite performance as shown in Appendix 24. However, the effect of the Z to Y ratio on normalized impact energy did not show any significant difference illustrated in Appendix 26. The only noticeable difference is the decrease in a p-value for the Z to Y ratio as shown in the Table 5.6.

Table 5.6. Comparison of the p-value of total energy and p-value of energy normalized by the thickness.

Ratio	**P-value (total energy, J)**	**P-value (energy normalized by thickness, J/mm)**
1:1	0.96	0.28
1:2	1.00	0.62
1:3	0.98	0.83

The effect of weave design on normalized impact energy remained unchanged when compared with normalized value with the non-normalized energy, shown in Appendix 25.

Thus, it can be concluded that the total energy normalized by the composite thickness generally reduced the effect of altering the structural parameters except weave design which remains mostly unchanged. However, the alteration in the number of layers or thickness and Z to Y ratio indicated that these parameters have a significant effect on the composite impact penetration energy normalized by thickness. Additionally, it indicated that increasing the number of layers didn't change the resin flow in the preform during resin infusion because if increasing the number of layers reduced the normalized impact energy, then there would be defects associated with increasing the number of layers.

The results of the total energy were normalized by the composite areal density shows similar trends. Total penetration energy is normalized by composite areal density in order to exclude the effect of composite weight. This will give a fair comparison between all the samples irrespective of the weight. Appendix 27 shows the main effect of the structural parameters on the total penetration energy normalized by composite areal density. The effect of decreasing Z to Y ratio in the structure resulted in a significant change in Tup impact. Tukey output, illustrated in Appendix 30, shows that even though the ratio of Z to Y is still insignificant as compared to the non-normalized energy, the p-value has significantly gone down as indicated in Table 5.7.

Table 5.7. Comparison of the p-value of total energy and p-value of energy normalized by composite areal density.

Ratio	P-value (total energy, J)	P-value (energy normalized by Composite areal density, kJ/g/mm^2)
1:1	0.96	0.24
1:2	1.00	0.44
1:3	0.98	0.92

Thus, it can be concluded that the total energy normalized by the composite areal density generally reduced the effect of altering the structural parameters except weave design which remains mostly unchanged (Appendix 29). However, the alteration in the number of layers or thickness and Z to Y ratio indicated that these parameters have a significant effect on the impact penetration energy normalized by composite areal density. The effect of changing the weave pattern on Tup impact energy remains unchanged in which 2x2 warp rib shows the highest mean followed by 3x3 warp rib and plain weave (see Appendix 29).The responses were very similar to the responses of the previous case when the energy was normalized by the composite thickness. Thus, it can be concluded that the composite thickness and composite weight (represented by composite areal density) has a similar effect on the total penetration energy where thickness or number of layers has the most significant effect on the energy, as shown in Appendix 28.

Lastly, total penetration energy was normalized using preform density. The concept is similar to the previous normalization except preform density was used in order to eliminate the effect of the preform weight from the analysis. This will give a fair chance of a comparison between all the samples irrespective of the original preform weight. The analysis shows no major shift in trends in terms of a number of layers, change in weave design and change in Z to Y ratio. Unlike the previous normalization with composite areal density where there was a significant drop in p-value in terms of Z to Y ratio, normalization using preform density only shows a slight decrease in the p-value. This suggests that normalization using preform density has less effect on total penetration energy. The ANOVA output shows that parameter estimates still suggests Z to Y ratio is significantly different so changing the ratio impacts the overall energy. The same is

true for a number of layers and had the most significant effect on impact energy. ANOVA and Tukey outputs are listed in Appendices 8.31, 8.32, 8.33 and 8.34.

5.1.2.2. Charpy Impact – result and discussion

The Charpy impact is a low impact destructive test where a hammer is used to break the specimens. In this test, the tested specimen is supported as a simple beam. Then the hammer is released from a position with known potential energy to impact the specimen in the middle and the energy absorbed by the sample is reported. The test was performed both in X- and Y-direction to understand the performance in terms of the reinforcement in X- and Y-directions. The X-direction specimens indicate impact resistance of X-yarns whereas the Y-direction specimens specify impact resistance on Y- and Z- yarns combined. The overall failure analysis indicates higher impact resistance in X-direction compared to Y-direction impact energy. The results of the Charpy impact test in both Y- and X- direction is listed in Table 5.8 and 5.9, respectively.

Table 5.8. Charpy impact test results – Warp direction.

Sample ID	Thickness (mm)	Preform Areal Density (g/m^2)	Composite Areal Density (g/m^2)	Energy (J)	CV, %	Energy/ thickness, J/mm	Energy Normalized by Comp. Areal Density ($kJ/g/mm^2$)	Energy Normalized by Preform Areal Density ($kJ/g/mm^2$)
1	2.67	888.81	2835.37	0.42	21.90	0.16	0.15	0.48
2	2.70	885.17	2813.89	0.36	18.72	0.13	0.13	0.41
3	2.77	868.82	2826.10	0.31	16.40	0.11	0.11	0.35
4	2.83	915.89	3076.36	0.38	26.80	0.13	0.12	0.41
5	2.89	915.65	3082.46	0.36	23.25	0.13	0.12	0.40
6	2.71	978.72	2966.49	0.41	17.25	0.15	0.14	0.42
7	2.78	855.39	3028.47	0.31	23.66	0.11	0.10	0.36
8	2.73	850.10	2967.90	0.32	22.98	0.12	0.11	0.37
9	2.63	881.96	2749.85	0.23	14.37	0.09	0.08	0.26
10	5.06	1632.76	5499.60	0.54	11.43	0.11	0.10	0.33
11	5.15	1648.20	5615.58	0.71	17.06	0.14	0.13	0.43
12	4.96	1656.96	5798.69	0.68	20.11	0.14	0.12	0.41
13	4.91	1623.53	5469.08	0.85	27.86	0.17	0.15	0.52
14	4.88	1629.19	5377.53	0.61	20.82	0.13	0.11	0.38
15	5.02	1693.40	6018.43	0.77	24.23	0.15	0.13	0.45
16	4.95	1640.00	6123.56	0.69	33.27	0.14	0.11	0.42
17	5.09	1598.16	5741.97	0.71	17.16	0.14	0.12	0.44
18	4.86	1582.11	5548.15	0.54	21.79	0.11	0.10	0.34
19	7.05	2706.06	8325.70	1.10	17.49	0.16	0.13	0.41
20	7.54	2648.20	8856.74	0.83	17.47	0.11	0.09	0.31
21	7.39	2661.36	8607.43	1.10	15.64	0.15	0.13	0.41
22	7.39	2661.36	8607.43	1.10	21.42	0.15	0.13	0.41
23	7.19	2602.81	8472.20	0.91	20.22	0.13	0.11	0.35
24	7.17	2655.30	8258.56	0.83	18.97	0.12	0.10	0.31
25	7.46	2428.77	8849.18	0.90	14.68	0.12	0.10	0.37
26	7.38	2483.07	8740.16	0.90	16.18	0.12	0.10	0.36
27	7.23	2435.68	7928.53	0.80	13.32	0.11	0.10	0.33

Table 5.9. Charpy impact test results – Weft direction.

Sample ID	Thickness (mm)	Preform Areal Density (g/m^2)	Composite Areal Density (g/m^2)	Energy (J)	CV, %	Energy/ thickness, J/mm	Energy Normalized by Comp. Areal Density ($kJ/g/mm^2$)	Energy Normalized by Preform Areal Density ($kJ/g/mm^2$)
2	2.83	885.17	2862.72	1.40	19.97	0.49	0.49	1.58
3	3.06	868.82	2862.72	0.79	24.59	0.26	0.28	0.91
4	2.84	915.89	3106.88	0.93	12.12	0.33	0.30	1.01
5	3.08	915.65	2942.07	0.77	21.44	0.25	0.26	0.84
6	2.89	978.72	2960.39	1.06	7.17	0.37	0.36	1.08
7	2.89	978.72	2960.39	1.06	24.95	0.37	0.36	1.08
8	2.82	850.10	2889.16	0.89	23.54	0.32	0.31	1.05
9	2.80	881.96	2858.87	0.65	22.87	0.23	0.23	0.74
10	5.05	1632.76	5548.43	1.49	12.36	0.29	0.27	0.91
11	5.11	1648.20	5719.34	1.45	28.90	0.28	0.25	0.88
12	5.62	1656.96	5853.63	1.52	25.37	0.27	0.26	0.92
13	5.13	1623.53	5694.93	1.66	11.08	0.32	0.29	1.02
14	4.93	1629.19	5316.49	1.35	22.91	0.27	0.25	0.83
15	5.22	1693.40	5835.32	1.74	25.36	0.33	0.30	1.03
16	5.06	1640.00	6184.13	1.32	7.92	0.26	0.21	0.80
17	5.21	1598.16	5651.12	1.50	21.55	0.29	0.26	0.94
18	5.09	1582.11	5517.87	1.35	28.63	0.27	0.24	0.85
19	7.08	2706.06	8606.48	1.95	16.16	0.28	0.23	0.72
20	7.76	2648.20	8911.68	2.14	21.89	0.28	0.24	0.81
21	7.51	2641.10	8618.69	1.91	18.59	0.25	0.22	0.72
22	7.13	2661.36	8453.89	1.97	4.39	0.28	0.23	0.74
23	7.14	2602.81	7544.41	1.68	8.99	0.23	0.22	0.64
24	7.22	2655.30	8228.04	1.77	15.46	0.24	0.21	0.66
25	7.35	2428.77	8661.42	1.94	9.38	0.26	0.22	0.80
26	7.47	2483.07	8746.21	2.28	8.85	0.30	0.26	0.92
27	7.34	2435.68	8443.37	2.13	24.80	0.29	0.25	0.87

The Charpy test is subject to four types of break namely complete, hinged, and partial or non-break as listed in table 5.10. However, for this research only specimens with complete or hinge break were considered for the failure analysis.

Table 5.10. Types of Charpy break along with description.

Symbol	Break Type	Description
C	Complete	Specimen breaks into two or more pieces
H	Hinged	A stable cracking where part of the impacted specimen cannot support itself when held vertically
P	Partial	A stable cracking of at least 90% of the width of the specimen
N	Non-break	An incomplete or no break where no valid result is available

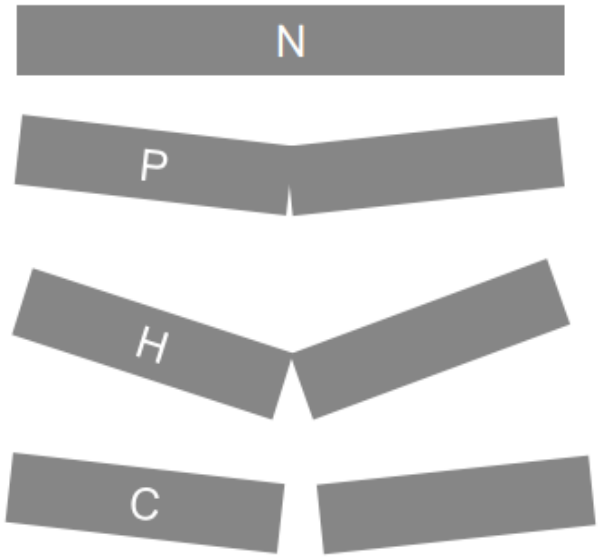

Figure 5.20 (a) Type of breaks in Charpy (b) Specimens showing complete and hinge break

Almost all of the 275 specimens tested showed complete or hinge break as shown in figure 5.20 (b). The test results of the Charpy impact were derived from 135 specimens from warp direction and 135 specimens from weft direction. The test data was analyzed to investigate the effect of structural variables including a number of layers (thickness), Z to Y ratio and weave design, on total energy. The analysis was based on the univariate analysis of variance, which was further confirmed by the Tukey test. The ANOVA analysis was done both in X (weft) and Y (warp) directions. The statistical analyses output for warp and weft direction specimens are listed

in Appendices 35 and 51. Also, the graphs highlighting the main effects of each of the structural parameters are listed in Figures 5.21(a, b) and 5.22.

Figure 5.21 (a) shows that changing the number of layers (thickness) has significantly increased the total impact energy (Appendix 36). However, changing the weave design and Z to Y ratio did not significantly altered the total impact as shown in Figure 5.21 (b) and Figure 5.22. In order to prove the observation, ANOVA and Tukey test were performed. According to ANOVA test, Appendix 35, it was confirmed that there is no significant difference between Z to Y ratio which proves that changing Z to Y ratio does not significantly change total impact energy. Likewise, it was also confirmed that there is no significant difference between weave designs, which proves that changing the weave pattern does not significantly change total impact energy. It was further confirmed by Tukey test, which shows no significant difference between different levels of ratio shown in Appendix 38. Additionally, changing the weave pattern had shown no significant effect on the total energy as illustrated in Appendix 37, which was confirmed by performing a post hoc test.

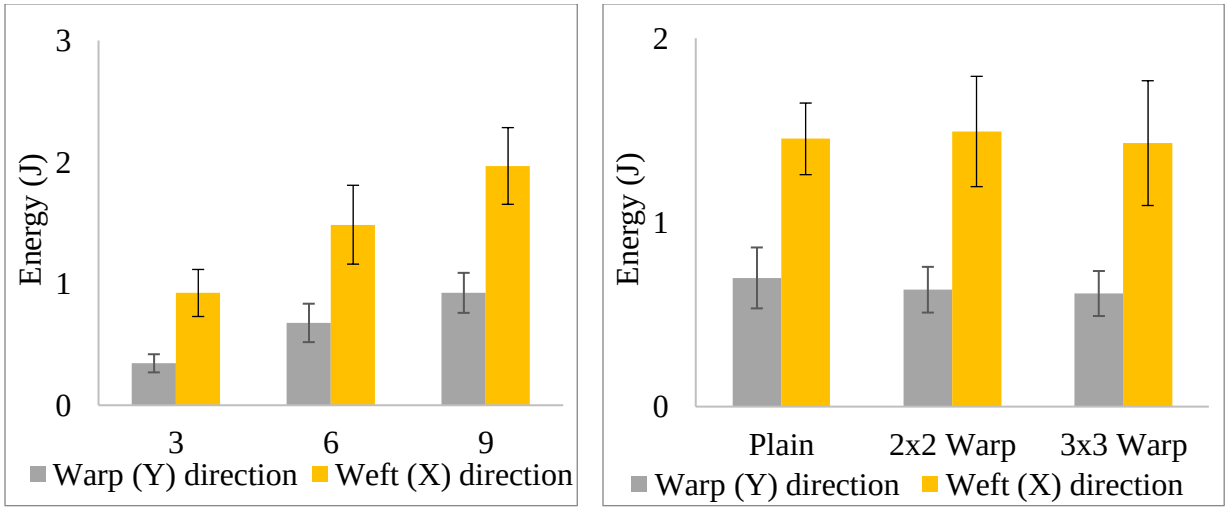

(a) (b)

Figure 5.21 (a) Main effect of number of layers on Charpy impact energy, (b) Main effect of weave on Charpy impact energy.

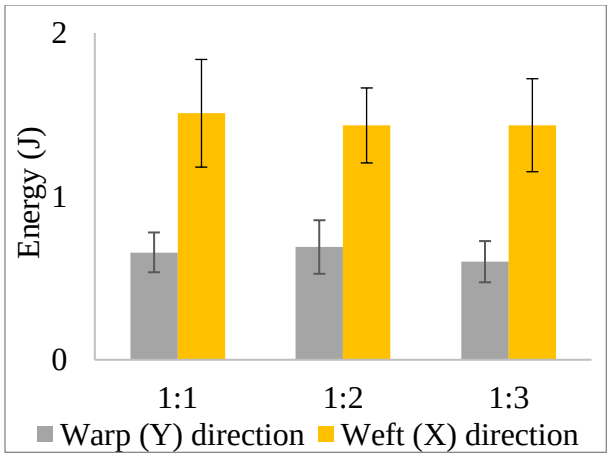

Figure 5.22. Main effect of Z to Y ratio contribution on Charpy impact energy.

The results of the total Charpy energy in the Y-yarn and X-yarn direction were normalized using three different normalization approaches including composite thickness, composite areal density, and preform areal density. The results of the statistical analysis of the total energy normalized by thickness in the Y-yarn and X-yarn direction are listed in Appendices 39 and 55.

Figure 5.23(a) illustrates the main effect of increasing the number of layers on the total energy normalized by composite thickness along with the effect of weave, in Figure 5.23(b) and effect of Z to Y ratio (Figure 5.24) for both X- and Y- yarn direction. All the layers levels show a similar impact energy. This is also proved in the ANOVA, which illustrates that when normalized by thickness, number of layers is not significantly different from each other. The Tukey output, shown in Appendix 40 also consistent with the ANOVA results. As for the effect of changing the Z to Y ratio is concerned, it was still found to have no significant difference similar to the non-normalized value as shown in Appendix 41. On the other hand, changing the weave pattern also show an insignificant effect on the normalized energy as shown in Appendix 42. However, the p-value of normalized energy compared to the non-normalized value is lowered. The trend is like Tup impact. Thus it can be concluded that normalizing the total energy by the composite thickness, reduced the significance of the number of layers, Z to Y ratio and weave pattern.

Tukey analysis illustrates that when normalized by thickness, number of layers does not have significant effect on energy as shown in Appendix 56. As for the effect of changing the Z to

Y ratio and weave pattern, it was still found to have no significant difference on the normalized energy as shown in Appendices 57 and 58, respectively. However, the p-value of normalized energy compared to the non-normalized value is lowered. The trend is similar to the warp (Y) direction impact results.

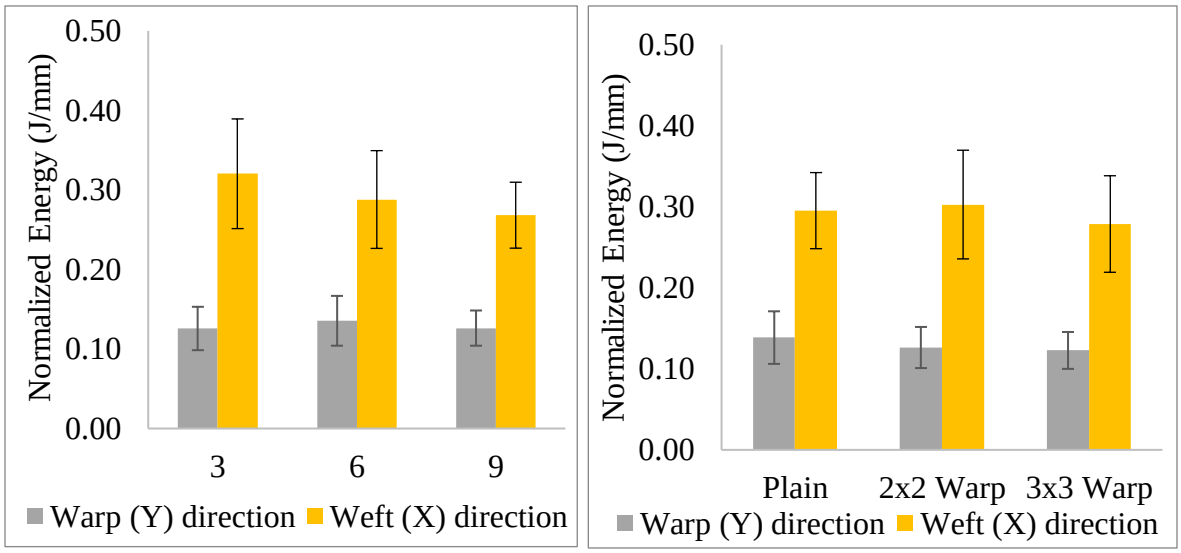

(a) (b)

Figure 5.23 (a) Main effect of number of layers on Charpy impact energy normalized by composite thickness, (b) Main effect of weave on impact energy normalized by composite thickness

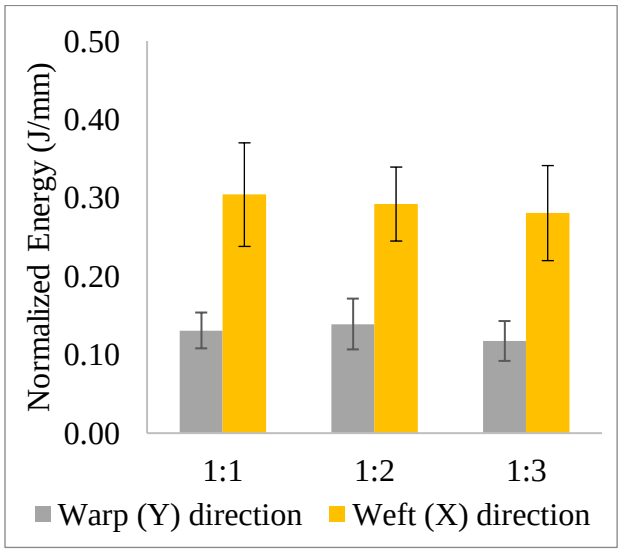

Figure 5.24. Main effect of Z to Y ratio on Charpy impact energy normalized by composite thickness

The results of the total energy were normalized by the composite areal density show similar trends. Figure 25 (a, b) and Figure 26 show the main effect of the structural parameters on the total penetration energy normalized by composite areal density for both X-yarn and Y-yarn direction. The effect of Z to Y ratio on normalized impact energy was statistically insignificant in both X and Y direction. Tukey output shows that even though the ratio of Z to Y is still insignificant as compared to the non-normalized energy, the p-value has significantly lowered (Appendix 45).

There was significant effect of number of layers (thickness) and Z to Y ratio on Charpy impact energy normalized by composite areal density however there was no significant effect of weave design in warp direction as shown in Appendix 43 However, the alteration in the number of layers or thickness indicated that the parameter has a significant effect on the composite impact energy normalized by thickness as shown in Appendix 44. The effect of changing the weave pattern on normalized impact energy remains unchanged where plain weave shows the highest mean followed by 2x2 warp rib and 3x3 warp rib as illustrated in Appendix 46. The Z to Y ratio on normalized energy was significantly different for 1:2 and 1:3 ratio (Appendix 45).

The ANOVA result of Charpy energy for weft yarns shows the effect of layers on the normalized value of impact energy is significantly different (Appendix 59) which is also confirmed by Tukey output in Appendix 60. The effect of Z to Y ratio and weave on normalized energy remains statistically insignificant as show in Appendices 61 and 62, respectively.

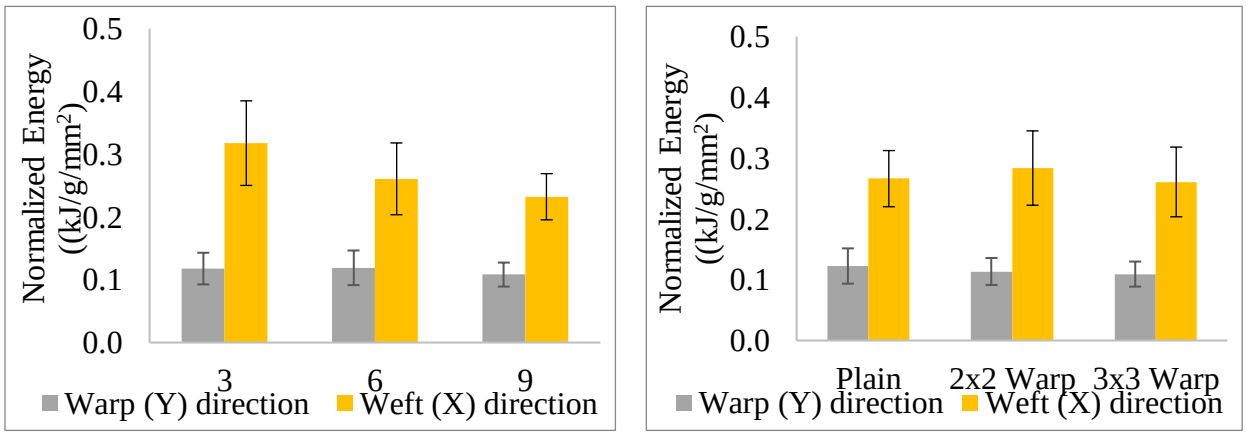

(a) (b)

Figure 5.25 (a) Main effect of number of layers on Charpy impact energy normalized by composite areal density, (b) Main effect of weave on Charpy impact energy normalized by composite areal density.

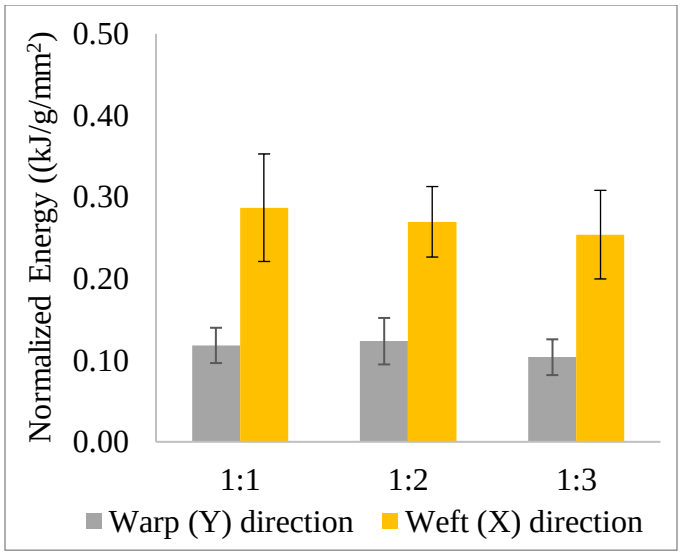

Figure 5.26. Main effect of Z to Y ratio contribution on Charpy impact energy normalized by composite areal density.

Figure 27 (a, b) and Figure 28 shows the main effect of the structural parameters on the total penetration energy normalized by preform areal density in both warp and weft direction. The analysis shows no major shift in trends in terms of number of layers, Z to Y ratio and weave design in warp direction as shown in Appendices 48, 49 and 50, respectively. Unlike the previous normalization with composite areal density where there was a significant drop in p-value in terms of Z to Y ratio. Normalization using preform density only shows a slight decrease in the p-value. This suggests that normalization using preform density has less effect on the total penetration energy. The effect of Z to Y ratio on normalized impact energy was statistically significant as suggested in Appendix 47. The same is true for a number of layers and had the most significant effect of impact energy. The ANOVA and Tukey results for Charpy energy normalized by preform density show similar result as shown in Appendices 63, 64, 65 and 66.

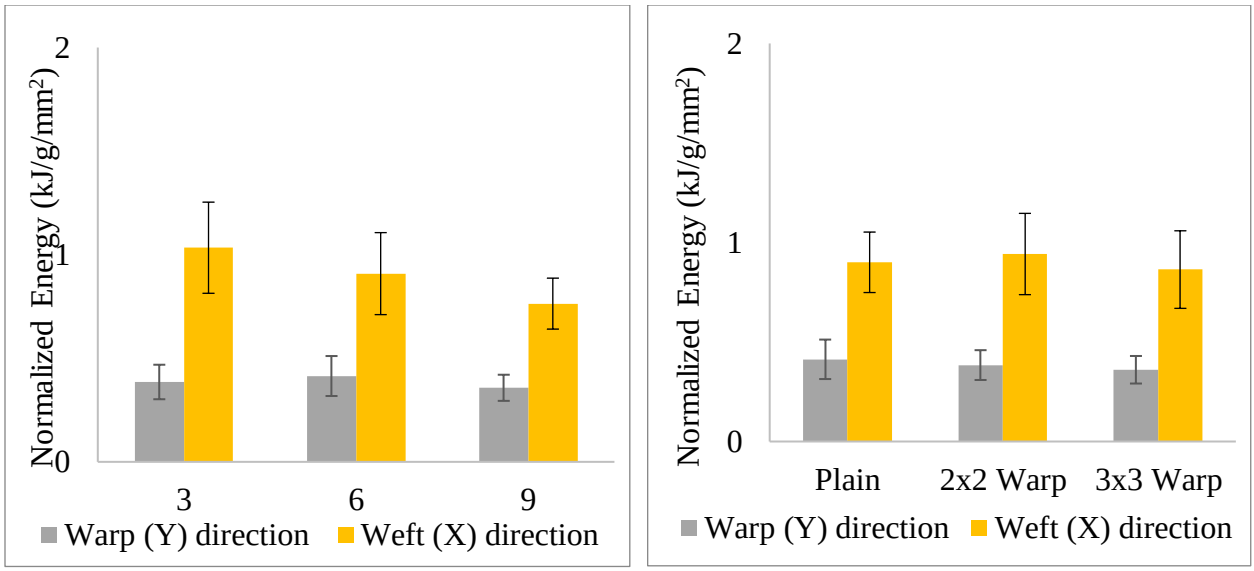

(a) (b)

Figure 5.27 (a) Main effect of number of layers on Charpy impact energy normalized by preform areal density, (b) Main effect of weave on Charpy impact energy normalized by preform areal density.

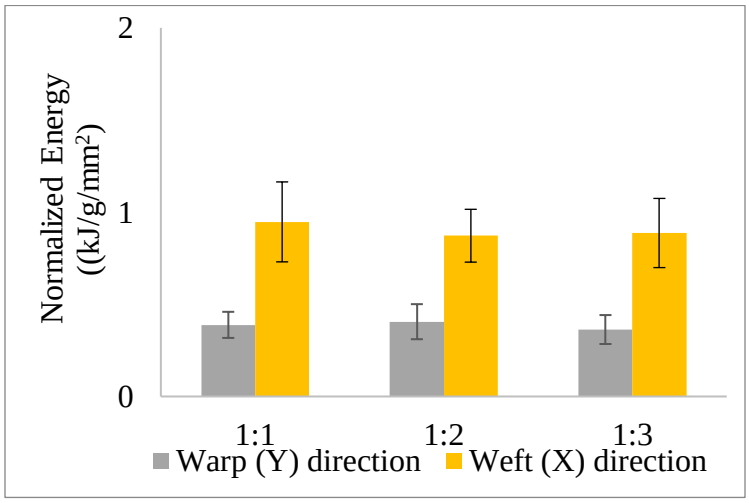

Figure 5.28. Main effect of Z to Y ratio contribution on Charpy impact energy normalized by preform areal density.

5.1.2.3. Comparison of impact properties of hemp composites with glass composites

Similar to the tensile properties comparison, impact properties of HFR composites were compared with GFR composites in terms of Tup and Charpy. The impact energy of hemp and glass was used for comparison along with normalized value in terms of thickness, composite

areal density and preform areal density as shown in Table 5.11. The data was derived from Midani's dissertation (Midani, 2016). The total penetration energy for E-glass and hemp are comparable alongside with energy normalized by preform areal density. However, Charpy impact energy for hemp was lower than e-glass.

Table 5.11. Comparison of impact (Tup and Charpy) properties of hemp-fiber composites with glass-fiber composites.

	Tup			
Fiber	**Total energy, J**	**Normalized by thickness, J/mm**	**Normalized by composite areal density, kJ/g/mm^2**	**Normalized by preform areal density, kJ/g/mm^2**
E-glass	26 - 70	13.5 - 19.8	7.5 - 10.6	10.5 - 15.2
Hemp	3.1 - 33	1.1 - 5.1	1.1 - 4.2	3.5 - 13.4
	Charpy - Warp			
Fiber	**Total energy, J**	**Normalized by thickness, J/mm**	**Normalized by composite areal density, kJ/g/mm^2**	**Normalized by preform areal density, kJ/g/mm^2**
E-glass	2.2 - 11.5	1.2 - 3.6	0.7 - 1.9	0.9 - 2.6
Hemp	0.2 - 1.1	0.1 - 0.2	0.1 - 0.2	0.3 - 0.5
	Charpy - Weft			
Fiber	**Total energy, J**	**Normalized by thickness, J/mm**	**Normalized by composite areal density, kJ/g/mm^2**	**Normalized by preform areal density, kJ/g/mm^2**
E-glass	2.6 - 13	1.3 - 3.7	0.8 - 2.1	1.2 - 2.9
Hemp	0.7 - 2.3	0.2 - 0.5	0.2 - 0.5	0.6 - 1.6

5.1.2.4. Conclusion – Tup & Charpy

Tup

In the Tup impact test, it can be concluded that the effect of changing the number of layers increased the total impact energy significantly. The effect of weave has no significant effect on the penetration energy. The weave pattern had a minimal effect on the total energy with 2x2 warp rib being the highest followed by 3x3 warp rib and plain. The effect of a change in Z to Y ratio is significantly different however, the results are different in Tukey analysis where it shows that the change in Z to Y ratio does not significantly change the energy and ratio 1:1, 1:2

and 1:3 are not different from each other. Regardless of the normalization technique, the number of layers significantly influences the composite Charpy impact energy. The effect of changing the Z to Y ratio in the structure and changing the weave pattern has less influence on the overall penetration energy.

Charpy

In the case of Charpy impact energy, it can be concluded that increasing the number of layers or thickness, increased the total energy in both warp and weft directions. However the weave pattern and Z to Y ratio contribution do not have a significant effect on the impact energy for both warp (Y) and Weft (X) direction. The analysis is similar in both ANOVA and Tukey results. However, after normalizing the total penetration energy, the effects of the structural parameters became less significant with lower p-values. The number of layers have significant effect on the normalized impact energy including normalized by thickness, composite areal density and preform areal density. The effect of changing the Z to Y ratio in the structure, and changing the weave pattern has less influence on the overall normalized impact energy. The impact energy in the X-yarn direction was generally higher than that of the Y-yarn direction, and they remained significant even after the normalization. This is because there are number of yarns in weft (X) direction that warp (Y) direction which provide resistance to the impact energy as X-yarns have higher yarn tenacity compared to Y- yarns (Appendix 83).

Moreover, Tup energy levels are overall higher than the Charpy impact as Tup is a high impact energy test compared to Charpy, which is a low impact energy test. The other reason for the difference in the energy levels is because of the way the specimens are placed during the test. The Tup impact is a flexed plate impact test, where the sample is supported as a flat plate laying horizontally, and the strike mode is on the flat face. Tup impact specimens are independent of the yarns orientation as they are square (101.6 mm x 101.6 mm) and all yarn contributes to the impact resistance mutually. Hence, the energy required to puncture the specimen is much higher compared to Charpy impact test, due to the combined effect of X-, Y- and Z- direction yarns. The role of Z to Y ratio is particularly significant in Tup impact since it strengthens through-thickness properties, damage tolerance and the delamination resistance of the 3DOW composite. On the other hand, the Charpy is a flexed beam test, where the specimens are placed on a simple beam and then a swinging pendulum strikes the specimen on the longer side of the specimen. In

such a case, the impact resistance only comes either from Y- and Z- yarns in case of warp direction impacts or from X- yarns in case of weft direction impact.

5.1.3. Compression test

The combines loading compression (CLC) governs compression and stiffness properties of the composite panels. This test was specifically applicable to a balanced and symmetric structure which fits perfect with the samples. This research used untabbed specimens due to its low strength and its orthotropic (elastic properties in two or three planes perpendicular to each other). This test represents a combination of end loading and shear-loading where the main goal is to induce optimum shear loading so that the end loading does not crush the specimens at the ends. Figure 5.29 represents possible failure schematics and three-part failure identification codes in the CLC test. Most of the specimens tested fall into the category of the accepted failure mode (BGM or HAT) as shown is Appendix 85. Appendix 88 shows graphs of every specimen from samples 1 through 27 both in warp and weft direction.

Compression properties of 3D orthogonal properties with different fiber volume fraction and different structural parameters including a number of Y-yarns layers or thickness, through-thickness reinforcing fibers (Z-binders) contribution and weave pattern were analyzed. CLC test is a destructive test, which is intended to measure the peak load, modulus, and compression stress.

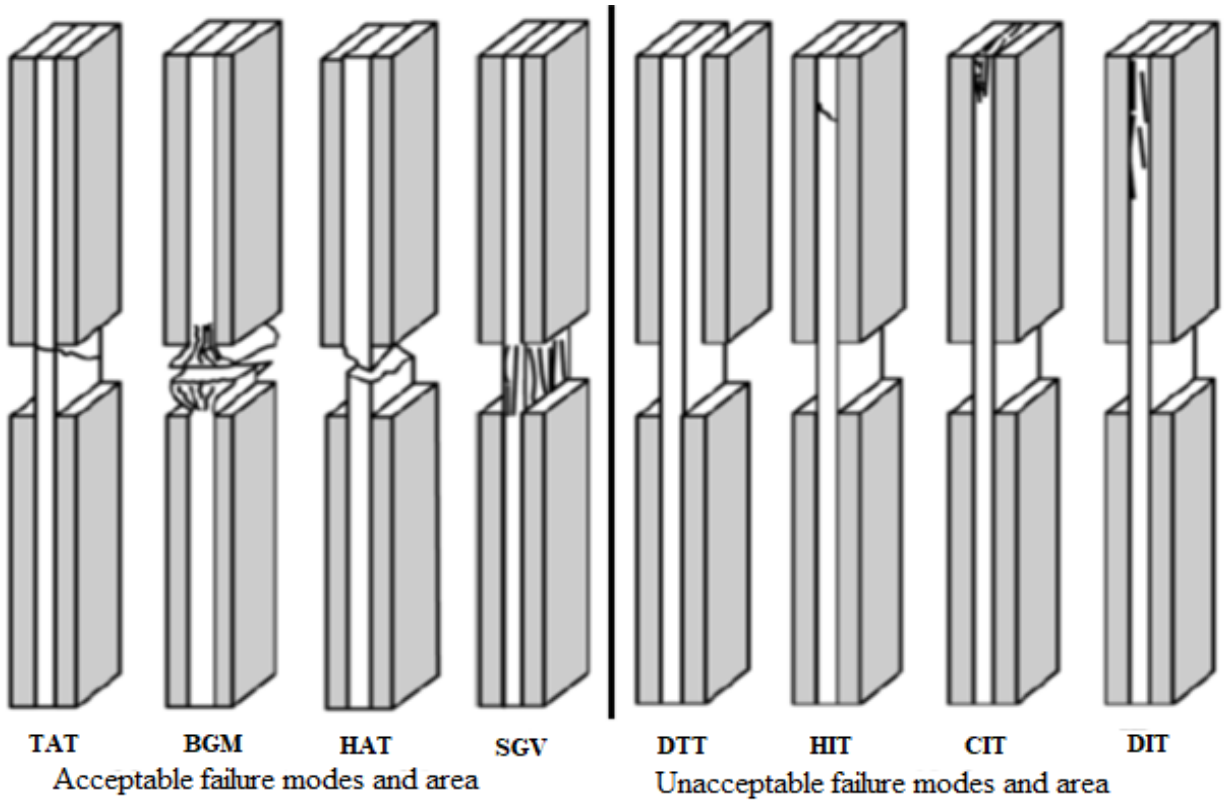

First character	Second character	Third character
B - Brooming	A - At grip/tab	T - Top
C - end Crushing	G - Gage	M - Middle
D - Delamination	I - Inside grip/tab	V - Various
H - tHrough thickness	T - Tab adhesive	
S - long Splitting		
T - Traverse shear		

Figure 5.29. Failure schematics and three-part failure identification codes in the CLC test (ASTM D6110).

A total of 128 specimens (27x5-7 defective specimens) in warp direction and 129 specimens (27x5-6 defective specimens) in weft (X-yarn) direction were analyzed using ANOVA and Tukey HSD to investigate the effect of the structural parameter on compression properties. The results of the CLC test from samples 1 through 27 in warp (Y) direction are listed in Table 5.12. The weft (X) direction compression data is shown in Table 5.13. The peak point and the breaking load corresponded to the same point and therefore, the peak load was generally

used to characterize the compression behavior of the composite in this analysis. Figure 30 shows a typical CLC test specimen set-up (a) and crushed specimen (b) after the test.

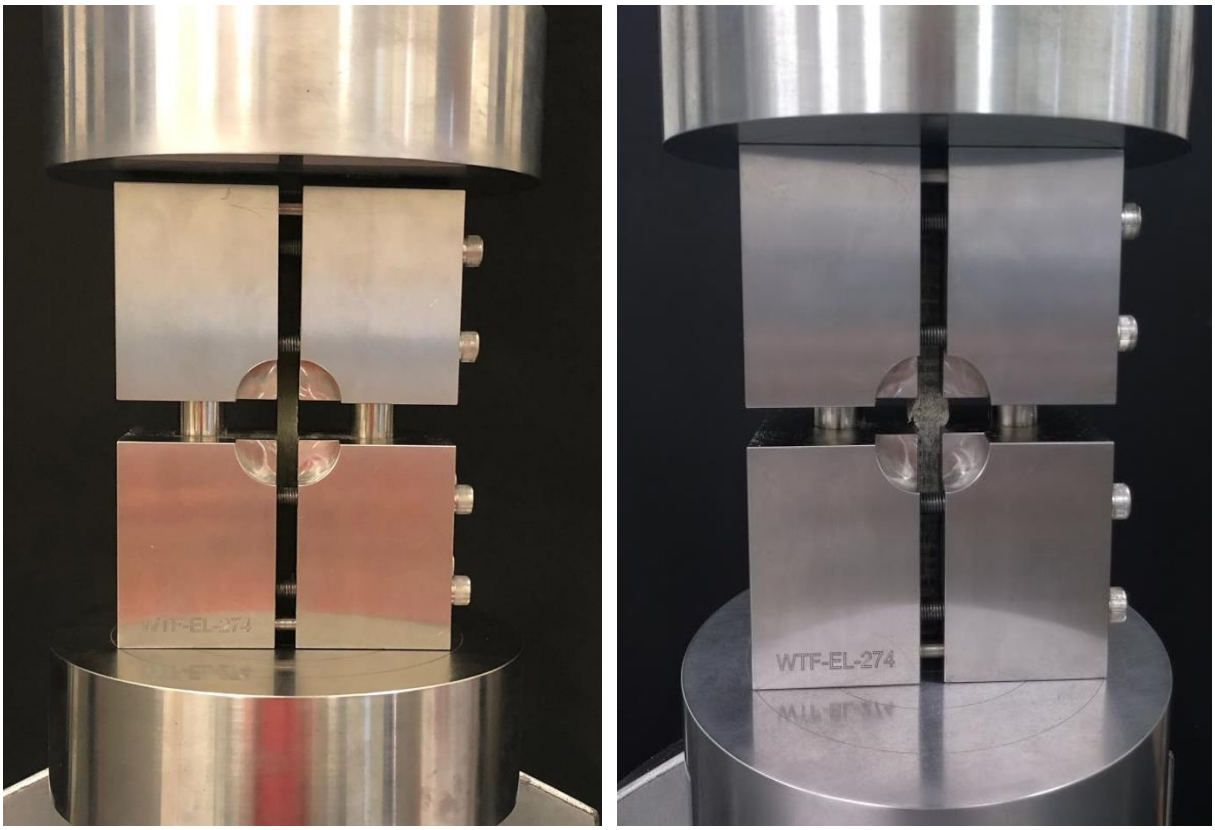

(a) (b)

Figure 5.30 (a) CLC test specimen set-up, (b) Crushed specimen after CLC test.

Table 5.12. Compression test results – Warp direction.

Sample ID	Composite areal density, g/m^2	Modulus, GPa	Peak compression stress, MPa	PEAK LOAD, N	Thickness, mm	Load normalized by composite thickness (N/mm)	Load normalized by composite areal density (kN/(g/mm^2))
1	2862.6	0.7	54.2	1910.7	2.7	704.5	1.3
2	2785.7	0.5	42.3	1480.1	2.7	549.7	0.9
3	2692.3	0.5	45.3	1613.3	2.7	589.3	1.1
4	3214.3	0.5	56.0	2089.4	2.9	728.6	1.5
5	3087.9	0.4	65.8	2551.0	3.0	855.2	1.9
6	2989.0	0.5	45.4	1736.3	3.0	590.1	1.2
7	2961.5	0.6	59.4	2229.3	2.9	772.6	1.6
8	3335.2	2.9	23.1	1690.3	2.9	588.0	1.1
9	2703.3	2.3	20.6	1494.2	2.9	524.5	1.0
10	5395.6	0.3	87.8	4380.8	5.2	847.6	5.6
11	5516.5	0.3	94.7	6310.3	5.1	1231.7	8.4
12	5730.8	0.3	108.0	7084.3	5.1	1403.8	9.6
13	5263.7	0.3	75.5	4742.1	4.8	981.5	6.0
14	5478.0	0.3	71.6	4497.2	4.8	930.2	5.5
15	6428.6	0.2	96.8	6453.6	5.1	1258.1	8.3
16	5549.5	0.4	82.0	5256.9	4.9	1065.4	6.6
17	5527.5	0.4	89.8	5912.0	5.0	1168.0	7.7
18	5587.9	0.3	85.9	5412.9	4.8	1116.1	6.8
19	8401.1	0.3	101.2	9429.6	7.2	1315.7	17.0
20	8631.9	0.3	107.2	10358.2	7.4	1393.5	20.5
21	8604.4	0.3	99.5	9652.8	7.5	1293.1	19.0
22	8593.4	0.3	99.3	9464.5	7.3	1291.2	18.0
23	8230.8	0.3	102.3	9760.6	7.3	1330.2	17.5
24	8395.6	0.3	122.0	11770.2	7.4	1586.3	22.1
25	8796.7	0.3	92.7	8918.9	7.4	1205.0	17.6
26	8549.5	0.3	116.7	11056.1	7.3	1517.0	21.3
27	8478.0	0.3	113.0	10500.4	7.2	1468.5	20.1

Table 5.13. Compression test results – Weft direction.

Sample ID	Composite areal density, g/m^2	Modulus, GPa	Peak compression stress, MPa	PEAK LOAD, N	Thickness, mm	Load normalized by composite thickness (N/mm)	Load normalized by composite areal density ($kN/(g/mm^2)$)
1	2857.1	0.9	53.8	1938.4	2.8	699.4	1.3
2	2895.6	0.7	42.5	1602.2	2.9	552.9	1.0
3	2901.1	0.7	62.4	2514.7	3.1	811.3	1.7
4	3049.5	0.6	63.8	2405.3	2.9	829.3	1.7
5	3104.4	0.7	63.4	2515.5	3.0	823.7	1.8
6	2901.1	0.7	59.4	2264.6	2.9	772.1	1.5
7	3115.4	0.7	61.8	2204.6	2.7	803.3	1.6
8	2945.1	0.8	72.3	2629.4	2.8	940.4	1.8
9	2862.6	0.9	66.6	2442.1	2.8	866.4	1.6
10	5670.3	0.3	90.8	5952.9	5.1	1180.5	7.6
11	5307.7	0.4	85.6	5694.5	5.1	1112.7	7.6
12	5769.2	0.4	93.9	6678.3	5.4	1221.0	9.0
13	5511.0	0.4	84.5	5703.9	5.3	1098.3	7.2
14	5302.2	0.3	87.2	5613.8	5.0	1133.2	6.9
15	5576.9	0.3	78.0	5167.0	5.1	1014.4	6.6
16	5598.9	5.7	63.5	3859.2	3.4	791.1	7.9
17	5780.2	0.4	91.6	6062.5	5.1	1190.8	7.9
18	6269.2	0.3	84.4	5594.9	5.1	1096.9	7.1
19	8384.6	0.3	98.1	9138.5	7.2	1275.6	16.5
20	8598.9	0.4	102.2	10093.7	7.6	1329.0	20.0
21	8736.3	0.4	92.7	9217.4	7.7	1204.8	18.1
22	8219.8	0.3	109.5	10133.4	7.1	1423.9	19.3
23	8340.7	0.3	110.8	10578.6	7.4	1440.5	19.0
24	8406.6	0.3	96.8	9398.5	7.5	1259.0	17.7
25	8873.6	0.3	110.4	10595.2	7.4	1435.7	20.9
26	8467.0	0.3	125.5	11861.3	7.3	1631.3	22.8
27	8631.9	0.4	94.4	8953.9	7.3	1227.8	17.1

5.1.3.1. Main effect of Layers on compression properties

The results for the main effect of different layers on compression properties of the composites was analyzed using a one-way ANOVA test. The data was tested both in the warp (Y-yarn) direction and weft (X-yarn) direction. Figure 5.31 (a) shows the effect of the layers on the compression peak load in the X- and Y- directions, in which the graph indicated that there is

a significant difference between the samples with different layers. This was also confirmed by the Tukey HSD test in Appendix 69. The 9 layers samples in the warp direction have the highest peak load compared to 3 layers and 6 layers of composite samples. This is due to the presence of more number of yarns in the 9 layers compared to 3 or 6 layers. In 9 layers, more yarns contribute towards the compression strength. As the layers were changed from 9 layers to 6 layers, there was a gradual decline in the compression peak load. Similarly, 6 layers of composite samples have higher compression peak load compared to the 3 layers samples because of the presence of a higher number of yarns. Following a similar trend, 9 layers samples in the weft direction have the highest compression peak load, followed by 6 layers and 3 layers. The compression load in the warp (Y) direction is similar to the weft (X) direction.

The compression stress in Y- and X-directions is illustrated in Figure 5.31 (b), indicated that the number of layers has a significant effect on the compression behaviors of the samples in both warp and weft direction. The compression stress is highest in 9 layers weave followed by 6 layers and 3 layers in warp and weft direction. The downward trend indicates thickness influence on compression strength. This trend is also consistent in the weft direction where we see 9 layers registers the highest tensile stress followed by 6 layers and 3 layers.

The results of the one-way ANOVA test were confirmed using a follow-up post hoc Tukey test. The statistical analysis results in warp and weft direction compression properties were mainly influenced by the number of layers of Y-yarns as illustrated in Appendices 67 and 68, respectively. ANOVA analysis illustrates that there was a significant difference between a number of layers or thickness. The combined Tukey and ANOVA results showing a significant difference between 3 layers, 6 layers, and 9 layers.

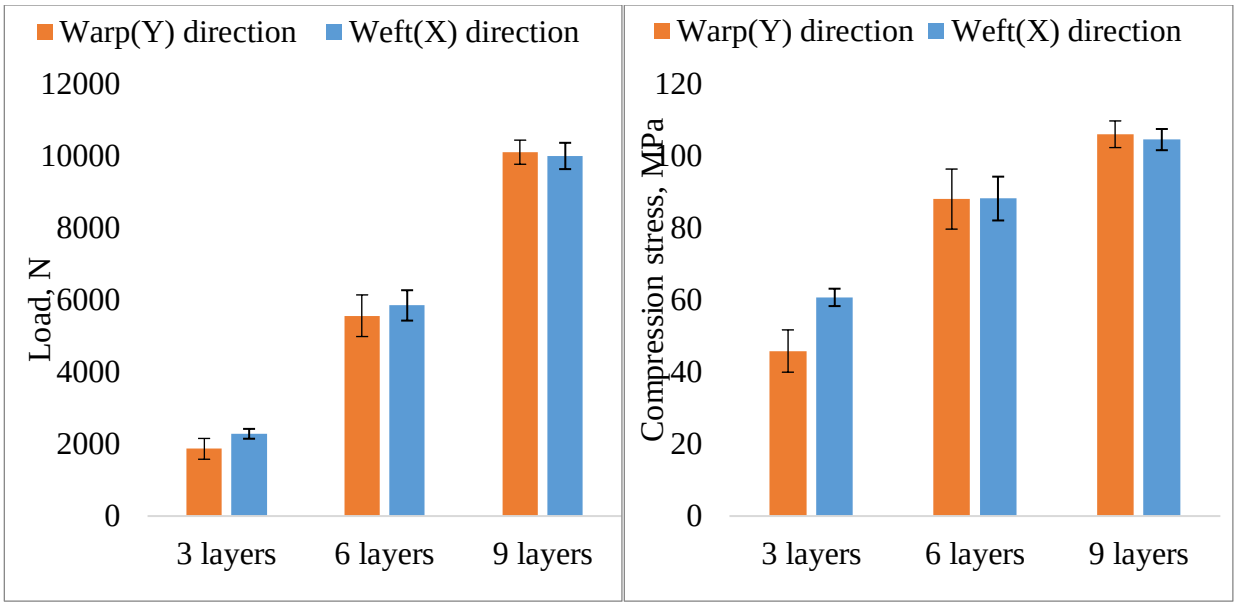

(a) (b)

Figure 5.31 (a) Main effect of layers on compression load, (b) Main effect of layers on compression stress.

5.1.3.2. Main effect of weave on compression properties

Figure 5.32 (a) shows the effect of the weave on the compression peak load in the X- and Y- directions, in which the graph indicated that there is no significant difference between the samples with different weaves. This was also confirmed by the Tukey HSD test in Appendix 70. The 2x2 warp rib samples in the warp direction have the highest peak load compared to plain and 3x3 warp rib composite samples. The compression load in the warp (Y) direction is similar to the weft (X) direction as was the case in the different layers.

The compression stress in Y- and X- direction indicated no significant difference as illustrated in Figure 5.32 (b). 3x3 warp rib had the highest compression stress compared to plain and 2x2 warp rib in warp direction. In weft direction, 2x2 warp rib showed highest compression stress followed by plain and 3x3 warp rib.

The statistical analysis (ANOVA) results in warp and weft direction are listed in Appendices 67 and 68, respectively. ANOVA analysis shows no significant difference between

different types of weaves in the warp direction.. The Tukey analysis also shows similar relationships like ANOVA results showing no significant difference between plain, 2x2 warp rib and 3x3 warp rib in Appendix 70.

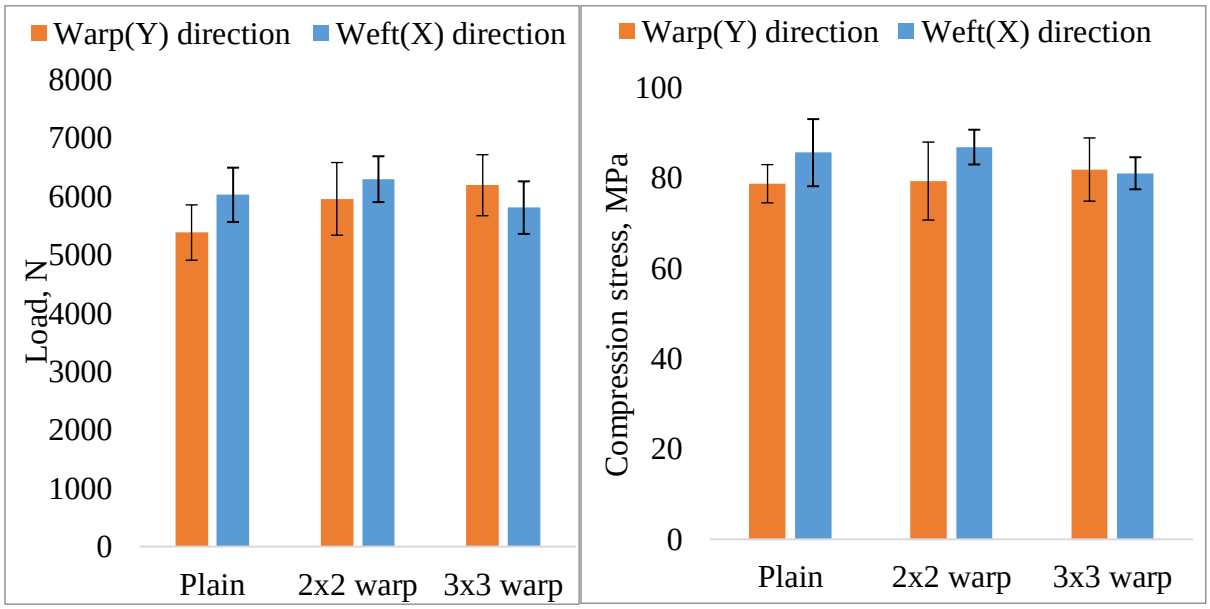

(a) (b)

Figure 5.32 (a) Main effect of weave on compression load, (b) Main effect of weave on compression stress.

5.1.3.3. Main effect of Z to Y ratio on compression properties

Figure 5.33 (a) shows the effect of Z to Y ratio on the compression peak load in the X- and Y- directions. Similar to effect of weaves, the effect of Z to Y ratio on compression load and stress does not show any significant difference. This was also confirmed by the Tukey HSD test in Appendix 71. The ratio 1:2 showed highest compression load followed by 1:1 and 1:3 in warp direction. In case of weft direction, 1:3 ratio had the highest compression load followed by 1:2 and 1:1. Similar to compression load, compression stress indicated no significant difference between the both warp and weft direction as illustrated in Figure 5.33 (b).

The results for the main effect of Z to Y ratio on compression properties of the composites was analyzed using a one-way ANOVA test. ANOVA analysis shows no significant difference between different ratios in the warp and weft direction as listed in Appendices 67 and

68, respectively. The Tukey analysis also shows similar relationships like ANOVA results showing no significant difference between ratio 1:1, 1:2 and 1:3 as shown in Appendix 71. Unlike warp direction, ANOVA analysis in weft direction was significantly different in terms of the weave.

The peak load was further normalized using thickness. There was no significant change in terms of main effect of layers, weave and Z to Y ratio on normalized peak load as illustrated in Appendices 72, 73 and 74, respectively.

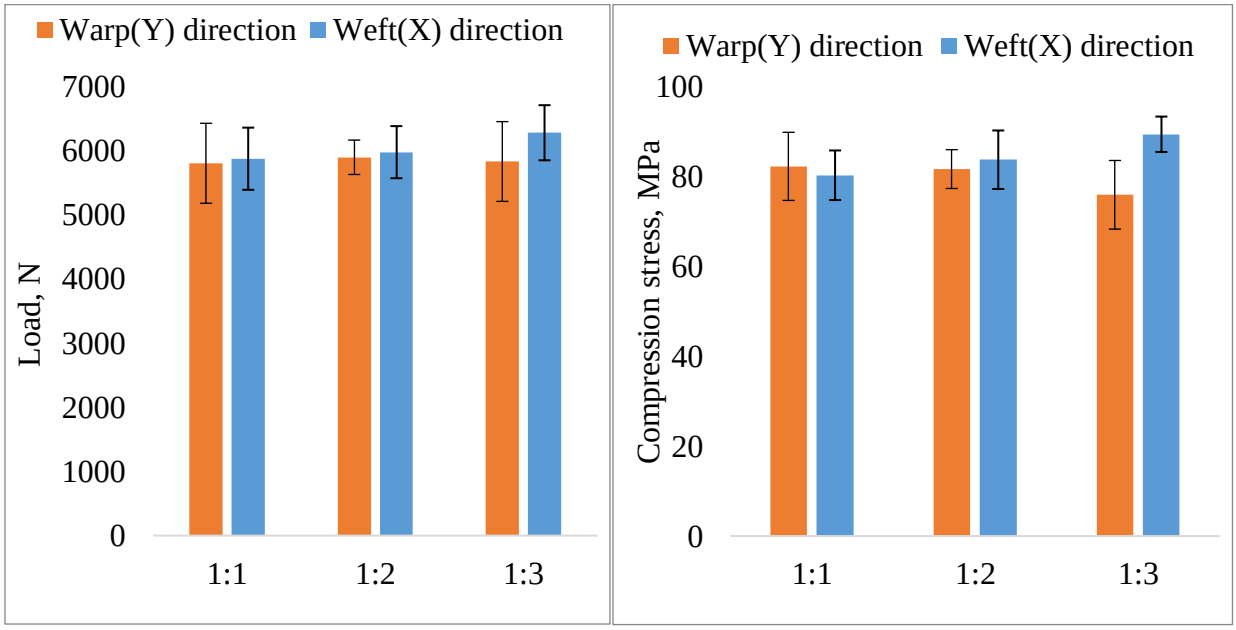

(a) (b)

Figure 5.33 (a) Main effect of Z to Y ratio on compression load, (b) Main effect of Z to Y ratio on compression stress.

5.1.3.4. Conclusion

Compression testing is subject to out-of-plane bending due to non-uniform strain and stress points across the specimen thickness. This results in a reduction in compression properties. The main cause of thickness variation is specimen fabrication, which leads to bending. As in the case of tensile test, thickness has the highest contributing factor in compression strength. . The yarn strength measured as tenacity was higher for X-yarn compared to Y-yarn as shown in Appendix 83. Tenacity does not influence compression properties and therefore there was no

significant difference between warp and weft direction. Weave design and Z-yarns did not affect compression properties.

5.2. Experiment A1

The objective of experiment A1 is to remove excess moisture from the samples. One of the problem areas of natural fiber is its hydrophilic nature, which is naturally ingrained in the fiber. The moisture content of hemp fiber is high and can vary somewhere between 8% to 10%, which leads to dimensional variation in composites. It directly impacts the mechanical properties of the composites, which restricts the applications of hemp in high-performance textiles. The tensile properties of the composites is the reflection of matrix properties whereas the modulus is reliant on the fiber properties.

The desiccated samples were cut using the cutting plan shown in Figure 4.11. The only structural parameter compared was the effect of weave on the treated samples. The number of y-yarn layers and Z-binder contribution remained unaltered. The treated specimens were compared with the untreated ones with similar construction. Mechanical properties in terms of tensile and compression strength and impact energy for both Tup and Charpy were compared and discussed below in details.

5.2.1. Main effect of moisture on tensile properties

A total of 30 (5x3x2) specimens in warp (Y) direction and 30 (5x3x2) specimens in weft (X) direction from treated and desiccated samples were analyzed. The results for the main effect of different weave on the tensile strength of desiccated composites samples were analyzed and compared with untreated samples using Tukey HSD test shown in Appendix 75 for warp direction & Appendix 76 in the weft direction. Tukey test indicates that there was no significant difference between the weave pattern namely plain, 2x2 warp rib and 3x3 warp rib in the warp and weft direction. Tukey also indicates there was no significant difference between untreated and desiccated samples. It was observed that only a minor change in weight recorded after desiccation illustrates in Table 5.14. Presence of moisture in the samples or a small amount of

moisture regain between removing the samples from the oven and infusion influenced the outcome of the test.

Table 5.14. Weight comparison before and after desiccation.

Sample ID	Weave	Weight before desiccation, g	Weight after desiccation, g	Change in weight, %
10M	Plain	720.1	704.9	2.1
11M	2x2 warp rib	711.3	699.3	1.7
12M	3x3 warp rib	698.4	683.8	2.1

5.2.2. Main effect of moisture on impact resistance

A total of 30 (5x3x2) specimens from untreated and desiccated samples were analyzed for tup impact test along with 30 (5x3x2) specimens in the warp and 30 (5x3x2) specimens in weft direction from untreated and desiccated samples were analyzed and compared for Charpy impact test. The results for the main effect of different weave on tup and Charpy energy impact of desiccated composites samples were analyzed and compared with untreated samples. Tukey results for Tup impact test is illustrated in Appendix 77. For Charpy test results were shown in Appendix 78 for warp direction and Appendix 79 for weft direction. Tukey test suggests that there was no significant difference between the weave pattern namely plain, 2x2 warp rib and 3x3 warp rib in the warp and weft direction. Tukey also indicates there was no significant difference between untreated and desiccated samples for both Tup and Charpy test.

5.2.3. Main effect of moisture on compression strength

A total of 30 (5x3x2) specimens in warp and 30 (5x3x2) specimens in weft direction from untreated and desiccated samples were analyzed and compared for a compression test. The results for the main effect of different weave on compression strength of desiccated composites samples were analyzed and compared with untreated specimens using the Tukey HSD test. Tukey test illustrated in Appendix 80 for warp direction and Appendix 81 for weft direction suggests that there is no significant difference between the weave pattern namely plain, 2x2 warp rib and 3x3 warp rib in the warp and weft direction. Tukey also indicates there is no significant difference between untreated and desiccated samples. It was observed that only a minor change

in weight recorded after desiccation illustrates in Table 5.12. There is a probability that there would be moisture present in the samples or a small amount of moisture regain between removing the samples from the oven and infusion.

5.2.4. Conclusion

To conclude, by changing the weave pattern, the mechanical properties of the treated samples did not demonstrate any major change in the samples for both X- and Y-direction. This was due to moisture present in the samples or a small amount of moisture regained after removing from the oven. A few future recommendations are to use higher temperature in the oven for an extended period of time and use of desiccant bags to protect for moisture regain might help to improve the mechanical properties of the treated samples.

5.3. Experiment A2

The objective of experiment A2 is to understand the effect of mercerization on the mechanical properties of the samples. The chemically treated samples were cut using the cutting plan shown in Figure 4.11. The only structural parameter compared was the effect of weave on the treated samples. The number of y-yarn layers and Z-binder contribution remained unaltered. The treated specimens were compared with the untreated ones with similar construction. Mechanical properties in terms of tensile and compression strength and impact energy for both Tup and Charpy were compared and discussed.

5.3.1. Main effect of mercerization on tensile properties

A total of 30 (5x3x2) specimens in warp (Y) direction and 30 (5x3x2) specimens in weft direction were analyzed. The results for the main effect of different weave on the tensile strength of the mercerized composites samples were analyzed and compared with untreated ones using Tukey HSD test. Tukey test illustrated in Appendix 75 suggests that there is no significant difference between the weave pattern namely plain, 2x2 warp rib and 3x3 warp rib in the warp direction. In the case of weft direction, the treated samples were significantly different from untreated ones as shown in Appendix 76. The graph presented in Figure 34 (a) shows an increase in tensile load in Plain, 2x2 warp rib and 3x3 warp rib. Like the warp direction, the plain weave

of the mercerized specimens in the weft direction has the highest tensile load followed by 2x2 warp rib and 3x3 warp rib depicted in Figure 36 (a). This could be due to the fact that plain woven structures are more compact with a less open spot for the resin to accumulate compared to the 2x2 warp rib and 3x3 warp rib weave structure. Unlike the warp direction, tensile load in weft direction shows a decreasing trend in all the three weaves. This was due to yarn waviness which is higher in weft direction compared to warp direction. During weaving, continuous tension was applied to warp yarns which helped in curtailing yarn waviness. However, weft yarns had tension applied only during rapier insertion resulting in waviness. The waviness continued from weaving to infusion.

Furthermore, the load-strain curves in Y- and X-directions illustrated in Figure 34 (b) & 36 (b) respectively, indicated a decreasing trend as compared to untreated samples. There was no significant difference between the tensile behaviors of the samples in both warp and weft direction. The tensile strain is highest in plain weave followed by 2x2 warp rib and 3x3 warp rib in both warp and weft direction. This trend was also consistent in the weft direction where we see plain registers the highest tensile strain followed by 2x2 warp rib and 3x3 warp rib. Plain has better structural integrity where the x and y yarns are distributed more uniformly compared to 2x2 warp rib and 3x3 warp rib. Pre-existing defects during the formation stages could also contribute difference in the tensile strain between weaves. Yarn waviness in both directions was also a contributing factor.

The tensile stress curves in Y- and X-directions illustrated in Figure 35 and Figure 37 respectively indicated that there was no significant difference between the tensile behaviors of the samples in both warp and weft direction. The tensile stress was highest in plain weave followed by 2x2 warp rib and 3x3 warp rib in warp and weft direction. Even though the difference is not significant, the downward trend indicates weave influence on the tensile strength. This trend was also consistent in the weft direction where we see plain registers the highest tensile strain followed by 2x2 warp rib and 3x3 warp rib. Pre-existing defects during the formation stages could also contribute difference in the tensile stress between weaves.

5.3.2. Main effect of mercerization on impact resistance

A total of 30 (5x3x2) specimens from untreated and mercerized samples were analyzed and compared for the Tup impact test. The results for the main effect of different weaves on Tup impact of the treated composites were analyzed using the Tukey HSD test shown in Appendix 77. Tukey test suggests there was a significant difference between treated and untreated samples. Also, within the treated samples, there were discrepancies. There was no significant difference between plain and 2x2 warp weave and there was no significant difference between 2x2 warp and 3x3 warp weave as shown in Figure 38. However, there was a significant difference between plain and 3x3 warp rib weave. Impact energy in all the three weaves has significantly increased after mercerization. Tup impact specimens were independent of the yarns orientation as they are square and all yarn contributes to the impact resistance mutually. The effect of yarn waviness has less impact as Tup impact is independent of yarn orientation and is minimized by mercerization. Mercerization has resulted in enhancing the fiber-matrix bonding as there is more number of cross-over points per specimen.

A total of 30 (5x3x2) specimens in the warp direction and 30 (5x3x2) specimens in weft direction from untreated and mercerized samples were analyzed and compared for Charpy impact test. The results for the main effect of different weaves on Charpy impact of the treated composites were analyzed in both warp and weft direction using Tukey HSD test shown in Appendices 87 & 79 respectively. Tukey test suggests that there was no significant difference between treated and untreated samples in X-yarn and Y-yarn direction. There was no significant difference between plain, 2x2 warp rib and 3x3 warp rib weave as presented in Figure 39 (a) and 39 (b). The impact energy in most of the three weaves has decreased after mercerization. Pre-existing defects during the formation stages could also contribute difference in the tensile strain between weaves. Yarn waviness in both directions was also a contributing factor. Since Charpy is a low impact test compared to Tup, the effect of mercerization is also low.

5.3.3. Main effect of mercerization on compression properties

A total of 30 (5x3x2) specimens in warp (Y) direction and 30 (5x3x2) specimens in weft (X) direction were analyzed. The results for the main effect of different weave on the compression strength of the treated composites were analyzed and compared with untreated ones using Tukey HSD test shown in Appendix 80. Tukey test suggests there was no significant

difference between the weave pattern namely plain, 2x2 warp rib and 3x3 warp rib in the warp direction compared to untreated samples with the weaves. Although, there was no significant difference between plain, 2x2 warp rib and 3x3 warp rib within the treated samples in both warp and weft direction as shown in Figure 40 (a) & Figure 41 (a) respectively. It was observed that the compression strength of all the composite samples increased after mercerization treatment. The increase was highest in plain weave in the warp direction and 2x2 warp in weft direction as shown in Table 5.15. The variation denoted by standard deviation is also reduced after alkali treatment. This was due to yarn waviness which is higher in weft direction compared to warp direction. During weaving, continuous tension was applied to warp yarns which helped in curtailing yarn waviness. However, weft yarns had tension applied only during rapier insertion resulting in waviness. The waviness continued from weaving to infusion.

The compression stress curves in Y- and X-directions illustrated in Figure 40 (b) & 41 (b) respectively, indicated that there was no significant difference between the tensile behaviors of the samples in both warp and weft direction. The compression stress is highest in plain weave followed by 2x2 warp rib and 3x3 warp rib in warp and weft direction. Even though the difference is not significant, the downward trend indicates weave influence on the compression strength. This trend is also consistent in the weft direction where we see plain registers the highest compression stress followed by 2x2 warp rib and 3x3 warp rib. Pre-existing defects during the formation stages could also contribute difference in the compression stress between weaves.

Table 5.15. Comparison of compression strength before and after mercerization.

Compression LOAD, N	**Warp (Y)**			**Weft (X)**		
	Untreated	**Mercerized**	**% change in compression load**	**Untreated**	**Mercerized**	**% change in compression Load**
Plain	4380.8	8587.0	96.0	5952.9	8055.2	35.3
2x2 Warp	6310.3	7675.5	21.6	5694.5	8529.0	49.8
3x3 Warp	7084.3	8195.1	15.7	6678.3	7441.4	11.4

5.3.4. Conclusion

To conclude, by changing the weave pattern, the tensile strength of the treated samples decreased in weft direction along with a decrease in tensile stress and tensile strain. Plain weave has the highest values due to better structural integrity. The other contributing factor was that plain weave has a shorter float with more number of x-y intersections. These crossover points have better adhesion after mercerization thereby improving the tensile strength of plain weave. Yarn waviness also is the contributing factor, especially in the weft direction. During mercerization, no additional tension was applied to keep the samples straight. This lead to shrinkage (about 9.8% in warp direction and about 7.5% in weft direction) and additional waviness in both direction resulting in lower tensile strength of alkali treated samples compared to untreated samples.

Other contributing factors are level of yarn twist and yarn linear density (denier) for X-, Y- and Z-direction yarns. The yarn twist was measured in terms of twist per meter (TPM). The twist was 172 TPM for X-yarn, 351 TPM for Y-yarn and 291 TPM for Z-yarn. The optimum level of yarn twist will maintain structural integrity as well as resin absorbency into the yarns. Composites made with higher yarn linear density exhibit better mechanical strength. The yarn linear density was measured to be 1462 denier for X-yarn, 1207 denier for Y-yarn and 234 denier for Z-yarn.

Sodium hydroxide (NaOH) is used to interrupt hydrogen bonding in the cellulose structure of the fiber. This helps to make the fiber surface rough for better resin adhesion. Mercerization is used to remove any excessive lignin, wax, and oil from the fiber surface, which will negatively influence the fiber-matrix bonding. The alkali treatment tends to improve the mechanical and thermal properties of the composites.

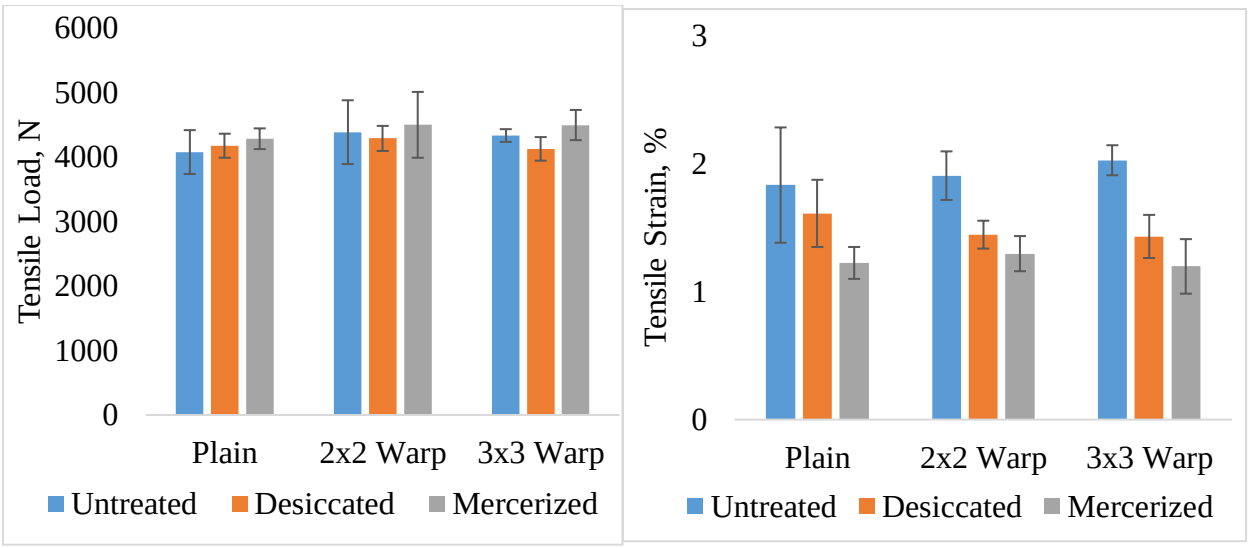

(a) (b)

Figure 5.34 (a) Effect of weave and treatments on tensile load (treated Vs untreated) - Warp direction, (b) Effect of weave on tensile strain (treated Vs untreated) - Warp direction.

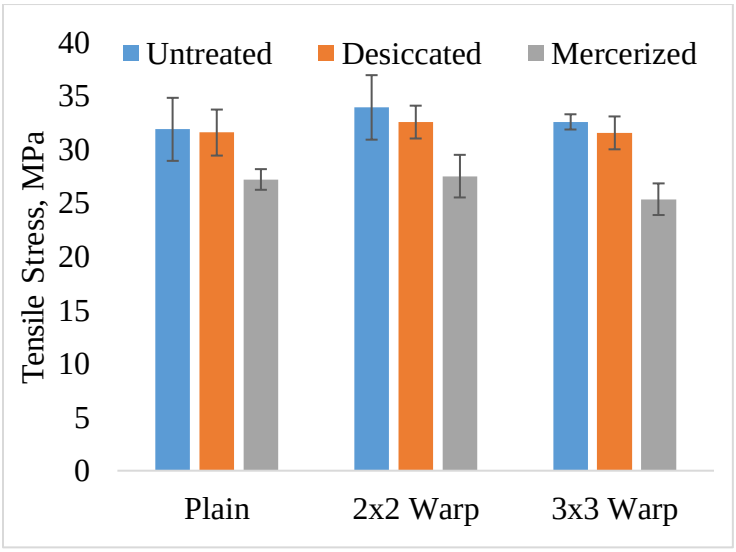

Figure 5.35 (a) Effect of weave and treatments on tensile stress (treated Vs untreated) – Warp direction.

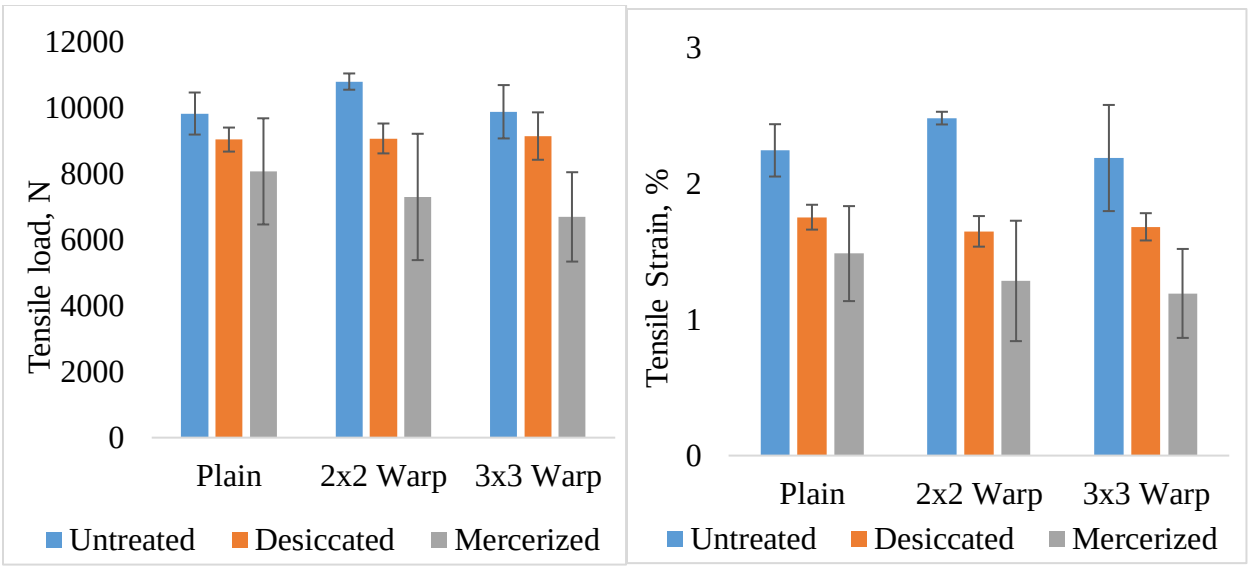

(a) (b)

Figure 5.36 (a) Effect of weave and treatments on tensile load (treated Vs untreated) - Weft direction, (b) Effect of weave on tensile strain (treated Vs untreated) - Weft direction

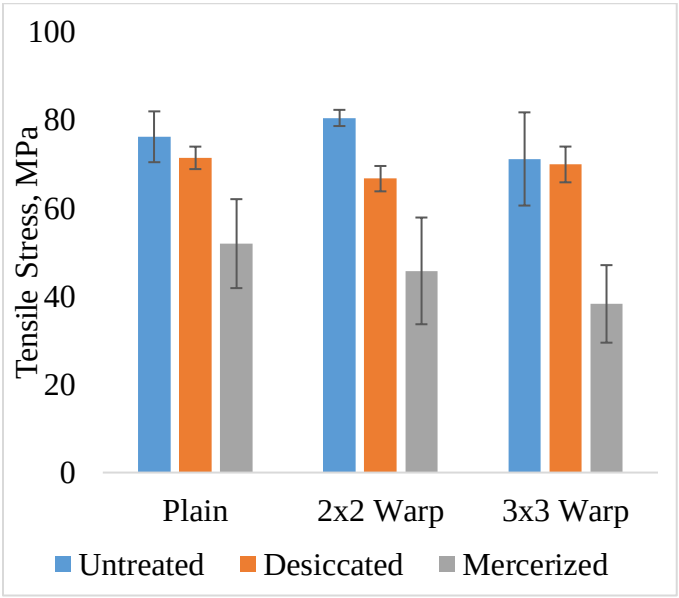

Figure 5.37 Effect of weave and treatments on tensile stress (treated Vs untreated) - Weft direction

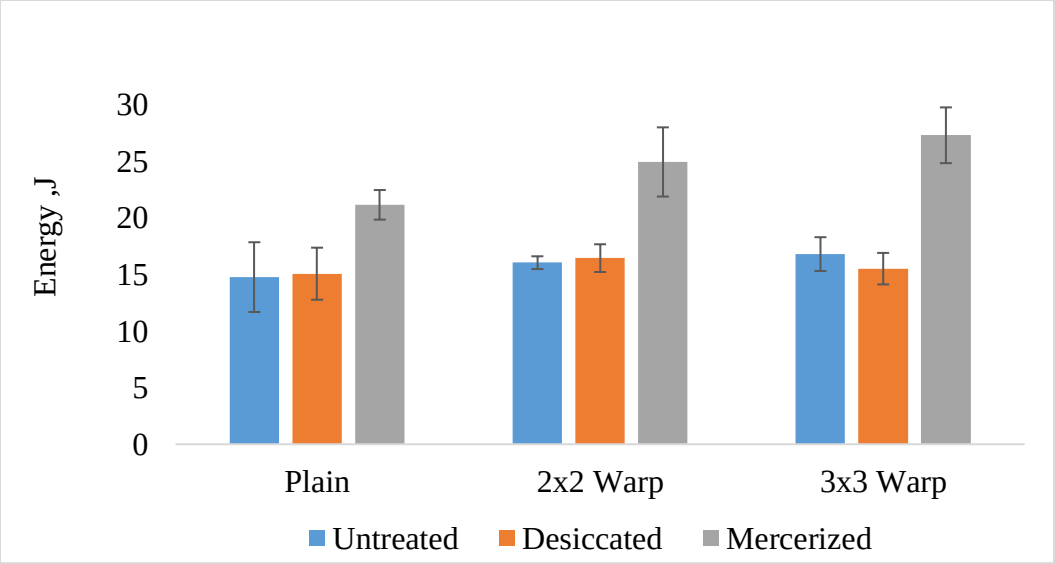

Figure 5.38 Effect of weave and treatments on Tup impact energy (Treated Vs Untreated)

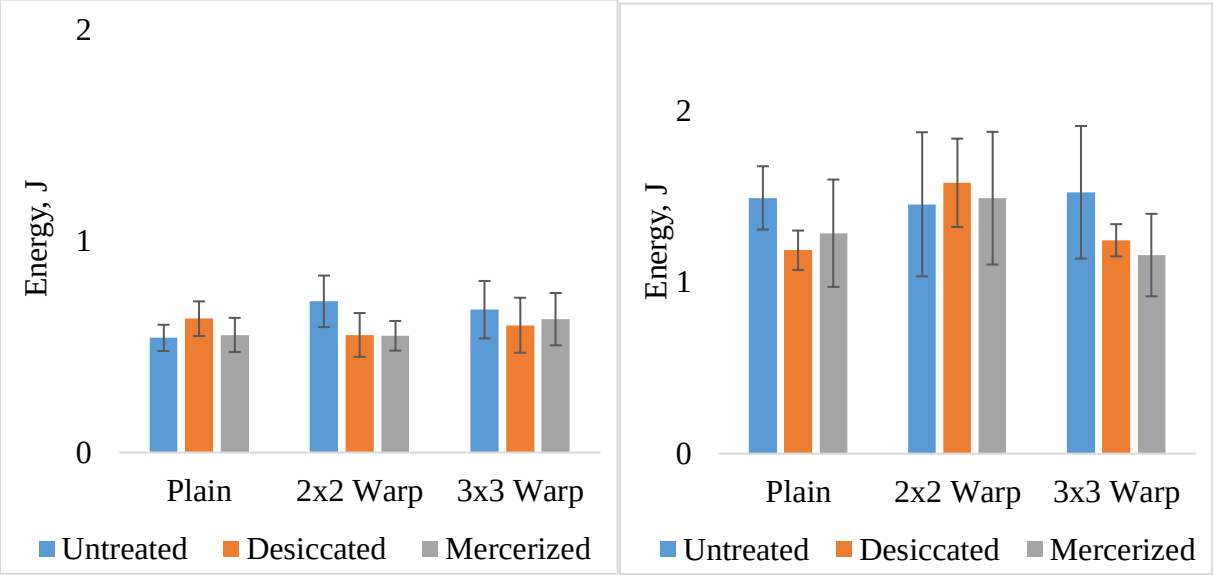

(a) (b)

Figure 5.39 (a) Effect of weave and treatments on Charpy impact energy (treated Vs untreated) - Warp direction, (b) Effect of weave on Charpy impact energy – Warp direction (treated Vs untreated) - Weft direction.

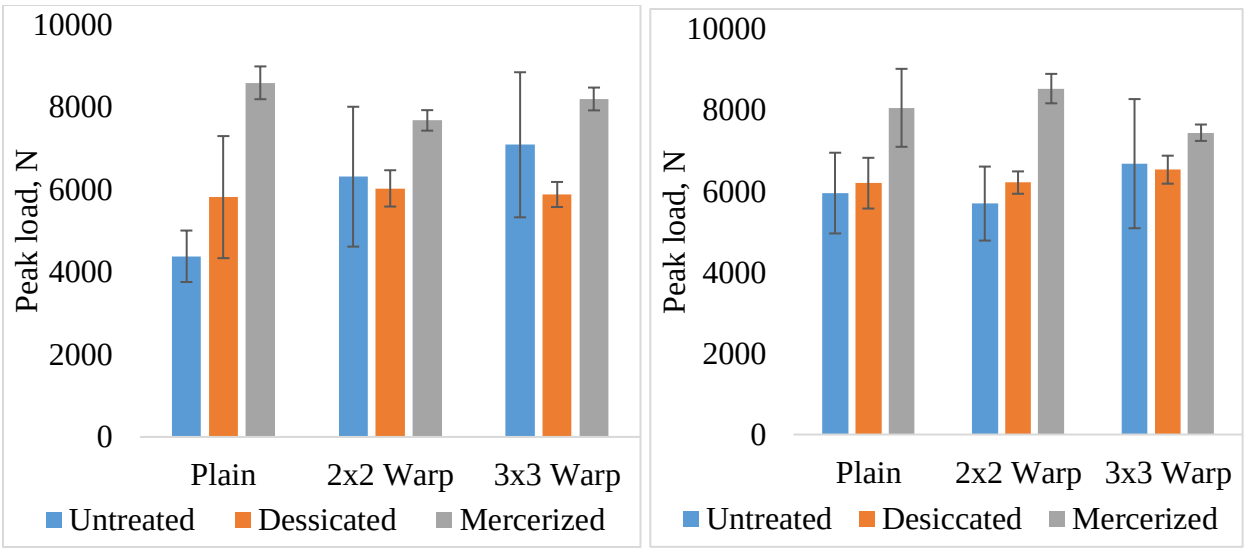

(a) (b)

Figure 5.40 (a) Compression load comparison for treated and untreated samples - warp direction, (b) Compression load comparison for treated and untreated samples - weft direction.

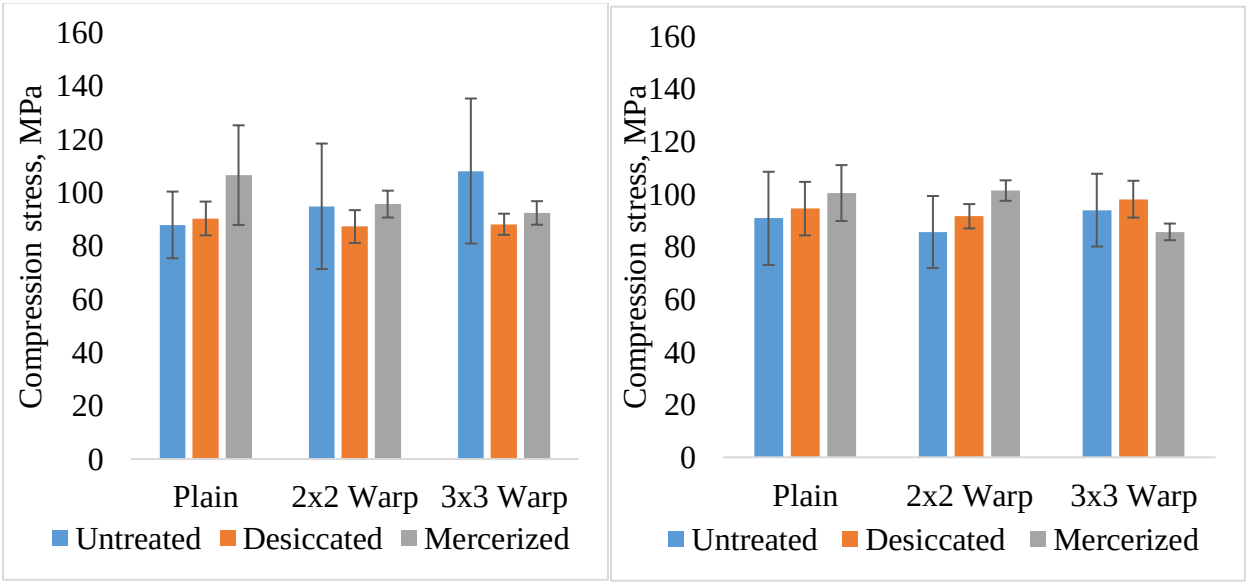

(a) (b)

Figure 5.41(a) Compression Stress comparison for treated and untreated samples - warp direction, (b) Compression stress comparison for treated and untreated samples - weft direction

CHAPTER 6 - MARKET POTENTIAL OF INDUSTRIAL HEMP IN THE US

6.1. Introduction

Hemp is considered as one of the high-performance natural fiber due to its mechanical properties. Hemp is one of the oldest bast plant known to man. It is estimated that it was used over 6000 years ago with a wide range of applications from food, rope, sail, paper, textiles, and oil, etc. with references dating back to ancient China and Mesopotamia. Industrial hemp was used in a wide variety of industrial and consumer products for centuries. Although, industrial hemp is grown in many developed and developing countries around the world, the United States had strict control on hemp cultivation until 2014. The restriction was under the authority of the Drug Enforcement Administration (DEA). Industrial hemp is now treated as an agricultural commodity after revised Farm bill Act, 2018 that allow hemp to be cultivated for use in the production of a wide range of products. There was no full-scale commercial production in the United States until 2014 when Farm Bill was introduced which permitted certain research institutions to collaborate with the State Department of Agriculture to establish a pilot program.

According to Section 7606 of Farm Bill Act, 2014, industrial hemp is defined as "the plant Cannabis sativa L. and any part of such plant, whether growing or not, with a delta-9 tetrahydrocannabinol concentration of not more than 0.3 percent on a dry weight basis." Delta-9 tetrahydrocannabinol (THC) is the psychoactive drug present in cannabis. Industrial hemp belongs to Cannabis is a classification of plants with various species, and Hemp and Marijuana are both species of plant within the Cannabis family. Industrial hemp is known as "*Cannabis sativa*" whereas marijuana is *"Cannabis indica".* Although Hemp and Marijuana are both species of Cannabis, they have several distinct differences in terms of their physical appearance, chemical composition, and applications. Marijuana has broad leaves, dense buds concentrated at the top like a crown, and has a short and bushy appearance which are grown in a very controlled environment with regulated temperature and humidity as shown in Figure 6.1. In stark contrast, hemp plants are slender, taller with narrower leaves, with fewer branches and are grown in open field like any other crop illustrated in Figure 6.2.

Figure 6.1. Marijuana plant in controlled environment.

Figure 6.2. Industrial hemp in open field.

Apart from contrasting physical appearance, its chemical make-up is also significantly different, specifically in terms of THC and Cannabidiol (CBD). THC is the chemical responsible for marijuana's psychological effects in cannabis. On average, marijuana usually contains anywhere from 5-20% THC. Some strains of marijuana can have up to 35% THC (Vantreese, 1998). Due to the high percentage of THC in marijuana, it is used for recreational purpose. Unlike marijuana, hemp has a very low level of THC, approximately 0.3%, which make it nearly impossible to trigger any psychoactive effect or get a "high". This threshold is heavily regulated in other countries that have legalized hemp including the United States. Another factor, which differentiates industrial hemp from marijuana, is high CBD which acts as THC's antagonist

restricting THC effect to minimal. Table 6.1 shows the main differentiating factors between industrial hemp and marijuana.

Table 6.1. List of differences between industrial hemp and marijuana.

Industrial hemp	Marijuana
• *Cannabis sativa L.*	*Cannabis indica*
• Used for seeds, stalk and fiber	Used for seeds, buds and leaves
• Low Tetra Hydro Cannabinol (THC) level (< 0.3%)	Contain high THC level (5% - 35%)
• High levels of Cannabidiol (CBD)	Low levels of Cannabidiol (CBD)
• Requires minimal care with adaptability to most climates.	Grown in carefully controlled area
• Agricultural crop used in automobiles, personal care, clothing, construction, food, etc.	Medical and recreational use

Some estimate suggests that the global market for hemp has possible applications of more than 25,000 products. Since hemp is fairly a new crop in the United States, precise data are not available on the size of the U.S. market for hemp-based products. The focus of this chapter was to highlight the importance of industrial hemp, revisit the past glorious years of hemp, and discuss new measures taken by the previous and current government in advancing and promoting hemp as an agricultural product. This chapter also looked at the future of hemp market in the US and its applications.

6.2. Past (the 1700s – 1970)

Newly popularized hemp topic today, after legalization in 2014, actually dates way back to early 1700s. It was first introduced in North America around 1611 in Jamestown. American farmers grew the crop for a multitude of purposes, including rope, paper, and lantern oil.

Fast forward to the 1700s, to an era which was an agriculturally-driven economy, where hemp played a vital role in driving the economy. In America particularly, hemp was very popular and was treated as legal money and was used to pay taxes. People were forced to cultivate hemp because of the shortage. It was not only cultivated by local people but also by President George Washington and Thomas Jefferson. The declaration of independence and the U.S. Constitution

was first drafted on hemp paper. Hemp fabric was used to make U.S. first flag by Betsy Ross as hemp was the finest and strongest fiber available at that time.

Previously, hemp fiber was used for ropes, sails, textiles, and paper. Hemp seeds can be used for its oil and other medicinal properties. Hemp Hurd can be used in construction. The rising popularity of hemp decreased in the 19th century due to cheaper alternative hemp fiber from foreign sources and competition from cotton, sisal, and jute. After World War I, hemp attractiveness further decreased within the farmer's community, especially in Kentucky, which was accountable for the majority of the nation's hemp fiber production.

In 1938, Popular Mechanics published an article that promoted industrial hemp as the "new billion dollar crop". The article focused on hemp applications by demonstrating "over 25,000 uses for the plant ranging from dynamite to cellophane." However, this movement was short-lived as the federal government's increased efforts to criminalize all cannabis including industrial hemp by introducing the Marihuana Tax Act of 1937, which placed heavy taxes on the sale of cannabis. There has been some controversy over this bill, as some have argued that this policy was aimed to reduce the size of the hemp industry in order to lobby and promote emerging plastic and nylon industries.

This significantly declined hemp cultivation in the United States. Hemp experienced a slight resurgence during World War II when the US Government recognized the importance of hemp to support the war and briefly lifted enforcement of the Marihuana Tax Act. This was primarily because hemp imports were cut off by Japan from the Philippines, which was a major importer of hemp in the US. That is when hemp was briefly legalized by the US government to minimize the dependency on foreign countries. US government released a pro-hemp documentary, "Hemp for Victory", to promote hemp cultivation which would support the war by using hemp in ship sail, ropes, etc. The documentary made a huge impact and led to over 400,000 acres of hemp cultivation during 1942-1945. It was during this time, Henry Ford used hemp-based plastic in the body of an automotive in 1941. By replacing metal with hemp significantly reduced its weight and increased impact strength without denting. He also used hemp ethanol as fuel for the car.

By the end of World War II, the restriction was reinstated and industrial hemp was again treated as an “illegal crop”. The farmers again were discouraged to grow hemp as cheaper synthetic fiber became widely available. The US government went back to its original stance on hemp again and the industry continued to decline. This led to fewer farmers cultivating hemp and many hemp processors declaring bankruptcy. The last commercial hemp farm in the US was planted in Wisconsin in 1957.

Shortly after, combined with conflicts with other big business, like tobacco, petrochemical, oil, and anti-marijuana political movements, the entire cannabis family, including hemp, fell to opposition campaigns and propaganda. Hemp farming was eventually officially banned altogether in 1970 with the passage of the Controlled Substances Act in which hemp was included as a Schedule 1 drug, grouping this crop with drugs like heroin and LSD, making all cannabis and hemp cultivation federally illegal. All important milestones of hemp in the US is shown in figure 6.3.

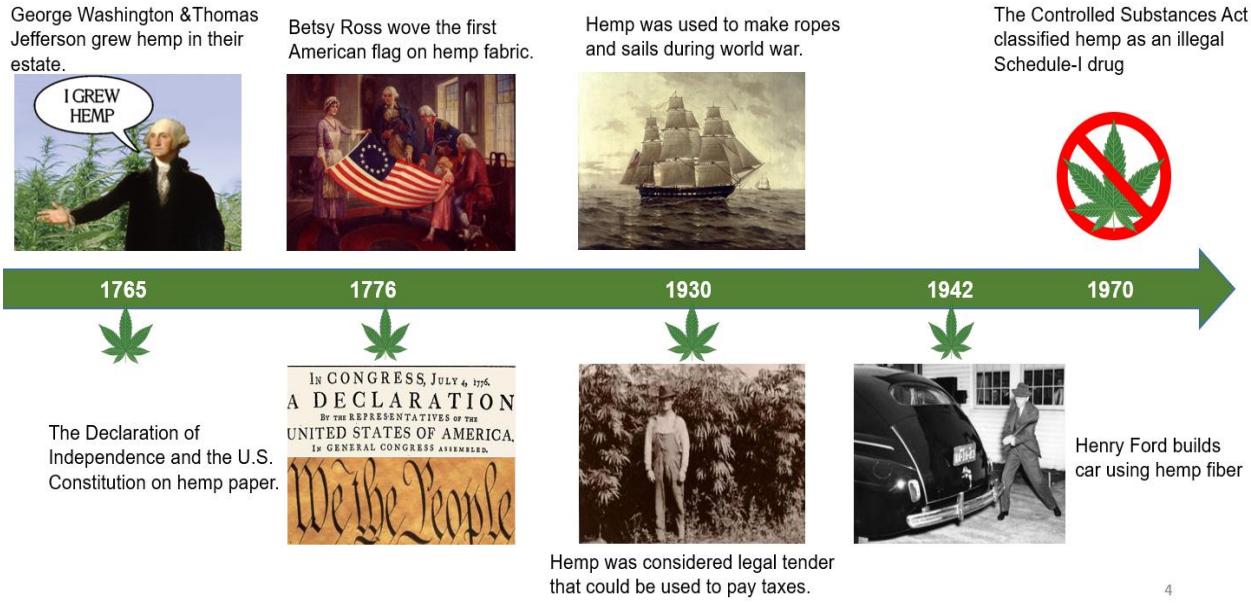

Figure 6.3 Highlights of glorious past of hemp from the 1700s to 1970.

6.3. Present (2000 – 2018)

After decades of hibernation, Industrial hemp in the US was revived by introducing Farm Bill, 2014, which authorized institutions of higher learning and state department of agriculture to regulate and conduct research and pilot programs. These pilot programs aimed at researching industrial hemp upon the approval of the U.S. Department of Agriculture (USDA) and Drug Enforcement Administration (DEA). This program also allowed small scale expansion of hemp cultivation for restricted research purposes only.

North Carolina legalized industrial hemp production in October 2015. The North Carolina Industrial Hemp Commission (NCIHC) and North Carolina Department of Agriculture are responsible to oversee agricultural hemp pilot program. The commission also collaborated with North Carolina State University and North Carolina A&T University to manage the pilot program. This legalization will change the whole dynamics of the usage of industrial hemp in various sectors in the US. Figure 6.4 shows the current status of hemp state wise from the National Conference of State Legislation (NCSL, 2018). There are 41 states that have already legalized hemp or are in the process of legalization.

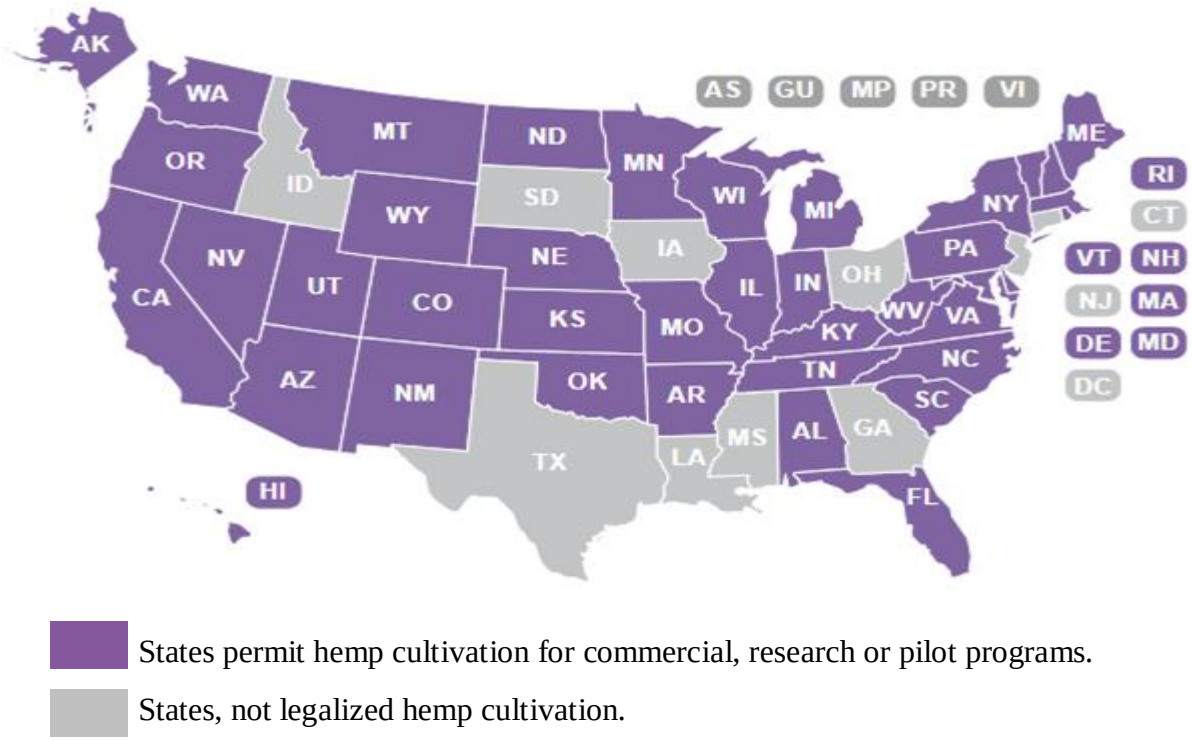

Figure 6.4. Current state-wise hemp status (NCSL, 2018).

The motivation for introducing Farm Bill, 2014 was to encourage research on hemp. This was further boosted by revising Farm Bill in 2018. This bill is more expansive and overtly allows inter-state trade of hemp-based products for commercial purposes. There are no restrictions on sales, transport or possession of hemp-derived products, as long as they are produced under legal guidelines. This encouraged many states to legalize hemp and boost production of already legalized states. Table 6.2 illustrates the growth in hemp production in various states within two years of legalization.

Table 6.2. State wise hemp production from 2016-2018 (Vote hemp, 2018; Vote Hemp, 2019).

State	Acres planted, 2016	Acres planted, 2017	Acres planted, 2018	% change
Colorado	5921	9700	21578	264.4
Hawaii	1	1	2	100.0
Indiana	2	5	5	150.0
Kentucky	2525	3271	6700	165.3
Maine	1	30	550	54900.0
Minnesota	51	1205	710	1292.2
Nebraska	1	1	0.5	-50.0
Nevada	216	417	1881	770.8
New York	30	2000	2240	7366.7
North Dakota	70	3020	2778	3868.6
Oregon	500	3469	7808	1461.6
Tennessee	225	200	3338	1383.6
Vermont	60	575	1820	2933.3
Virginia	37	87	135	264.9
West Virginia	10	14	155	1450.0
Massachusetts	*	**	21	N/A
Montana	*	542	22000	3959.0
North Carolina	*	965	3184	229.9
Oklahoma	*	**	445	N/A
Pennsylvania	*	36	580	1511.1
South Carolina	*	**	256	N/A
Washington	*	175	142	-18.9
Wisconsin	*	**	1850	N/A
Illinois	*	**	0.1	N/A
	2016	2017	2018	% change
Total acres	9649	25713	78176	710.2
University involvement	30	32	40	33.3
No. of licenses issued	817	1456	3546	334.0
* Hemp cultivation started after 2016				
** Hemp cultivation started after 2017				

The biggest development in the Farm Bill, 2018 (Section 7606) was that hemp was removed from the controlled substance, schedule-I list and is now treated as an agricultural crop. Although the Farm Bill, 2018, removed industrial hemp from the controlled substances list, it

also made industrial hemp production compulsory to get USDA license either issued under a federal USDA plan or state USDA approved industrial hemp production plan. Therefore, hemp will be treated illegally until plans are approved and licenses issued under Agricultural Marketing Services (AMS) regulations with a DEA permit.

Section 7501 of the Farm Bill categorizes hemp under Critical Agricultural Materials Act which further strengthens hemp prospects by recognizing the importance and multiplicity of the hemp plant and its applications. This section also emphasizes on the commercial and market viability of hemp.

Section 7605 further extends the protections for hemp research including the ways and means research should be conducted. Similarly, several other changes were made to the existing provisions to protect the hemp farmers as well. Section 11101 of the Farm Bill includes hemp farmers' protection under the Federal Crop Insurance Act, which will safeguard hemp farmers in case of crop loss. Since hemp is a fairly new crop and farmers are still in the learning mode, this will provide assistance and encouragement to grow more hemp in the US.

6.4. Future (2019 and beyond)

Industrial Hemp Farm Bill Act has proven to be a giant step forward for hemp status in the United States. For the time of legalization until the present date, thousands of acres of land has been used for growing industrial hemp, start harvesting their crops and see the impact it brings to its local economy. The revised Farm Bill Act, 2018, which removed industrial hemp from the controlled substance, Schedule I drug and categorized it as an agricultural product. This will further strengthen hemp prospects in the US market and lower the dependency on foreign countries for hemp consumption.

Natural fiber composites have great potential as the focus of many industries is shifting from conventional fiber to more sustainable natural resources. According to a recent report from Market and Markets, natural fiber composite market will be worth 6.5 billion USD by the year 2021. Hemp will also play a big contributor to this market. Currently, the US relies mostly on imports from countries like Canada, China, and Europe for hemp. However, the recent developments to cultivate industrial hemp has increased the chance of using home-grown products. In the past two decades, various feasibility and marketing studies have been conducted

by researchers at the USDA and various land grant universities and state agencies to understand the market potential of hemp. However, there are various external forces like customers, suppliers, competitors, distributors, regulators, technology, etc. that will shape the hemp market in the USA. This will contribute to economic growth and decrease the dependency on imports. One of the disadvantages of using imported hemp is the variability in fibers in a different region. This is one of the biggest hurdle faced by the composite market using hemp is the inherent variability that exists in hemp fiber and processing. If hemp is cultivated on a large scale in US soil, there will be better control over the quality of fibers.

Many studies were done in Canada and many state agencies explain the positive results based on the optimistic market approach, consumer sensitiveness and the potential range of product uses for hemp. Some reports also indicate the positive impact of growing hemp on agricultural producers if the current restriction were removed. The US is one of the biggest importers of hemp in the world. The imports as indicated in Figure 6.5 demonstrates an increasing trend, which validates the need to grow hemp in the US, rather than depending on imports.

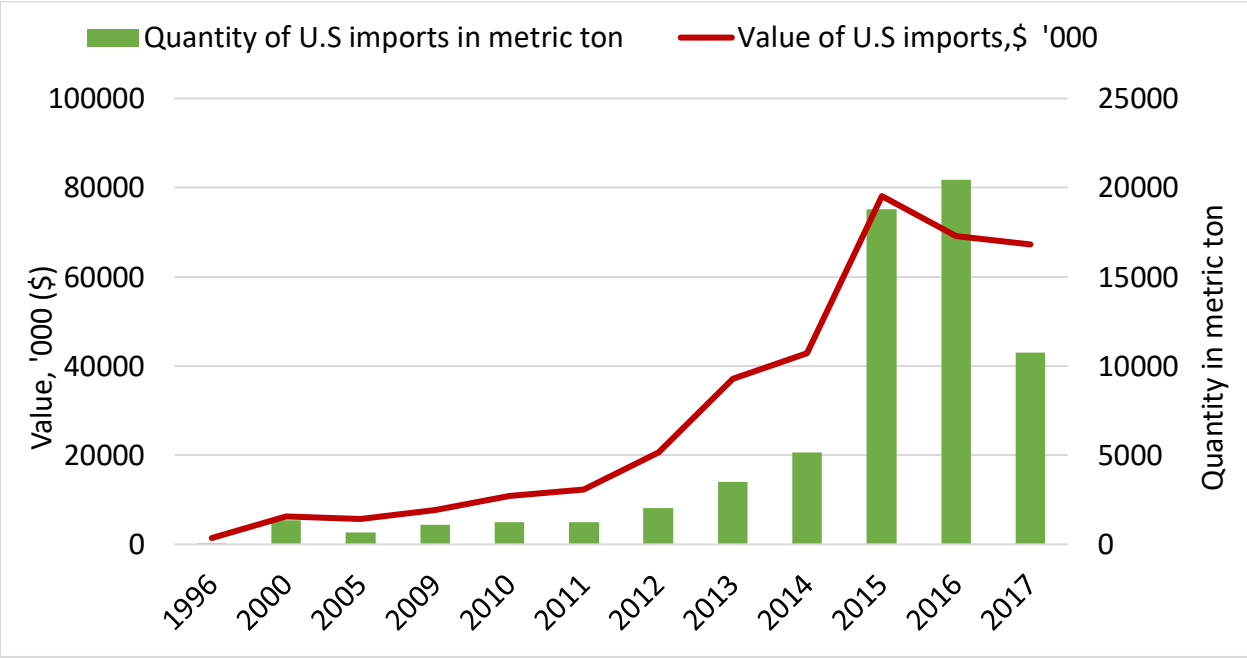

Figure 6.5. Value and Quantity of U.S. Imports of Selected Hemp Products, 1996-2017 (Johnson, 2017).

The following are the characteristics of hemp, which make it attractive for various applications.

- Hemp has higher specific properties with lower prices
- Good anti-vibration properties for higher adoption of natural fiber composites in the sporting goods segment
- Hemp has a lower life-cycle cost and comparatively low maintenance than wood plastics composites helps to play a key role in building & construction applications
- Hemp can also be used in Electrical & Electronics applications where these companies are looking for eco-friendly alternatives.
- Automotive industry could be the major user of hemp due to rising prices of petroleum-based products, strong government support to eco-friendly products, higher acceptance and positive growth of end-user industries.

The composite market still remains an untapped area and has potential worth billions of dollars. Sectors like consumer goods, aerospace, construction, electrical and electronics (E & E) are a few examples where market potential is enormous. Europe is one of the largest markets in natural fiber composites for automotive applications whereas North America is the largest region for Building & Construction applications. Environmental concerns are making natural fiber composites suitable in various new applications. Figure 6.6 explains the growing market for natural fiber composites.

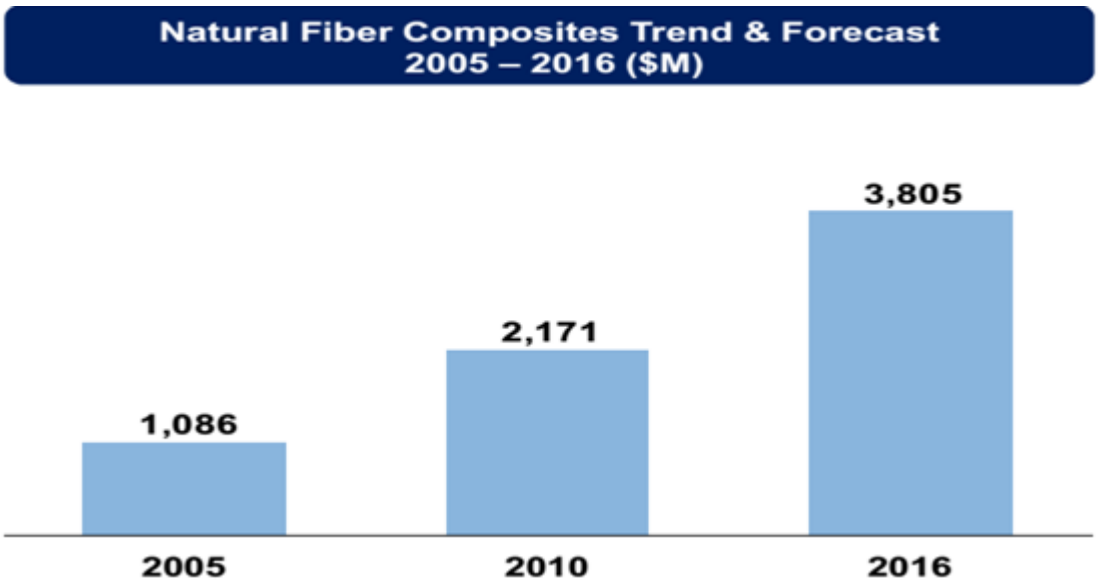

Figure 6.6. Market Trend of Natural Fiber Composites (Lucintel report, 2011).

There are also a few trends which indicate the growth of natural fiber composites markets like the emphasis on recyclability and global warming concerns. Figure 6.7 illustrates hemp market growth compared to the current global hemp market which is expected to rise three-fold by the year 2020. Also, global players are inclining towards natural fiber composites like Asian countries are focusing on green electronics and European market is heavily interested in natural fiber composites in automotive (Lucintel report, 2011).

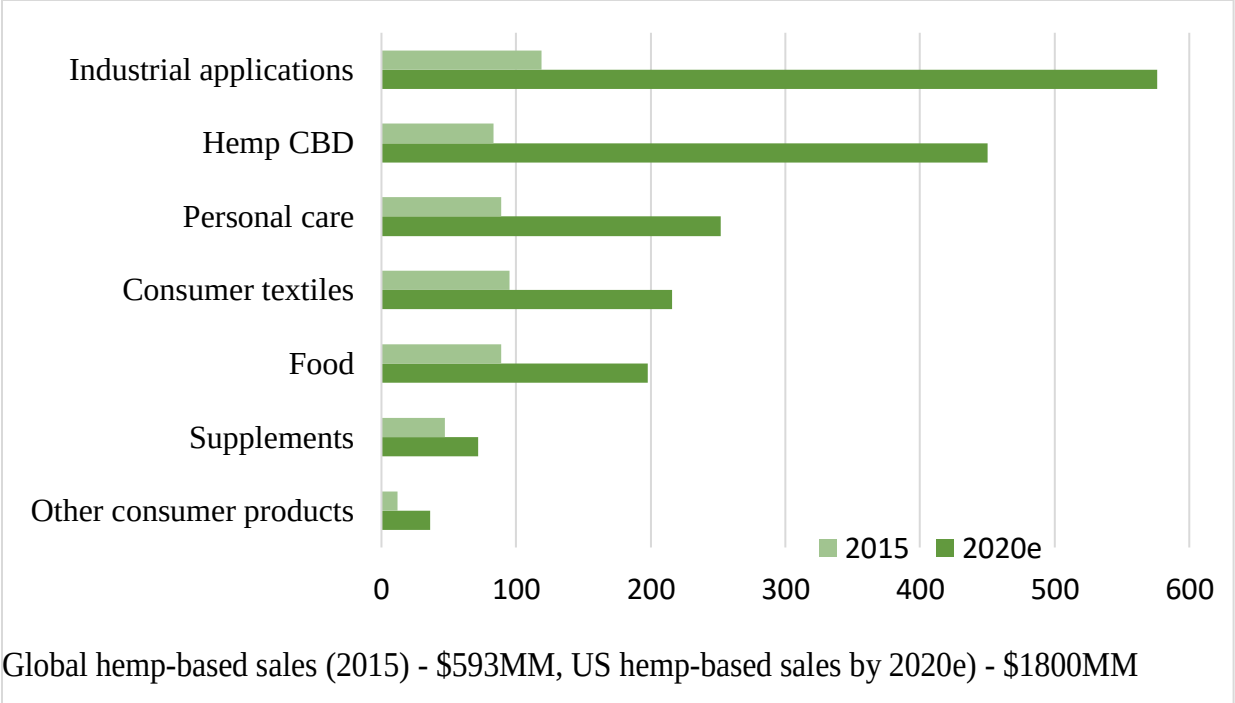

Figure 6.7. Future hemp market growth in the US compared to current global market (Hemp Business Journal, 2016).

Industrial hemp is not restricted by the optimum conditions to grow and can be grown in a variety of climates, altitudes, soils and weather conditions. Moreover, they grow up to 12 feet in just about 3 months. One of the most unique properties of hemp is fiber length and strength. Hemp has been used in making paper centuries ago. Today, about 95% of paper is made from wood pulp. Hemp can be a good alternative and therefore save trees from deforestations. Hemp has tremendous opportunities and can have multiple applications as every part of the hemp plant can be put to good use starting from seed, and stalk as illustrated in Figure 6.8.

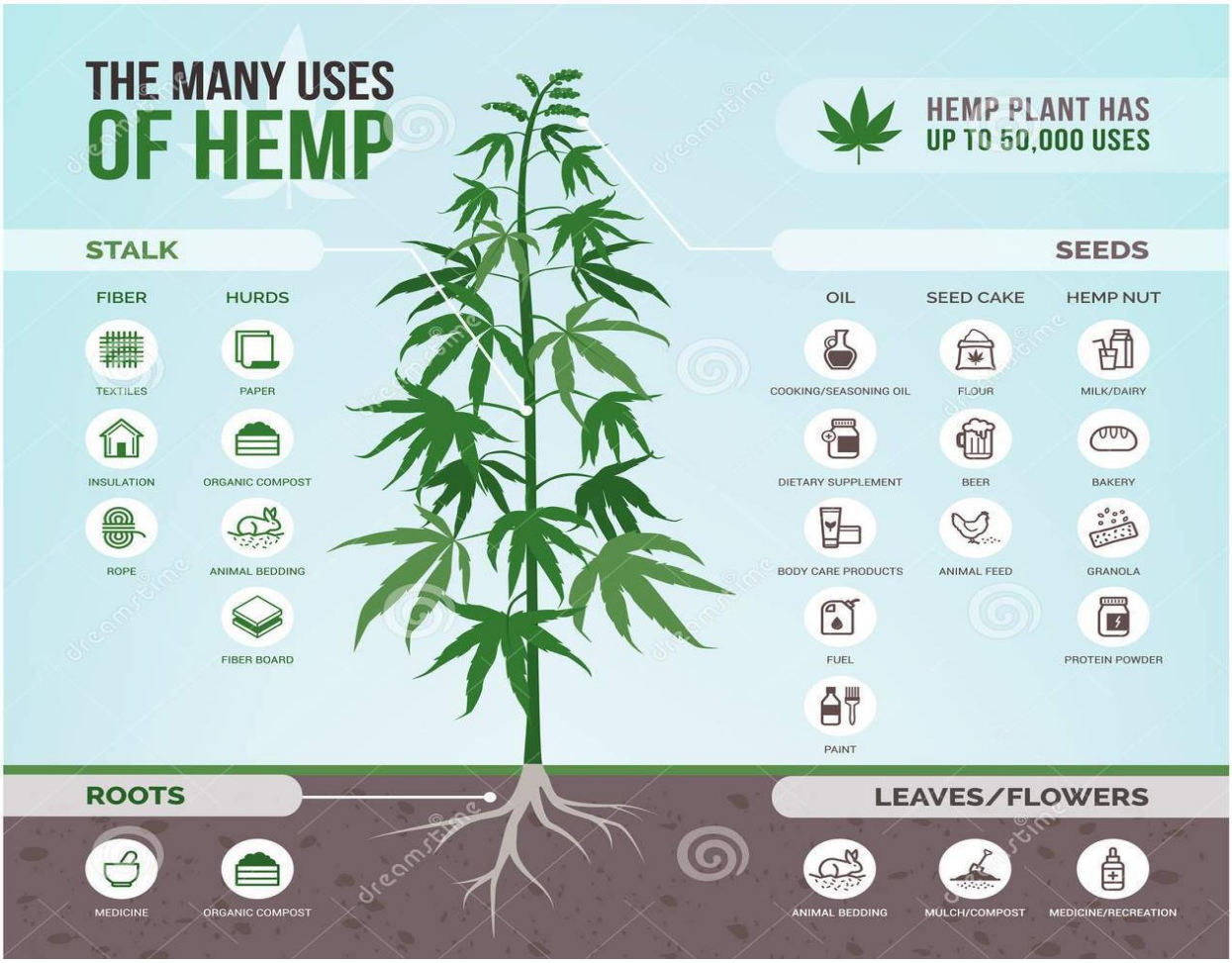

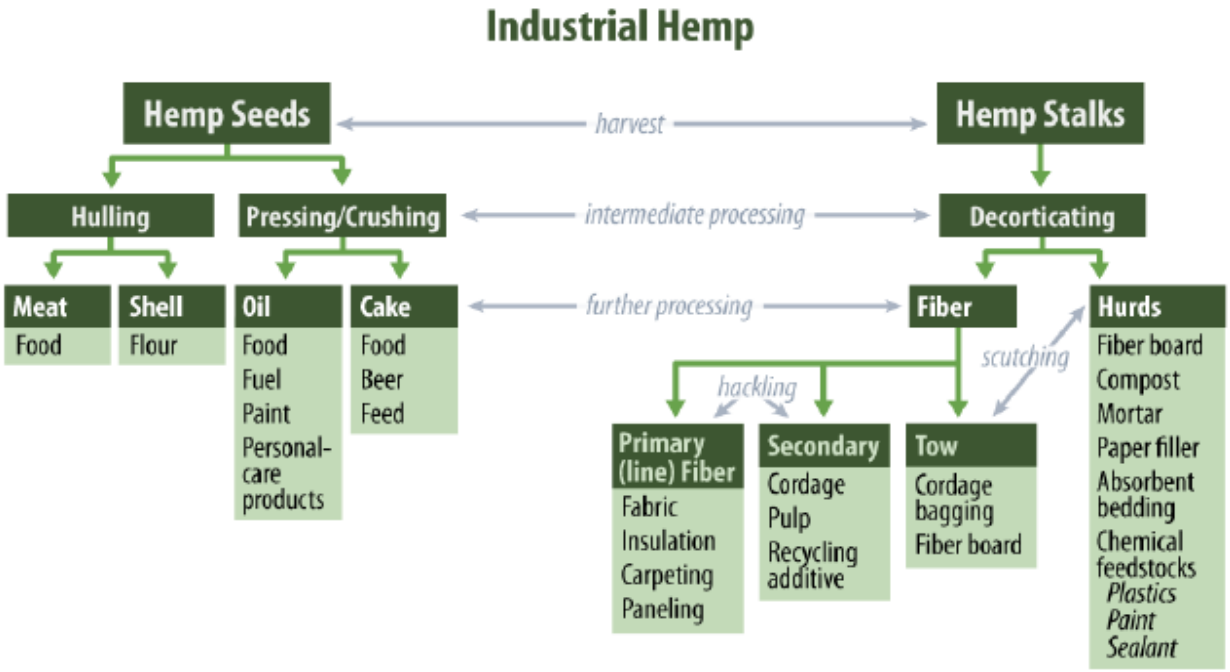

Figure 6.8. Hemp application from a different part of the plant (Follow, 2018; Johnson, 2017).

To understand the potential of hemp in the US. Demand forecasting is a combined effect of art and science, which helps in predicting the demand for the product and services in anticipation of variation that can be transformed into business planning and management. This is helpful for both governments to alter the existing policies as well as businesses to make strategic decisions. The strategic and quantitative forecasting has become an essential decision support tool in holistic execution of government functions and corporate supply chain management. Hemp forecasting can be used in production planning, inventory management, and at times in assessing future capacity requirements.

Due to lack of historical data, demand forecasting depended heavily on qualitative methods, such as expert opinion, online research and reports, educated guesses, and personal views of people from industry from various reports. Observations and individual views are based on historical facts, sales data, and any relevant information that add value to the forecast. However, to get an overview of future hemp market in the United States, it is important to look at other hemp growing countries.

Forecasting can be done based on recent market growth in the United States as well as comparative analysis with other hemp growing countries like France, Germany, and Canada. Figure 6.9 & 6.10 illustrates the market growth of European countries and Canada respectively. The figure clearly shows an upward trend in hemp production indicating an increase in hemp demand. However, in Figure 6.10, the downturn or dips in the year 2000 and 2007 is assumed as correction due to overproduction in the year 1999 and 2006 respectively. It is also attributed to "increasingly positive economics of growing other crops" as indicated by Manitoba Agriculture, National Industrial Hemp Strategy, March 2008.

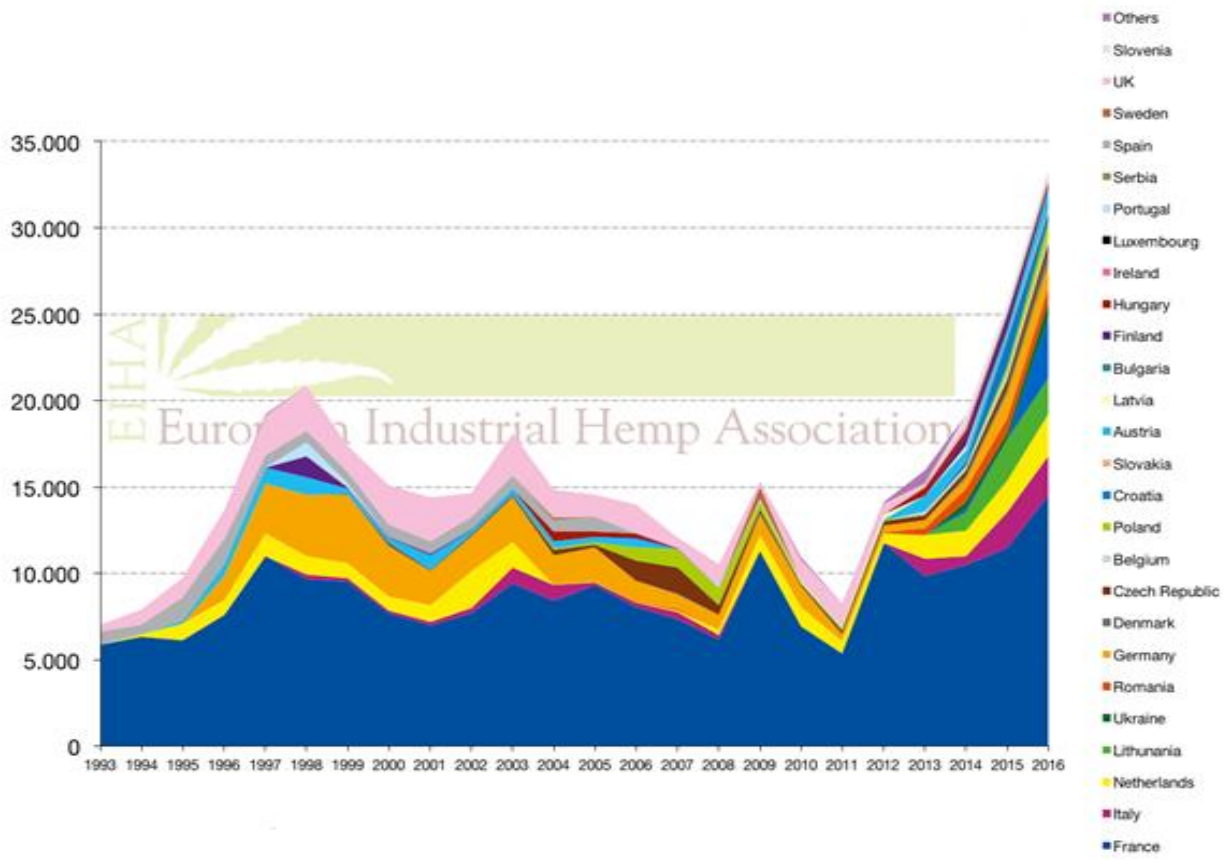

Figure 6.9 European hemp market (EIHA), 2017)

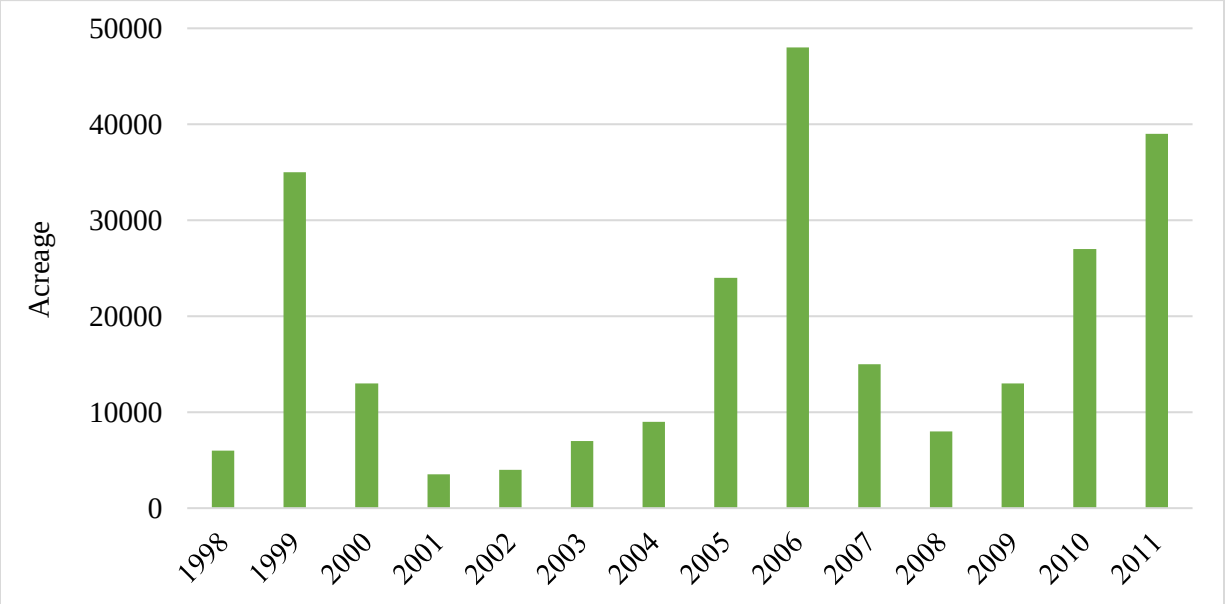

Figure 6.10 Acreage used to cultivate hemp in Canada (Johnson, 2017, Industrial Hemp Statistics, Agriculture and Agro-food, Canada)

Product Life Cycle (PLC)

Definition

Another aspect to look at it is the product life cycle method. Product life cycle (PLC) is the cycle, which is related to four phases namely introduction, growth, maturity and decline, which product has to go through. It explains the product from the time of its birth to complete decline at a macro level. The development of PLC to a given time point enables an estimate for the future time horizon. The size and shape of a product life cycle are unique to each commodity and cannot be generalized, however there are a few common traits which can fit all products and technologies. One cannot accurately predict the market and time spread for the stages, nevertheless, the development of PLC to a given time point facilitates a prediction for the future time horizon.

Stages of PLC

As mentioned above, product life cycle normally consists of four or five stages; introduction, growth, maturity, saturation, and decline. Saturation and decline may be combined into just decline stage [5]. In the introduction stage, the product is first introduced in the market. The product may occupy a small market share and then is followed by a growth stage which may be short or long. When the growth rate accelerates significantly, it is recognized as a growth stage. It is followed by maturity stage then the products are widely used and saturate the market. The growth rate is decreased in the maturity stage and the manufacturers make an effort to maintain its competitiveness as much as possible. The next step is a decline stage but timing is quite difficult to predict as it depends on the business strategy of the company as well as the emergence of new technologies. In this stage, the growth rate becomes negative. Usually, a decline stage is determined by new products in the market or change of consumer preference, lifestyle changes, and a strong cost competition from new processing technologies. This term ‘market’ means sales of a product or usage of a product. The strength of a product remains is retained until new products replace it.

Usefulness of applying PLC

There is no such thing as an 'ideal model' for predicting future demand especially when there is very minimal historical data. A product life cycle approach is used primarily for prediction of demand for a product in a long macro scale. Many examples exist for predicting product demand through product life cycles with success. While the usefulness of the PLC approach has been cited, one shortcoming is that the usefulness and appropriateness cannot be judged until the PLC is completed. In this sense, PLC could be viewed as an art in addition to being a science-based and shapes and numerical analysis. It is simply a well-recognized tool in studying the long term trends of a product in economic research. The fact that many products historically follow a long term trend similar to that postulated by the life cycle concept has been validated by Polli and Cook (Polli & Cook, 2002)

While the PLC concept is descriptive and heuristic in nature, it still has to be formulated and validated through a mathematical model. Often 'S-curve' is selected as a model from the introduction stage to maturity stage especially when historical data are not abundant. As this is also called a logistic function, the general equation will be given in a subsequent section.

The current market of hemp is in the introduction stage as States legalized industrial hemp after Farm bill 2014 shown in Figure 6.11. Due to inadequate data points available, we cannot rely on time series analysis to forecast demand. "S-curve" or Sigmoidal curve is used as a model for products in the introduction and growth stage, especially when historical data is not available. This is also called a logistic growth curve as shown below with the hemp market featuring in the introduction stage.

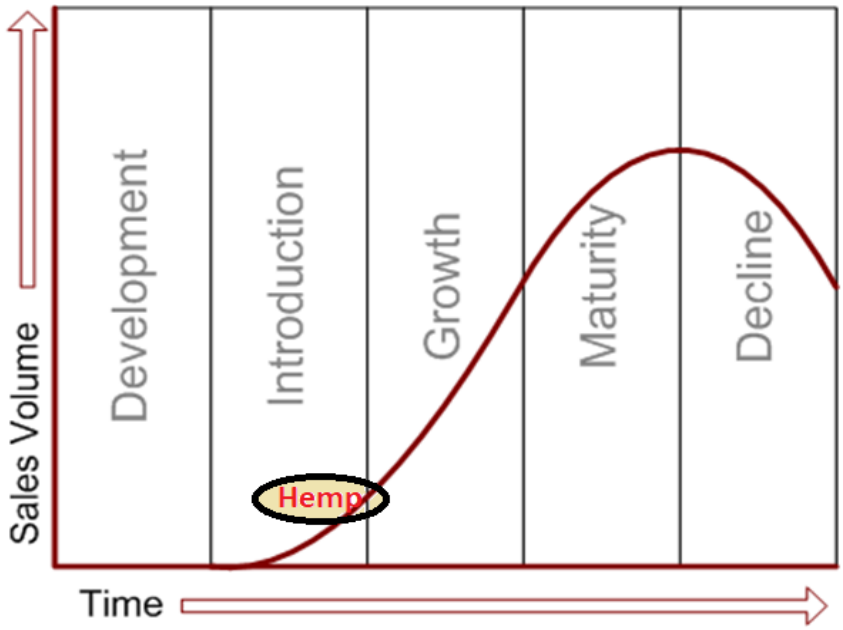

Figure 6.11. Product life cycle showing hemp in introduction stage in the US.

6.5. Conclusion

Although hemp policy in the US has significantly changed by the Farm Bill, hemp still has to make giant leaps to catch-up with the growing global hemp market. Even after legalization, industrial hemp has to go through a lot of scrutinizes and remains a highly regulated crop in the United States for personal and commercial production. The ramification about hemp still exists and there are a number of hindrances like the complicated government policies that have been modified still need to be addressed. Also, commercial cultivation could influence the surreptitious production of marijuana (high-THC source). This significantly increases surveillance in an effort to legalize industrial hemp and not promote marijuana.

From the logistics side, obstacles like processing, transportation, and agricultural infrastructure need to overcome. Increases in fiber harvesting and processing technology have allowed rapid advancements in hemp's use in composites and building applications.

Apart from the local challenges, the United States also faces competition from other hemp growing countries like Canada, France, Germany, China, etc. China remains the world's largest hemp fiber and seed producer and will likely to continue to reign the hemp market including hemp market price. Canada's investment in the North American hemp market,

especially hemp seed and oil, would also likely affect the hemp market growth in the United States.

Nevertheless, the hemp market in the United States has shown an upward trend, which looks very promising in multiple facets. Commercial hemp industry in the United States could provide opportunities as an economically viable alternative crop. The wide array applications of industrial hemp like specialty textiles, paper, and composites from bast fibers, animal bedding, composites and paper from hemp hurds are expected to grow with legislature change in the United States. However, for all these applications to develop or expand, hemp will have to compete with current advanced raw materials and manufacturing practices from other countries. Since the US hemp market is in at the introduction stage, it might take a couple of years to establish a strong market with continuous home-grown hemp supply.

CHAPTER 7 - OVERALL CONCLUSION AND FUTURE RESEARCH SUGGESTIONS

7.1. Key findings and conclusions

3DOW was used to develop composites using hemp as the reinforcement and vinyl ester as a matrix. The objective was to develop "green composites" by substituting glass fiber with more sustainable natural fiber. 3DOW was opted due to its crimpless weaving and minimal possibility of delamination. The advantage of low inter-fiber friction between the yarns during weaving leads to high drapability and low bending rigidity structure.

A full numerical parametric study was conducted to understand the structure potential of 3DOW composites. In order to understand the mechanical properties of the composite panels, structural parameters were altered including a number of Y-layers or thickness, weave design and amount of Z-yarns to Y- yarns ratio. A wide range of 3DOW was developed and put to test under different mechanical tests to study their response. Mechanical tests including tensile test, impact test (Tup & Charpy) and compression test were performed.

The tensile strength of the composite samples, due to changing the number of Y-yarn layers or thickness, had a very significant effect on the tensile peak load in both warp and weft direction. The contribution of thickness in the overall structure in this research was very substantial compared to the contribution of Z-binders and weave pattern. However, it was observed that 9 layer samples have the highest peak load, tensile stress and tensile strain compared to 6 layers and 3 layers had the lowest values. This was due to the fact that as we progressively increase the number of Y-yarn layers, the tensile strength goes higher due to an increase in the number of yarns with any additional layers. While comparing hemp composites with glass composites, it was found that the specific tensile stress of glass was significantly higher compared to hemp specific tensile stress. Unlike tensile stress, specific modulus of hemp and glass composite was found to be comparable.

In the Tup impact test, it can be concluded that changing the number of layers increased the total impact energy significantly and the layers are significantly different from each other. The effect of weave has no significant effect on the penetration energy. The weave pattern had a minimal significant effect on the total energy with 2x2 warp rib being the highest followed by 3x3 warp rib and plain. The effect of a change in Z to Y ratio is significantly different however,

the results are different in Tukey analysis where it shows that the change in Z to Y ratio does not significantly change the energy and ratio 1:1, 1:2 and 1:3 is not different from each other. Further, after normalizing the total penetration energy, the effects of the structural parameters became less significant. However, the presence of increasing trend by changing the number of layers (thickness) indicated that those three parameters have a significant effect on the composite impact energy irrespective of composite thickness, composite weight, or preform weight. The effect of changing the ratio of Z-binders contribution in the structure, and changing the weave pattern has less impact on the overall penetration energy.

In the case of Charpy impact energy, the increase in the number of layers or thickness increased the total energy in both warp and weft directions. However the effect of weave pattern and Z to Y contribution does not have a significant effect on the impact energy for both warp (Y) and Weft (X) direction. After normalizing the total penetration energy, the effects of the structural parameters became less significant with lower p-values. The presence of increasing trend by changing the number of layers (thickness) indicated that those three parameters have a significant effect on the composite impact energy irrespective of composite thickness, composite weight, or preform weight.

The impact properties of HFR composites were compared to GFR composites and was found that the total penetration energy for e-glass and hemp are comparable alongside with energy normalized by preform areal density. Charpy impact energy for hemp was significantly lower to e-glass.

In the case of a compression test, the main cause of thickness variation is specimen fabrication which leads to bending. As in the case of tensile test, thickness has the highest contributing factor in compression strength. It was found that there is a significant difference between warp and weft direction in terms of compression. Weave design and Z-yarns did not affect compression strength. The actual binder path of the weaves is affected by the interlacing movement which largely depends on the weave architectures. The degree of yarn waviness present in a 3D woven fabric can be affected by a range of factors including weave parameters and manufacturing-induced distortions such as fabric compaction. Any misalignment in the internal architecture such as yarn waviness can reduce in-plane compression effect.

For experiment A1, where the samples were desiccated to remove excess moisture from the preform, weave pattern change did not indicate a significant effect on the mechanical properties of the treated samples for both X- and Y-direction. This was due to moisture present in the samples or a small amount of moisture regained after removing from the oven. A few future recommendations are to use higher temperature in the oven for an extended period of time and use of desiccant bags to protect for moisture regain might help to improve the mechanical properties of the treated samples.

However, in the case of mercerization, by changing the weave pattern, the tensile strength of the treated samples decreased in weft direction along with a decrease in tensile stress and tensile strain. Plain weave has the highest values due to better structural integrity. The other contributing factor was that plain weave has a shorter float with more number of x-y intersections. These crossover points have better adhesion after mercerization thereby improving the tensile strength of plain weave. Yarn waviness also is the contributing factor, especially in the weft direction. Other important elements which influence the mechanical properties of composites are fiber length and yarn orientation during weaving. Tup impact energy in all the three weaves has significantly increased after mercerization. The effect of yarn waviness has less impact as tup impact is independent of yarn orientation and is minimized by mercerization. There was no significant difference between treated and untreated samples in X-yarn and Y-yarn direction as well as weave pattern for Charpy impact test. It was observed that the compression strength of all the composite samples increased after mercerization treatment. The variation denoted by standard deviation is also reduced after alkali treatment.

After decades of hibernation, Industrial hemp in the US was revived by introducing Farm Bill, 2014 and shows an upward trend which looks very promising in multiple facets. Natural fiber composites, especially hemp and flax, has great potential as the focus of many industries is shifting from conventional fiber to more sustainable natural resources. This shift can be made without compromising of the mechanical strength of the composites. However, there are various external forces like customers, suppliers, competitors, distributors, regulators, technology, etc. that will shape the hemp market in the USA. This will contribute to economic growth and decrease the dependency on imports.

7.2. Future research

This research work involving 3DOW using hemp-fiber reinforcement could open new research avenues in the future. Since hemp is a new crop in the US, it is subject to a variety of research. As every research work, this project had its own limitations which can be tackled through future research.

Sourcing 100% hemp-fiber required for thesis research was challenging, especially at the time when hemp was being considered for legalization. However, the legal scenario has changed dramatically over the past few years where industrial hemp is made legal in 41 states. This opens up areas for more research opportunities, especially in the area of high-performance technical textiles.

Although using 3DOW technique successfully eliminated the delamination failure mechanism, it also introduced fiber waviness in warp and weft direction through weave geometry limitations. Fiber waviness resulted in a substantial reduction in mechanical strength, especially compression strength. The pick density used in this research was chosen in order to manufacture square fabric. However, this created fabric with low fiber volume fraction and low structural integrity, which ultimately affected the mechanical properties of the composites. Also, weave design with similar weave repeat was chosen to understand the effect of float on the mechanical strength. For future studies, the analysis should be extended to high pick density and other weave patterns which could result in better mechanical properties.

VARTM has proved to be a very effective way to infuse 3DOW preforms. Vinyl ester used in this research could be substituted with plant-based resin in order to produce 100% green composite in the future.

Further mechanical tests to understand the flexural properties should be performed to expand the application prospect in composites. Also, in order to improve the fiber and matrix bonding for natural-fiber based composites, other chemical treatment should be considered.

It can be concluded that with systematic and persistent research there will be a good scope and better future for hemp-fiber reinforced composites for suitable composite applications ranging from high-performance applications to low load-bearing applications.

REFERENCES

(EIHA), E. I. H. A. (2017). Press Release : Record cultivation of industrial hemp in Europe in 2016 Especially hemp food and pharmaceuticals face strong demand –, *1994*.

Agoudjil, B., Benchabane, A., Boudenne, A., Ibos, L., & Fois, M. (2011). Renewable materials to reduce building heat loss: Characterization of date palm wood. *Energy and Buildings*, *43*(2–3), 491–497. https://doi.org/10.1016/j.enbuild.2010.10.014

AL-Oqla, F. M., & Sapuan, S. M. (2014). Natural fiber reinforced polymer composites in industrial applications: feasibility of date palm fibers for sustainable automotive industry. *Journal of Cleaner Production*, *66*, 347–354. https://doi.org/10.1016/j.jclepro.2013.10.050

Anandjiwala, R. D., & Blouw, S. (2007). Composites from Bast Fibres-Prospects and Potential in the Changing Market Environment. *Journal of Natural Fibers*, *4*(2), 91–109. https://doi.org/10.1300/J395v04n02_07

Arbelaiz, a., Fernández, B., Ramos, J. a., & Mondragon, I. (2006). Thermal and crystallization studies of short flax fibre reinforced polypropylene matrix composites: Effect of treatments. *Thermochimica Acta*, *440*(2), 111–121. https://doi.org/10.1016/j.tca.2005.10.016

Ashland chemicals. (2006). DERAKANE 8084 Epoxy Vinyl Ester Resin, 2002–2004.

B. Singh, A. Verma, and A. G. (1998). Studies on Adsorptive Interaction Between Natural Fiber and Coupling Agents. *Journal of Applied Polymer Science*, (70), 1847–1858.

Baiardo, M., Frisoni, G., Scandola, M., & Licciardello, A. (2002). Surface chemical modification of natural cellulose fibers. *Journal of Applied Polymer Science*, *83*(1), 38–45. https://doi.org/10.1002/app.2229

Baiardo, M., Zini, E., & Scandola, M. (2004). Flax fibre-polyester composites. *Composites Part A: Applied Science and Manufacturing*, *35*(6), 703–710. https://doi.org/10.1016/j.compositesa.2004.02.004

Barnett, J. R., & Bonham, V. a. (2004). Cellulose microfibril angle in the cell wall of wood fibres. *Biological Reviews of the Cambridge Philosophical Society*, *79*(2), 461–472. https://doi.org/Doi 10.1017/S1464793103006377

Belgacem, M. N., & Gandini, A. (2005). The surface modification of cellulose fibres for use as reinforcing elements in composite materials. *Composite Interfaces*, *12*(1–2), 41–75. https://doi.org/10.1163/1568554053542188

Bledzki, a. K., & Gassan, J. (1999). Composites reinforced with cellulose based fibres. *Progress in Polymer Science (Oxford)*, *24*(2), 221–274. https://doi.org/10.1016/S0079-6700(98)00018-5

Campbell, F. C. (2010). Introduction to composites material. In *Structural composites material*. ASM International.

Cardarelli, F. (2001). Materials Handbook — a concise desktop reference. *Materials & Design*. https://doi.org/10.1016/S0261-3069(00)00075-3

Chandramohan, D., & Marimuthu, K. (2011). A review on natural fibers. *International Journal of Research and Reviews in Applied Sciences*, *8*(2), 194–206. Retrieved from http://www.arpapress.com/Volumes/Vol8Issue2/IJRRAS_8_2_09.pdf

Chou, T. W. (1993). *Polymer-matrix composites*.

Craig MC, D. F. (2005). Natural Fibers. In X. M (Ed.), *Functional fillers for plastics* (pp. 195–206). Weinheim: Wiley-VCH Verlag.

Dash BN, Rana AK, Mishra HK, Nayak SK, T. S. (2000). Novel low-cost jute–polyester composites. III. Weathering and Thermal Behavior. *Journal of Applied Polymer Science*, *78*, 1671–1679.

De, S. K., & White, J. R. (Eds.). (1996). *Short fibre-polymer composites*. Elsevier.

Deve, H., & McCullough, C. (1995). Continuous-fiber reinforced composites: A new generation. *JOM*, *47*(7), 33–37. https://doi.org/10.1007/BF03221227

Dhakal, H. N., Zhang, Z. Y., & Richardson, M. O. W. (2007). SCIENCE AND Effect of water absorption on the mechanical properties of hemp fibre reinforced unsaturated polyester composites, *67*, 1674–1683. https://doi.org/10.1016/j.compscitech.2006.06.019

Eichhorn, S. J., Baillie, C. a., Zafeiropoulos, N., Mwaikambo, L. Y., Ansell, M. P., Dufresne, a., … Wild, P. M. (2001). Current international research into cellulosic fibres and composites. *Journal of Materials Science*, *36*(9), 2107–2131. https://doi.org/10.1023/A:1017512029696

Elliott-Sink, S. (2005). *Cars Made of Plants*. Retrieved from www.edmunds.com/advice/

F. Stig. (n.d.). 3D-woven reinforcement in composites.

Faruk, O., Bledzki, A. K., Fink, H. P., & Sain, M. (2012). Biocomposites reinforced with natural fibers: 2000-2010. *Progress in Polymer Science*, *37*(11), 1552–1596. https://doi.org/10.1016/j.progpolymsci.2012.04.003

Follow, A. C. (2018). Hemp 101 : Everything You Need to Know How is Hemp Different from

Marijuana and Cannabis ?

Francucci, G., Manthey, N. W., Cardona, F., & Aravinthan, T. (2014). Processing and characterization of 100% hemp-based biocomposites obtained by vacuum infusion. *Journal of Composite Materials*, *48*(11), 1323–1335. https://doi.org/10.1177/0021998313485266

Frisoni, G., Baiardo, M., Scandola, M., Lednická, D., Cnockaert, M. C., Mergaert, J., & Swings, J. (2001). Natural cellulose fibers: Heterogeneous acetylation kinetics and biodegradation behavior. *Biomacromolecules*, *2*(2), 476–482. https://doi.org/10.1021/bm0056409

Gassan, J., & Gutowski, V. S. (2000). Effects of corona discharge and UV treatment on the properties of jute-fibre expoxy composites. *Composites Science and Technology*, *60*(15), 2857–2863. https://doi.org/10.1016/S0266-3538(00)00168-8

George, J., Sreekala, M. S., & Thomas, S. (2001). A review on interface modification and characterization of natural fiber reinforced plastic composites. *Polymer Engineering & Science*, *41*(9), 1471–1485. https://doi.org/10.1002/pen.10846

Ghobakhloo, M., Tang, S., Zulkifli, N., & Ariffin, M. (2013). An Integrated Framework of Green Supply Chain Management Implementation. *Ijimt.Org*, *4*(1). https://doi.org/10.7763/IJIMT.2013.V4.364

Hemp Business Journal. (2016). HBJ_StateofHemp_2016.pdf.

Herrera-Franco, P. J., & Valadez-González, a. (2005). A study of the mechanical properties of short natural-fiber reinforced composites. *Composites Part B: Engineering*, *36*(8), 597–608. https://doi.org/10.1016/j.compositesb.2005.04.001

Hoa, S. V. (2009). *ebook-Principles of the MANUFACTURING OF COMPOSITE MATERIALS*. *Industrial Engineering*.

Holbery, J., & Houston, D. (2006). Natural-fiber-reinforced polymer composites in automotive applications. *Jom*, *58*(November), 80–86. https://doi.org/10.1007/s11837-006-0234-2

Hull, D., & Clyne, T. W. (1996). *An Introduction to Composite Materials*. Cambridge University Press. Retrieved from https://books.google.co.in/books?id=BRcdDu4bUhMC

Ince, M. E. (2013). Performance of Composites from 3D Orthogonal Woven Preforms in terms of Architecture and Sample Location during Resin Infusion.

Islam, M. S., Pickering, K. L., & Foreman, N. J. (2010). Composites : Part A Influence of alkali treatment on the interfacial and physico-mechanical properties of industrial hemp fibre reinforced polylactic acid composites. *Composites Part A*, *41*(5), 596–603.

https://doi.org/10.1016/j.compositesa.2010.01.006

JOHN, M., & THOMAS, S. (2008). Biofibres and biocomposites. *Carbohydrate Polymers*, *71*(3), 343–364. https://doi.org/10.1016/j.carbpol.2007.05.040

Johnson, R. (2017). Hemp as an Agricultural Commodity. *Congressional Research Service*, 1–40. Retrieved from https://fas.org/sgp/crs/misc/RL32725.pdf

Joshi, S. V., Drzal, L. T., Mohanty, a. K., & Arora, S. (2004). Are natural fiber composites environmentally superior to glass fiber reinforced composites? *Composites Part A: Applied Science and Manufacturing*, *35*(3), 371–376. https://doi.org/10.1016/j.compositesa.2003.09.016

Khokar, N. (1996). 3D Fabric-forming Processes: Distinguishing Between 2D-weaving, 3D-weaving and an Unspecified Non-interlacing Process. *Journal of the Textile Institute*. https://doi.org/10.1080/00405009608659059

Khot, S. N., Lascala, J. J., Can, E., Morye, S. S., Williams, G. I., Palmese, G. R., … Wool, R. P. (2001). Development and application of triglyceride-based polymers and composites. *Journal of Applied Polymer Science*, *82*(3), 703–723. https://doi.org/10.1002/app.1897

Lee, S. M. (1991). *International encyclopedia of composites* (2nd editio).

Lewin, M. (2006). *Handbook of Fiber Chemistry*. *Handbook of Fiber Chemistry*. https://doi.org/10.1002/1521-3773(20010316)40:6<9823::AID-ANIE9823>3.3.CO;2-C

Lucintel report, 2011. (2011). Potential of Natural fiber Composites, Lucintel Consulting. *Energy Weekly News*, 107. Retrieved from http://www.lucintel.com/

Madsen, B. (2004). *Properties of Plant Fibre Yarn Polymer Composites*. *Thesis*.

Mallick, P. K. (1993). *Fiber-Reinforced Composites: Materials, Manufacturing, and Design.* CRC Press.

Manikandan Nair, K. C., Diwan, S. M., & Thomas, S. (1996). Tensile properties of short sisal fiber reinforced polystyrene composites. *Journal of Applied Polymer Science*, *60*(9), 1483–1497. https://doi.org/10.1002/(SICI)1097-4628(19960531)60:9<1483::AID-APP23>3.3.CO;2-L

Manson, R. T. and J.-A. E. (2001). *Polymer Matrix Composites*. Elsevier, Amsterdam.

Matthews, de FL, and R. D. R. (1999). *Composite materials: engineering and science.* Elsevier.

Midani, M., "The Influence of Weave and Structural Parameters on the Performance of Composites from 3D Orthogonal Woven Preforms" Dissertation. North Carolina State

University, 2016. Electronic Thesis and Dissertation.

Mike, & Brady, P. (2008). Developments in automotive plastics. *Reinforced Plastics*, *52*(10), 37–40. https://doi.org/10.1016/S0034-3617(08)70374-6

Mohamed, et al, 2001. (2001). A new generation of 3D woven fabric preforms and composites. In *SAMPE Journal* (Vol. 37, pp. 8–17).

Mohamed, M. H., & Zhang, Z.-H. (1992). *5,085,252*. United States of America: United States Patent. https://doi.org/US005485919A

Mohanty, a. K., Misra, M., & Drzal, L. T. (2001). Surface modifications of natural fibers and performance of the resulting biocomposites: An overview. *Composite Interfaces*, *8*(5), 313–343. https://doi.org/10.1163/156855401753255422

Mohanty, a. K., Misra, M., & Drzal, L. T. (2002). Sustainable Bio-Composites from renewable resources: Opportunities and challenges in the green materials world. *Journal of Polymers and the Environment*, *10*(1–2), 19–26. https://doi.org/10.1023/A:1021013921916

Mohanty, A. K., Misra, M., & Drzal, L. T. (2005). *Natural Fibers, Biopolymers, and Biocomposites*. *Most*. https://doi.org/10.1201/9780203508206

Mohanty, K. A., Drzal, L. T., & Misra, M. (2002). Engineered natural fiber reinforced polypropylene composites : influence of surface modifications and novel powder impregnation processing. *Journal of Adhesion Science and Technology*, *16*(8), 999–1015. https://doi.org/10.1163/156856102760146129

NCSL. (2018). State Industrial Hemp Statutes. *National Conference of State Legislatures* . Retrieved from http://www.ncsl.org/research/agriculture-and-rural-development/state-industrial-hemp-statutes.aspx

Netravali, A. N., & Chabba, S. (2003). Composites get greener. *Materials Today*, *6*(4), 22–29. https://doi.org/10.1016/S1369-7021(03)00427-9

Odian, G. (2004). *Principles of Polymerization (3. Kapitel)*. *Principles of Polymerization, Fourth Edition*. https://doi.org/10.1002/047147875X

Ouajai, S., & Shanks, R. A. (2005). Composition, structure and thermal degradation of hemp cellulose after chemical treatments. *Polymer Degradation and Stability*, *89*(2), 327–335. https://doi.org/10.1016/j.polymdegradstab.2005.01.016

Pathak, S., Sneha, C. L. R., & Mathew, B. B. (2016). Bioplastics : Its Timeline Based Scenario & Challenges, *2*(January 2014), 84–90. https://doi.org/10.12691/jpbpc-2-4-5

Polli, R., & Cook, V. (2002). Validity of the Product Life Cycle. *The Journal of Business*, *42*(4), 385. https://doi.org/10.1086/295215

Prasad, R. C., & Ramakrishnan, P. (2000). *Composites, Science, and Technology*. New Age International. Retrieved from https://books.google.co.in/books?id=6QsoU6HtQAoC

R. Karnani, M. Krishnan, and R. N. (1997).). *Polymer Engineering & Science*, 476.

Rong, M. Z., Zhang, M. Q., Liu, Y., Yang, G. C., & Zeng, H. M. (2001). The effect of fiber treatment on the mechanical properties of unidirectional sisal-reinforced epoxy composites. *Composites Science and Technology*, *61*, 1437–1447. https://doi.org/10.1016/S0266-3538(01)00046-X

Samuel, O. D., Agbo, S., & Adekanye, T. A. (2012). Assessing Mechanical Properties of Natural Fibre Reinforced Composites for Engineering Applications, *2012*(August), 780–784.

Sawpan, M. A., Pickering, K. L., & Fernyhough, A. (2011). Composites : Part A Effect of fibre treatments on interfacial shear strength of hemp fibre reinforced polylactide and unsaturated polyester composites. *Composites Part A*, *42*(9), 1189–1196. https://doi.org/10.1016/j.compositesa.2011.05.003

Scarponi, C., & Messano, M. (2015). Comparative evaluation between E-Glass and hemp fiber composites application in rotorcraft interiors. *Composites Part B: Engineering*, *69*, 542–549. https://doi.org/10.1016/j.compositesb.2014.09.010

Seile, A., Belakova, D., & Technologies, D. (2014). Hemp Made Bio-Composites, 22–28. https://doi.org/10.7250/mstct.2014.004

Sgriccia, N., Hawley, M. C., & Misra, M. (2008). Characterization of natural fiber surfaces and natural fiber composites. *Composites Part A: Applied Science and Manufacturing*, *39*(10), 1632–1637. https://doi.org/10.1016/j.compositesa.2008.07.007

Shahzad, A. (2011). Hemp fiber and its composites – a review. https://doi.org/10.1177/0021998311413623

Siqueira, G., Bras, J., & Dufresne, A. (2010). Cellulosic bionanocomposites: A review of preparation, properties and applications. *Polymers*. https://doi.org/10.3390/polym2040728

Sydenstricker, T. H. D., Mochnaz, S., & Amico, S. C. (2003). Pull-out and other evaluations in sisal-reinforced polyester biocomposites. *Polymer Testing*, *22*(4), 375–380. https://doi.org/10.1016/S0142-9418(02)00116-2

Tran, P., Graiver, D., & Narayan, R. (2006). Biocomposites synthesized from chemically

modified soy oil and biofibers. *Journal of Applied Polymer Science*, *102*(1), 69–75. https://doi.org/10.1002/app.22265

Tsoumis, G. (1991). *Science and technology of wood. Structure, properties, utilization*. *Science and technology of wood. Structure, properties, utilization.*

Van Vuure, A. W., Baets, J., Wouters, K., & Hendrickx, K. (2015). Compressive properties of natural fibre composites. *Materials Letters*, *149*, 138–140. https://doi.org/10.1016/j.matlet.2015.01.158

Vantreese, V. L. (1998). Industrial Hemp Global Operations , Local Implications, *0276*(July), 1–32.

Vigo, T. L. and Kinzig, B. J. (1992). *An overview of organic polymeric matrix resins for composites*.

Vinay, H. B., Govindaraju, H. K., & Banakar, P. (2014). A Review on Investigation on the Influence of Reinforcement on Mechanical Properties of Hybrid Composites Introduction : Fibers / Reinforcement Materials :, *24*(2), 39–48.

Vote hemp. (2018). US Hemp report, 2017, *2016*, 7606. Retrieved from https://www.votehemp.com/wp-content/uploads/2018/09/Vote-Hemp-2017-US-Hemp-Crop-Report.pdf

Vote Hemp. (2019). US hemp report, 2018, 578.

Wu, C. S. (2009). No Title. *Polymer Degradation and Stability.*, 1076.

Zampaloni, M. (2007). Kenaf natural fiber reinforced polypropylene composites : A discussion on manufacturing problems and solutions, *38*, 1569–1580. https://doi.org/10.1016/j.compositesa.2007.01.001

Zini, E., & Scandola, M. (2011). Green composites: An overview. *Polymer Composites*, *32*, 1905–1915. https://doi.org/10.1002/pc.21224

Zini, E., Scandola, M., & Gatenholm, P. (2003). Heterogeneous acylation of flax fibers. Reaction kinetics and surface properties. *Biomacromolecules*, *4*(3), 821–827. https://doi.org/10.1021/bm034040h

https://ministryofhemp.com/hemp/history/

https://www.hempbasics.com/shop/general-hemp-information

https://www.brookings.edu/blog/fixgov/2018/12/14/the-farm-bill-hemp-and-cbd-explainer/

http://www.hemptrade.ca/eguide/background/history-of-hemp

https://hempindustrydaily.com/chart-farmers-and-ranchers-show-interest-in-growing-and-using-hemp/

http://www.ncsl.org/research/agriculture-and-rural-development/state-industrial-hemp-statutes.aspx

https://www.grandviewresearch.com/industry-analysis/industrial-hemp-market

APPENDICES

Appendix 1. Calculation of single fiber diameter

Preform Length, m	1.2
Preform Width, m	0.4
Preform Width, cm	40
Creel capacity	1088
Weave	Plain
No. of Y-yarns per layer	102
Number of Y-yarn Layers	6
Number of X-yarn Layers	7
Y/Z yarn ratio	1
Number of Preforms	40

Yarn	Numerical count, Nm	Denier	Tex	Packing Factor (spun yarn)	Specific Gravity, kg/m^3	Diamter, m	Diamter, cm
X	6	1500	167	0.65	1480	0.0005	0.04698
Y	8.5	1059	118	0.65	1480	0.0004	0.03947
Z	36	250	28	0.65	1480	0.0002	0.01918

Appendix 2. Calculation of pick density for balanced structure for different layers

Y-yarns/inch/layer	
inches/cm	2.54
No.of yarns/layer	102
Preform Width (cm)	40
y-yarns/inch/layer	6.5

For balanced structure	
No. of ends/pacakge (X)	2
No. of ends/pacakge (Y)	3
No. of X-yarns insertions/shed	2

No. of layers (X)	No. of layers (Y)	of Y-yarns (in denier)	No. of Y-yarns/inch/layer	Total denier(Y)/inch	Linear density of X-yarns (in denier)	No. of X-yarns/inch/layer
4	3	1059	6.5	61722	1500	5.14
7	6	1059	6.5	123444	1500	5.88
10	9	1059	6.5	185166	1500	6.17

Appendix 3. Formula and nomenclature for FVF calculation (theoretical)

$$F_{fx} = \frac{\frac{n_x \rho_{lx}}{\rho_{vx} 10^3}}{p_x(n_y d_y + n_x d_x + 2d_z)} \quad F_{fy} = \frac{\frac{n_y \rho_{ly}}{\rho_{vx} 10^3}}{p_y(n_y d_y + n_x d_x + 2d_z)}$$

$$F_{fz} = \frac{\frac{[\frac{L_{Ioz}}{M_z} + (1 - \frac{1}{M_z}) p_x] N_z \rho_{lz}}{\rho_{vz} 10^3}}{N_y p_y p_x (n_y d_y + n_x d_x + 2d_z)}$$

The diameter of the yarns is calculated by using the formula below.

$$d = \frac{1}{280.2} \sqrt{\frac{N_t}{\phi \rho_f}}$$

F_{fx}	FVF (X-yarns)
F_{fy}	FVF (Y-yarns)
F_{fz}	FVF (Z-yarns)
T_x	Thread density (No. of x-yarns/cm)
P_{ox} (mm)	X-yarn spacing (1/thread density)
n_x	No. of X-yarn layers
n_y	No. of Y-yarn layers
dx	No. of Z-yarn layers
d_x (mm)	X-yarn diameter
d_y (mm)	Y-yarn diameter
d_z (mm)	Z-yarn diameter
ρ_{lx} (tex)	Linear density of X-yarns
ρ_{ly} (tex)	Linear density of Y-yarns
ρ_{lz} (tex)	Linear density of Z-yarns
ρ_{vx} (g/cm3)	Volumetric density of X-yarns
ρ_{vy} (g/cm3)	Volumetric density of Y-yarns
ρ_{vz} (g/cm3)	Volumetric density of Z-yarns
L_{ioz} (mm)	inclined length of Z-yarns
M_z	Weave factor of Z-yarn
N_x	Weave repeat of X-yarn
N_y	Weave repeat of Y-yarn
N_z	Weave repeat of Z-yarn
N_t	Yarn number (tex)
ρ_f	Fiber density
ρ_y	Yarn density
ø	Yarn packing factor, ρ_y/ρ_f

Appendix 4. Nomenclature of variables used in statistical analysis

Variable	Levels	Nomenclature
Number of layers	9 layers	9 , A
	6 layers	6 , B
	3 layers	3 , C
Weave pattern	Plain	WA , 1
	2x2 warp rib	WB , 2
	3x3 warp rib	WC , 3
Z to Y ratio	1:1	1
	1:2	0.5
	1:3	0.33
Warp/ weft direction	-	y/x
Normalized by thickness	Warp	ynormthick
	Weft	xnormthick
Normalized by composite areal density	Warp	ynormcden
	Weft	xnormcden
Normalized by preform areal density	Warp	ynormpden
	Weft	xnormpden
Thickness	Warp	ythick
	Weft	xthick
Total penetration energy	Warp	yenergy
	Weft	xenergy
Z to Y Ratio 1:1	Warp, weft	AY , AX
Z to Y Ratio 1:2	Warp, weft	BY , BX
Z to Y Ratio 1:3	Warp, weft	CY , CX
Chemical treatment (mercerization)		C
Moisture treatment (desiccation)		M
10		6 layer+1:1+WA
11		6 layer+1:1+WB
12		6 layer+1:1+WA

Appendix 5. ANOVA result – Tensile Test (Warp direction)

Dependent Variable: ythick

Number of Observations Read	126
Number of Observations Used	126

Analysis of Variance

Source	DF	Sum of Squares	Mean Square	F Value	Pr > F
Model	3	436.66706	145.55569	6092.48	<.0001
Error	122	2.91471	0.02389		
Corrected Total	125	439.58177			

Root MSE	0.15457	R-Square	0.9934
Dependent Mean	5.07897	Adj R-Sq	0.9932
Coeff Var	3.04328		

Parameter Estimates

Variable	DF	Parameter Estimate	Standard Error	t Value	Pr > |t|
Intercept	1	0.48277	0.05864	8.23	<.0001
ZYRatio	1	0.03151	0.04735	0.67	0.5071
layers	1	0.75538	0.00559	135.12	<.0001
weave	1	0.03097	0.01701	1.82	0.0711

Appendix 6. Tukey HSD Tensile result – Effect of layers on tensile peak load (Warp direction)

Oneway Analysis of PEAK LOAD, N By # of LAYERS

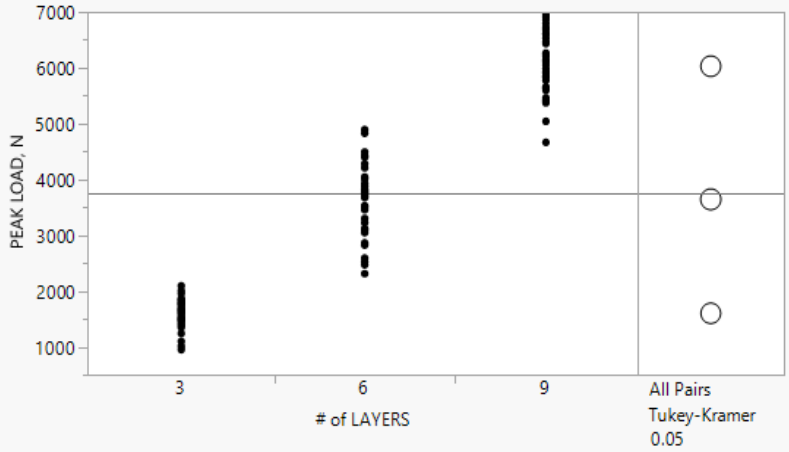

Means Comparisons

Comparisons for all pairs using Tukey-Kramer HSD

Difference Matrix

Dif=Mean[i]-Mean[j]

	9	6	3
9	0.0	2386.4	4429.3
6	-2386.4	0.0	2042.9
3	-4429.3	-2042.9	0.0

Connecting Letters Report

Level		Mean
9	A	6029.9671
6	B	3643.5917
3	C	1600.6760

Levels not connected by same letter are significantly different.

Ordered Differences Report

Level	- Level	Difference	Std Err Dif	Lower CL	Upper CL	p-Value
9	3	4429.291	110.0673	4168.162	4690.421	<.0001*
9	6	2386.375	111.3859	2122.118	2650.633	<.0001*
6	3	2042.916	110.7442	1780.180	2305.651	<.0001*

Appendix 7. Tukey HSD Tensile result – Effect of layers on tensile load normalized by thickness (Warp direction)

Oneway Analysis of Normaized by thickness, N/mm By # of LAYERS

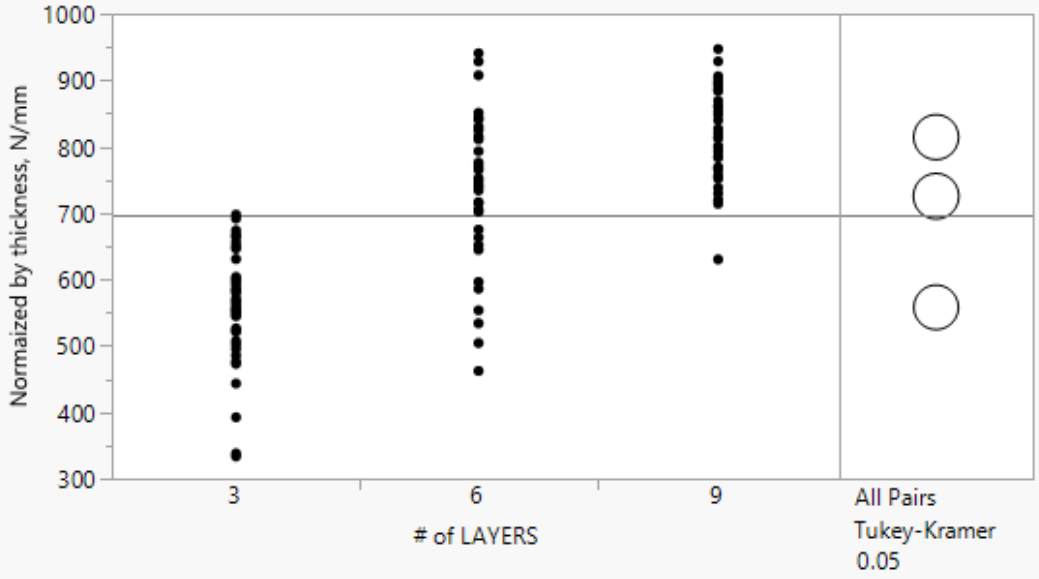

Means Comparisons

Comparisons for all pairs using Tukey-Kramer HSD

Difference Matrix

Dif=Mean[i]-Mean[j]

	9	6	3
9	0.00	88.95	256.40
6	-88.95	0.00	167.45
3	-256.40	-167.45	0.00

Connecting Letters Report

Level				Mean
9	A			814.46663
6		B		725.51728
3			C	558.07032

Levels not connected by same letter are significantly different.

Ordered Differences Report

Level	- Level	Difference	Std Err Dif	Lower CL	Upper CL	p-Value
9	3	256.3963	20.13573	208.6253	304.1674	<.0001*
6	3	167.4470	20.25957	119.3821	215.5118	<.0001*
9	6	88.9494	20.37695	40.6060	137.2927	<.0001*

Appendix 8. Tukey HSD Tensile result – Effect of weave on tensile load (Warp direction)

Oneway Analysis of PEAK LOAD, N By WEAVE

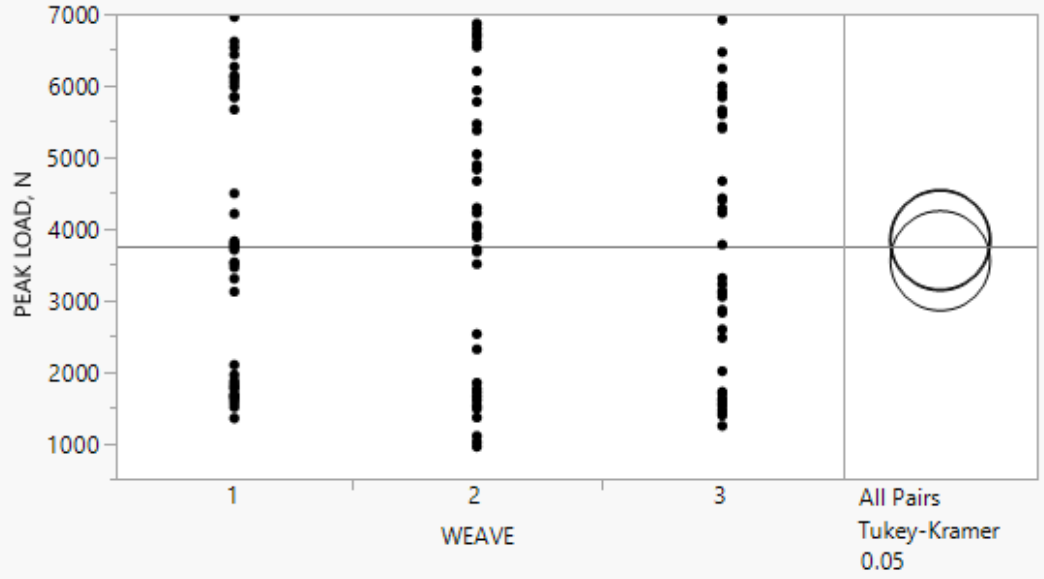

Means Comparisons

Comparisons for all pairs using Tukey-Kramer HSD

Difference Matrix

Dif=Mean[i]-Mean[j]

	2	1	3
2	0.00	1.22	288.42
1	-1.22	0.00	287.20
3	-288.42	-287.20	0.00

Connecting Letters Report

Level		Mean
2	A	3838.4040
1	A	3837.1812
3	A	3549.9798

Levels not connected by same letter are significantly different.

Ordered Differences Report

Level	- Level	Difference	Std Err Dif	Lower CL	Upper CL	p-Value
2	3	288.4242	413.4643	-692.500	1269.349	0.7653
1	3	287.2015	418.4176	-705.475	1279.877	0.7719
2	1	1.2227	416.0073	-985.735	988.180	1.0000

Appendix 9. Tukey HSD Tensile result – Effect of weave on tensile load normalized by thickness (Warp direction)

Oneway Analysis of Normaized by thickness, N/mm By WEAVE

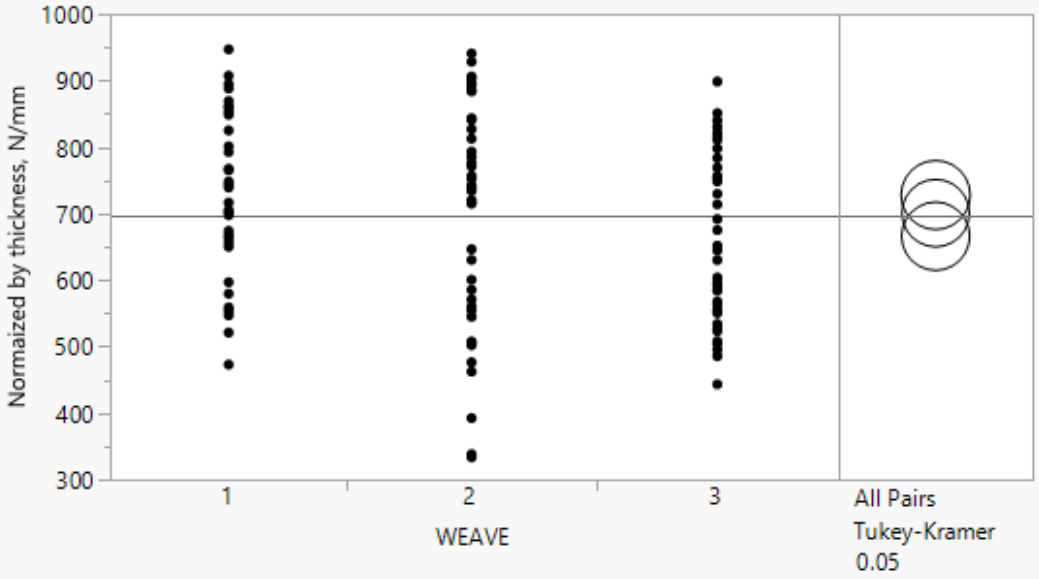

Means Comparisons

Comparisons for all pairs using Tukey-Kramer HSD

Difference Matrix

Dif=Mean[i]-Mean[j]

	1	2	3
1	0.000	27.308	62.027
2	-27.308	0.000	34.719
3	-62.027	-34.719	0.000

Connecting Letters Report

Level		Mean
1	A	728.01754
2	A	700.70961
3	A	665.99044

Levels not connected by same letter are significantly different.

Ordered Differences Report

Level	- Level	Difference	Std Err Dif	Lower CL	Upper CL	p-Value
1	3	62.02710	30.80757	-11.0624	135.1166	0.1133
2	3	34.71917	30.44287	-37.5051	106.9434	0.4911
1	2	27.30793	30.63011	-45.3606	99.9764	0.6467

Appendix 10. Tukey HSD Tensile result – Effect of Z to Y ratio on tensile load (Warp direction)

Oneway Analysis of PEAK LOAD, N By Z yarn:Yyarn Ratio

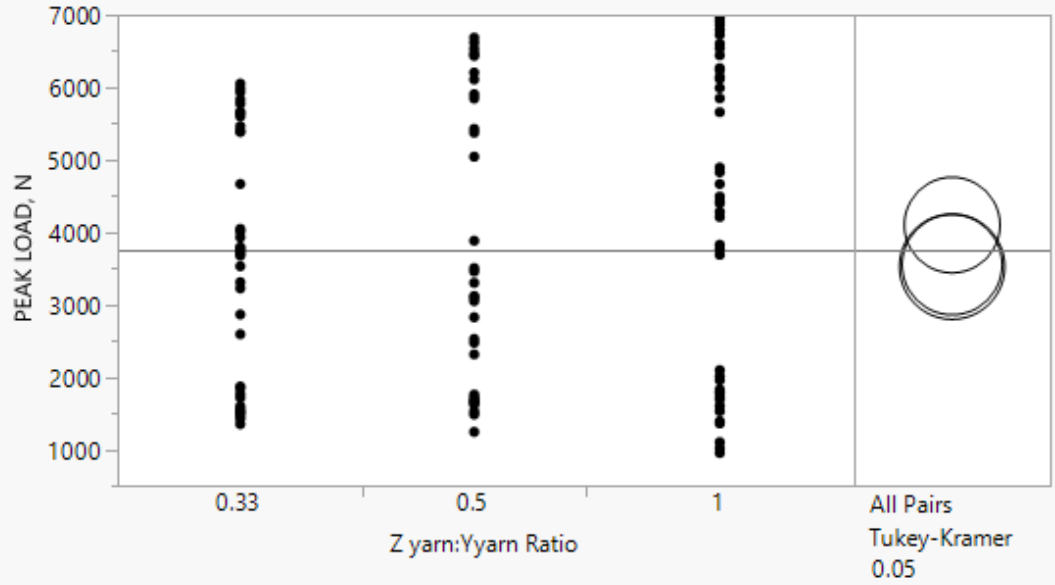

Means Comparisons

Comparisons for all pairs using Tukey-Kramer HSD

Difference Matrix

Dif=Mean[i]-Mean[j]

	1	0.33	0.5
1	0.00	547.60	575.08
0.33	-547.60	0.00	27.48
0.5	-575.08	-27.48	0.00

Connecting Letters Report

Level		Mean
1	A	4097.8346
0.33	A	3550.2329
0.5	A	3522.7574

Levels not connected by same letter are significantly different.

Ordered Differences Report

Level	- Level	Difference	Std Err Dif	Lower CL	Upper CL	p-Value
1	0.5	575.0772	414.5610	-408.449	1558.604	0.3507
1	0.33	547.6017	403.6057	-409.934	1505.137	0.3668
0.33	0.5	27.4755	423.3973	-977.015	1031.966	0.9977

Appendix 11. Tukey HSD Tensile result – Effect of Z to Y ratio on tensile load, normalized by thickness (Warp direction)

Oneway Analysis of Normaized by thickness, N/mm By Z yarn:Yyarn Ratio

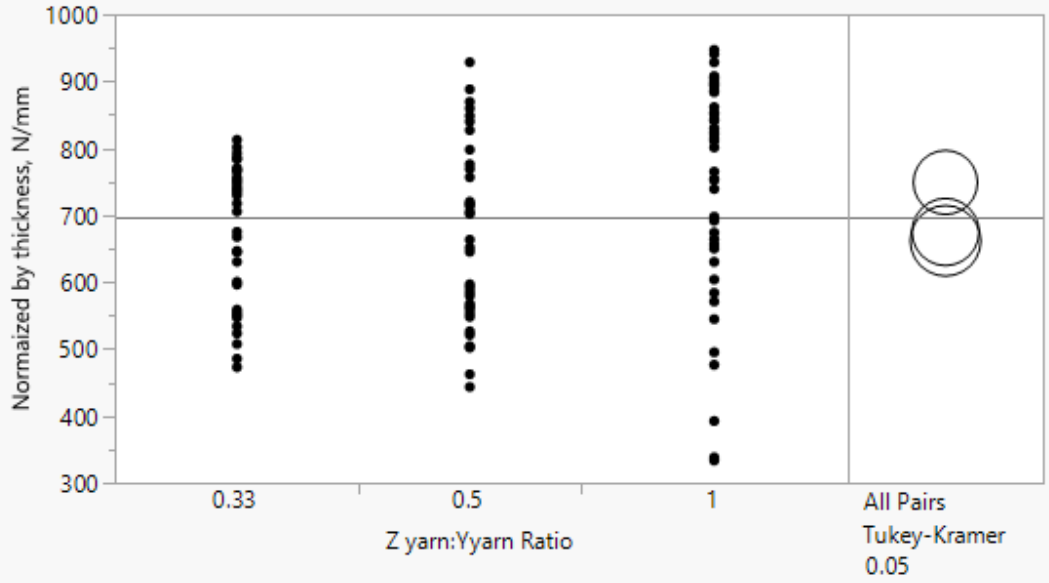

Means Comparisons

Comparisons for all pairs using Tukey-Kramer HSD

Difference Matrix

Dif=Mean[i]-Mean[j]

	1	0.33	0.5
1	0.000	74.000	87.223
0.33	-74.000	0.000	13.223
0.5	-87.223	-13.223	0.000

Connecting Letters Report

Level		Mean
1	A	748.99435
0.33	B	674.99433
0.5	B	661.77180

Levels not connected by same letter are significantly different.

Ordered Differences Report

Level	- Level	Difference	Std Err Dif	Lower CL	Upper CL	p-Value
1	0.5	87.22255	30.04529	15.9415	158.5036	0.0121*
1	0.33	74.00002	29.25131	4.6027	143.3974	0.0337*
0.33	0.5	13.22253	30.68570	-59.5779	86.0229	0.9028

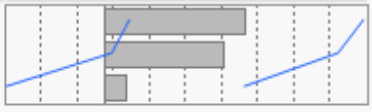

Appendix 12. ANOVA result – Tensile Test (Weft direction)

Dependent Variable: xthick

Number of Observations Read	160
Number of Observations Used	160

Analysis of Variance

Source	DF	Sum of Squares	Mean Square	F Value	Pr > F
Model	3	509.82432	169.94144	9052.77	<.0001
Error	156	2.92848	0.01877		
Corrected Total	159	512.75280			

Root MSE	0.13701	R-Square	0.9943
Dependent Mean	5.22250	Adj R-Sq	0.9942
Coeff Var	2.62350		

Parameter Estimates

Variable	DF	Parameter Estimate	Standard Error	t Value	Pr > |t|
Intercept	1	0.52969	0.04670	11.34	<.0001
ZYRatio	1	0.10913	0.03896	2.80	0.0057
layers	1	0.74458	0.00453	164.29	<.0001
weave	1	0.05007	0.01379	3.63	0.0004

Appendix 13. Tukey HSD Tensile result – Effect of layers on tensile load (Weft direction)

Oneway Analysis of PEAK LOAD, N By # of LAYERS

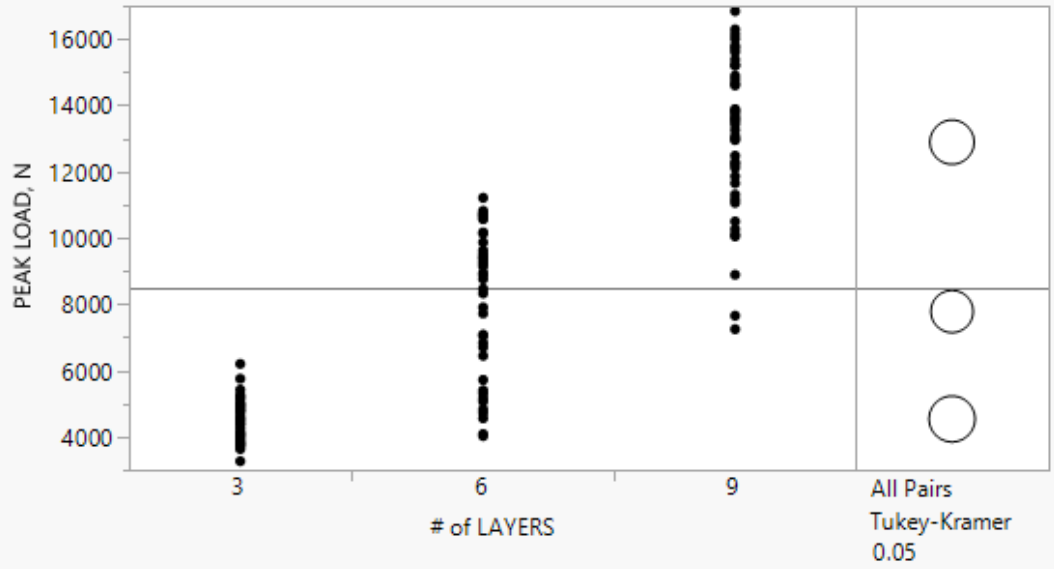

Means Comparisons

Comparisons for all pairs using Tukey-Kramer HSD

Difference Matrix

Dif=Mean[i]-Mean[j]

	9	6	3
9	0.0	5108.0	8349.7
6	-5108.0	0.0	3241.6
3	-8349.7	-3241.6	0.0

Connecting Letters Report

Level				Mean
9	A			12888.760
6		B		7780.741
3			C	4539.107

Levels not connected by same letter are significantly different.

Ordered Differences Report

Level	- Level	Difference	Std Err Dif	Lower CL	Upper CL	p-Value
9	3	8349.653	408.3844	7383.336	9315.970	<.0001*
9	6	5108.019	391.5747	4181.477	6034.561	<.0001*
6	3	3241.634	399.8388	2295.538	4187.730	<.0001*

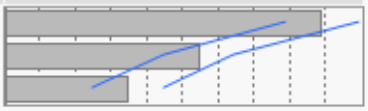

Appendix 14. Tukey HSD Tensile result – Effect of layers on tensile load, normalized by thickness (Weft direction)

Oneway Analysis of Normalized by thickness, N/mm By # of LAYERS

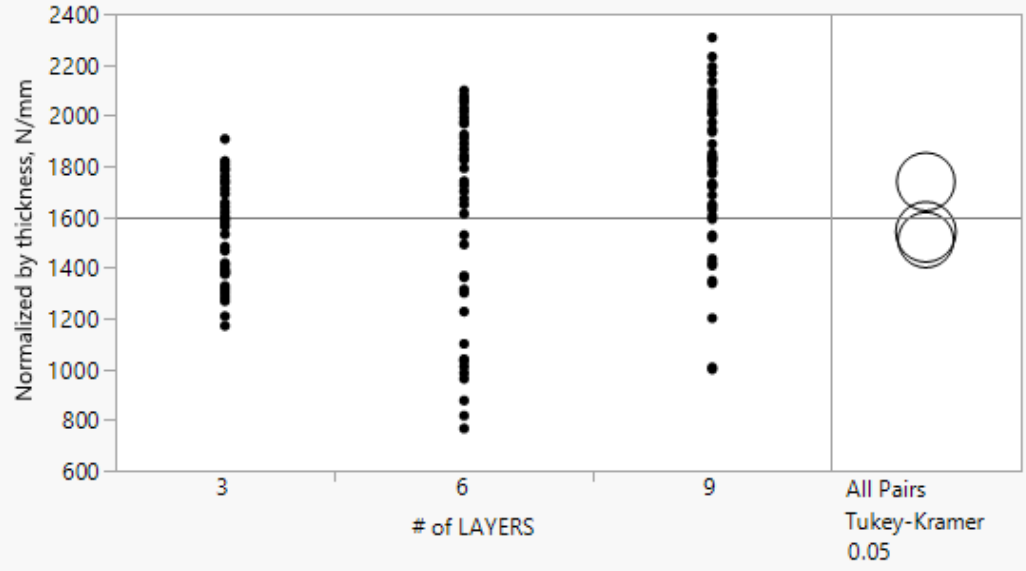

Means Comparisons

Comparisons for all pairs using Tukey-Kramer HSD

Difference Matrix

Dif=Mean[i]-Mean[j]

	9	3	6
9	0.00	198.31	229.87
3	-198.31	0.00	31.55
6	-229.87	-31.55	0.00

Connecting Letters Report

Level		Mean
9	A	1739.1031
3	B	1540.7909
6	B	1509.2360

Levels not connected by same letter are significantly different.

Ordered Differences Report

Level	- Level	Difference	Std Err Dif	Lower CL	Upper CL	p-Value
9	6	229.8671	66.87232	71.634	388.1000	0.0022*
9	3	198.3122	69.74305	33.287	363.3378	0.0139*
3	6	31.5549	68.28364	-130.017	193.1273	0.8891

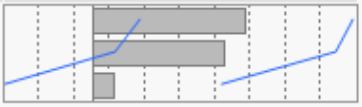

Appendix 15. Tukey HSD Tensile result – Effect of weave on tensile load (Weft direction)

Oneway Analysis of PEAK LOAD, N By WEAVE

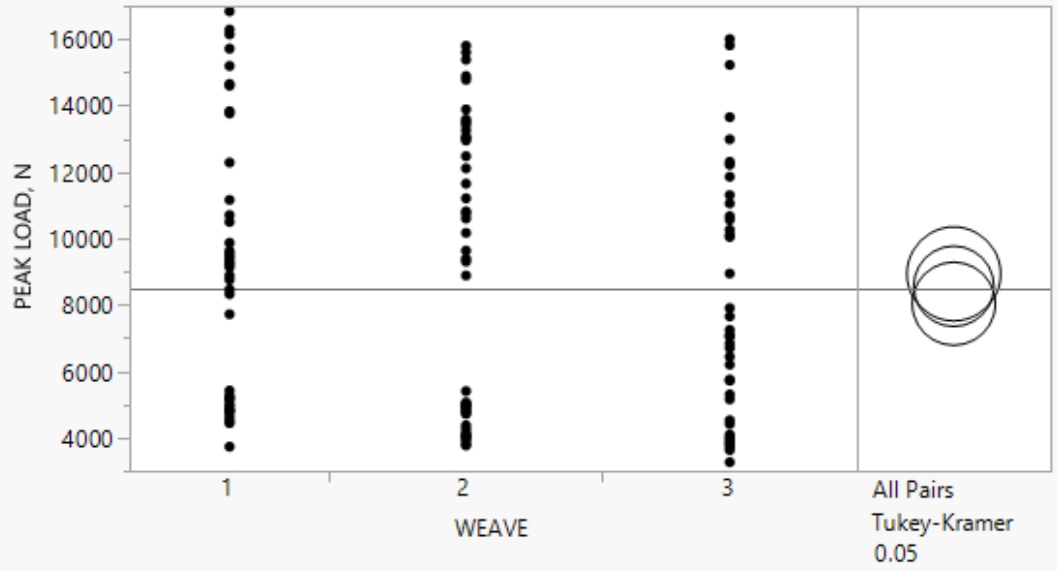

Means Comparisons

Comparisons for all pairs using Tukey-Kramer HSD

Difference Matrix

Dif=Mean[i]-Mean[j]

	1	2	3
1	0.00	373.56	897.81
2	-373.56	0.00	524.24
3	-897.81	-524.24	0.00

Connecting Letters Report

Level		Mean
1	A	8934.3400
2	A	8560.7762
3	A	8036.5341

Levels not connected by same letter are significantly different.

Ordered Differences Report

Level	- Level	Difference	Std Err Dif	Lower CL	Upper CL	p-Value
1	3	897.8059	798.3641	-991.28	2786.890	0.5004
2	3	524.2421	736.3439	-1218.09	2266.575	0.7568
1	2	373.5638	786.5676	-1487.61	2234.736	0.8832

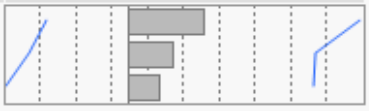

Appendix 16. Tukey HSD Tensile result – Effect of weave on tensile load normalized by thickness (Weft direction)

Oneway Analysis of Normalized by thickness, N/mm By WEAVE

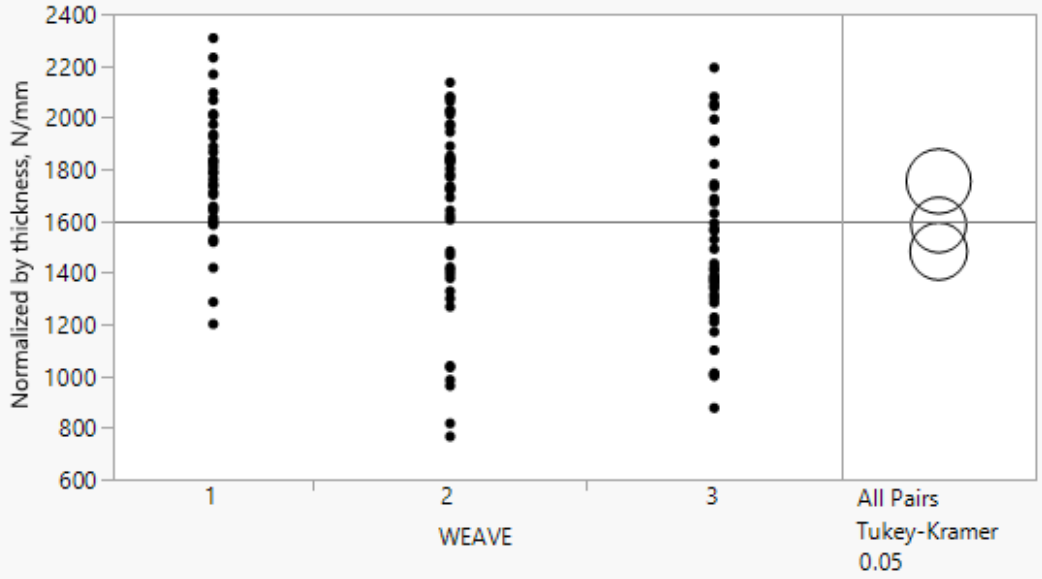

Means Comparisons

Comparisons for all pairs using Tukey-Kramer HSD

Difference Matrix

Dif=Mean[i]-Mean[j]

	1	2	3
1	0.00	168.62	270.68
2	-168.62	0.00	102.05
3	-270.68	-102.05	0.00

Connecting Letters Report

Level		Mean
1	A	1753.0125
2	B	1584.3912
3	B	1482.3371

Levels not connected by same letter are significantly different.

Ordered Differences Report

Level	- Level	Difference	Std Err Dif	Lower CL	Upper CL	p-Value
1	3	270.6754	70.63038	103.550	437.8006	0.0005*
1	2	168.6213	69.58676	3.965	333.2771	0.0434*
2	3	102.0541	65.14353	-52.088	256.1964	0.2632

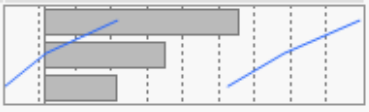

Appendix 17. Tukey HSD Tensile result – Effect of Z to Y ratio on tensile load (Weft direction)

Oneway Analysis of PEAK LOAD, N By Z yarn:Yyarn Ratio

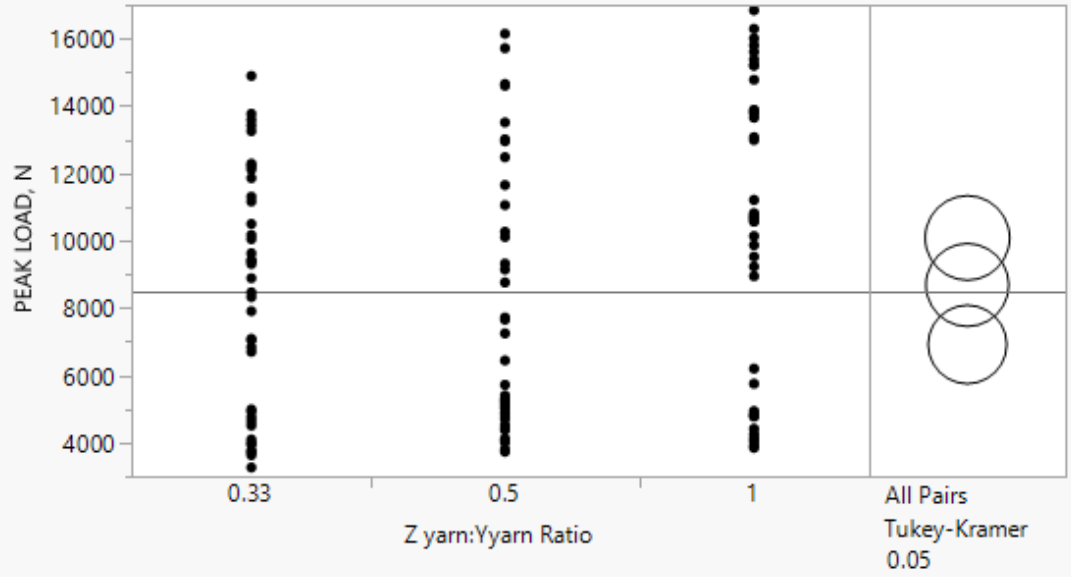

Means Comparisons

Comparisons for all pairs using Tukey-Kramer HSD

Difference Matrix

Dif=Mean[i]-Mean[j]

	1	0.33	0.5
1	0.0	1396.1	3163.1
0.33	-1396.1	0.0	1767.0
0.5	-3163.1	-1767.0	0.0

Connecting Letters Report

Level		Mean
1	A	10080.363
0.33	A	8684.273
0.5	B	6917.294

Levels not connected by same letter are significantly different.

Ordered Differences Report

Level	- Level	Difference	Std Err Dif	Lower CL	Upper CL	p-Value
1	0.5	3163.068	724.7437	1448.18	4877.953	<.0001*
0.33	0.5	1766.979	717.2198	69.90	3464.060	0.0392*
1	0.33	1396.089	743.8494	-364.00	3156.182	0.1488

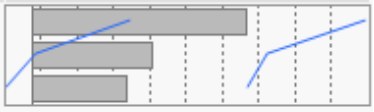

Appendix 18. Tukey HSD Tensile result – Effect of Z to Y ratio on tensile load normalized by thickness (Weft direction)

Oneway Analysis of Normalized by thickness, N/mm By Z yarn:Yarn Ratio

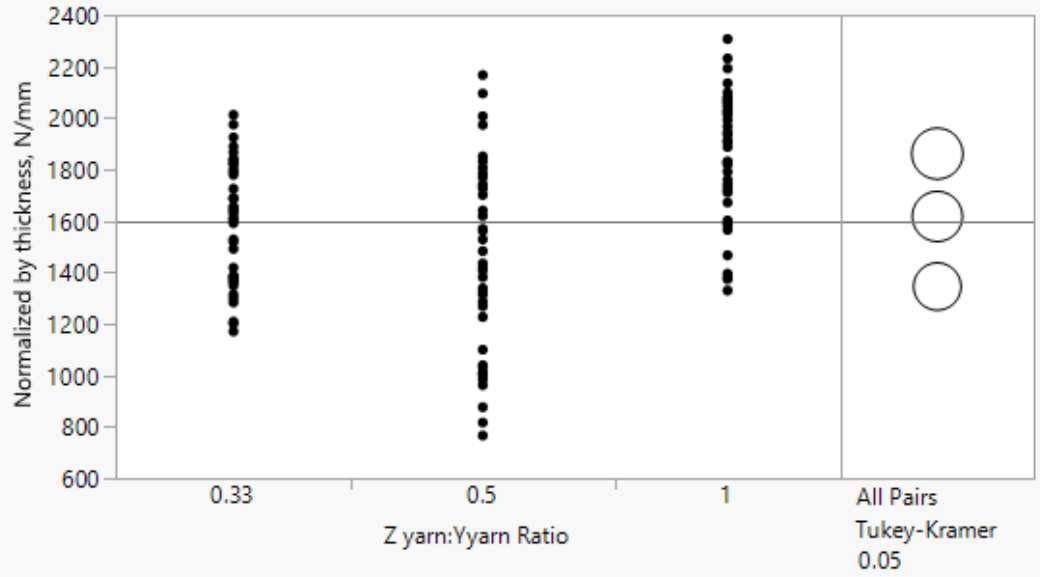

Means Comparisons

Comparisons for all pairs using Tukey-Kramer HSD

Difference Matrix

Dif=Mean[i]-Mean[j]

	1	0.33	0.5
1	0.00	243.95	516.17
0.33	-243.95	0.00	272.22
0.5	-516.17	-272.22	0.00

Connecting Letters Report

Level		Mean
1	A	1861.4390
0.33	B	1617.4903
0.5	C	1345.2665

Levels not connected by same letter are significantly different.

Ordered Differences Report

Level	- Level	Difference	Std Err Dif	Lower CL	Upper CL	p-Value
1	0.5	516.1725	57.46551	380.1979	652.1470	<.0001*
0.33	0.5	272.2237	56.86893	137.6608	406.7867	<.0001*
1	0.33	243.9487	58.98042	104.3896	383.5078	0.0002*

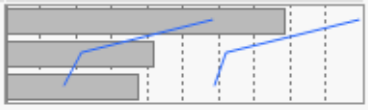

Appendix 19. ANOVA result – Tup impact test

Dependent Variable: energy

Number of Observations Read	125
Number of Observations Used	125

Analysis of Variance

Source	DF	Sum of Squares	Mean Square	F Value	Pr > F
Model	4	14959	3739.67689	549.73	<.0001
Error	120	816.33381	6.80278		
Corrected Total	124	15775			

Root MSE	2.60821	R-Square	0.9483
Dependent Mean	17.14622	Adj R-Sq	0.9465
Coeff Var	15.21160		

Parameter Estimates

Variable	DF	Parameter Estimate	Standard Error	t Value	Pr > |t|
Intercept	1	47.97365	10.52026	4.56	<.0001
ZYRatio	1	2.16301	0.83364	2.59	0.0106
layers	1	6.51448	0.39994	16.29	<.0001
xden	1	-12.12303	2.24515	-5.40	<.0001
weave	1	-0.57221	0.29464	-1.94	0.0545

Appendix 20. Tukey HSD Tup result – Effect of layers on total energy

Oneway Analysis of TOTAL PENETRATION ENERGY, J By # of LAYERS

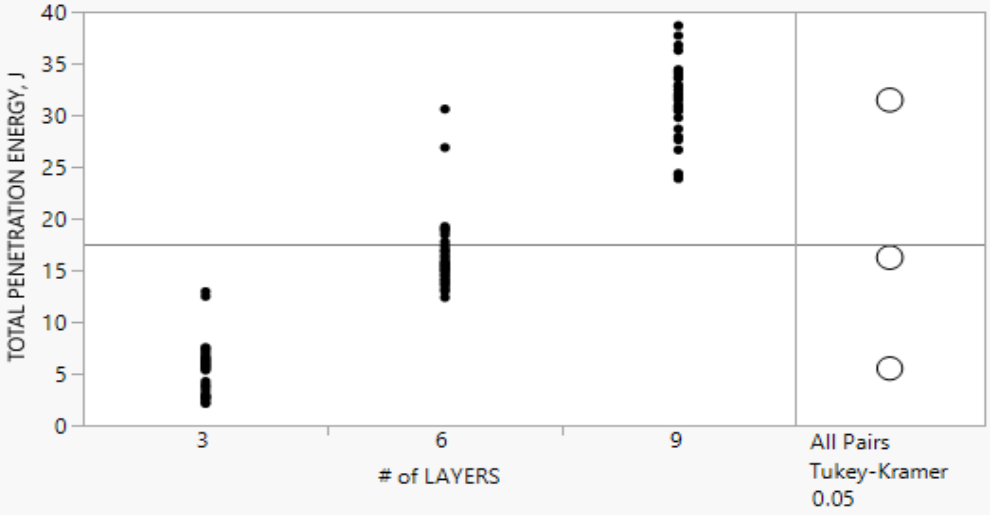

Means Comparisons

Comparisons for all pairs using Tukey-Kramer HSD

Difference Matrix

Dif=Mean[i]-Mean[j]

	9	6	3
9	0.000	15.230	25.964
6	-15.230	0.000	10.734
3	-25.964	-10.734	0.000

Connecting Letters Report

Level		Mean
9	A	31.466851
6	B	16.237261
3	C	5.503060

Levels not connected by same letter are significantly different.

Ordered Differences Report

Level	- Level	Difference	Std Err Dif	Lower CL	Upper CL	p-Value
9	3	25.96379	0.6698517	24.37395	27.55363	<.0001*
9	6	15.22959	0.6779714	13.62047	16.83871	<.0001*
6	3	10.73420	0.6698517	9.14436	12.32404	<.0001*

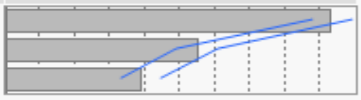

Appendix 21. Tukey HSD Tup result – Effect of weave on total energy

Oneway Analysis of TOTAL PENETRATION ENERGY, J By Weave

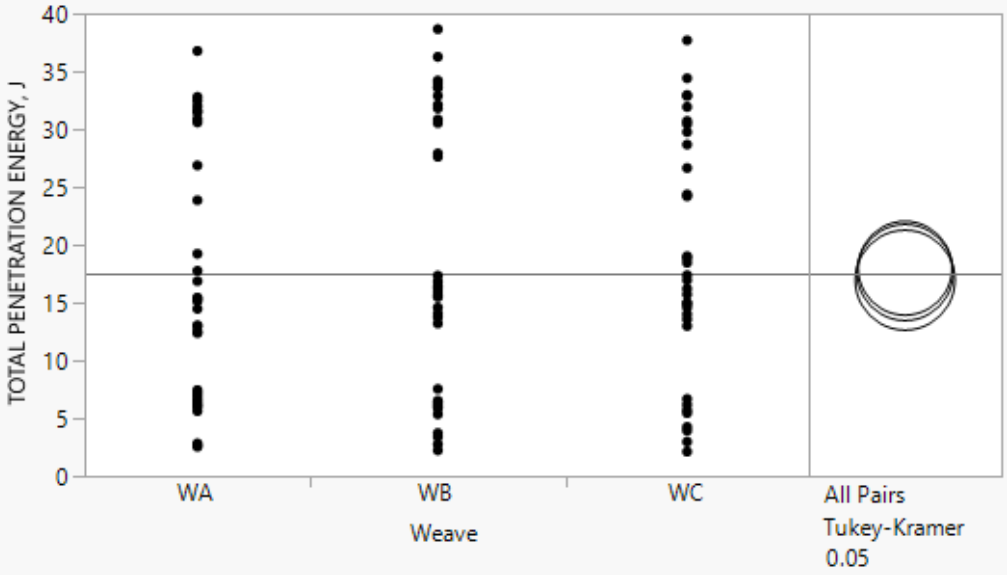

Means Comparisons

Comparisons for all pairs using Tukey-Kramer HSD

Difference Matrix

Dif=Mean[i]-Mean[j]

	WB	WC	WA
WB	0.0000	0.3655	1.0306
WC	-0.3655	0.0000	0.6652
WA	-1.0306	-0.6652	0.0000

Connecting Letters Report

Level		Mean
WB	A	17.979028
WC	A	17.613567
WA	A	16.948382

Levels not connected by same letter are significantly different.

Ordered Differences Report

Level	- Level	Difference	Std Err Dif	Lower CL	Upper CL	p-Value
WB	WA	1.030646	2.498338	-4.89898	6.960270	0.9105
WC	WA	0.665185	2.526763	-5.33190	6.662273	0.9625
WB	WC	0.365461	2.449335	-5.44786	6.178780	0.9878

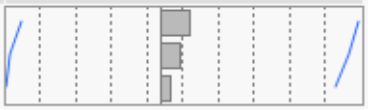

Appendix 22. Tukey HSD Tup result – Effect of Z to Y ratio on total energy

Oneway Analysis of TOTAL PENETRATION ENERGY, J By Z yarn:Yyarn Ratio

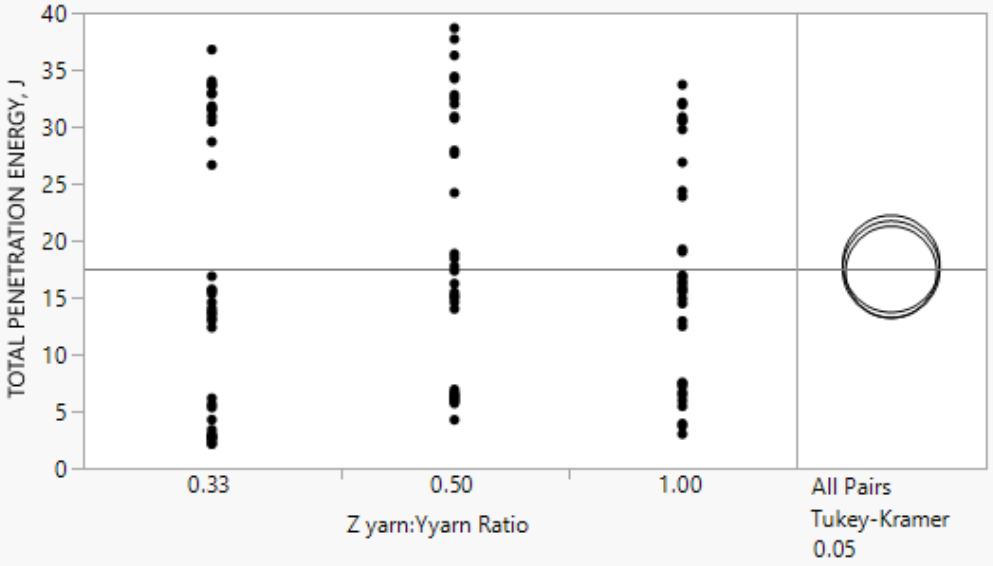

Means Comparisons

Comparisons for all pairs using Tukey-Kramer HSD

Difference Matrix

Dif=Mean[i]-Mean[j]

	0.50	1.00	0.33
0.50	0.00000	0.48721	0.70520
1.00	-0.48721	0.00000	0.21799
0.33	-0.70520	-0.21799	0.00000

Connecting Letters Report

Level		Mean
0.50	A	17.945270
1.00	A	17.458060
0.33	A	17.240071

Levels not connected by same letter are significantly different.

Ordered Differences Report

Level	- Level	Difference	Std Err Dif	Lower CL	Upper CL	p-Value
0.50	0.33	0.7051992	2.468750	-5.15420	6.564598	0.9560
0.50	1.00	0.4872102	2.542023	-5.54610	6.520516	0.9800
1.00	0.33	0.2179890	2.468750	-5.64141	6.077388	0.9957

Appendix 23. ANOVA Tup result – Effect of layers on total energy normalized by thickness

Dependent Variable: normthick

Number of Observations Read	125
Number of Observations Used	125

Analysis of Variance

Source	DF	Sum of Squares	Mean Square	F Value	Pr > F
Model	4	128172028	32043007	134.38	<.0001
Error	120	28613312	238444		
Corrected Total	124	156785339			

Root MSE	488.30755	R-Square	0.8175
Dependent Mean	2983.67339	Adj R-Sq	0.8114
Coeff Var	16.36599		

Parameter Estimates

Variable	DF	Parameter Estimate	Standard Error	t Value	Pr > |t|
Intercept	1	974.60897	1969.59381	0.49	0.6216
ZYRatio	1	392.25362	156.07384	2.51	0.0133
layers	1	430.88367	74.87551	5.75	<.0001
xden	1	-105.65802	420.33456	-0.25	0.8020
weave	1	-72.20777	55.16193	-1.31	0.1930

Appendix 24. Tukey HSD Tup result – Effect of layers on total energy normalized by thickness

Oneway Analysis of Total Energy Normalized by Thickness (J/mm) By # of LAYERS

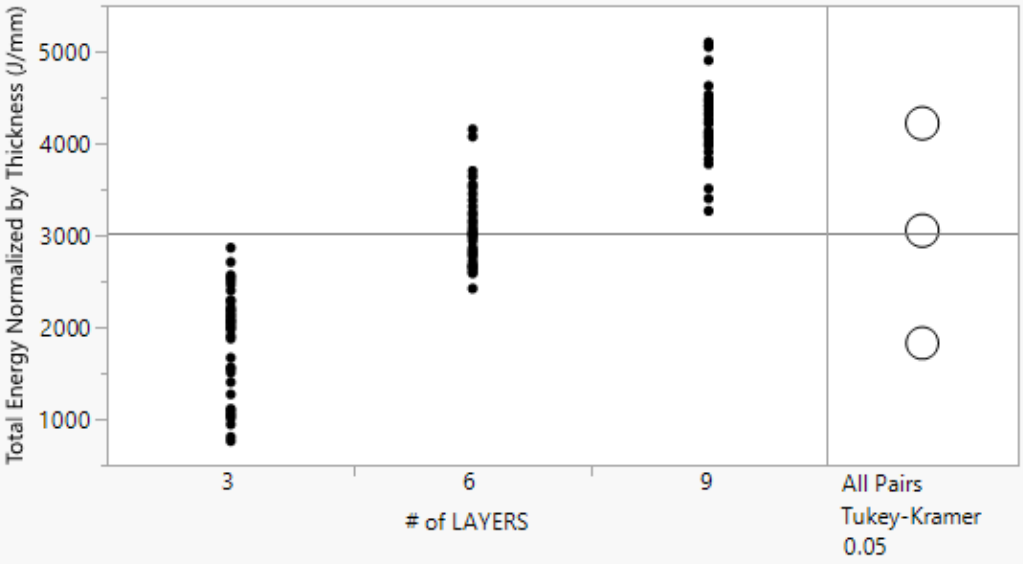

Means Comparisons

Comparisons for all pairs using Tukey-Kramer HSD

Difference Matrix

Dif=Mean[i]-Mean[j]

	9	6	3
9	0.0	1167.4	2391.5
6	-1167.4	0.0	1224.1
3	-2391.5	-1224.1	0.0

Connecting Letters Report

Level				Mean
9	A			4218.1358
6		B		3050.7781
3			C	1826.6562

Levels not connected by same letter are significantly different.

Ordered Differences Report

Level	- Level	Difference	Std Err Dif	Lower CL	Upper CL	p-Value
9	3	2391.480	105.5016	2141.079	2641.880	<.0001*
6	3	1224.122	105.5016	973.721	1474.522	<.0001*
9	6	1167.358	106.7805	913.922	1420.793	<.0001*

Appendix 25. Tukey HSD Tup result – Effect of weave on total energy normalized by thickness

Oneway Analysis of Total Energy Normalized by Thickness (J/mm) By Weave

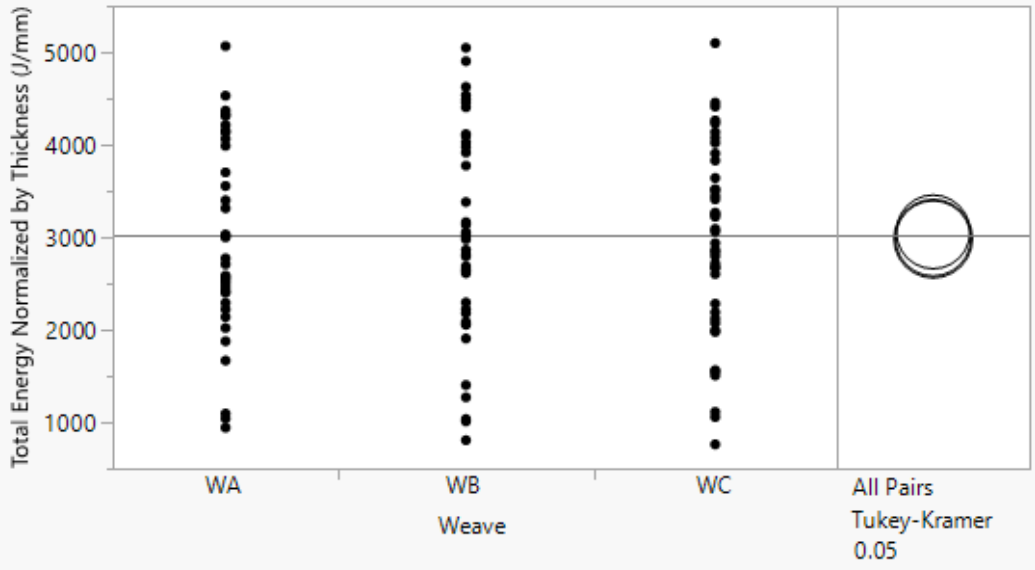

Means Comparisons

Comparisons for all pairs using Tukey-Kramer HSD

Difference Matrix

Dif=Mean[i]-Mean[j]

	WB	WC	WA
WB	0.000	69.152	72.768
WC	-69.152	0.000	3.617
WA	-72.768	-3.617	0.000

Connecting Letters Report

Level		Mean
WB	A	3058.0043
WC	A	2988.8527
WA	A	2985.2359

Levels not connected by same letter are significantly different.

Ordered Differences Report

Level	- Level	Difference	Std Err Dif	Lower CL	Upper CL	p-Value
WB	WA	72.76840	245.1403	-509.054	654.5909	0.9526
WB	WC	69.15163	240.3320	-501.259	639.5621	0.9554
WC	WA	3.61678	247.9294	-584.825	592.0590	0.9999

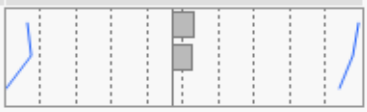

Appendix 26. Tukey HSD Tup result – Effect of Z to Y ratio on total energy normalized by thickness

Oneway Analysis of Total Energy Normalized by Thickness (J/mm) By Z yarn:Yyarn Ratio

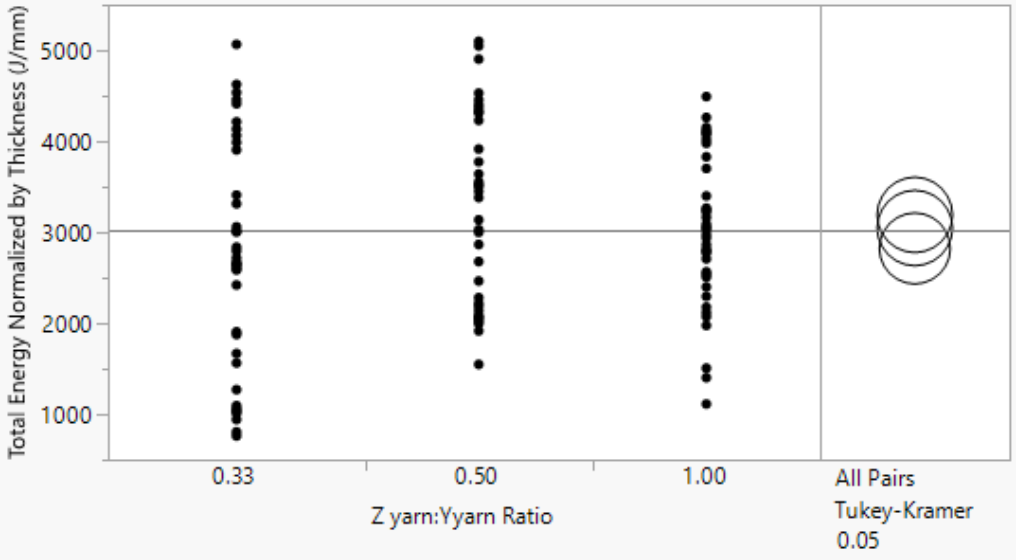

Means Comparisons

Comparisons for all pairs using Tukey-Kramer HSD

Difference Matrix

Dif=Mean[i]-Mean[j]

	0.50	1.00	0.33
0.50	0.00	143.85	368.55
1.00	-143.85	0.00	224.70
0.33	-368.55	-224.70	0.00

Connecting Letters Report

Level		Mean
0.50	A	3191.0052
1.00	A	3047.1519
0.33	A	2822.4542

Levels not connected by same letter are significantly different.

Ordered Differences Report

Level	- Level	Difference	Std Err Dif	Lower CL	Upper CL	p-Value
0.50	0.33	368.5510	239.8373	-200.685	937.7875	0.2776
1.00	0.33	224.6977	239.8373	-344.539	793.9342	0.6181
0.50	1.00	143.8533	246.9557	-442.278	729.9847	0.8297

Appendix 27. ANOVA Tup result – Effect of layers on total energy normalized by thickness

Dependent Variable: normcden

Number of Observations Read	124
Number of Observations Used	124

Analysis of Variance

Source	DF	Sum of Squares	Mean Square	F Value	Pr > F
Model	4	85.24267	21.31067	105.59	<.0001
Error	119	24.01691	0.20182		
Corrected Total	123	109.25958			

Root MSE	0.44925	R-Square	0.7802
Dependent Mean	2.65777	Adj R-Sq	0.7728
Coeff Var	16.90318		

Parameter Estimates

Variable	DF	Parameter Estimate	Standard Error	t Value	Pr > |t|
Intercept	1	-0.36013	1.81549	-0.20	0.8431
ZYRatio	1	0.39096	0.14361	2.72	0.0075
layers	1	0.30448	0.06916	4.40	<.0001
xden	1	0.19369	0.38751	0.50	0.6181
weave	1	-0.04692	0.05075	-0.92	0.3571

Appendix 28. Tukey HSD Tup result – Effect of layers on total energy normalized by composite areal density

Oneway Analysis of Total Energy Normalized by Comp. Areal desnity (kJ/g/mm2) By # of LAYERS

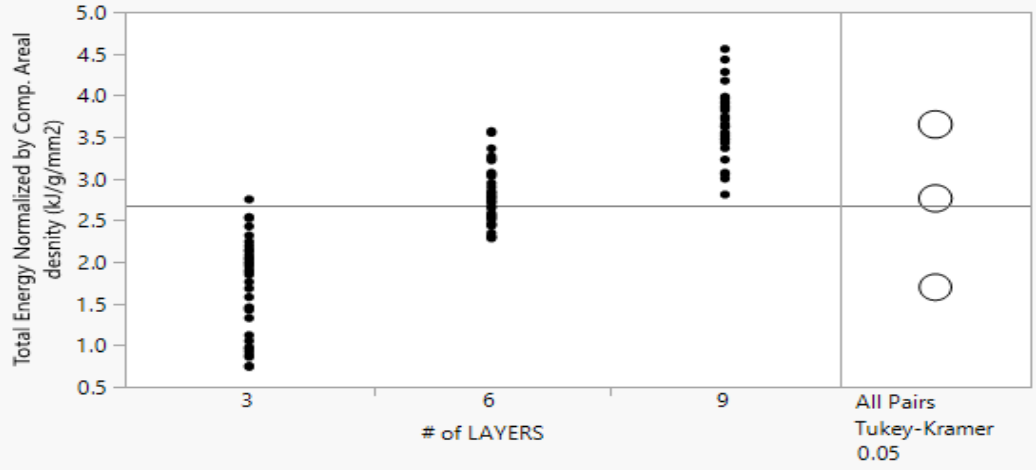

Means Comparisons

Comparisons for all pairs using Tukey-Kramer HSD

Confidence Quantile

q*	Alpha
2.37368	0.05

Difference Matrix

Dif=Mean[i]-Mean[j]

	9	6	3
9	0.0000	0.8880	1.9541
6	-0.8880	0.0000	1.0661
3	-1.9541	-1.0661	0.0000

Connecting Letters Report

Level		Mean
9	A	3.6512181
6	B	2.7632273
3	C	1.6971201

Levels not connected by same letter are significantly different.

Ordered Differences Report

Level	- Level	Difference	Std Err Dif	Lower CL	Upper CL	p-Value
9	3	1.954098	0.0959999	1.726225	2.181971	<.0001*
6	3	1.066107	0.0953757	0.839716	1.292499	<.0001*
9	6	0.887991	0.0971486	0.657391	1.118591	<.0001*

Appendix 29. Tukey HSD Tup result – Effect of weave on total energy normalized by composite areal density

Oneway Analysis of Total Energy Normalized by Comp. Areal desnity (kJ/g/mm2) By Weave

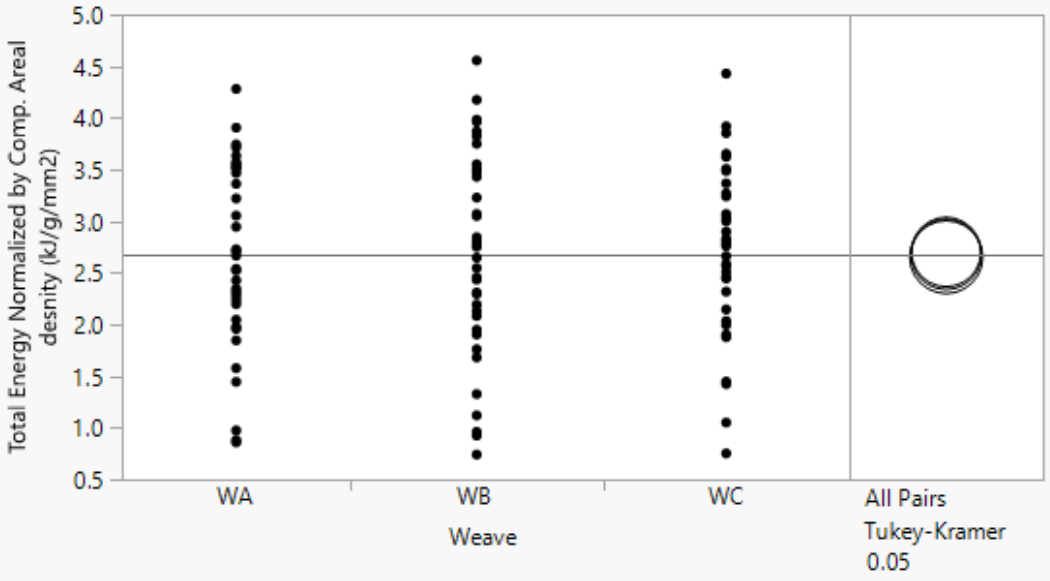

Means Comparisons

Comparisons for all pairs using Tukey-Kramer HSD

Confidence Quantile

q*	Alpha
2.37368	0.05

Difference Matrix

Dif=Mean[i]-Mean[j]

	WB	WC	WA
WB	0.00000	0.02191	0.04882
WC	-0.02191	0.00000	0.02691
WA	-0.04882	-0.02691	0.00000

Connecting Letters Report

Level		Mean
WB	A	2.7021407
WC	A	2.6802315
WA	A	2.6533220

Levels not connected by same letter are significantly different.

Ordered Differences Report

Level	- Level	Difference	Std Err Dif	Lower CL	Upper CL	p-Value
WB	WA	0.0488187	0.2056737	-0.439385	0.5370225	0.9694
WC	WA	0.0269095	0.2068617	-0.464114	0.5179331	0.9907
WB	WC	0.0219092	0.2016846	-0.456826	0.5006440	0.9935

Appendix 30. Tukey HSD Tup result – Effect of Z to Y ratio on total energy normalized by composite areal density

Oneway Analysis of Total Energy Normalized by Comp. Areal desnity (kJ/g/mm2) By Z yarn:Yyarn Ratio

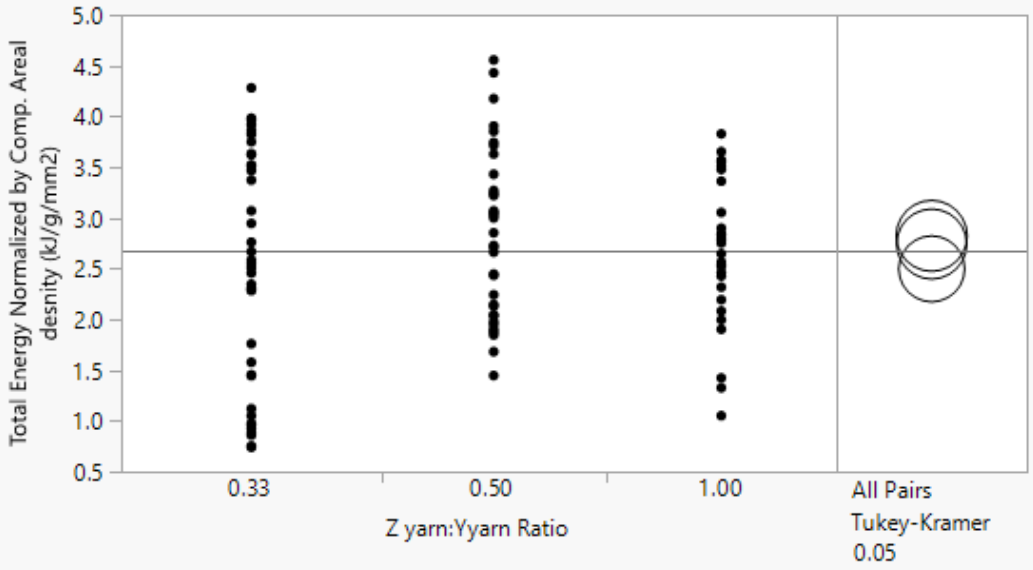

Means Comparisons

Comparisons for all pairs using Tukey-Kramer HSD

Confidence Quantile

q*	Alpha
2.37368	0.05

Difference Matrix

Dif=Mean[i]-Mean[j]

	0.50	1.00	0.33
0.50	0.00000	0.08008	0.32519
1.00	-0.08008	0.00000	0.24510
0.33	-0.32519	-0.24510	0.00000

Connecting Letters Report

Level		Mean
0.50	A	2.8234475
1.00	A	2.7433644
0.33	A	2.4982596

Levels not connected by same letter are significantly different.

Ordered Differences Report

Level	- Level	Difference	Std Err Dif	Lower CL	Upper CL	p-Value
0.50	0.33	0.3251878	0.2010325	-0.151999	0.8023748	0.2423
1.00	0.33	0.2451048	0.1996447	-0.228788	0.7189976	0.4393
0.50	1.00	0.0800831	0.2069182	-0.411075	0.5712409	0.9208

Appendix 31. ANOVA Tup result – Effect of layers on total energy normalized by preform areal density

Dependent Variable: normpden

Number of Observations Read	124
Number of Observations Used	124

Analysis of Variance

Source	DF	Sum of Squares	Mean Square	F Value	Pr > F
Model	4	933.59943	233.39986	102.74	<.0001
Error	119	270.34801	2.27183		
Corrected Total	123	1203.94745			

Root MSE	1.50726	R-Square	0.7754
Dependent Mean	9.06669	Adj R-Sq	0.7679
Coeff Var	16.62415		

Parameter Estimates

Variable	DF	Parameter Estimate	Standard Error	t Value	Pr > |t|
Intercept	1	-6.58525	6.09113	-1.08	0.2818
ZYRatio	1	1.00269	0.48182	2.08	0.0396
layers	1	0.78508	0.23204	3.38	0.0010
xden	1	1.92136	1.30012	1.48	0.1421
weave	1	-0.23210	0.17028	-1.36	0.1754

Appendix 32. Tukey HSD Tup result – Effect of layers on total energy normalized by preform areal density

Oneway Analysis of Total Energy Normalized by Preform Areal desnity (kJ/g/mm2) By # of LAYERS

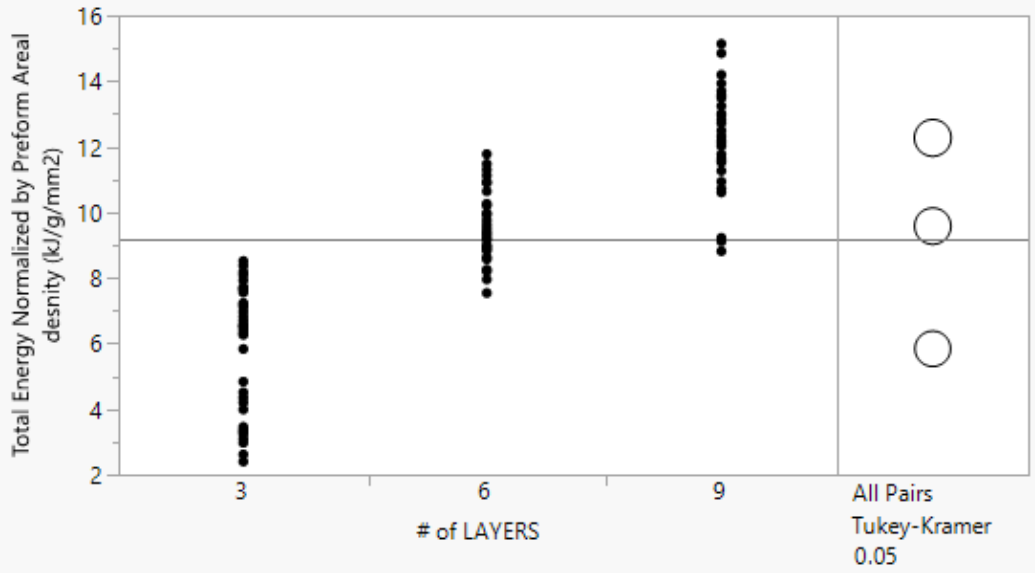

Means Comparisons

Comparisons for all pairs using Tukey-Kramer HSD

Difference Matrix

Dif=Mean[i]-Mean[j]

	9	6	3
9	0.0000	2.6904	6.4311
6	-2.6904	0.0000	3.7407
3	-6.4311	-3.7407	0.0000

Connecting Letters Report

Level		Mean
9	A	12.270701
6	B	9.580322
3	C	5.839618

Levels not connected by same letter are significantly different.

Ordered Differences Report

Level	- Level	Difference	Std Err Dif	Lower CL	Upper CL	p-Value
9	3	6.431083	0.3301039	5.647522	7.214645	<.0001*
6	3	3.740705	0.3279574	2.962238	4.519171	<.0001*
9	6	2.690379	0.3340537	1.897442	3.483316	<.0001*

Appendix 33. Tukey HSD Tup result – Effect of weave on total energy normalized by preform areal density

Oneway Analysis of Total Energy Normalized by Preform Areal desnity (kJ/g/mm2) By Weave

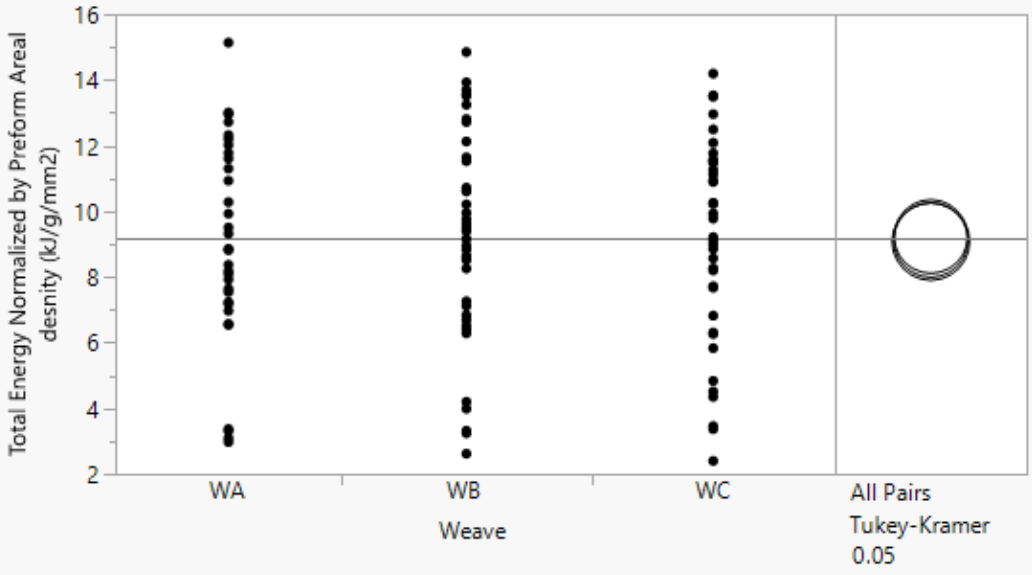

Means Comparisons

Comparisons for all pairs using Tukey-Kramer HSD

Difference Matrix

Dif=Mean[i]-Mean[j]

	WB	WC	WA
WB	0.00000	0.10433	0.15190
WC	-0.10433	0.00000	0.04757
WA	-0.15190	-0.04757	0.00000

Connecting Letters Report

Level		Mean
WB	A	9.2320996
WC	A	9.1277693
WA	A	9.0801955

Levels not connected by same letter are significantly different.

Ordered Differences Report

Level	- Level	Difference	Std Err Dif	Lower CL	Upper CL	p-Value
WB	WA	0.1519042	0.6857481	-1.47584	1.779651	0.9733
WB	WC	0.1043304	0.6724477	-1.49185	1.700507	0.9868
WC	WA	0.0475738	0.6897090	-1.58958	1.684723	0.9974

Appendix 34. Tukey HSD Tup result – Effect of Z to Y ratio on total energy normalized by preform areal density

Oneway Analysis of Total Energy Normalized by Preform Areal desnity (kJ/g/mm2) By Z yarn:Yyarn Ratio

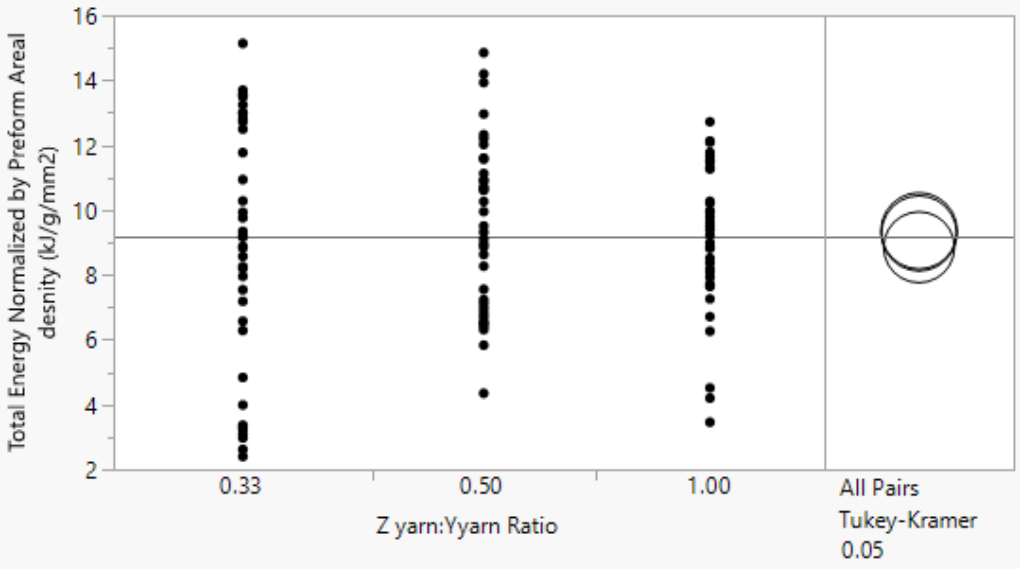

Means Comparisons

Comparisons for all pairs using Tukey-Kramer HSD

Difference Matrix

Dif=Mean[i]-Mean[j]

	0.50	1.00	0.33
0.50	0.00000	0.07819	0.50611
1.00	-0.07819	0.00000	0.42791
0.33	-0.50611	-0.42791	0.00000

Connecting Letters Report

Level		Mean
0.50	A	9.3582840
1.00	A	9.2800907
0.33	A	8.8521778

Levels not connected by same letter are significantly different.

Ordered Differences Report

Level	- Level	Difference	Std Err Dif	Lower CL	Upper CL	p-Value
0.50	0.33	0.5061062	0.6765492	-1.09981	2.112018	0.7354
1.00	0.33	0.4279129	0.6718789	-1.16691	2.022739	0.8001
0.50	1.00	0.0781933	0.6963569	-1.57474	1.731122	0.9931

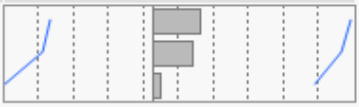

Appendix 35. ANOVA result – Charpy impact test (warp direction)

Dependent Variable: energy

Number of Observations Read	136
Number of Observations Used	136

Analysis of Variance

Source	DF	Sum of Squares	Mean Square	F Value	Pr > F
Model	3	7.76924	2.58975	119.14	<.0001
Error	132	2.86936	0.02174		
Corrected Total	135	10.63860			

Root MSE	0.14744	R-Square	0.7303
Dependent Mean	0.65015	Adj R-Sq	0.7242
Coeff Var	22.67744		

Parameter Estimates

Variable	DF	Parameter Estimate	Standard Error	t Value	Pr > |t|
Intercept	1	0.11997	0.05254	2.28	0.0240
ZYRatio	1	0.05516	0.04422	1.25	0.2144
layers	1	0.09593	0.00513	18.69	<.0001
weave	1	-0.04079	0.01575	-2.59	0.0107

Appendix 36. Tukey HSD Charpy result – Effect of layers on total energy (warp direction)

Oneway Analysis of Energy (J) By Layers

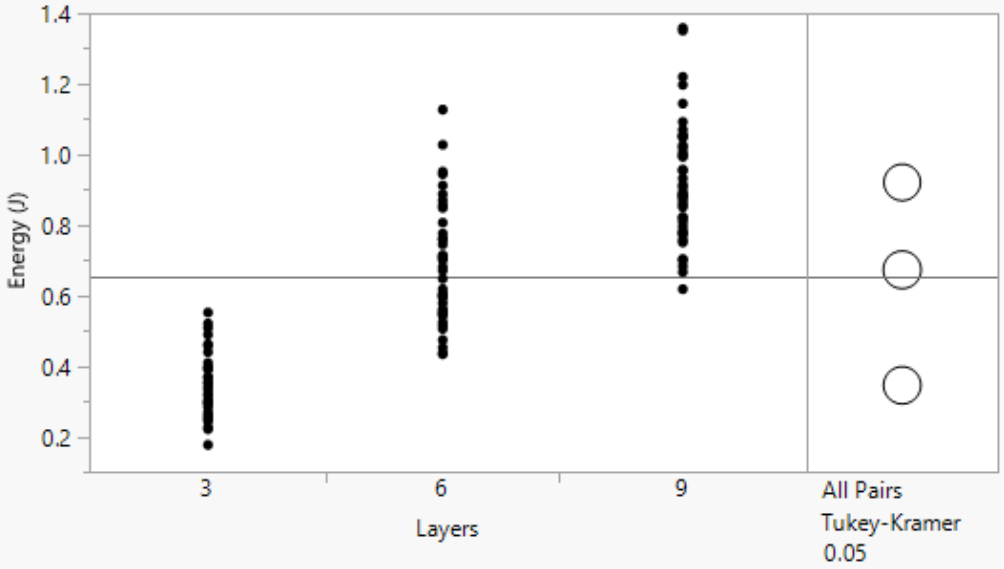

Means Comparisons

Comparisons for all pairs using Tukey-Kramer HSD

Difference Matrix

Dif=Mean[i]-Mean[j]

	9	6	3
9	0.00000	0.24785	0.57531
6	-0.24785	0.00000	0.32746
3	-0.57531	-0.32746	0.00000

Connecting Letters Report

Level		Mean
9	A	0.92050000
6	B	0.67265227
3	C	0.34519111

Levels not connected by same letter are significantly different.

Ordered Differences Report

Level	- Level	Difference	Std Err Dif	Lower CL	Upper CL	p-Value
9	3	0.5753089	0.0312809	0.5011646	0.6494532	<.0001*
6	3	0.3274612	0.0317982	0.2520907	0.4028317	<.0001*
9	6	0.2478477	0.0314619	0.1732742	0.3224212	<.0001*

Appendix 37. Tukey HSD Charpy result – Effect of weave on total energy (warp direction)

Oneway Analysis of Energy (J) By Weave

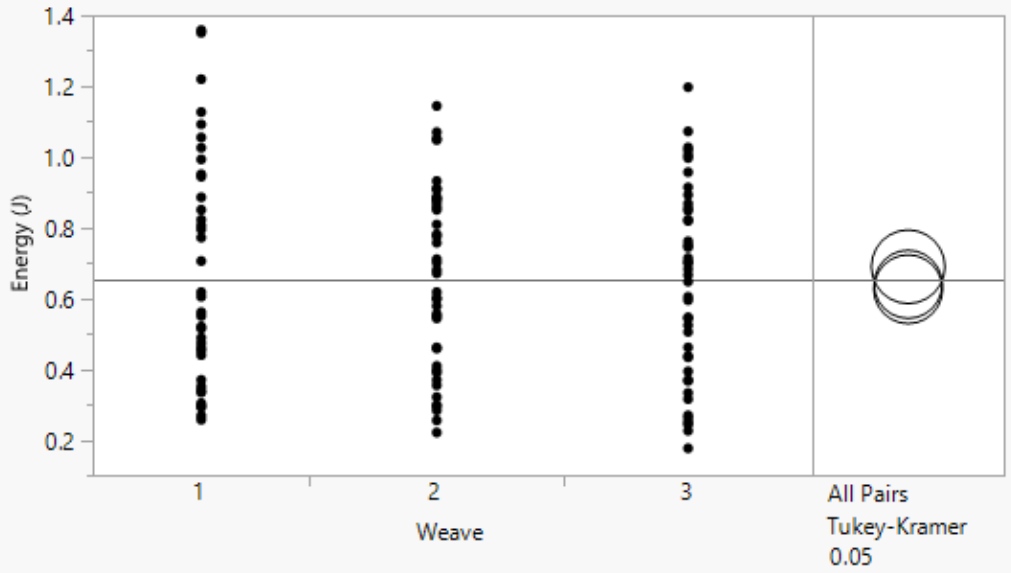

Means Comparisons

Comparisons for all pairs using Tukey-Kramer HSD

Difference Matrix

Dif=Mean[i]-Mean[j]

	1	2	3
1	0.00000	0.04972	0.06347
2	-0.04972	0.00000	0.01376
3	-0.06347	-0.01376	0.00000

Connecting Letters Report

Level		Mean
1	A	0.68943659
2	A	0.63972083
3	A	0.62596383

Levels not connected by same letter are significantly different.

Ordered Differences Report

Level	- Level	Difference	Std Err Dif	Lower CL	Upper CL	p-Value
1	3	0.0634728	0.0601533	-0.079107	0.2060526	0.5436
1	2	0.0497158	0.0598606	-0.092170	0.1916020	0.6848
2	3	0.0137570	0.0577632	-0.123158	0.1506717	0.9692

Appendix 38. Tukey HSD Charpy result – Effect of Z to Y ratio on total energy (warp direction)

Oneway Analysis of Energy (J) By Z:Y ratio

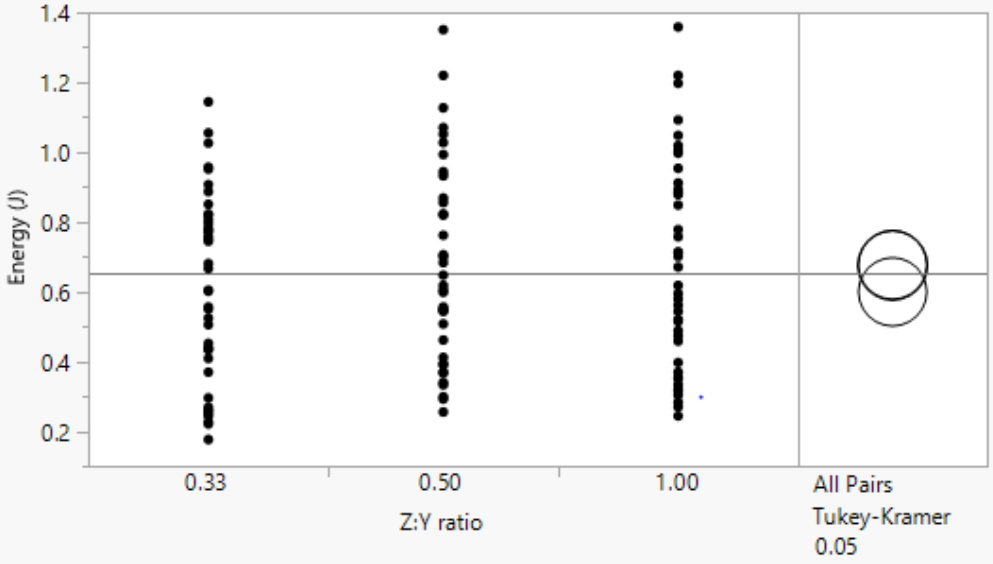

Means Comparisons

Comparisons for all pairs using Tukey-Kramer HSD

Difference Matrix

Dif=Mean[i]-Mean[j]

	1.00	0.50	0.33
1.00	0.00000	0.00099	0.07694
0.50	-0.00099	0.00000	0.07595
0.33	-0.07694	-0.07595	0.00000

Connecting Letters Report

Level		Mean
1.00	A	0.67629783
0.50	A	0.67531136
0.33	A	0.59935652

Levels not connected by same letter are significantly different.

Ordered Differences Report

Level	- Level	Difference	Std Err Dif	Lower CL	Upper CL	p-Value
1.00	0.33	0.0769413	0.0584654	-0.061638	0.2155204	0.3888
0.50	0.33	0.0759548	0.0591260	-0.064190	0.2160999	0.4063
1.00	0.50	0.0009865	0.0591260	-0.139159	0.1411315	0.9998

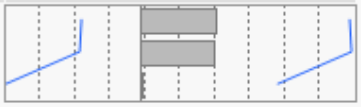

Appendix 39. ANOVA Charpy result – Total energy normalized by thickness (warp direction)

The REG Procedure
Model: MODEL1
Dependent Variable: ynormthick

Number of Observations Read	131
Number of Observations Used	131

Analysis of Variance

Source	DF	Sum of Squares	Mean Square	F Value	Pr > F
Model	3	0.00357	0.00119	1.53	0.2091
Error	127	0.09869	0.00077710		
Corrected Total	130	0.10227			

Root MSE	0.02788	R-Square	0.0350
Dependent Mean	0.12626	Adj R-Sq	0.0122
Coeff Var	22.07881		

Parameter Estimates

Variable	DF	Parameter Estimate	Standard Error	t Value	Pr > |t|
Intercept	1	0.13514	0.01006	13.43	<.0001
ZYRatio	1	0.00861	0.00855	1.01	0.3154
layers	1	-0.00044801	0.00098164	-0.46	0.6489
weave	1	-0.00553	0.00306	-1.81	0.0727

Appendix 40. Tukey HSD Charpy result – Effect of layers on total energy normalized by thickness (warp direction)

Oneway Analysis of Energy Normalized by Thickness (J/mm) By Layers

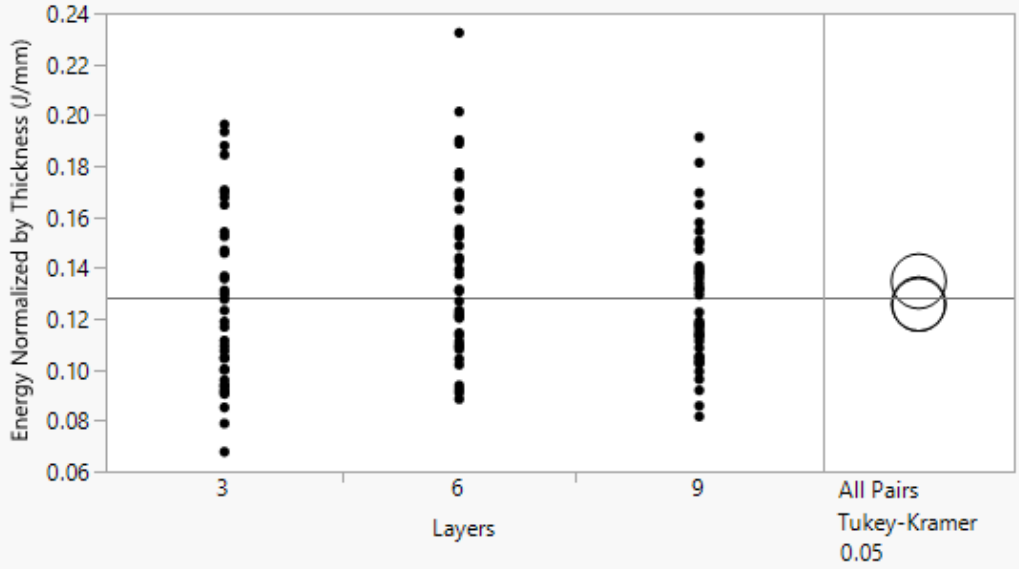

Means Comparisons

Comparisons for all pairs using Tukey-Kramer HSD

Difference Matrix

Dif=Mean[i]-Mean[j]

	6	3	9
6	0.00000	0.00891	0.00919
3	-0.00891	0.00000	0.00028
9	-0.00919	-0.00028	0.00000

Connecting Letters Report

Level		Mean
6	A	0.13473193
3	A	0.12582182
9	A	0.12553994

Levels not connected by same letter are significantly different.

Ordered Differences Report

Level	- Level	Difference	Std Err Dif	Lower CL	Upper CL	p-Value
6	9	0.0091920	0.0062952	-0.005729	0.0241134	0.3134
6	3	0.0089101	0.0063625	-0.006171	0.0239910	0.3436
3	9	0.0002819	0.0062590	-0.014554	0.0151174	0.9989

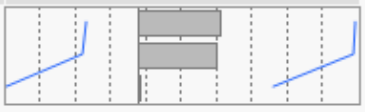

Appendix 41. Tukey HSD Charpy result – Effect of Z to Y ratio on total energy normalized by thickness (warp direction)

Oneway Analysis of Energy Normalized by Thickness (J/mm) By Z:Y ratio

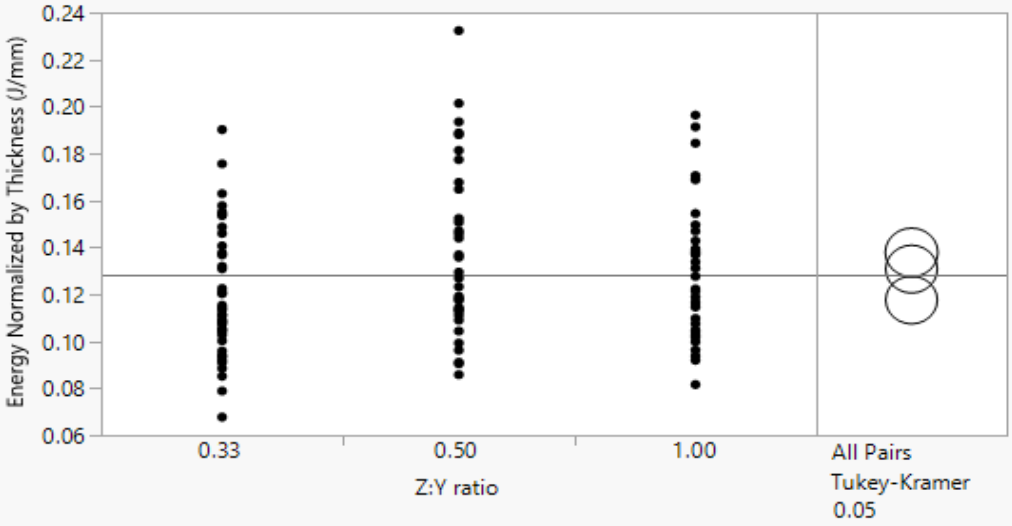

Means Comparisons

Comparisons for all pairs using Tukey-Kramer HSD

Difference Matrix

Dif=Mean[i]-Mean[j]

	0.50	1.00	0.33
0.50	0.00000	0.00712	0.02027
1.00	-0.00712	0.00000	0.01315
0.33	-0.02027	-0.01315	0.00000

Connecting Letters Report

Level			Mean
0.50	A		0.13787067
1.00	A	B	0.13075280
0.33		B	0.11760056

Levels not connected by same letter are significantly different.

Ordered Differences Report

Level	- Level	Difference	Std Err Dif	Lower CL	Upper CL	p-Value
0.50	0.33	0.0202701	0.0061373	0.005723	0.0348172	0.0035*
1.00	0.33	0.0131522	0.0060687	-0.001232	0.0275368	0.0807
0.50	1.00	0.0071179	0.0061373	-0.007429	0.0216649	0.4793

Appendix 42. Tukey HSD Charpy result – Effect of weave on total energy normalized by thickness (warp direction)

Oneway Analysis of Energy Normalized by Thickness (J/mm) By Weave

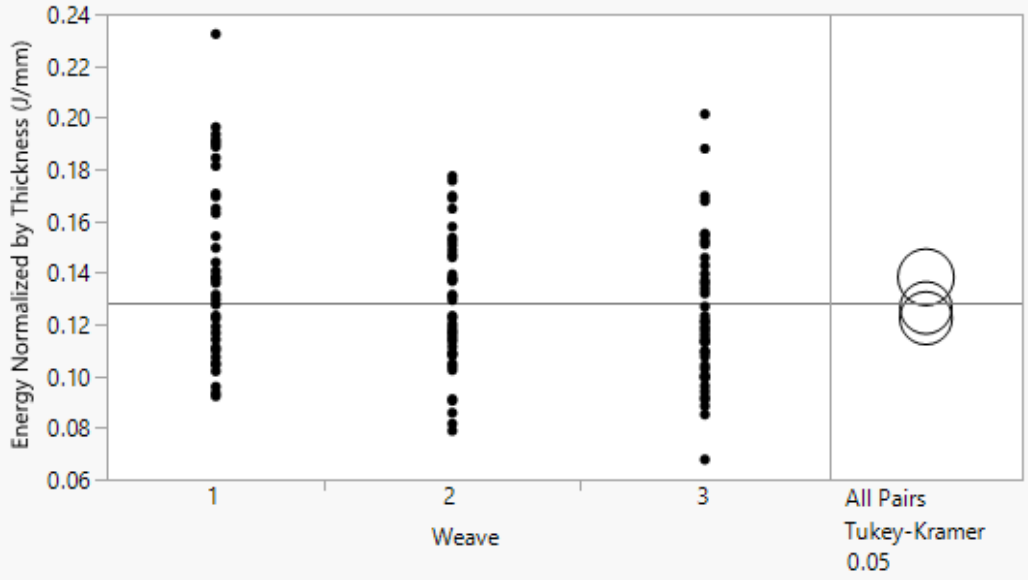

Means Comparisons

Comparisons for all pairs using Tukey-Kramer HSD

Difference Matrix

Dif=Mean[i]-Mean[j]

	1	2	3
1	0.00000	0.01185	0.01587
2	-0.01185	0.00000	0.00401
3	-0.01587	-0.00401	0.00000

Connecting Letters Report

Level			Mean
1	A		0.13827368
2	A	B	0.12642108
3		B	0.12240706

Levels not connected by same letter are significantly different.

Ordered Differences Report

Level	- Level	Difference	Std Err Dif	Lower CL	Upper CL	p-Value
1	3	0.0158666	0.0063207	0.000885	0.0308484	0.0352*
1	2	0.0118526	0.0062899	-0.003056	0.0267615	0.1472
2	3	0.0040140	0.0060695	-0.010372	0.0184005	0.7863

Appendix 43. ANOVA Charpy result – Total energy normalized by composite areal density (warp direction)

Dependent Variable: ynormcden

Number of Observations Read	131
Number of Observations Used	131

Analysis of Variance

Source	DF	Sum of Squares	Mean Square	F Value	Pr > F
Model	3	0.00690	0.00230	3.92	0.0103
Error	127	0.07458	0.00058725		
Corrected Total	130	0.08148			

Root MSE	0.02423	R-Square	0.0847
Dependent Mean	0.11249	Adj R-Sq	0.0631
Coeff Var	21.54309		

Parameter Estimates

Variable	DF	Parameter Estimate	Standard Error	t Value	Pr > |t|
Intercept	1	0.12746	0.00874	14.58	<.0001
ZYRatio	1	0.01171	0.00743	1.58	0.1174
layers	1	-0.00205	0.00085334	-2.41	0.0176
weave	1	-0.00472	0.00266	-1.78	0.0778

Appendix 44. Tukey HSD Charpy result – Effect of layers on total energy normalized by composite areal density (warp direction)

Oneway Analysis of energycden By Layers

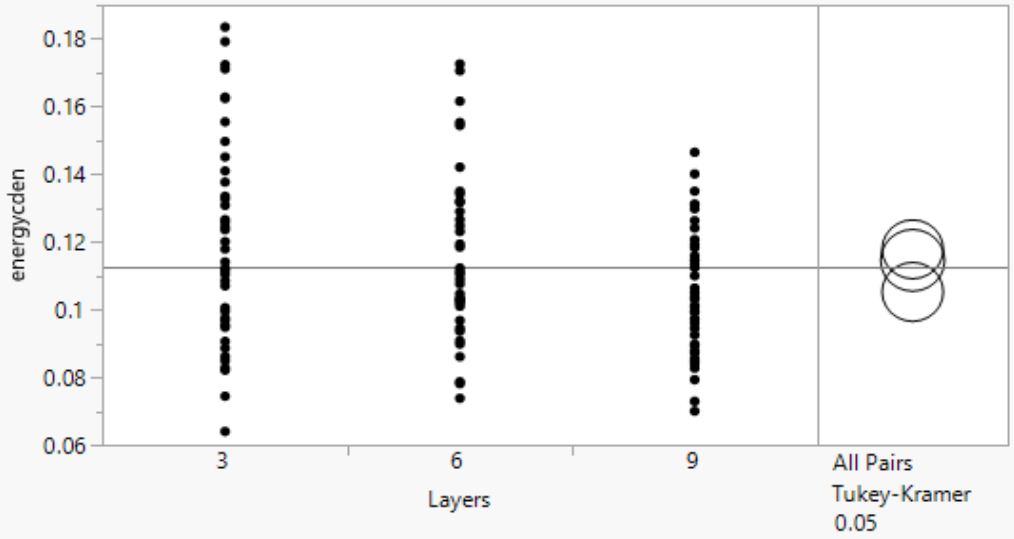

Means Comparisons

Comparisons for all pairs using Tukey-Kramer HSD

Difference Matrix

Dif=Mean[i]-Mean[j]

	3	6	9
3	0.00000	0.00325	0.01258
6	-0.00325	0.00000	0.00933
9	-0.01258	-0.00933	0.00000

Connecting Letters Report

Level			Mean
3	A		0.11782667
6	A	B	0.11457317
9		B	0.10524667

Levels not connected by same letter are significantly different.

Ordered Differences Report

Level	- Level	Difference	Std Err Dif	Lower CL	Upper CL	p-Value
3	9	0.0125800	0.0051929	0.000266	0.0248940	0.0441*
6	9	0.0093265	0.0053180	-0.003284	0.0219373	0.1895
3	6	0.0032535	0.0053180	-0.009357	0.0158643	0.8140

Appendix 45. Tukey HSD Charpy result – Effect Z to Y ratio on total energy normalized by composite areal density (warp direction)

Oneway Analysis of energycden By Ratio

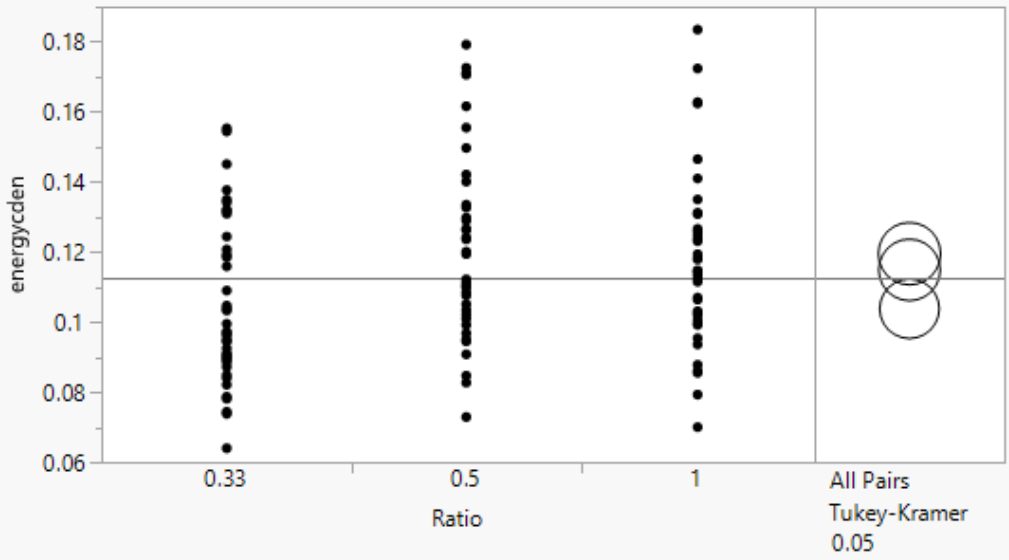

Means Comparisons

Comparisons for all pairs using Tukey-Kramer HSD

Difference Matrix

Dif=Mean[i]-Mean[j]

	0.5	1	0.33
0.5	0.00000	0.00464	0.01572
1	-0.00464	0.00000	0.01107
0.33	-0.01572	-0.01107	0.00000

Connecting Letters Report

Level			Mean
0.5	A		0.11953095
1	A	B	0.11488605
0.33		B	0.10381304

Levels not connected by same letter are significantly different.

Ordered Differences Report

Level	- Level	Difference	Std Err Dif	Lower CL	Upper CL	p-Value
0.5	0.33	0.0157179	0.0051898	0.003411	0.0280247	0.0083*
1	0.33	0.0110730	0.0051582	-0.001159	0.0233048	0.0846
0.5	1	0.0046449	0.0052755	-0.007865	0.0171549	0.6536

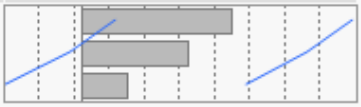

Appendix 46. Tukey HSD Charpy result – Effect of weave on total energy normalized by composite areal density (warp direction)

Oneway Analysis of energycden By Weave

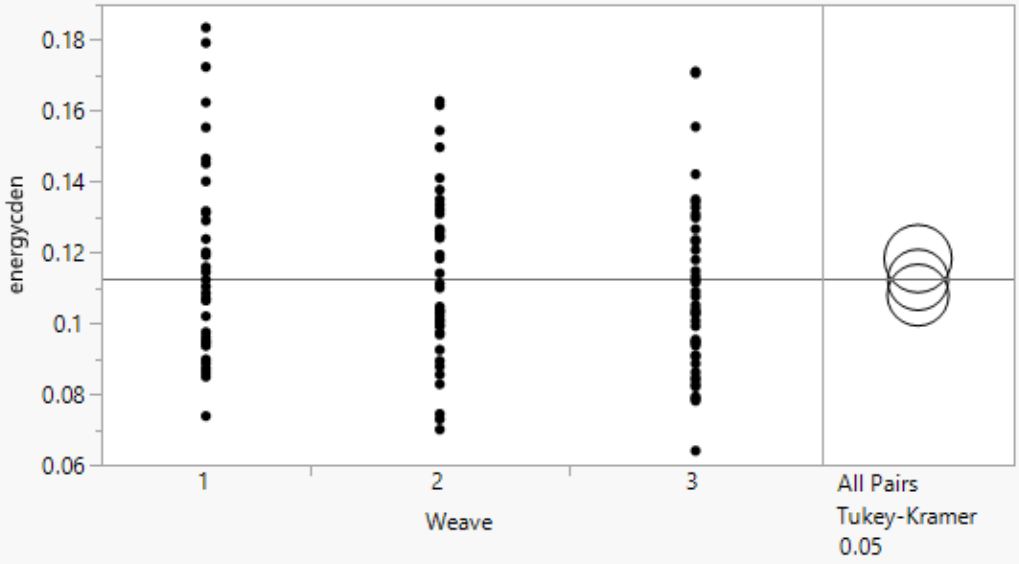

Means Comparisons

Comparisons for all pairs using Tukey-Kramer HSD

Difference Matrix

Dif=Mean[i]-Mean[j]

	1	2	3
1	0.00000	0.00599	0.01029
2	-0.00599	0.00000	0.00430
3	-0.01029	-0.00430	0.00000

Connecting Letters Report

Level		Mean
1	A	0.11825000
2	A	0.11225957
3	A	0.10795870

Levels not connected by same letter are significantly different.

Ordered Differences Report

Level	- Level	Difference	Std Err Dif	Lower CL	Upper CL	p-Value
1	3	0.0102913	0.0054555	-0.002645	0.0232280	0.1468
1	2	0.0059904	0.0054292	-0.006884	0.0188647	0.5137
2	3	0.0043009	0.0051615	-0.007939	0.0165405	0.6831

Appendix 47. ANOVA Charpy result – Total energy normalized by preform areal density (warp direction)

Dependent Variable: normpden

Number of Observations Read	135
Number of Observations Used	135

Analysis of Variance

Source	DF	Sum of Squares	Mean Square	F Value	Pr > F
Model	3	0.07176	0.02392	3.40	0.0199
Error	131	0.92270	0.00704		
Corrected Total	134	0.99446			

Root MSE	0.08393	R-Square	0.0722
Dependent Mean	0.38146	Adj R-Sq	0.0509
Coeff Var	22.00098		

Parameter Estimates

Variable	DF	Parameter Estimate	Standard Error	t Value	Pr > |t|
Intercept	1	0.44209	0.03007	14.70	<.0001
ZYRatio	1	0.02488	0.02519	0.99	0.3250
layers	1	-0.00494	0.00292	-1.69	0.0931
weave	1	-0.02242	0.00902	-2.48	0.0142

Appendix 48. Tukey HSD Charpy result – Effect of layers on total energy normalized by preform areal density (warp direction)

Oneway Analysis of Energy Normalized by Preform Areal Density (kJ/g/mm2) By Layers

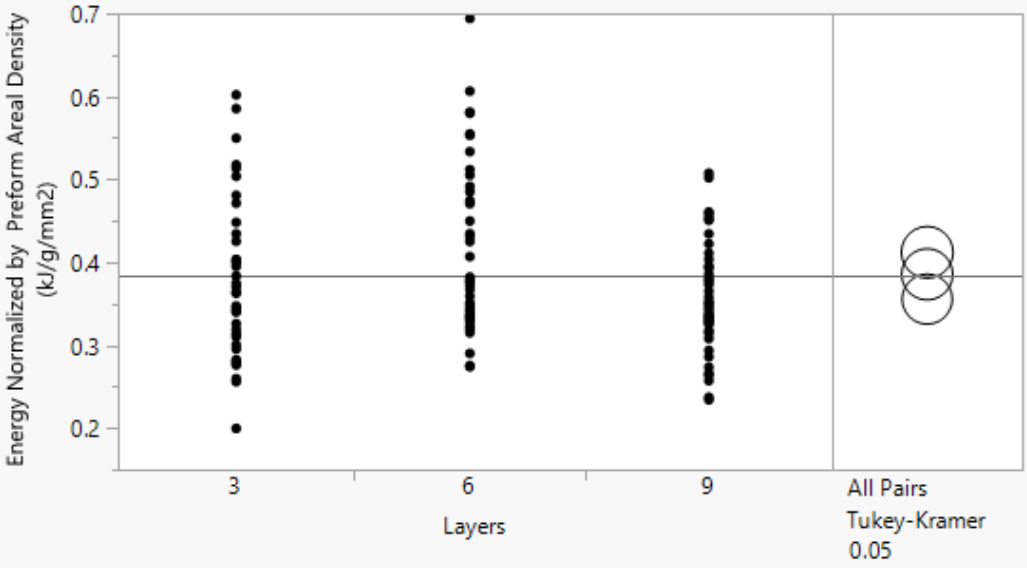

Means Comparisons

Comparisons for all pairs using Tukey-Kramer HSD

Difference Matrix

Dif=Mean[i]-Mean[j]

	6	3	9
6	0.00000	0.02645	0.05634
3	-0.02645	0.00000	0.02989
9	-0.05634	-0.02989	0.00000

Connecting Letters Report

Level			Mean
6	A		0.41198537
3	A	B	0.38553260
9		B	0.35564406

Levels not connected by same letter are significantly different.

Ordered Differences Report

Level	- Level	Difference	Std Err Dif	Lower CL	Upper CL	p-Value
6	9	0.0563413	0.0183624	0.012817	0.0998652	0.0073*
3	9	0.0298885	0.0182567	-0.013385	0.0731619	0.2337
6	3	0.0264528	0.0185586	-0.017536	0.0704418	0.3308

Appendix 49. Tukey HSD Charpy result – Effect of Z to Y ratio on total energy normalized by preform areal density (warp direction)

Oneway Analysis of Energy Normalized by Preform Areal Density (kJ/g/mm2) By Z:Y ratio

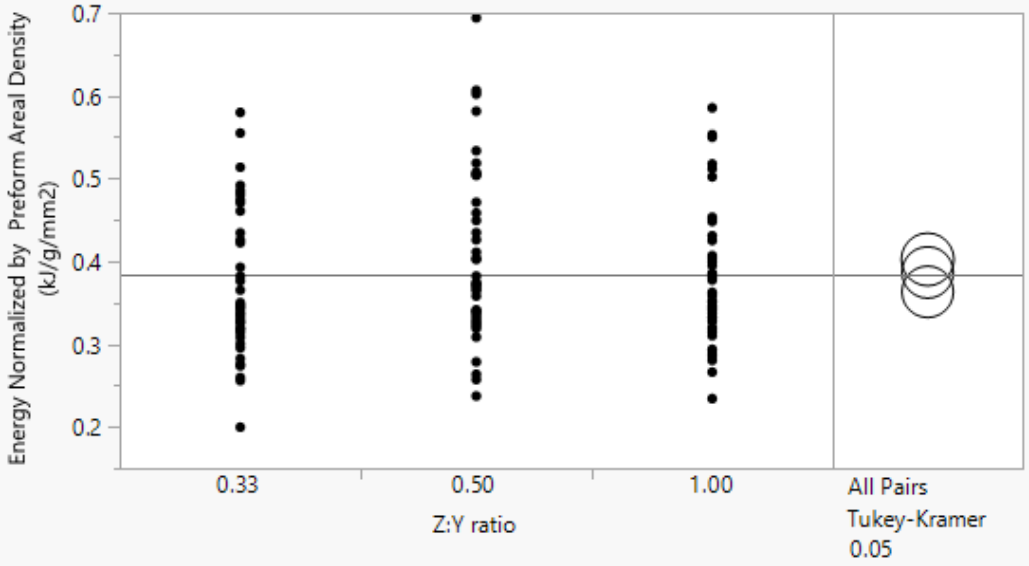

Means Comparisons

Comparisons for all pairs using Tukey-Kramer HSD

Difference Matrix

Dif=Mean[i]-Mean[j]

	0.50	1.00	0.33
0.50	0.00000	0.01572	0.03911
1.00	-0.01572	0.00000	0.02339
0.33	-0.03911	-0.02339	0.00000

Connecting Letters Report

Level		Mean
0.50	A	0.40230781
1.00	A	0.38658637
0.33	A	0.36319734

Levels not connected by same letter are significantly different.

Ordered Differences Report

Level	- Level	Difference	Std Err Dif	Lower CL	Upper CL	p-Value
0.50	0.33	0.0391105	0.0187942	-0.005437	0.0836580	0.0977
1.00	0.33	0.0233890	0.0185842	-0.020661	0.0674388	0.4212
0.50	1.00	0.0157214	0.0187942	-0.028826	0.0602689	0.6811

Appendix 50. Tukey HSD Charpy result – Effect of weave on total energy normalized by preform areal density (warp direction)

Oneway Analysis of Energy Normalized by Preform Areal Density (kJ/g/mm2) By Weave

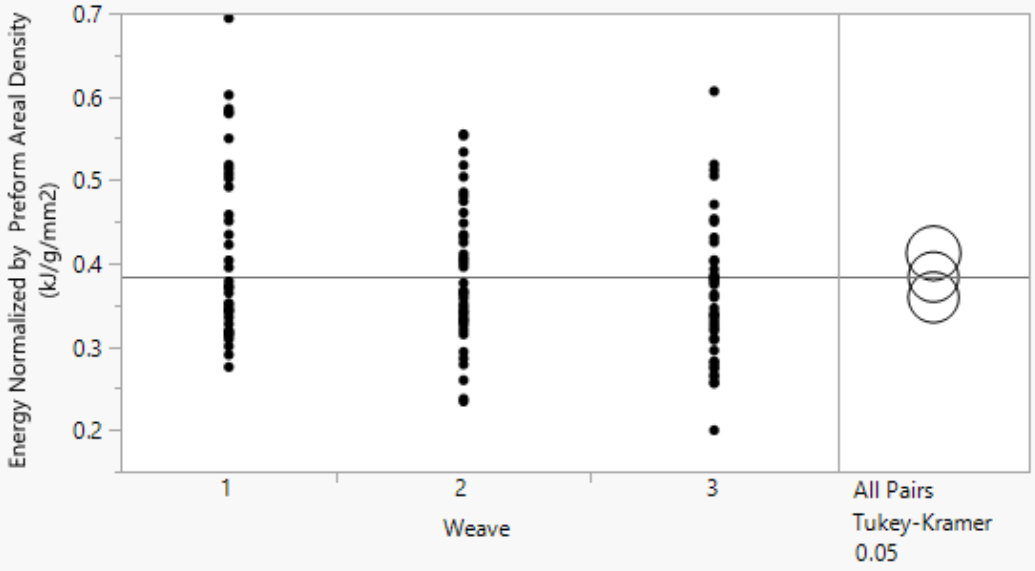

Means Comparisons

Comparisons for all pairs using Tukey-Kramer HSD

Difference Matrix

Dif=Mean[i]-Mean[j]

	1	2	3
1	0.00000	0.02853	0.05287
2	-0.02853	0.00000	0.02433
3	-0.05287	-0.02433	0.00000

Connecting Letters Report

Level			Mean
1	A		0.41210267
2	A	B	0.38356842
3		B	0.35923618

Levels not connected by same letter are significantly different.

Ordered Differences Report

Level	- Level	Difference	Std Err Dif	Lower CL	Upper CL	p-Value
1	3	0.0528665	0.0188081	0.008286	0.0974470	0.0156*
1	2	0.0285343	0.0187166	-0.015829	0.0728978	0.2827
2	3	0.0243322	0.0180608	-0.018477	0.0671414	0.3717

Appendix 51. ANOVA result – Charpy impact test (weft direction)

Dependent Variable: xenergy

Number of Observations Read	135
Number of Observations Used	135

Analysis of Variance

Source	DF	Sum of Squares	Mean Square	F Value	Pr > F
Model	3	22.84749	7.61583	93.22	<.0001
Error	131	10.70181	0.08169		
Corrected Total	134	33.54930			

Root MSE	0.28582	R-Square	0.6810
Dependent Mean	1.44193	Adj R-Sq	0.6737
Coeff Var	19.82212		

Parameter Estimates

Variable	DF	Parameter Estimate	Standard Error	t Value	Pr > |t|
Intercept	1	0.42262	0.10243	4.13	<.0001
ZYRatio	1	0.11586	0.08579	1.35	0.1792
layers	1	0.16791	0.01011	16.62	<.0001
weave	1	-0.03131	0.03087	-1.01	0.3123

Appendix 52. Tukey HSD Charpy result – Effect of layers on total energy (weft direction)

Oneway Analysis of Energy (J) 2 By Layers 2

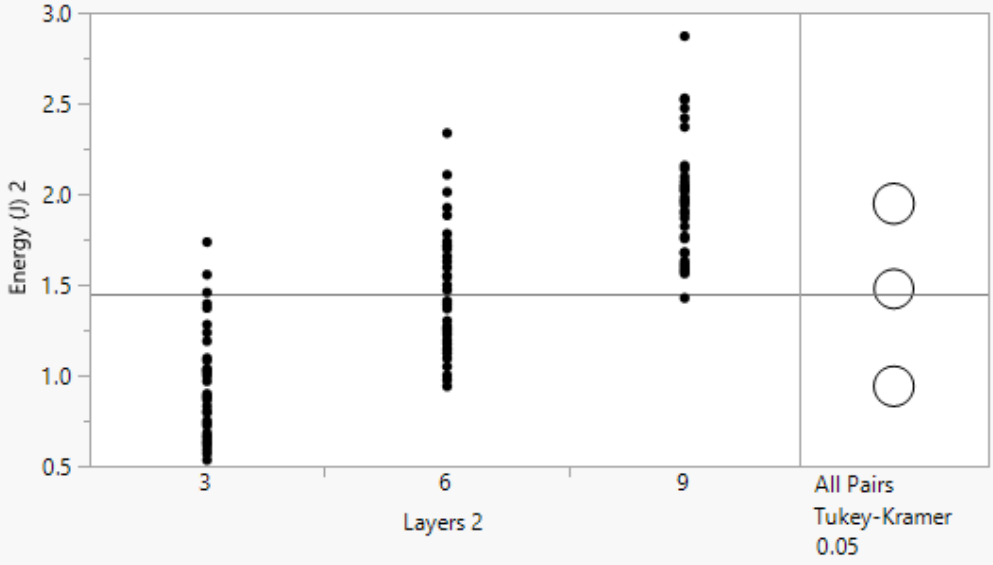

Means Comparisons

Comparisons for all pairs using Tukey-Kramer HSD

Difference Matrix

Dif=Mean[i]-Mean[j]

	9	6	3
9	0.0000	0.4698	1.0069
6	-0.4698	0.0000	0.5371
3	-1.0069	-0.5371	0.0000

Connecting Letters Report

Level		Mean
9	A	1.9472045
6	B	1.4774064
3	C	0.9402822

Levels not connected by same letter are significantly different.

Ordered Differences Report

Level	- Level	Difference	Std Err Dif	Lower CL	Upper CL	p-Value
9	3	1.006922	0.0663644	0.8496203	1.164224	<.0001*
6	3	0.537124	0.0652847	0.3823813	0.691867	<.0001*
9	6	0.469798	0.0656626	0.3141596	0.625437	<.0001*

Appendix 53. Tukey HSD Charpy result – Effect of weave on total energy (weft direction)

Oneway Analysis of Energy (J) 2 By Weave 2

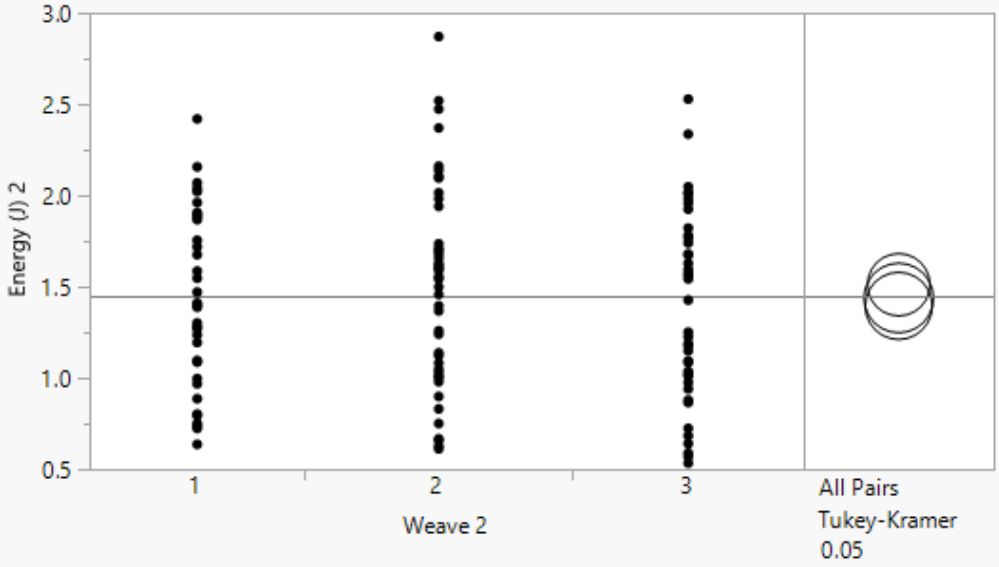

Means Comparisons

Comparisons for all pairs using Tukey-Kramer HSD

Difference Matrix

Dif=Mean[i]-Mean[j]

	2	1	3
2	0.00000	0.07279	0.11629
1	-0.07279	0.00000	0.04350
3	-0.11629	-0.04350	0.00000

Connecting Letters Report

Level		Mean
2	A	1.5112431
1	A	1.4384537
3	A	1.3949500

Levels not connected by same letter are significantly different.

Ordered Differences Report

Level	- Level	Difference	Std Err Dif	Lower CL	Upper CL	p-Value
2	3	0.1162931	0.1060100	-0.134980	0.3675662	0.5176
2	1	0.0727895	0.1080721	-0.183371	0.3289501	0.7793
1	3	0.0435037	0.1118376	-0.221582	0.3085896	0.9200

Appendix 54. Tukey HSD Charpy result – Effect of Z to Y ratio on total energy (weft direction)

Oneway Analysis of Energy (J) 2 By Z:Y ratio 2

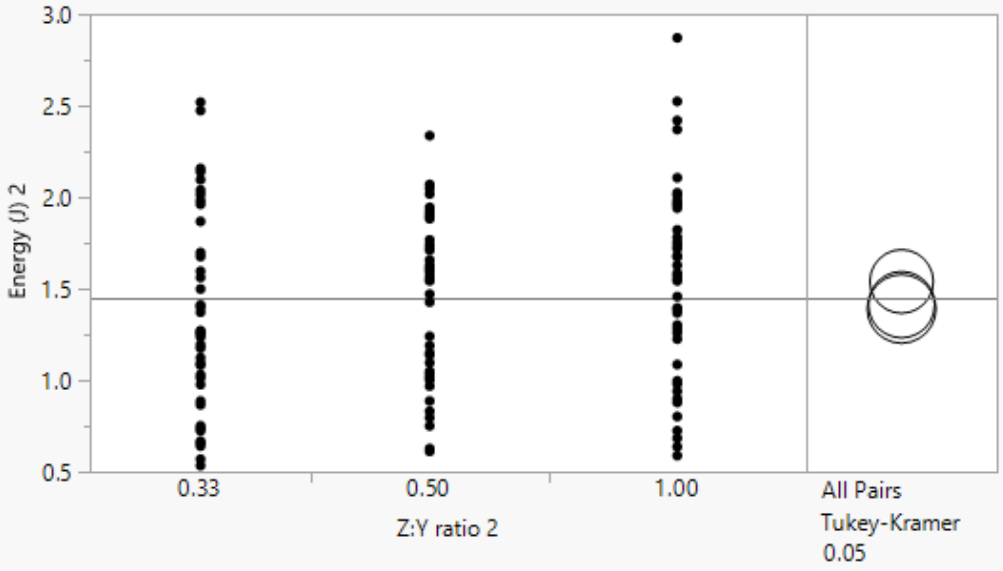

Means Comparisons

Comparisons for all pairs using Tukey-Kramer HSD

Difference Matrix

Dif=Mean[i]-Mean[j]

	1.00	0.50	0.33
1.00	0.00000	0.12702	0.15002
0.50	-0.12702	0.00000	0.02300
0.33	-0.15002	-0.02300	0.00000

Connecting Letters Report

Level		Mean
1.00	A	1.5400327
0.50	A	1.4130156
0.33	A	1.3900119

Levels not connected by same letter are significantly different.

Ordered Differences Report

Level	- Level	Difference	Std Err Dif	Lower CL	Upper CL	p-Value
1.00	0.33	0.1500207	0.1079113	-0.105759	0.4058003	0.3489
1.00	0.50	0.1270171	0.1059567	-0.124130	0.3781638	0.4560
0.50	0.33	0.0230037	0.1101026	-0.237970	0.2839772	0.9762

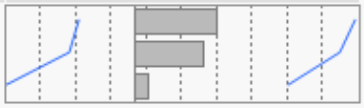

Appendix 55. ANOVA Charpy result – Total energy normalized by thickness (weft direction)

Dependent Variable: xnormthick

Number of Observations Read	134
Number of Observations Used	134

Analysis of Variance

Source	DF	Sum of Squares	Mean Square	F Value	Pr > F
Model	3	0.07177	0.02392	6.25	0.0005
Error	130	0.49739	0.00383		
Corrected Total	133	0.56916			

Root MSE	0.06186	R-Square	0.1261
Dependent Mean	0.28619	Adj R-Sq	0.1059
Coeff Var	21.61305		

Parameter Estimates

Variable	DF	Parameter Estimate	Standard Error	t Value	Pr > |t|
Intercept	1	0.34916	0.02218	15.74	<.0001
ZYRatio	1	0.01819	0.01870	0.97	0.3325
layers	1	-0.00858	0.00220	-3.90	0.0002
weave	1	-0.01099	0.00668	-1.64	0.1024

Appendix 56. Tukey HSD Charpy result – Effect of layers on total energy normalized by thickness (weft direction)

Oneway Analysis of Energy Normalized by Thickness (J/mm) 2 By Layers 2

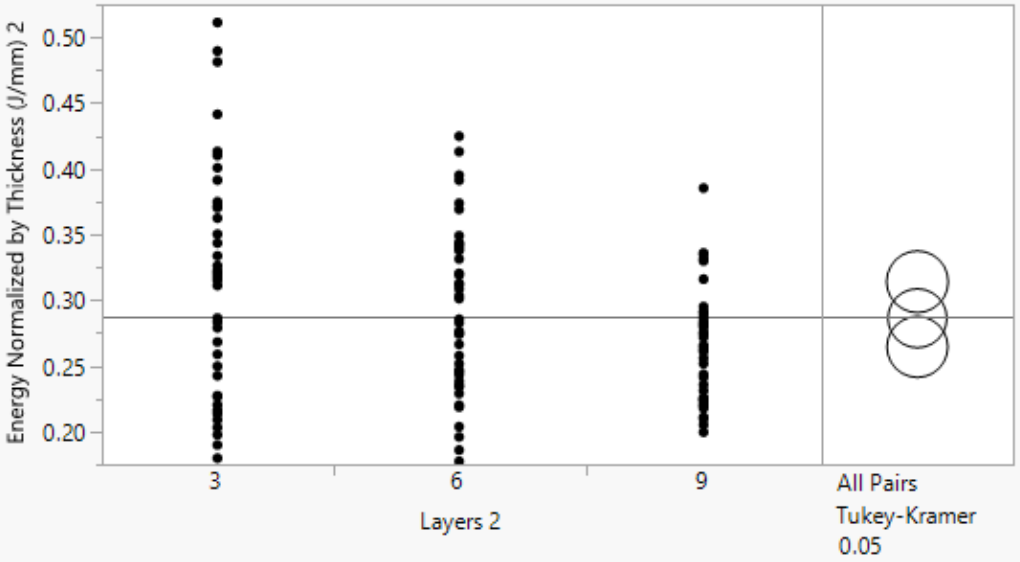

Means Comparisons

Comparisons for all pairs using Tukey-Kramer HSD

Difference Matrix

Dif=Mean[i]-Mean[j]

	3	6	9
3	0.00000	0.02777	0.04957
6	-0.02777	0.00000	0.02180
9	-0.04957	-0.02180	0.00000

Connecting Letters Report

Level			Mean
3	A		0.31401760
6	A	B	0.28624911
9		B	0.26444471

Levels not connected by same letter are significantly different.

Ordered Differences Report

Level	- Level	Difference	Std Err Dif	Lower CL	Upper CL	p-Value
3	9	0.0495729	0.0139196	0.016574	0.0825719	0.0015*
3	6	0.0277685	0.0136983	-0.004706	0.0602428	0.1097
6	9	0.0218044	0.0136167	-0.010477	0.0540854	0.2487

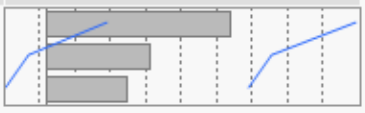

Appendix 57. Tukey HSD Charpy result – Effect of Z to Y ratio on total energy normalized by thickness (weft direction)

Oneway Analysis of Energy Normalized by Thickness (J/mm) 2 By Z:Y ratio 2

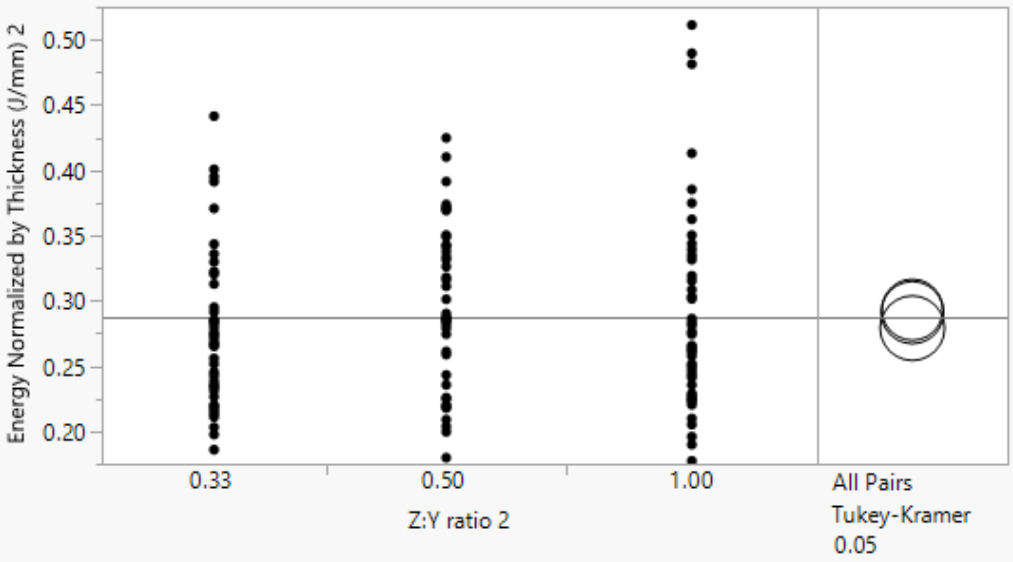

Means Comparisons

Comparisons for all pairs using Tukey-Kramer HSD

Difference Matrix

Dif=Mean[i]-Mean[j]

	1.00	0.50	0.33
1.00	0.00000	0.00219	0.01413
0.50	-0.00219	0.00000	0.01194
0.33	-0.01413	-0.01194	0.00000

Connecting Letters Report

Level		Mean
1.00	A	0.29316466
0.50	A	0.29097529
0.33	A	0.27903346

Levels not connected by same letter are significantly different.

Ordered Differences Report

Level	- Level	Difference	Std Err Dif	Lower CL	Upper CL	p-Value
1.00	0.33	0.0141312	0.0143776	-0.019954	0.0482159	0.5890
0.50	0.33	0.0119418	0.0145276	-0.022498	0.0463821	0.6901
1.00	0.50	0.0021894	0.0141222	-0.031290	0.0356687	0.9868

Appendix 58. Tukey HSD Charpy result – Effect of weave on total energy normalized by thickness (weft direction)

Oneway Analysis of Energy Normalized by Thickness (J/mm) 2 By Weave 2

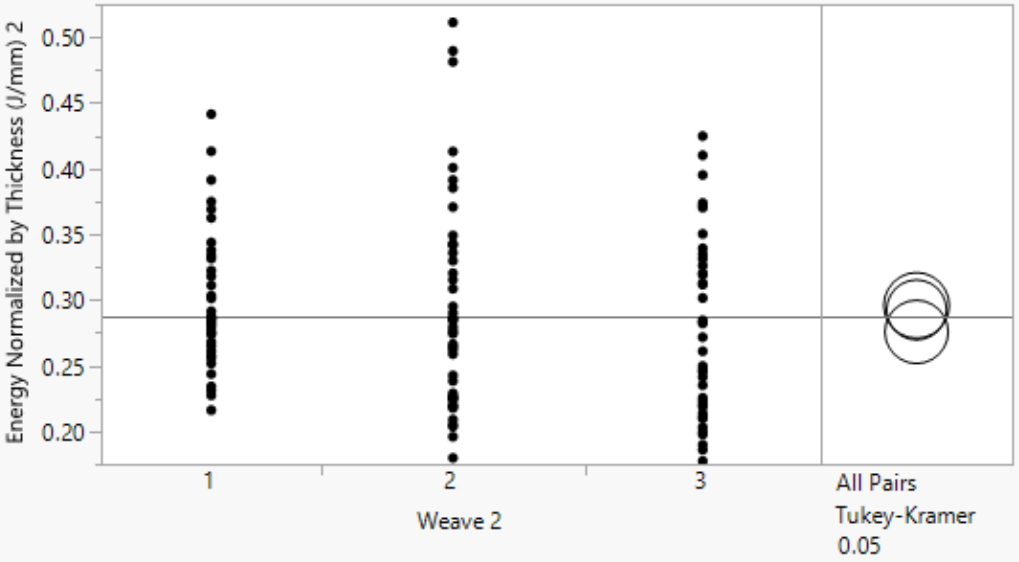

Means Comparisons

Comparisons for all pairs using Tukey-Kramer HSD

Difference Matrix

Dif=Mean[i]-Mean[j]

	1	2	3
1	0.00000	0.00342	0.02016
2	-0.00342	0.00000	0.01674
3	-0.02016	-0.01674	0.00000

Connecting Letters Report

Level		Mean
1	A	0.29586876
2	A	0.29245337
3	A	0.27570904

Levels not connected by same letter are significantly different.

Ordered Differences Report

Level	- Level	Difference	Std Err Dif	Lower CL	Upper CL	p-Value
1	3	0.0201597	0.0146350	-0.014535	0.0548548	0.3556
2	3	0.0167443	0.0140030	-0.016452	0.0499409	0.4578
1	2	0.0034154	0.0142703	-0.030415	0.0372458	0.9689

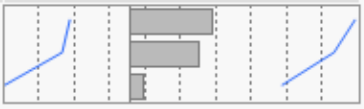

Appendix 59. ANOVA Charpy result – Total energy normalized by composite areal density (weft direction)

Dependent Variable: xnormcden

Number of Observations Read	134
Number of Observations Used	134

Analysis of Variance

Source	DF	Sum of Squares	Mean Square	F Value	Pr > F
Model	3	0.17159	0.05720	16.17	<.0001
Error	130	0.45995	0.00354		
Corrected Total	133	0.63154			

Root MSE	0.05948	R-Square	0.2717
Dependent Mean	0.26470	Adj R-Sq	0.2549
Coeff Var	22.47122		

Parameter Estimates

Variable	DF	Parameter Estimate	Standard Error	t Value	Pr > |t|
Intercept	1	0.34315	0.02133	16.09	<.0001
ZYRatio	1	0.03236	0.01798	1.80	0.0743
layers	1	-0.01420	0.00212	-6.71	<.0001
weave	1	-0.00617	0.00642	-0.96	0.3388

Appendix 60. Tukey HSD Charpy result – Effect of layers on total energy normalized by composite areal density (weft direction)

Oneway Analysis of Energy Normalized by Comp. Areal Density (kJ/g/mm2) 2 By Layers 2

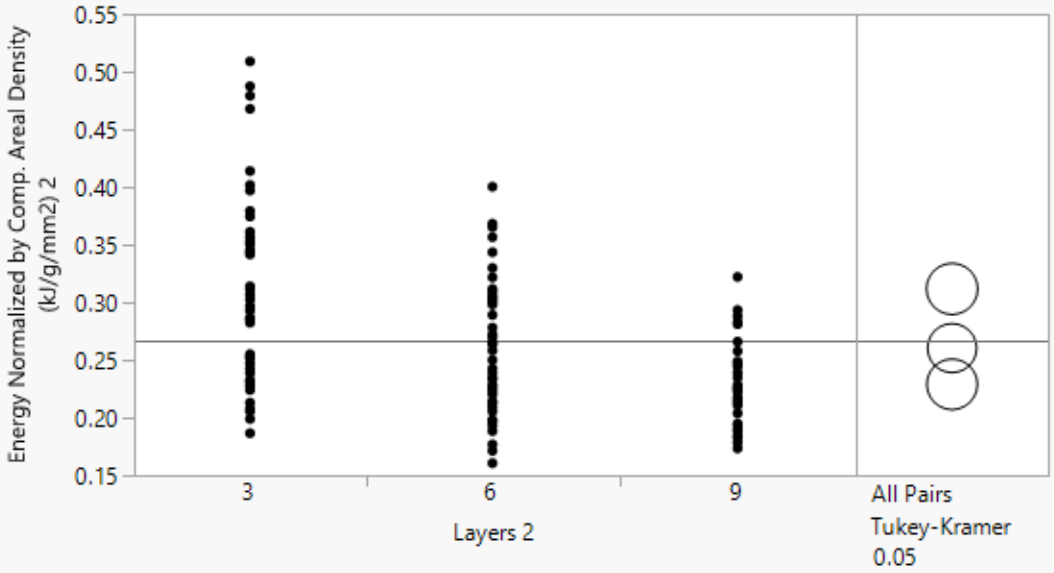

Means Comparisons

Comparisons for all pairs using Tukey-Kramer HSD

Difference Matrix

Dif=Mean[i]-Mean[j]

	3	6	9
3	0.00000	0.05137	0.08278
6	-0.05137	0.00000	0.03141
9	-0.08278	-0.03141	0.00000

Connecting Letters Report

Level		Mean
3	A	0.31173961
6	B	0.26036949
9	C	0.22895570

Levels not connected by same letter are significantly different.

Ordered Differences Report

Level	- Level	Difference	Std Err Dif	Lower CL	Upper CL	p-Value
3	9	0.0827839	0.0131801	0.0515381	0.1140297	<.0001*
3	6	0.0513701	0.0129705	0.0206211	0.0821191	0.0004*
6	9	0.0314138	0.0128933	0.0008478	0.0619798	0.0425*

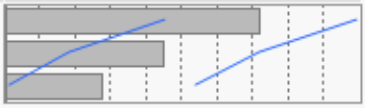

Appendix 61. Tukey HSD Charpy result – Effect of ratio on total energy normalized by composite areal density (weft direction)

Oneway Analysis of Energy Normalized by Comp. Areal Density (kJ/g/mm2) 2 By Z:Y ratio 2

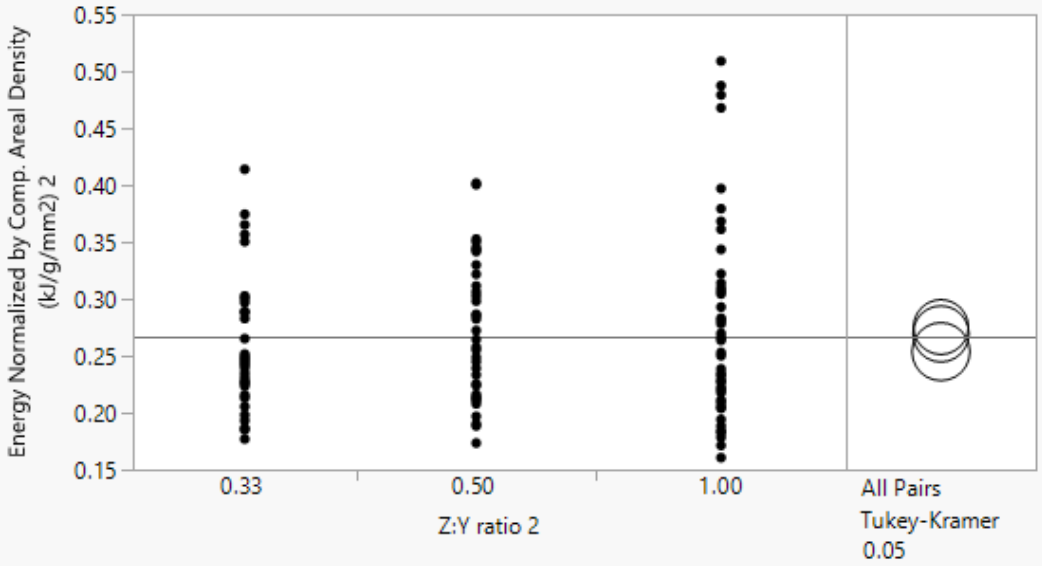

Means Comparisons

Comparisons for all pairs using Tukey-Kramer HSD

Difference Matrix

Dif=Mean[i]-Mean[j]

	1.00	0.50	0.33
1.00	0.00000	0.00602	0.02164
0.50	-0.00602	0.00000	0.01561
0.33	-0.02164	-0.01561	0.00000

Connecting Letters Report

Level		Mean
1.00	A	0.27534215
0.50	A	0.26932116
0.33	A	0.25370683

Levels not connected by same letter are significantly different.

Ordered Differences Report

Level	- Level	Difference	Std Err Dif	Lower CL	Upper CL	p-Value
1.00	0.33	0.0216353	0.0147924	-0.013433	0.0567034	0.3123
0.50	0.33	0.0156143	0.0149467	-0.019820	0.0510482	0.5501
1.00	0.50	0.0060210	0.0145297	-0.028424	0.0404662	0.9098

Appendix 62. Tukey HSD Charpy result – Effect of weave on total energy normalized by composite areal density (weft direction)

Oneway Analysis of Energy Normalized by Comp. Areal Density (kJ/g/mm2) 2 By Weave 2

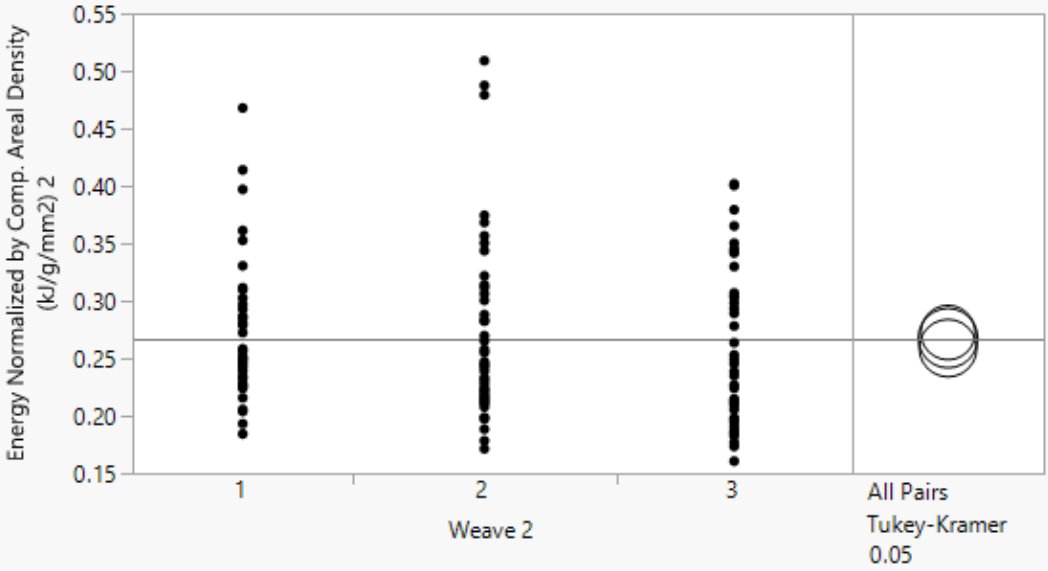

Means Comparisons

Comparisons for all pairs using Tukey-Kramer HSD

Difference Matrix

Dif=Mean[i]-Mean[j]

	2	1	3
2	0.00000	0.00487	0.01357
1	-0.00487	0.00000	0.00870
3	-0.01357	-0.00870	0.00000

Connecting Letters Report

Level		Mean
2	A	0.27248410
1	A	0.26761589
3	A	0.25891472

Levels not connected by same letter are significantly different.

Ordered Differences Report

Level	- Level	Difference	Std Err Dif	Lower CL	Upper CL	p-Value
2	3	0.0135694	0.0145434	-0.020908	0.0480472	0.6204
1	3	0.0087012	0.0151999	-0.027333	0.0447353	0.8350
2	1	0.0048682	0.0148211	-0.030268	0.0400044	0.9423

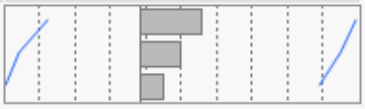

Appendix 63. ANOVA Charpy result – Total energy normalized by preform areal density (weft direction)

Dependent Variable: xnormpden

Number of Observations Read	134
Number of Observations Used	134

Analysis of Variance

Source	DF	Sum of Squares	Mean Square	F Value	Pr > F
Model	3	1.67993	0.55998	14.45	<.0001
Error	130	5.03837	0.03876		
Corrected Total	133	6.71830			

Root MSE	0.19687	R-Square	0.2501
Dependent Mean	0.88386	Adj R-Sq	0.2327
Coeff Var	22.27354		

Parameter Estimates

Variable	DF	Parameter Estimate	Standard Error	t Value	Pr > |t|
Intercept	1	1.16899	0.07058	16.56	<.0001
ZYRatio	1	0.06620	0.05951	1.11	0.2680
layers	1	-0.04465	0.00700	-6.37	<.0001
weave	1	-0.02759	0.02126	-1.30	0.1967

Appendix 64. Tukey HSD Charpy result – Effect of layers on total energy normalized by composite areal density (weft direction)

Oneway Analysis of Energy Normalized by Preform Areal Density (kJ/g/mm2) 2 By Layers 2

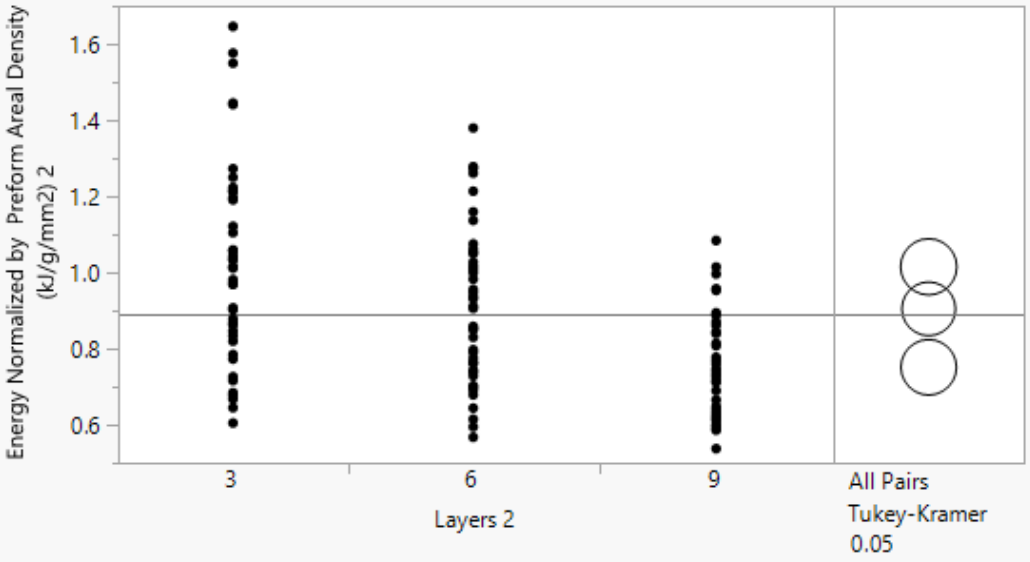

Means Comparisons

Comparisons for all pairs using Tukey-Kramer HSD

Difference Matrix

Dif=Mean[i]-Mean[j]

	3	6	9
3	0.00000	0.11045	0.26383
6	-0.11045	0.00000	0.15338
9	-0.26383	-0.15338	0.00000

Connecting Letters Report

Level		Mean
3	A	1.0149878
6	B	0.9045414
9	C	0.7511568

Levels not connected by same letter are significantly different.

Ordered Differences Report

Level	- Level	Difference	Std Err Dif	Lower CL	Upper CL	p-Value
3	9	0.2638310	0.0437602	0.1600894	0.3675726	<.0001*
6	9	0.1533846	0.0428081	0.0519001	0.2548690	0.0014*
3	6	0.1104464	0.0430644	0.0083543	0.2125386	0.0306*

Appendix 65. Tukey HSD Charpy result – Effect of Z to Y ratio on total energy normalized by composite areal density (weft direction)

Oneway Analysis of Energy Normalized by Preform Areal Density (kJ/g/mm2) 2 By Z:Y ratio 2

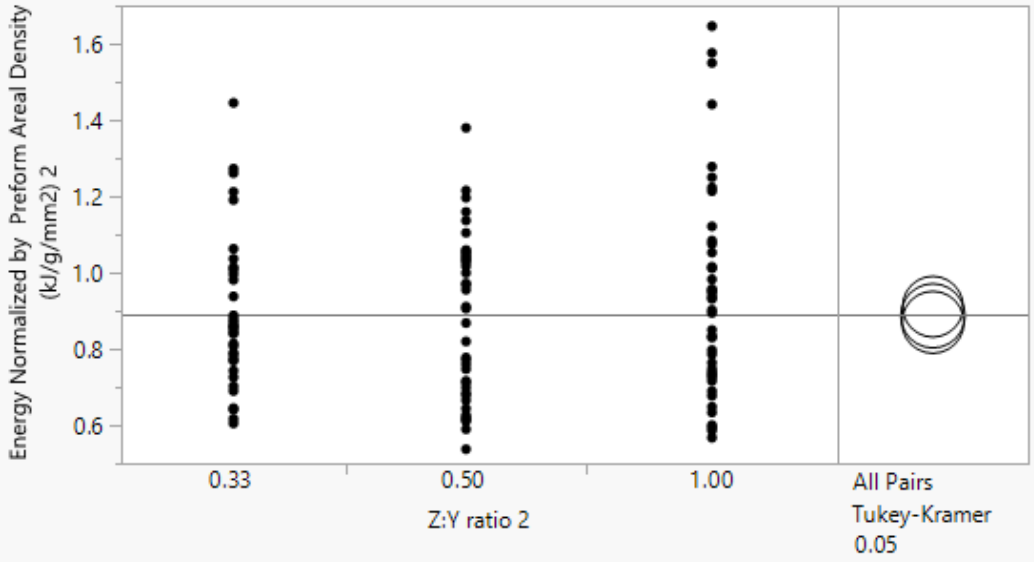

Means Comparisons

Comparisons for all pairs using Tukey-Kramer HSD

Difference Matrix

Dif=Mean[i]-Mean[j]

	1.00	0.33	0.50
1.00	0.00000	0.02408	0.04107
0.33	-0.02408	0.00000	0.01699
0.50	-0.04107	-0.01699	0.00000

Connecting Letters Report

Level		Mean
1.00	A	0.91095638
0.33	A	0.88687885
0.50	A	0.86988792

Levels not connected by same letter are significantly different.

Ordered Differences Report

Level	- Level	Difference	Std Err Dif	Lower CL	Upper CL	p-Value
1.00	0.50	0.0410685	0.0480257	-0.072785	0.1549222	0.6694
1.00	0.33	0.0240775	0.0488941	-0.091835	0.1399900	0.8750
0.33	0.50	0.0169909	0.0494042	-0.100131	0.1341127	0.9369

Appendix 66. Tukey HSD Charpy result – Effect of weave on total energy normalized by composite areal density (weft direction)

Oneway Analysis of Energy Normalized by Preform Areal Density (kJ/g/mm2) 2 By Weave 2

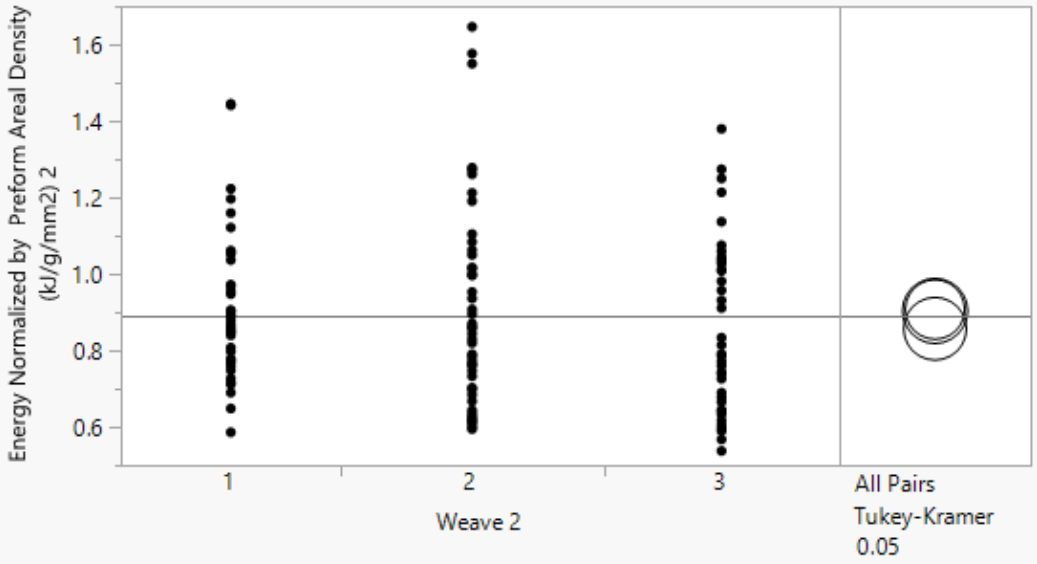

Means Comparisons

Comparisons for all pairs using Tukey-Kramer HSD

Difference Matrix

Dif=Mean[i]-Mean[j]

	2	1	3
2	0.00000	0.00384	0.05039
1	-0.00384	0.00000	0.04655
3	-0.05039	-0.04655	0.00000

Connecting Letters Report

Level		Mean
2	A	0.90733929
1	A	0.90349912
3	A	0.85694838

Levels not connected by same letter are significantly different.

Ordered Differences Report

Level	- Level	Difference	Std Err Dif	Lower CL	Upper CL	p-Value
2	3	0.0503909	0.0477178	-0.062733	0.1635147	0.5431
1	3	0.0465507	0.0498717	-0.071679	0.1647809	0.6202
2	1	0.0038402	0.0486289	-0.111444	0.1191240	0.9966

Appendix 67. ANOVA result – Compression test (warp direction)

The REG Procedure
Model: MODEL1
Dependent Variable: ythick

Number of Observations Read	128
Number of Observations Used	128

Analysis of Variance

Source	DF	Sum of Squares	Mean Square	F Value	Pr > F
Model	3	444.20062	148.06687	4132.52	<.0001
Error	124	4.44288	0.03583		
Corrected Total	127	448.64350			

Root MSE	0.18929	R-Square	0.9901
Dependent Mean	5.01992	Adj R-Sq	0.9899
Coeff Var	3.77072		

Parameter Estimates

Variable	DF	Parameter Estimate	Standard Error	t Value	Pr > |t|
Intercept	1	0.51569	0.07010	7.36	<.0001
ZYRatio	1	0.01756	0.05906	0.30	0.7667
layers	1	0.74903	0.00673	111.31	<.0001
weave	1	0.01693	0.02056	0.82	0.4118

Appendix 68. ANOVA result – Compression test (weft direction)

The REG Procedure
Model: MODEL1
Dependent Variable: xthick

Number of Observations Read	128
Number of Observations Used	128

Analysis of Variance

Source	DF	Sum of Squares	Mean Square	F Value	Pr > F
Model	3	440.54182	146.84727	2503.06	<.0001
Error	124	7.27473	0.05867		
Corrected Total	127	447.81656			

Root MSE	0.24221	R-Square	0.9838
Dependent Mean	5.12836	Adj R-Sq	0.9834
Coeff Var	4.72301		

Parameter Estimates

Variable	DF	Parameter Estimate	Standard Error	t Value	Pr > |t|
Intercept	1	0.32601	0.09186	3.55	0.0005
ZYRatio	1	0.21923	0.07460	2.94	0.0039
layers	1	0.74547	0.00861	86.58	<.0001
weave	1	0.09408	0.02665	3.53	0.0006

Appendix 69. Tukey HSD Compression result – Effect of layers on peak load (warp & weft direction)

Oneway Analysis of PEAK LOAD, N By # of LAYERS

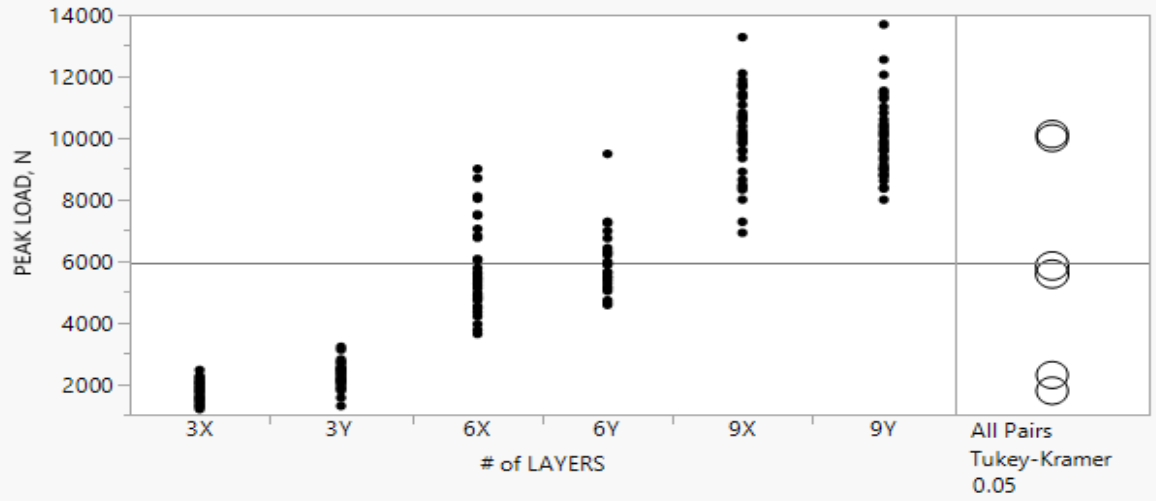

Means Comparisons

Comparisons for all pairs using Tukey-Kramer HSD

Connecting Letters Report

Level			Mean
9X	A		10123.984
9Y	A		9993.606
6Y		B	5836.603
6X		B	5571.868
3Y		C	2287.286
3X		C	1775.145

Levels not connected by same letter are significantly different.

Ordered Differences Report

Level	- Level	Difference	Std Err Dif	Lower CL	Upper CL	p-Value
9X	3X	8348.839	217.7761	7723.36	8974.323	<.0001*
9Y	3X	8218.461	216.5352	7596.54	8840.381	<.0001*
9X	3Y	7836.698	216.5352	7214.78	8458.618	<.0001*
9Y	3Y	7706.320	215.2871	7087.99	8324.655	<.0001*
9X	6X	4552.116	221.8218	3915.01	5189.220	<.0001*
9Y	6X	4421.738	220.6037	3788.13	5055.343	<.0001*
9X	6Y	4287.381	221.8218	3650.28	4924.485	<.0001*
9Y	6Y	4157.003	220.6037	3523.40	4790.608	<.0001*
6Y	3X	4061.458	221.8218	3424.35	4698.561	<.0001*
6X	3X	3796.723	221.8218	3159.62	4433.826	<.0001*
6Y	3Y	3549.317	220.6037	2915.71	4182.922	<.0001*
6X	3Y	3284.582	220.6037	2650.98	3918.187	<.0001*
3Y	3X	512.141	216.5352	-109.78	1134.060	0.1727
6Y	6X	264.735	225.7951	-383.78	913.250	0.8496
9X	9Y	130.378	216.5352	-491.54	752.298	0.9908

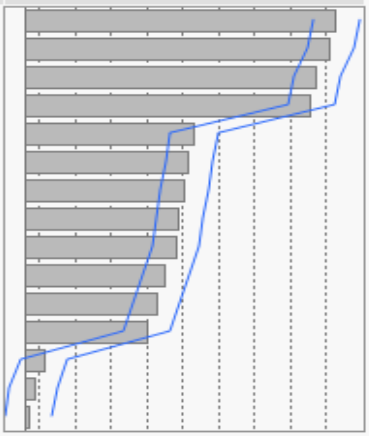

Appendix 70. Tukey HSD Compression result – Effect of weave on peak load (warp & weft direction)

Oneway Analysis of PEAK LOAD, N By WEAVE

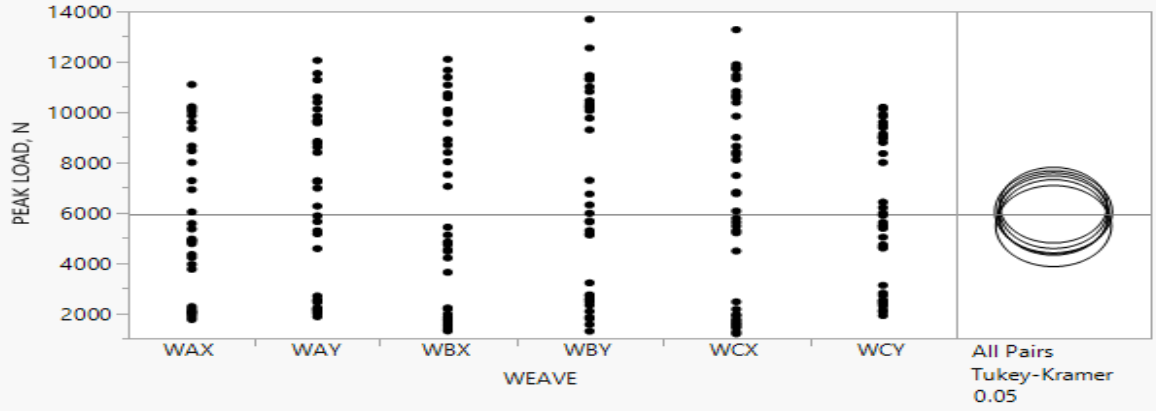

Means Comparisons

Comparisons for all pairs using Tukey-Kramer HSD

Connecting Letters Report

Level		Mean
WBY	A	6294.6124
WCX	A	6072.0367
WAY	A	6030.1989
WBX	A	5909.7927
WCY	A	5809.2953
WAX	A	5463.7017

Levels not connected by same letter are significantly different.

Ordered Differences Report

Level	- Level	Difference	Std Err Dif	Lower CL	Upper CL	p-Value
WBY	WAX	830.9107	767.3553	-1373.04	3034.863	0.8879
WCX	WAX	608.3350	767.3553	-1595.62	2812.287	0.9686
WAY	WAX	566.4972	799.4967	-1729.77	2862.764	0.9808
WBY	WCY	485.3171	739.4420	-1638.46	2609.099	0.9864
WBX	WAX	446.0910	779.9755	-1794.11	2686.291	0.9928
WBY	WBX	384.8197	752.5305	-1776.55	2546.193	0.9957
WCY	WAX	345.5936	767.3553	-1858.36	2549.546	0.9977
WBY	WAY	264.4135	772.7453	-1955.02	2483.847	0.9994
WCX	WCY	262.7414	739.4420	-1861.04	2386.523	0.9993
WBY	WCX	222.5757	739.4420	-1901.21	2346.357	0.9997
WAY	WCY	220.9037	772.7453	-1998.53	2440.337	0.9997
WCX	WBX	162.2440	752.5305	-1999.13	2323.618	0.9999
WAY	WBX	120.4062	785.2789	-2135.03	2375.838	1.0000
WBX	WCY	100.4975	752.5305	-2060.88	2261.871	1.0000
WCX	WAY	41.8378	772.7453	-2177.60	2261.271	1.0000

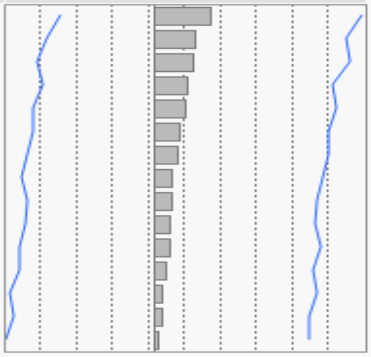

Appendix 71. Tukey HSD Compression result – Effect of Z to Y ratio on peak load (warp & weft direction)

Oneway Analysis of PEAK LOAD, N By Z yarn:Yyarn Ratio

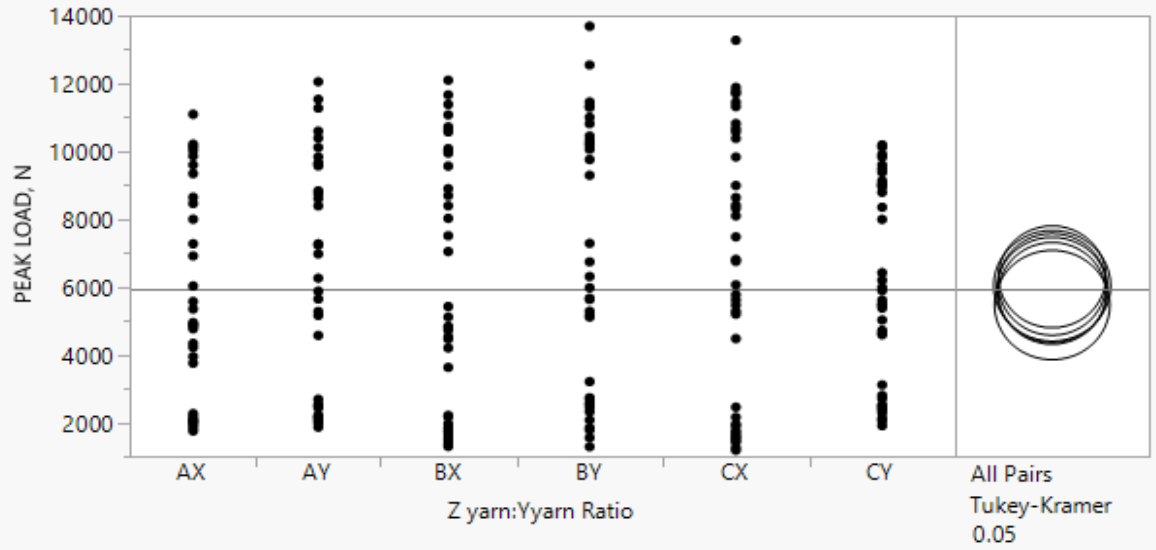

Means Comparisons

Comparisons for all pairs using Tukey-Kramer HSD

Connecting Letters Report

Level		Mean
BY	A	6294.6124
CX	A	6072.0367
AY	A	6030.1989
BX	A	5909.7927
CY	A	5809.2953
AX	A	5463.7017

Levels not connected by same letter are significantly different.

Ordered Differences Report

Level	- Level	Difference	Std Err Dif	Lower CL	Upper CL	p-Value
BY	AX	830.9107	767.3553	-1373.04	3034.863	0.8879
CX	AX	608.3350	767.3553	-1595.62	2812.287	0.9686
AY	AX	566.4972	799.4967	-1729.77	2862.764	0.9808
BY	CY	485.3171	739.4420	-1638.46	2609.099	0.9864
BX	AX	446.0910	779.9755	-1794.11	2686.291	0.9928
BY	BX	384.8197	752.5305	-1776.55	2546.193	0.9957
CY	AX	345.5936	767.3553	-1858.36	2549.546	0.9977
BY	AY	264.4135	772.7453	-1955.02	2483.847	0.9994
CX	CY	262.7414	739.4420	-1861.04	2386.523	0.9993
BY	CX	222.5757	739.4420	-1901.21	2346.357	0.9997
AY	CY	220.9037	772.7453	-1998.53	2440.337	0.9997
CX	BX	162.2440	752.5305	-1999.13	2323.618	0.9999
AY	BX	120.4062	785.2789	-2135.03	2375.838	1.0000
BX	CY	100.4975	752.5305	-2060.88	2261.871	1.0000
CX	AY	41.8378	772.7453	-2177.60	2261.271	1.0000

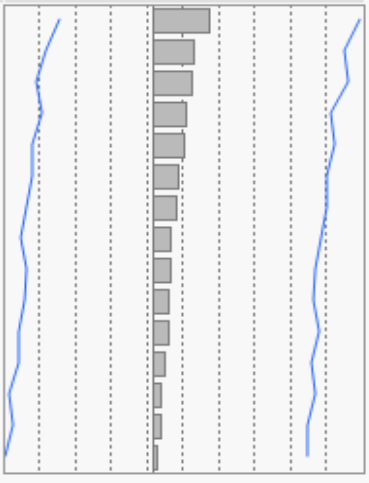

Appendix 72. Tukey HSD Compression result – Effect of layers on peak load normalized by thickness

Oneway Analysis of Load Normaized by thickness, N/mm By # of LAYERS

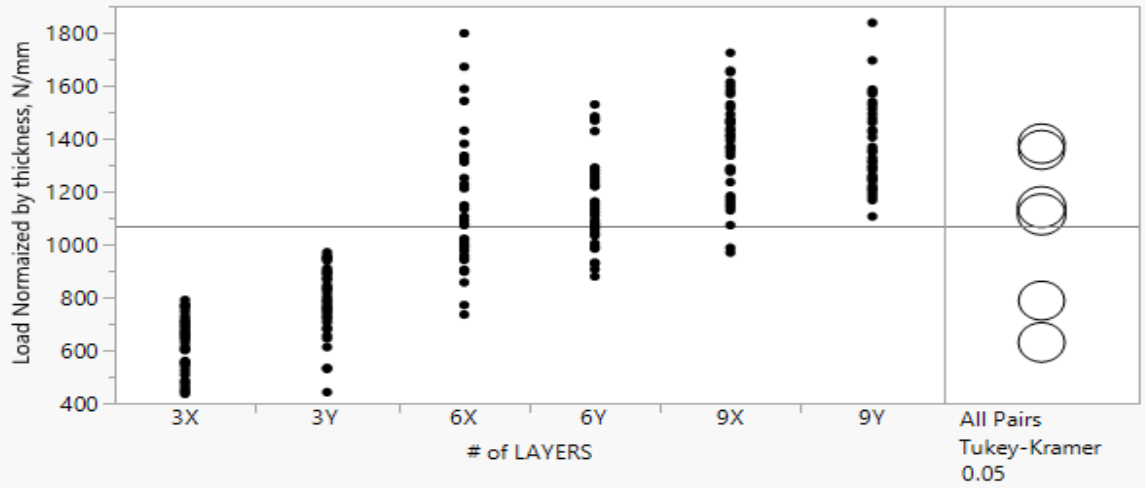

Means Comparisons

Comparisons for all pairs using Tukey-Kramer HSD

Connecting Letters Report

Level		Mean
9X	A	1380.9654
9Y	A	1357.1339
6Y	B	1141.3926
6X	B	1113.6441
3Y	C	787.6261
3X	D	630.1372

Levels not connected by same letter are significantly different.

Ordered Differences Report

Level	- Level	Difference	Std Err Dif	Lower CL	Upper CL	p-Value
9X	3X	750.8281	36.63839	645.598	856.0588	<.0001*
9Y	3X	726.9966	36.42962	622.366	831.6277	<.0001*
9X	3Y	593.3393	36.42962	488.708	697.9703	<.0001*
9Y	3Y	569.5078	36.21965	465.480	673.5357	<.0001*
6Y	3X	511.2554	37.31904	404.070	618.4409	<.0001*
6X	3X	483.5068	37.31904	376.321	590.6924	<.0001*
6Y	3Y	353.7665	37.11410	247.170	460.3634	<.0001*
6X	3Y	326.0180	37.11410	219.421	432.6149	<.0001*
9X	6X	267.3213	37.31904	160.136	374.5068	<.0001*
9Y	6X	243.4898	37.11410	136.893	350.0867	<.0001*
9X	6Y	239.5728	37.31904	132.387	346.7583	<.0001*
9Y	6Y	215.7413	37.11410	109.144	322.3382	<.0001*
3Y	3X	157.4889	36.42962	52.858	262.1199	0.0003*
6Y	6X	27.7485	37.98749	-81.357	136.8540	0.9780
9X	9Y	23.8315	36.42962	-80.800	128.4625	0.9866

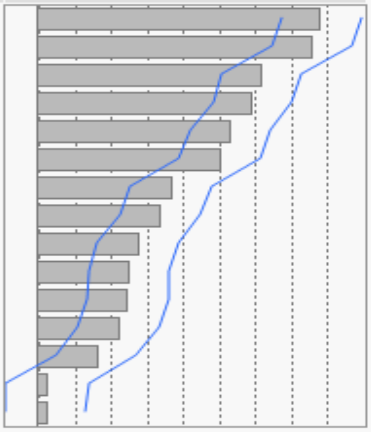

Appendix 73. Tukey HSD Compression result – Effect of weave on peak load normalized by thickness

Oneway Analysis of Load Normaized by thickness, N/mm By WEAVE

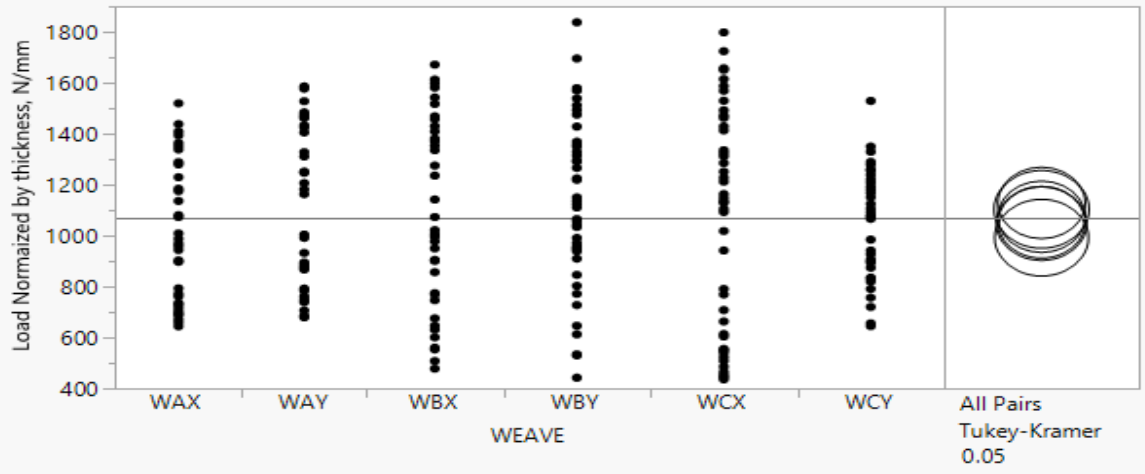

Means Comparisons

Comparisons for all pairs using Tukey-Kramer HSD

Connecting Letters Report

Level		Mean
WBY	A	1128.2741
WAY	A	1103.1429
WCX	A	1074.1095
WCY	A	1051.8529
WBX	A	1047.8113
WAX	A	991.7993

Levels not connected by same letter are significantly different.

Ordered Differences Report

Level	- Level	Difference	Std Err Dif	Lower CL	Upper CL	p-Value
WBY	WAX	136.4748	71.62563	-69.244	342.1937	0.4013
WAY	WAX	111.3435	74.62574	-102.992	325.6792	0.6697
WCX	WAX	82.3101	71.62563	-123.409	288.0290	0.8601
WBY	WBX	80.4628	70.24188	-121.282	282.2073	0.8618
WBY	WCY	76.4212	69.02019	-121.815	274.6569	0.8781
WCY	WAX	60.0536	71.62563	-145.665	265.7725	0.9600
WBX	WAX	56.0120	72.80362	-153.090	265.1142	0.9724
WAY	WBX	55.3316	73.29864	-155.192	265.8556	0.9746
WBY	WCX	54.1646	69.02019	-144.071	252.4003	0.9699
WAY	WCY	51.2900	72.12875	-155.874	258.4539	0.9805
WAY	WCX	29.0334	72.12875	-178.131	236.1973	0.9986
WCX	WBX	26.2981	70.24188	-175.446	228.0427	0.9990
WBY	WAY	25.1312	72.12875	-182.033	232.2951	0.9993
WCX	WCY	22.2566	69.02019	-175.979	220.4923	0.9995
WCY	WBX	4.0416	70.24188	-197.703	205.7861	1.0000

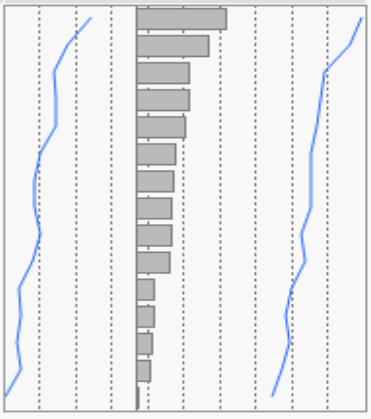

Appendix 74. Tukey HSD Compression result – Effect of Z to Y ratio on peak load normalized by thickness

Oneway Analysis of Load Normaized by thickness, N/mm By Z yarn:Yyarn Ratio

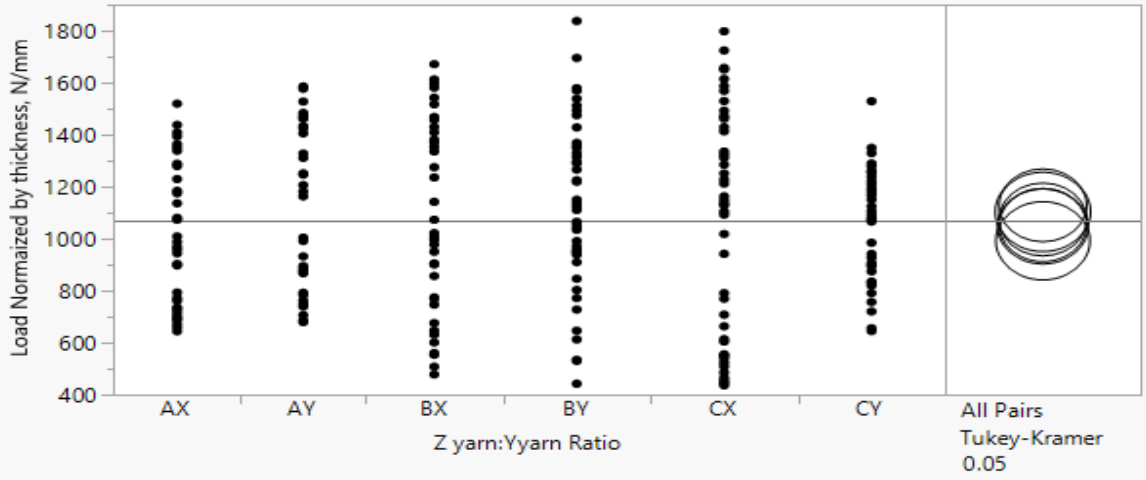

Means Comparisons

Comparisons for all pairs using Tukey-Kramer HSD

Connecting Letters Report

Level		Mean
BY	A	1128.2741
AY	A	1103.1429
CX	A	1074.1095
CY	A	1051.8529
BX	A	1047.8113
AX	A	991.7993

Levels not connected by same letter are significantly different.

Ordered Differences Report

Level	- Level	Difference	Std Err Dif	Lower CL	Upper CL	p-Value
BY	AX	136.4748	71.62563	-69.244	342.1937	0.4013
AY	AX	111.3435	74.62574	-102.992	325.6792	0.6697
CX	AX	82.3101	71.62563	-123.409	288.0290	0.8601
BY	BX	80.4628	70.24188	-121.282	282.2073	0.8618
BY	CY	76.4212	69.02019	-121.815	274.6569	0.8781
CY	AX	60.0536	71.62563	-145.665	265.7725	0.9600
BX	AX	56.0120	72.80362	-153.090	265.1142	0.9724
AY	BX	55.3316	73.29864	-155.192	265.8556	0.9746
BY	CX	54.1646	69.02019	-144.071	252.4003	0.9699
AY	CY	51.2900	72.12875	-155.874	258.4539	0.9805
AY	CX	29.0334	72.12875	-178.131	236.1973	0.9986
CX	BX	26.2981	70.24188	-175.446	228.0427	0.9990
BY	AY	25.1312	72.12875	-182.033	232.2951	0.9993
CX	CY	22.2566	69.02019	-175.979	220.4923	0.9995
CY	BX	4.0416	70.24188	-197.703	205.7861	1.0000

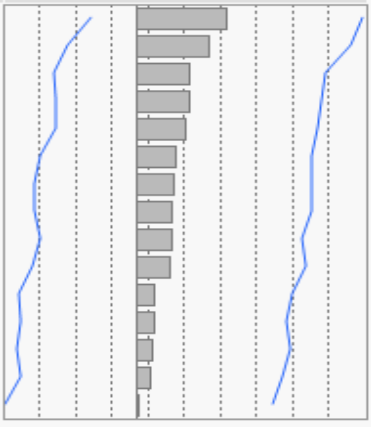

Appendix 75. Tukey HSD Tensile result– Effect of weave on peak load of treated & untreated samples (warp direction)

Oneway Analysis of PEAK LOAD, N By PANEL ID

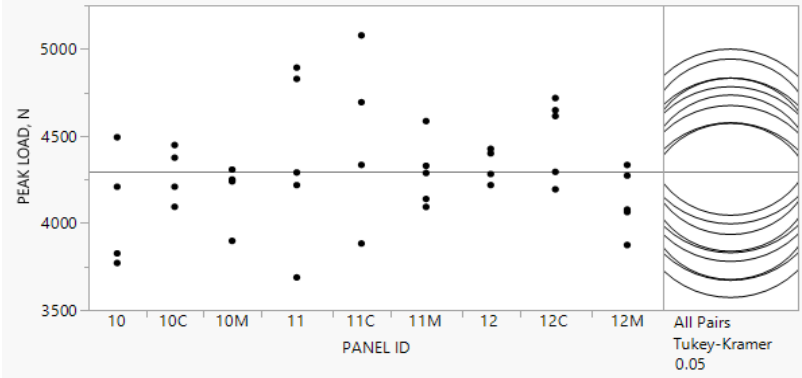

Means Comparisons

Comparisons for all pairs using Tukey-Kramer HSD

Connecting Letters Report

Level		Mean
11C	A	4496.9258
12C	A	4493.3742
11	A	4383.1073
12	A	4331.3209
11M	A	4286.4408
10C	A	4281.1348
10M	A	4173.2648
12M	A	4123.9810
10	A	4074.2931

Levels not connected by same letter are significantly different.

Ordered Differences Report

Level	- Level	Difference	Std Err Dif	Lower CL	Upper CL	p-Value
11C	10	422.6328	213.2171	-287.305	1132.571	0.5661
12C	10	419.0811	202.2755	-254.425	1092.587	0.5090
11C	12M	372.9448	202.2755	-300.561	1046.451	0.6544
12C	12M	369.3932	190.7071	-265.595	1004.381	0.5951
11C	10M	323.6611	213.2171	-386.277	1033.599	0.8387
12C	10M	320.1094	202.2755	-353.397	993.616	0.8067
11	10	308.8142	202.2755	-364.692	982.320	0.8345
11	12M	259.1263	190.7071	-375.861	894.114	0.9045
12	10	257.0278	213.2171	-452.910	966.966	0.9492
11C	10C	215.7910	213.2171	-494.147	925.729	0.9818
12C	10C	212.2394	202.2755	-461.267	885.745	0.9773
11M	10	212.1477	202.2755	-461.358	885.654	0.9773
11C	11M	210.4850	202.2755	-463.021	883.991	0.9784
11	10M	209.8425	202.2755	-463.664	883.349	0.9788
12	12M	207.3399	202.2755	-466.166	880.846	0.9803
12C	11M	206.9334	190.7071	-428.054	841.921	0.9722
10C	10	206.8417	213.2171	-503.096	916.780	0.9860
11C	12	165.6050	213.2171	-544.333	875.543	0.9968
11M	12M	162.4598	190.7071	-472.528	797.447	0.9940
12C	12	162.0533	202.2755	-511.453	835.559	0.9960
12	10M	158.0561	213.2171	-551.882	867.994	0.9977
10C	12M	157.1538	202.2755	-516.352	830.660	0.9968
11C	11	113.8185	202.2755	-559.688	787.325	0.9997
11M	10M	113.1760	202.2755	-560.330	786.682	0.9997
12C	11	110.2668	190.7071	-524.721	745.255	0.9996
10C	10M	107.8700	213.2171	-602.068	817.808	0.9999
11	10C	101.9725	202.2755	-571.534	775.479	0.9999
10M	10	98.9717	213.2171	-610.966	808.910	0.9999
11	11M	96.6665	190.7071	-538.321	731.654	0.9999
11	12	51.7864	202.2755	-621.720	725.293	1.0000
12	10C	50.1861	213.2171	-659.752	760.124	1.0000
12M	10	49.6879	202.2755	-623.818	723.194	1.0000
10M	12M	49.2838	202.2755	-624.222	722.790	1.0000
12	11M	44.8801	202.2755	-628.626	718.386	1.0000
11M	10C	5.3060	202.2755	-668.200	678.812	1.0000
11C	12C	3.5517	202.2755	-669.954	677.058	1.0000

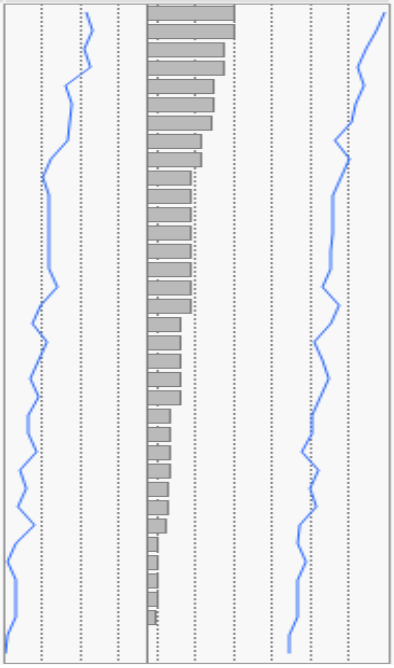

Appendix 76. Tukey HSD Tensile result– Effect of weave on peak load of treated & untreated samples (weft direction)

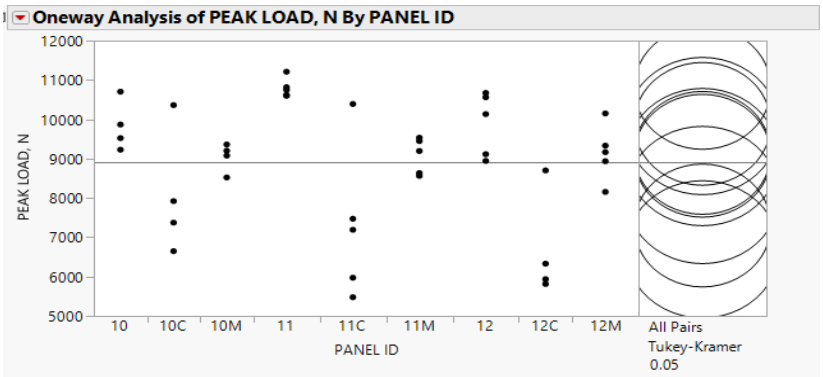

Means Comparisons

Comparisons for all pairs using Tukey-Kramer HSD

Connecting Letters Report

Level					Mean
11	A				10800.548
12	A	B			9885.544
10	A	B			9830.933
12M	A	B	C		9148.008
11M	A	B	C		9075.331
10M	A	B	C	D	9041.381
10C		B	C	D	8076.576
11C			C	D	7301.199
12C				D	6696.056

Levels not connected by same letter are significantly different.

Ordered Differences Report

Level	- Level	Difference	Std Err Dif	Lower CL	Upper CL	p-Value
11	12C	4104.492	705.0673	1762.05	6446.936	<.0001*
11	11C	3499.349	664.7439	1290.87	5707.826	0.0003*
12	12C	3189.488	705.0673	847.04	5531.932	0.0023*
10	12C	3134.877	743.2062	665.72	5604.030	0.0052*
11	10C	2723.972	705.0673	381.53	5066.416	0.0132*
12	11C	2584.344	664.7439	375.87	4792.822	0.0124*
10	11C	2529.734	705.0673	187.29	4872.178	0.0264*
12M	12C	2451.953	705.0673	109.51	4794.396	0.0346*
11M	12C	2379.275	705.0673	36.83	4721.719	0.0442*
10M	12C	2345.326	743.2062	-123.83	4814.478	0.0731
12M	11C	1846.809	664.7439	-361.67	4055.286	0.1616
12	10C	1808.967	705.0673	-533.48	4151.411	0.2403
11M	11C	1774.132	664.7439	-434.35	3982.609	0.1992
11	10M	1759.167	705.0673	-583.28	4101.611	0.2717
10	10C	1754.357	743.2062	-714.80	4223.509	0.3386
10M	11C	1740.182	705.0673	-602.26	4082.626	0.2843
11	11M	1725.217	664.7439	-483.26	3933.694	0.2279
11	12M	1652.540	664.7439	-555.94	3861.017	0.2759
10C	12C	1380.521	743.2062	-1088.63	3849.673	0.6457
12M	10C	1071.432	705.0673	-1271.01	3413.876	0.8381
11M	10C	998.755	705.0673	-1343.69	3341.198	0.8831
11	10	969.615	705.0673	-1372.83	3312.059	0.8989
10M	10C	964.805	743.2062	-1504.35	3433.958	0.9246
11	12	915.004	664.7439	-1293.47	3123.482	0.8984
12	10M	844.162	705.0673	-1498.28	3186.606	0.9513
12	11M	810.213	664.7439	-1398.26	3018.690	0.9462
10	10M	789.552	743.2062	-1679.60	3258.704	0.9756
10C	11C	775.377	705.0673	-1567.07	3117.821	0.9701
10	11M	755.602	705.0673	-1586.84	3098.046	0.9743
12	12M	737.535	664.7439	-1470.94	2946.013	0.9685
10	12M	682.925	705.0673	-1659.52	3025.369	0.9862
11C	12C	605.143	705.0673	-1737.30	2947.587	0.9937
12M	10M	106.627	705.0673	-2235.82	2449.071	1.0000
12M	11M	72.677	664.7439	-2135.80	2281.155	1.0000
12	10	54.611	705.0673	-2287.83	2397.055	1.0000
11M	10M	33.950	705.0673	-2308.49	2376.394	1.0000

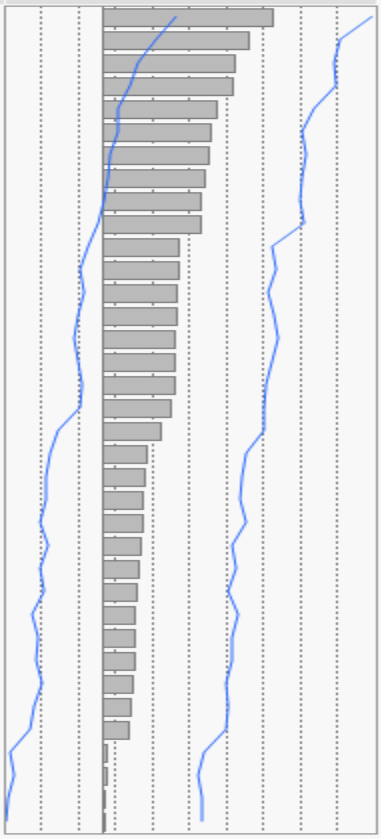

Appendix 77. Tukey HSD Tup Impact result– Effect of weave on peak load of treated & untreated samples

Oneway Analysis of TOTAL PENETRATION ENERGY, J By SAMPLE ID

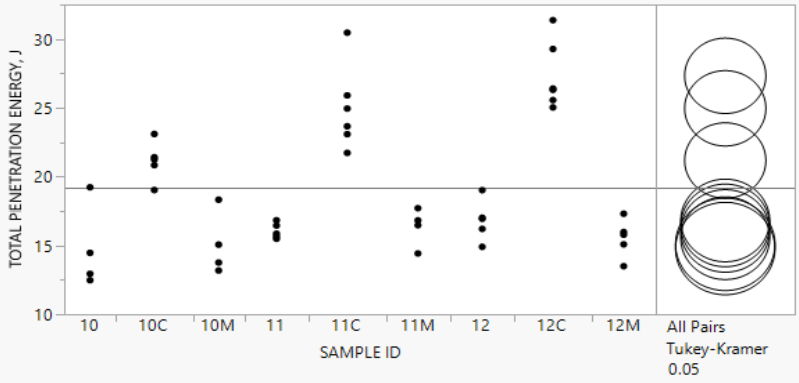

Means Comparisons

Comparisons for all pairs using Tukey-Kramer HSD

Connecting Letters Report

Level				Mean
12C	A			27.327082
11C	A	B		24.966743
10C		B		21.174636
12			C	16.817125
11M			C	16.459872
11			C	16.057617
12M			C	15.529173
10M			C	15.082682
10			C	14.779223

Levels not connected by same letter are significantly different.

Ordered Differences Report

Level	- Level	Difference	Std Err Dif	Lower CL	Upper CL	p-Value
12C	10	12.54786	1.318025	8.20936	16.88636	<.0001*
12C	10M	12.24440	1.318025	7.90590	16.58290	<.0001*
12C	12M	11.79791	1.236417	7.72803	15.86779	<.0001*
12C	11	11.26947	1.236417	7.19959	15.33934	<.0001*
12C	11M	10.86721	1.236417	6.79733	14.93709	<.0001*
12C	12	10.50996	1.236417	6.44008	14.57983	<.0001*
11C	10	10.18752	1.318025	5.84902	14.52602	<.0001*
11C	10M	9.88406	1.318025	5.54556	14.22257	<.0001*
11C	12M	9.43757	1.236417	5.36769	13.50745	<.0001*
11C	11	8.90913	1.236417	4.83925	12.97900	<.0001*
11C	11M	8.50687	1.236417	4.43699	12.57675	<.0001*
11C	12	8.14962	1.236417	4.07974	12.21950	<.0001*
10C	10	6.39541	1.318025	2.05691	10.73392	0.0007*
12C	10C	6.15245	1.178877	2.27197	10.03292	0.0002*
10C	10M	6.09195	1.318025	1.75345	10.43046	0.0013*
10C	12M	5.64546	1.236417	1.57559	9.71534	0.0016*
10C	11	5.11702	1.236417	1.04714	9.18690	0.0054*
10C	11M	4.71476	1.236417	0.64489	8.78464	0.0132*
10C	12	4.35751	1.236417	0.28763	8.42739	0.0281*
11C	10C	3.79211	1.178877	-0.08837	7.67258	0.0598
12C	11C	2.36034	1.178877	-1.52014	6.24082	0.5516
12	10	2.03790	1.369731	-2.47080	6.54661	0.8540
12	10M	1.73444	1.369731	-2.77426	6.24315	0.9348
11M	10	1.68065	1.369731	-2.82806	6.18936	0.9451
11M	10M	1.37719	1.369731	-3.13152	5.88590	0.9830
12	12M	1.28795	1.291395	-2.96290	5.53880	0.9838
11	10	1.27839	1.369731	-3.23031	5.78710	0.9894
11	10M	0.97493	1.369731	-3.53377	5.48364	0.9983
11M	12M	0.93070	1.291395	-3.32015	5.18155	0.9982
12	11	0.75951	1.291395	-3.49134	5.01036	0.9996
12M	10	0.74995	1.369731	-3.75876	5.25866	0.9997
11	12M	0.52844	1.291395	-3.72240	4.77929	1.0000
12M	10M	0.44649	1.369731	-4.06222	4.95520	1.0000
11M	11	0.40225	1.291395	-3.84859	4.65310	1.0000
12	11M	0.35725	1.291395	-3.89360	4.60810	1.0000
10M	10	0.30346	1.443824	-4.44913	5.05605	1.0000

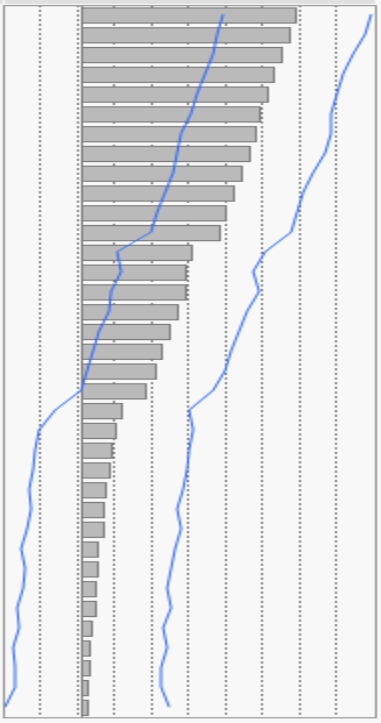

Appendix 78. Tukey HSD Charpy Impact result– Effect of weave on peak load of treated & untreated samples (warp direction)

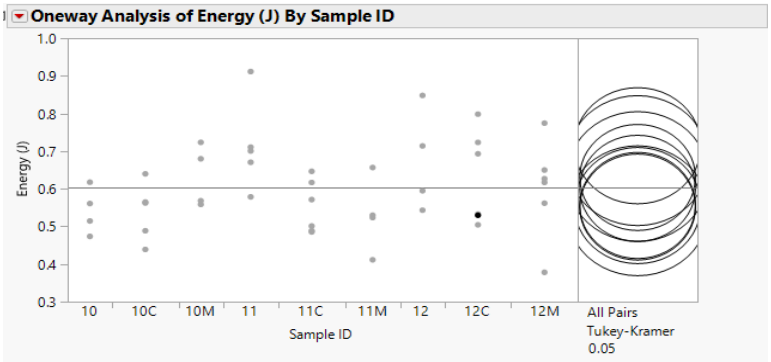

Means Comparisons

Comparisons for all pairs using Tukey-Kramer HSD

Connecting Letters Report

Level		Mean
11	A	0.71448000
12	A	0.67512500
10M	A	0.63262500
12C	A	0.63036667
12M	A	0.60145000
10C	A	0.55583333
11M	A	0.55564000
11C	A	0.55173333
10	A	0.54175000

Levels not connected by same letter are significantly different.

Ordered Differences Report

Level	- Level	Difference	Std Err Dif	Lower CL	Upper CL	p-Value
11	10	0.1727300	0.0703589	-0.058868	0.4043285	0.2862
11	11C	0.1627467	0.0635110	-0.046311	0.3718039	0.2368
11	11M	0.1588400	0.0663350	-0.059513	0.3771932	0.3167
11	10C	0.1586467	0.0635110	-0.050411	0.3677039	0.2657
12	10	0.1333750	0.0741648	-0.110751	0.3775012	0.6828
12	11C	0.1233917	0.0677029	-0.099464	0.3462474	0.6676
12	11M	0.1194850	0.0703589	-0.112113	0.3510835	0.7437
12	10C	0.1192917	0.0677029	-0.103564	0.3421474	0.7054
11	12M	0.1130300	0.0635110	-0.096027	0.3220872	0.6945
10M	10	0.0908750	0.0741648	-0.153251	0.3350012	0.9455
12C	10	0.0886167	0.0677029	-0.134239	0.3114724	0.9223
11	12C	0.0841133	0.0635110	-0.124944	0.2931706	0.9174
11	10M	0.0818550	0.0703589	-0.149743	0.3134535	0.9593
10M	11C	0.0808917	0.0677029	-0.141964	0.3037474	0.9526
12C	11C	0.0786333	0.0605553	-0.120695	0.2779616	0.9255
10M	11M	0.0769850	0.0703589	-0.154613	0.3085835	0.9715
10M	10C	0.0767917	0.0677029	-0.146064	0.2996474	0.9648
12C	11M	0.0747267	0.0635110	-0.134331	0.2837839	0.9566
12C	10C	0.0745333	0.0605553	-0.124795	0.2738616	0.9441
12	12M	0.0736750	0.0677029	-0.149181	0.2965308	0.9724
12M	10	0.0597000	0.0677029	-0.163156	0.2825558	0.9927
12M	11C	0.0497167	0.0605553	-0.149612	0.2490449	0.9955
12M	11M	0.0458100	0.0635110	-0.163247	0.2548672	0.9981
12M	10C	0.0456167	0.0605553	-0.153712	0.2449449	0.9975
12	12C	0.0447583	0.0677029	-0.178097	0.2676141	0.9990
12	10M	0.0425000	0.0741648	-0.201626	0.2866262	0.9996
11	12	0.0393550	0.0703589	-0.192243	0.2709535	0.9997
10M	12M	0.0311750	0.0677029	-0.191681	0.2540308	0.9999
12C	12M	0.0289167	0.0605553	-0.170412	0.2282449	0.9999
10C	10	0.0140833	0.0677029	-0.208772	0.2369391	1.0000
11M	10	0.0138900	0.0703589	-0.217708	0.2454885	1.0000
11C	10	0.0099833	0.0677029	-0.212872	0.2328391	1.0000
10C	11C	0.0041000	0.0605553	-0.195228	0.2034282	1.0000
11M	11C	0.0039067	0.0635110	-0.205151	0.2129639	1.0000
10M	12C	0.0022583	0.0677029	-0.220597	0.2251141	1.0000
10C	11M	0.0001933	0.0635110	-0.208864	0.2092506	1.0000

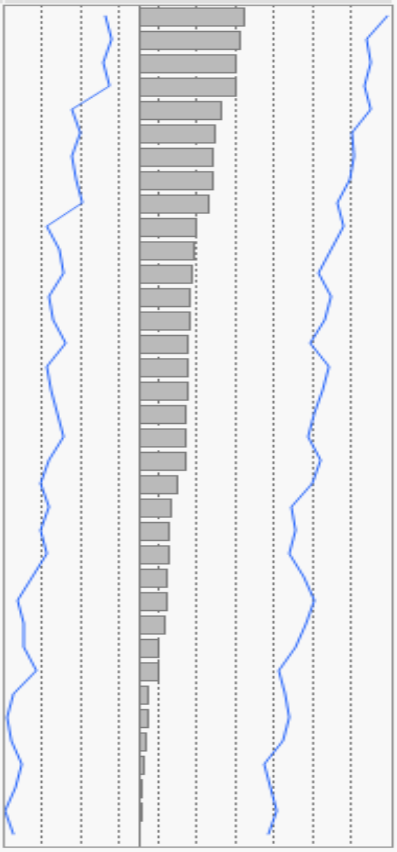

Appendix 79. Tukey HSD Charpy Impact result– Effect of weave on peak load of treated & untreated samples (weft direction)

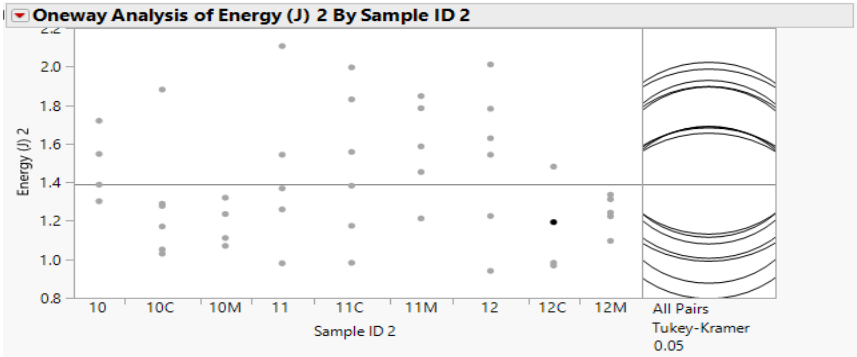

Means Comparisons

Comparisons for all pairs using Tukey-Kramer HSD

Connecting Letters Report

Level		Mean
11M	A	1.5765600
12	A	1.5214167
10	A	1.4887500
11C	A	1.4870333
11	A	1.4512600
10C	A	1.2830333
12M	A	1.2419800
10M	A	1.1839500
12C	A	1.1560750

Levels not connected by same letter are significantly different.

Ordered Differences Report

Level	- Level	Difference	Std Err Dif	Lower CL	Upper CL	p-Value
11M	12C	0.4204850	0.2029472	-0.248652	1.089622	0.5069
11M	10M	0.3926100	0.2029472	-0.276527	1.061747	0.5957
12	12C	0.3653417	0.1952861	-0.278535	1.009219	0.6369
12	10M	0.3374667	0.1952861	-0.306410	0.981344	0.7259
11M	12M	0.3345800	0.1913405	-0.296288	0.965448	0.7135
10	12C	0.3326750	0.2139252	-0.372657	1.038007	0.8217
11C	12C	0.3309583	0.1952861	-0.312919	0.974835	0.7456
10	10M	0.3048000	0.2139252	-0.400532	1.010132	0.8807
11C	10M	0.3030833	0.1952861	-0.340794	0.946960	0.8232
11	12C	0.2951850	0.2029472	-0.373952	0.964322	0.8684
11M	10C	0.2935267	0.1831946	-0.310484	0.897537	0.7973
12	12M	0.2794367	0.1831946	-0.324574	0.883447	0.8363
11	10M	0.2673100	0.2029472	-0.401827	0.936447	0.9195
10	12M	0.2467700	0.2029472	-0.422367	0.915907	0.9476
11C	12M	0.2450533	0.1831946	-0.358957	0.849064	0.9129
12	10C	0.2383833	0.1746692	-0.337518	0.814284	0.9035
11	12M	0.2092800	0.1913405	-0.421588	0.840148	0.9715
10	10C	0.2057167	0.1952861	-0.438160	0.849594	0.9772
11C	10C	0.2040000	0.1746692	-0.371901	0.779901	0.9582
11	10C	0.1682267	0.1831946	-0.435784	0.772237	0.9904
10C	12C	0.1269583	0.1952861	-0.516919	0.770835	0.9991
11M	11	0.1253000	0.1913405	-0.505568	0.756168	0.9991
10C	10M	0.0990833	0.1952861	-0.544794	0.742960	0.9999
11M	11C	0.0895267	0.1831946	-0.514484	0.693537	0.9999
11M	10	0.0878100	0.2029472	-0.581327	0.756947	1.0000
12M	12C	0.0859050	0.2029472	-0.583232	0.755042	1.0000
12	11	0.0701567	0.1831946	-0.533854	0.674167	1.0000
12M	10M	0.0580300	0.2029472	-0.611107	0.727167	1.0000
11M	12	0.0551433	0.1831946	-0.548867	0.659154	1.0000
10C	12M	0.0410533	0.1831946	-0.562957	0.645064	1.0000
10	11	0.0374900	0.2029472	-0.631647	0.706627	1.0000
11C	11	0.0357733	0.1831946	-0.568237	0.639784	1.0000
12	11C	0.0343833	0.1746692	-0.541518	0.610284	1.0000
12	10	0.0326667	0.1952861	-0.611210	0.676544	1.0000
10M	12C	0.0278750	0.2139252	-0.677457	0.733207	1.0000
10	11C	0.0017167	0.1952861	-0.642160	0.645594	1.0000

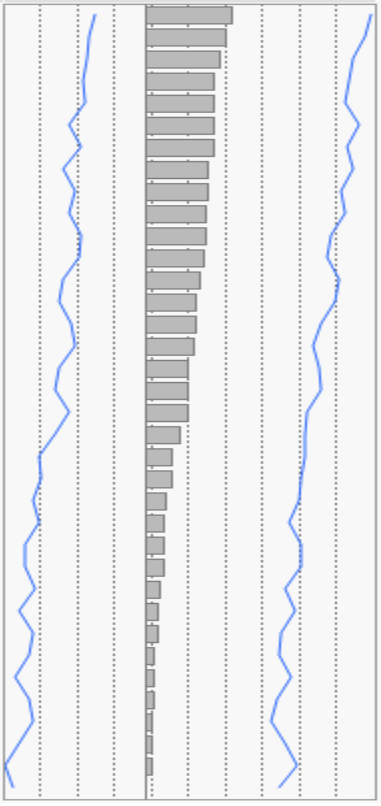

Appendix 80. Tukey HSD Compression result– Effect of weave on peak load of treated & untreated samples (warp direction)

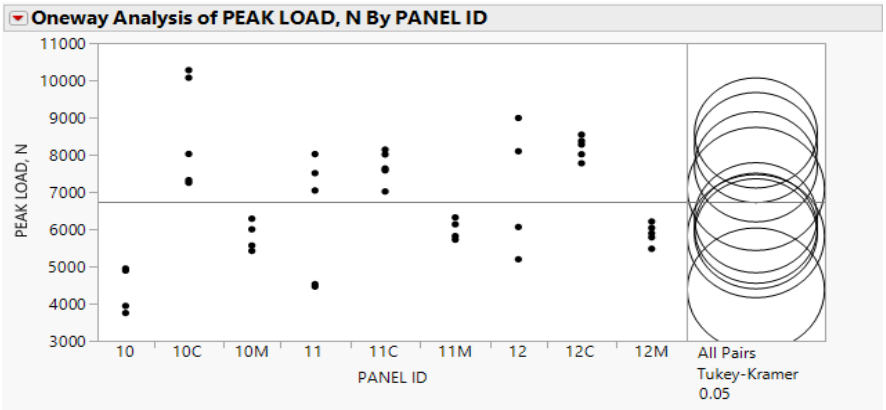

Means Comparisons

Comparisons for all pairs using Tukey-Kramer HSD

Connecting Letters Report

Level					Mean
10C	A				8586.9766
12C	A	B			8195.0667
11C	A	B	C		7675.4610
12	A	B	C		7084.3235
11		B	C	D	6310.3308
11M			C	D	6026.5109
12M			C	D	5878.5958
10M			C	D	5815.3248
10				D	4380.7776

Levels not connected by same letter are significantly different.

Ordered Differences Report

Level	- Level	Difference	Std Err Dif	Lower CL	Upper CL	p-Value
10C	10	4206.199	669.6210	1986.13	6426.265	<.0001*
12C	10	3814.289	669.6210	1594.22	6034.356	<.0001*
11C	10	3294.683	669.6210	1074.62	5514.750	0.0007*
10C	10M	2771.652	669.6210	551.59	4991.718	0.0062*
10C	12M	2708.381	631.3248	615.28	4801.480	0.0041*
12	10	2703.546	705.8425	363.39	5043.701	0.0140*
10C	11M	2560.466	631.3248	467.37	4653.564	0.0077*
12C	10M	2379.742	669.6210	159.68	4599.808	0.0281*
12C	12M	2316.471	631.3248	223.37	4409.570	0.0211*
10C	11	2276.646	631.3248	183.55	4369.745	0.0247*
12C	11M	2168.556	631.3248	75.46	4261.655	0.0376*
11	10	1929.553	669.6210	-290.51	4149.620	0.1303
12C	11	1884.736	631.3248	-208.36	3977.835	0.1049
11C	10M	1860.136	669.6210	-359.93	4080.203	0.1606
11C	12M	1796.865	631.3248	-296.23	3889.964	0.1401
11C	11M	1648.950	631.3248	-444.15	3742.049	0.2201
11M	10	1645.733	669.6210	-574.33	3865.800	0.2883
10C	12	1502.653	669.6210	-717.41	3722.720	0.4028
12M	10	1497.818	669.6210	-722.25	3717.885	0.4070
10M	10	1434.547	705.8425	-905.61	3774.703	0.5333
11C	11	1365.130	631.3248	-727.97	3458.229	0.4516
12	10M	1268.999	705.8425	-1071.16	3609.154	0.6831
12	12M	1205.728	669.6210	-1014.34	3425.794	0.6814
12C	12	1110.743	669.6210	-1109.32	3330.810	0.7659
12	11M	1057.813	669.6210	-1162.25	3277.879	0.8086
10C	11C	911.516	631.3248	-1181.58	3004.614	0.8723
12	11	773.993	669.6210	-1446.07	2994.059	0.9602
11C	12	591.138	669.6210	-1628.93	2811.204	0.9925
12C	11C	519.606	631.3248	-1573.49	2612.704	0.9953
11	10M	495.006	669.6210	-1725.06	2715.072	0.9977
11	12M	431.735	631.3248	-1661.36	2524.834	0.9987
10C	12C	391.910	631.3248	-1701.19	2485.009	0.9993
11	11M	283.820	631.3248	-1809.28	2376.919	0.9999
11M	10M	211.186	669.6210	-2008.88	2431.253	1.0000
11M	12M	147.915	631.3248	-1945.18	2241.014	1.0000
12M	10M	63.271	669.6210	-2156.80	2283.337	1.0000

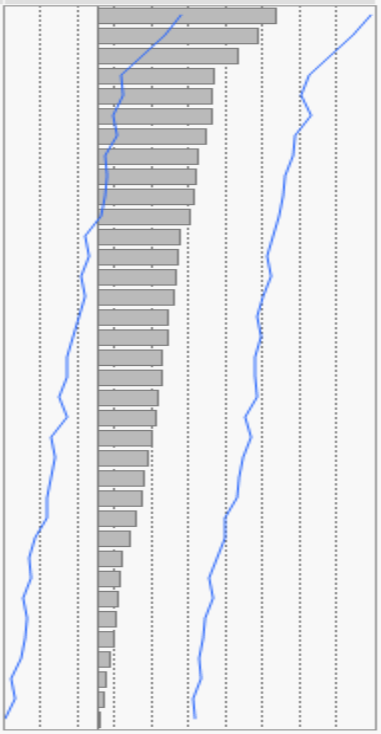

Appendix 81. Tukey HSD Compression result– Effect of weave on peak load of treated & untreated samples (warp direction)

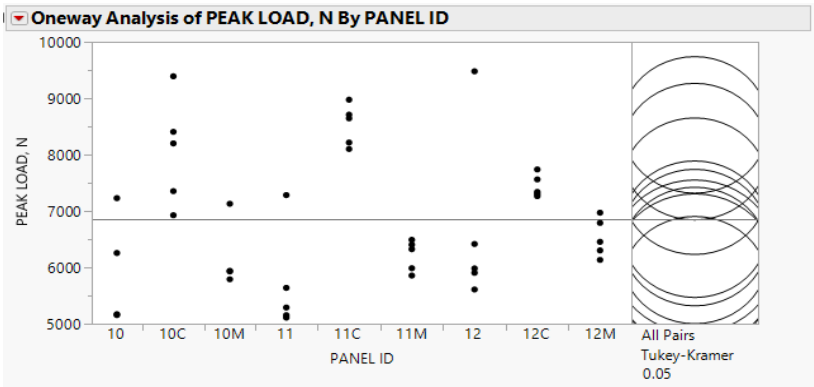

Means Comparisons

Comparisons for all pairs using Tukey-Kramer HSD

Connecting Letters Report

Level					Mean
11C	A				8528.9700
10C	A	B			8055.1933
12C	A	B	C		7441.4390
12		B	C	D	6678.3376
12M		B	C	D	6529.9565
11M			C	D	6212.0050
10M			C	D	6197.3850
10			C	D	5952.8676
11				D	5694.5180

Levels not connected by same letter are significantly different.

Ordered Differences Report

Level	- Level	Difference	Std Err Dif	Lower CL	Upper CL	p-Value
11C	11	2834.452	517.6248	1121.67	4547.238	0.0001*
11C	10	2576.102	549.0240	759.42	4392.787	0.0013*
10C	11	2360.675	517.6248	647.89	4073.462	0.0018*
11C	10M	2331.585	549.0240	514.90	4148.269	0.0044*
11C	11M	2316.965	517.6248	604.18	4029.751	0.0023*
10C	10	2102.326	549.0240	285.64	3919.010	0.0136*
11C	12M	1999.014	517.6248	286.23	3711.800	0.0125*
10C	10M	1857.808	549.0240	41.12	3674.493	0.0418*
11C	12	1850.632	517.6248	137.85	3563.419	0.0261*
10C	11M	1843.188	517.6248	130.40	3555.975	0.0271*
12C	11	1746.921	517.6248	34.13	3459.707	0.0427*
10C	12M	1525.237	517.6248	-187.55	3238.023	0.1128
12C	10	1488.571	549.0240	-328.11	3305.256	0.1817
10C	12	1376.856	517.6248	-335.93	3089.642	0.2003
12C	10M	1244.054	549.0240	-572.63	3060.738	0.3894
12C	11M	1229.434	517.6248	-483.35	2942.220	0.3291
11C	12C	1087.531	517.6248	-625.26	2800.317	0.4892
12	11	983.820	517.6248	-728.97	2696.606	0.6179
12C	12M	911.483	517.6248	-801.30	2624.269	0.7059
12M	11	835.438	517.6248	-877.35	2548.225	0.7907
12C	12	763.101	517.6248	-949.69	2475.888	0.8594
12	10	725.470	549.0240	-1091.21	2542.154	0.9178
10C	12C	613.754	517.6248	-1099.03	2326.541	0.9542
12M	10	577.089	549.0240	-1239.60	2393.773	0.9774
11M	11	517.487	517.6248	-1195.30	2230.273	0.9834
10M	11	502.867	549.0240	-1313.82	2319.551	0.9905
12	10M	480.953	549.0240	-1335.73	2297.637	0.9929
11C	10C	473.777	517.6248	-1239.01	2186.563	0.9905
12	11M	466.333	517.6248	-1246.45	2179.119	0.9914
12M	10M	332.571	549.0240	-1484.11	2149.256	0.9995
12M	11M	317.951	517.6248	-1394.83	2030.738	0.9994
11M	10	259.137	549.0240	-1557.55	2075.822	0.9999
10	11	258.350	549.0240	-1558.33	2075.034	0.9999
10M	10	244.517	578.7221	-1670.44	2159.471	1.0000
12	12M	148.381	517.6248	-1564.41	1861.168	1.0000
11M	10M	14.620	549.0240	-1802.06	1831.304	1.0000

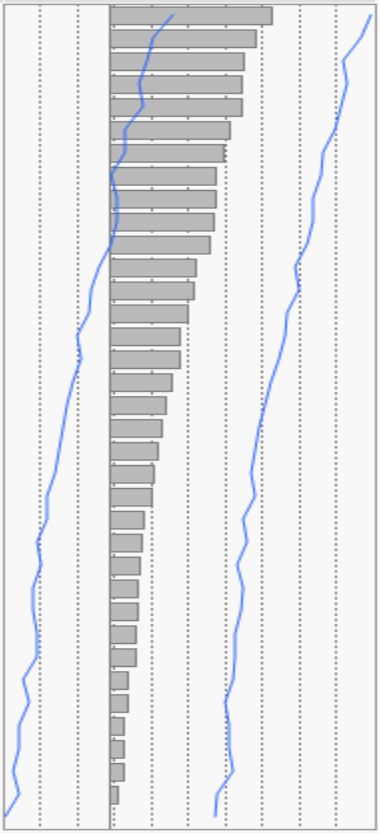

Appendix 82. Compression – warp and weft (treated)

Oneway Analysis of PEAK LOAD, N By PANEL ID

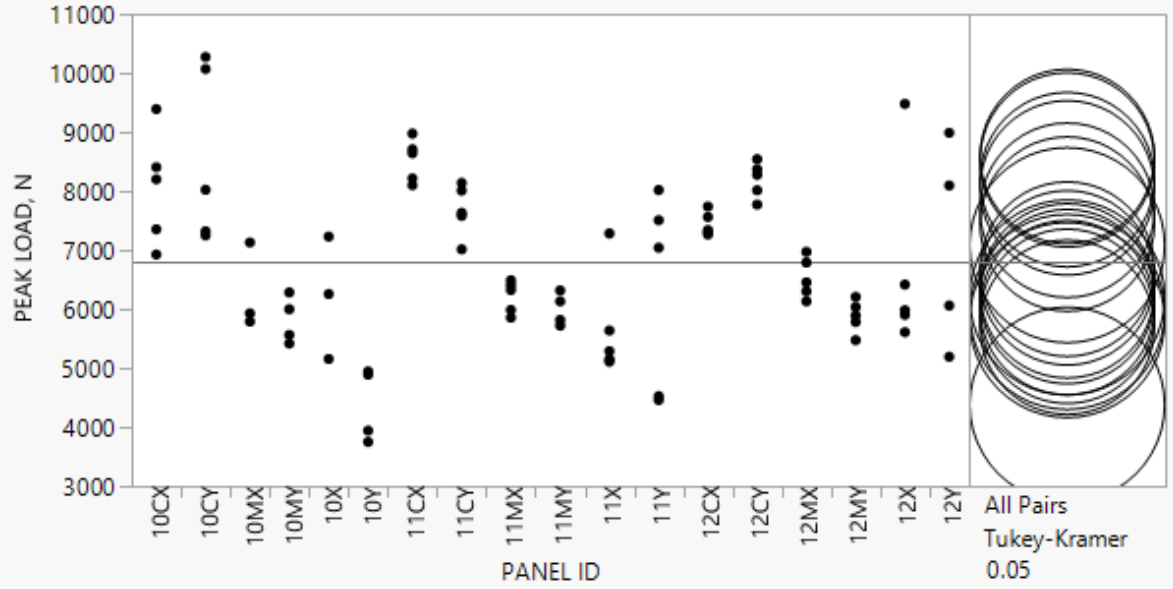

Means Comparisons

Comparisons for all pairs using Tukey-Kramer HSD

Connecting Letters Report

Level						Mean
10CY	A					8586.9766
11CX	A					8528.9700
12CY	A	B				8195.0667
10CX	A	B	C			8055.1933
11CY	A	B	C	D		7675.4610
12CX	A	B	C	D		7441.4390
12Y	A	B	C	D		7084.3235
12X	A	B	C	D		6678.3376
12MX	A	B	C	D	E	6529.9565
11Y		B	C	D	E	6310.3308
11MX		B	C	D	E	6212.0050
10MX		B	C	D	E	6197.3850
11MY			C	D	E	6026.5109
10X			C	D	E	5952.8676
12MY				D	E	5878.5958
10MY				D	E	5815.3248
11X				D	E	5694.5180
10Y					E	4380.7776

Levels not connected by same letter are significantly different.

Appendix 83. Comparision of X-, Y- and Z-yarn tenacity (Data provided by Hadir Eldeeb, NCSU)

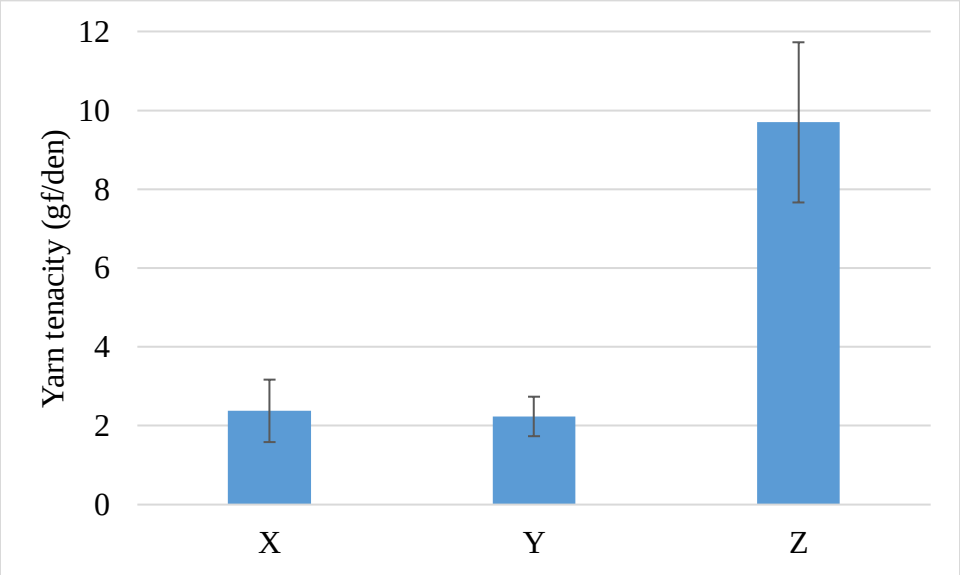

Appendix 84. Specimens after tup impact test

Appendix 85. Specimens after combined loading compression (CLC) test

Appendix 86. Test result from tensile test

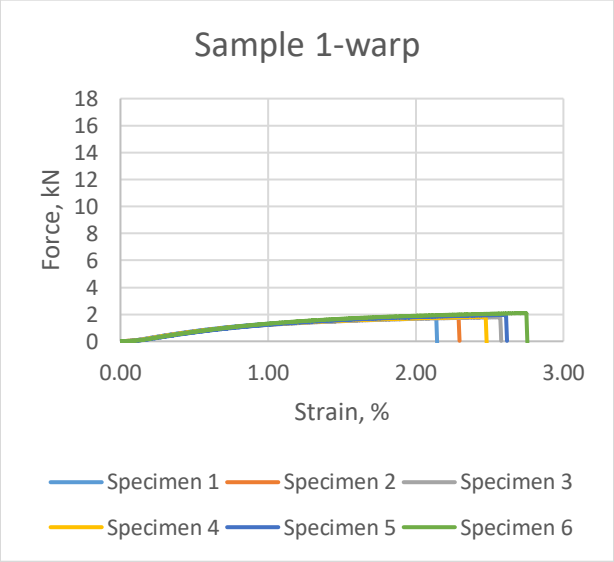

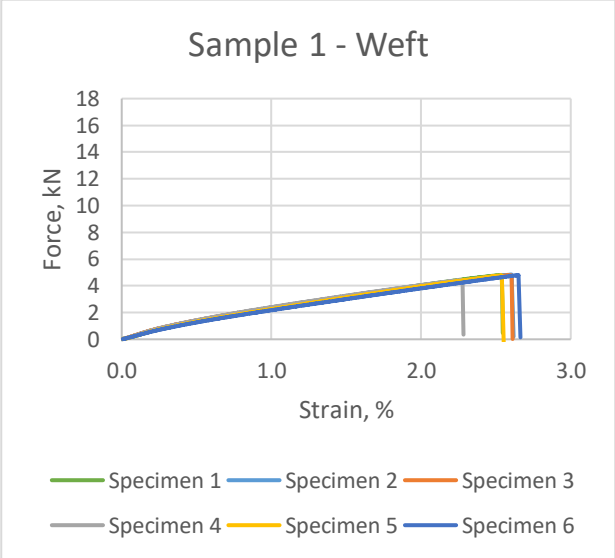

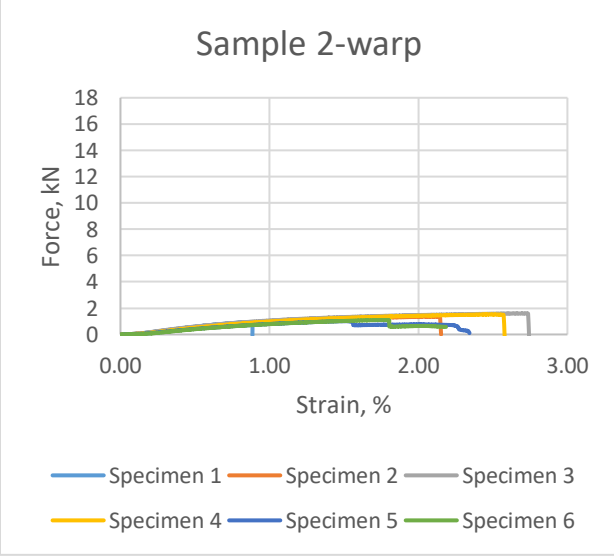

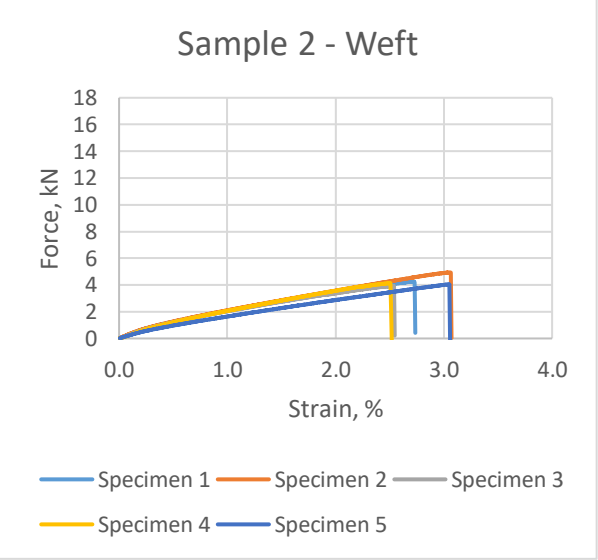

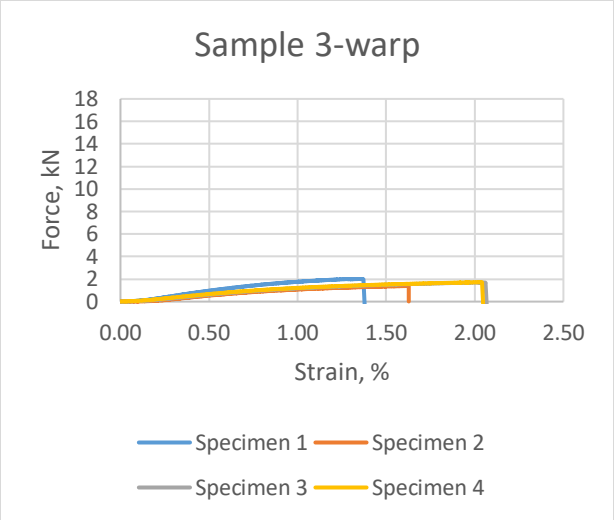
Sample 3-warp
Force, kN
Strain, %
Specimen 1
Specimen 2
Specimen 3
Specimen 4

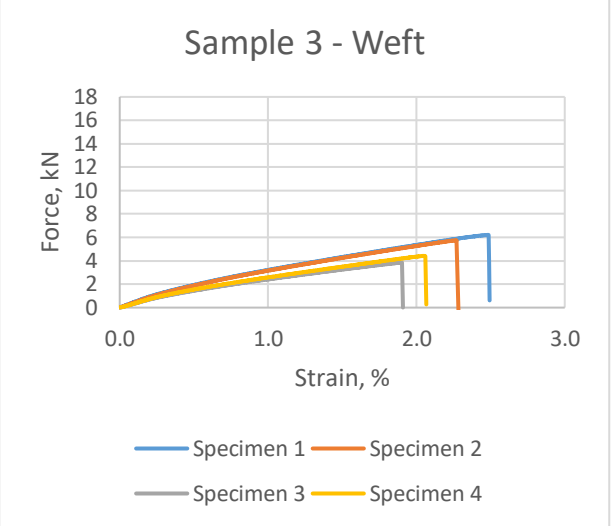
Sample 3 - Weft
Force, kN
Strain, %
Specimen 1
Specimen 2
Specimen 3
Specimen 4

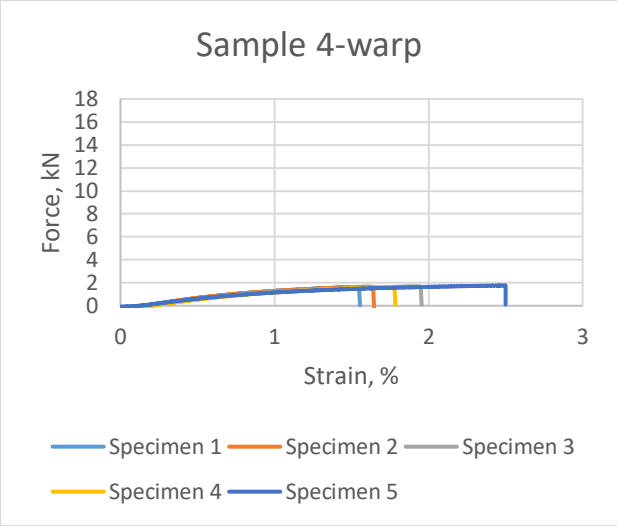
Sample 4-warp
Force, kN
Strain, %
Specimen 1
Specimen 2
Specimen 3
Specimen 4
Specimen 5

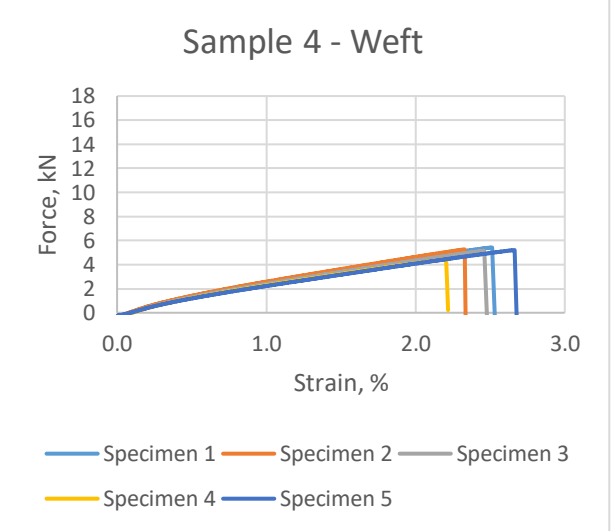
Sample 4 - Weft
Force, kN
Strain, %
Specimen 1
Specimen 2
Specimen 3
Specimen 4
Specimen 5

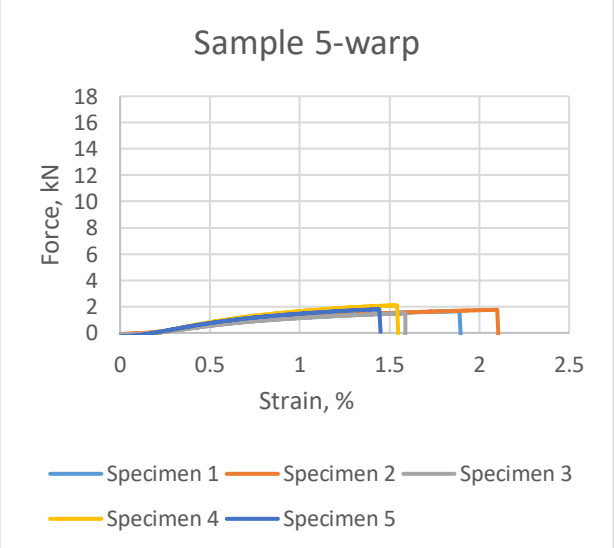
Sample 5-warp
Force, kN
Strain, %
Specimen 1
Specimen 2
Specimen 3
Specimen 4
Specimen 5

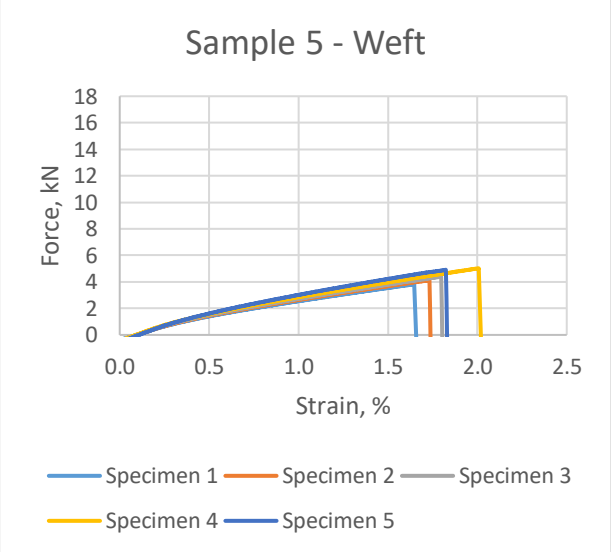
Sample 5 - Weft
Force, kN
Strain, %
Specimen 1
Specimen 2
Specimen 3
Specimen 4
Specimen 5

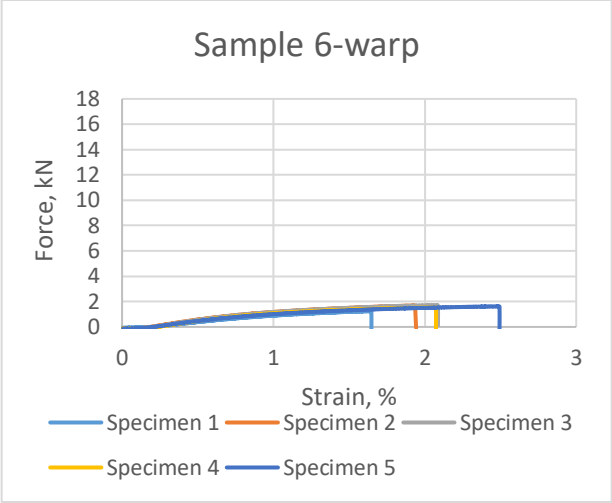
Sample 6-warp
Force, kN
Strain, %
Specimen 1
Specimen 2
Specimen 3
Specimen 4
Specimen 5

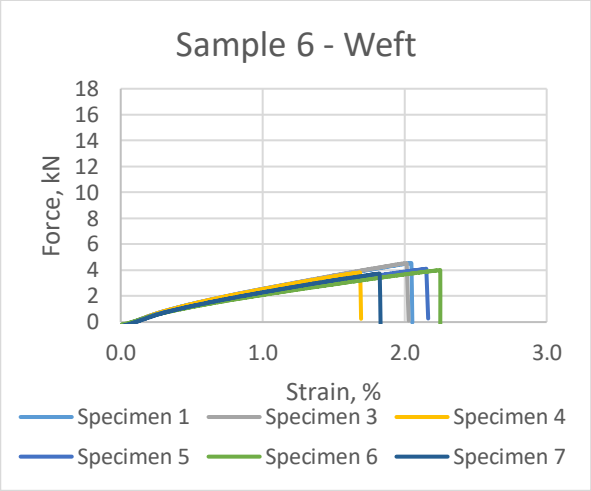
Sample 6 - Weft
Force, kN
Strain, %
Specimen 1
Specimen 3
Specimen 4
Specimen 5
Specimen 6
Specimen 7

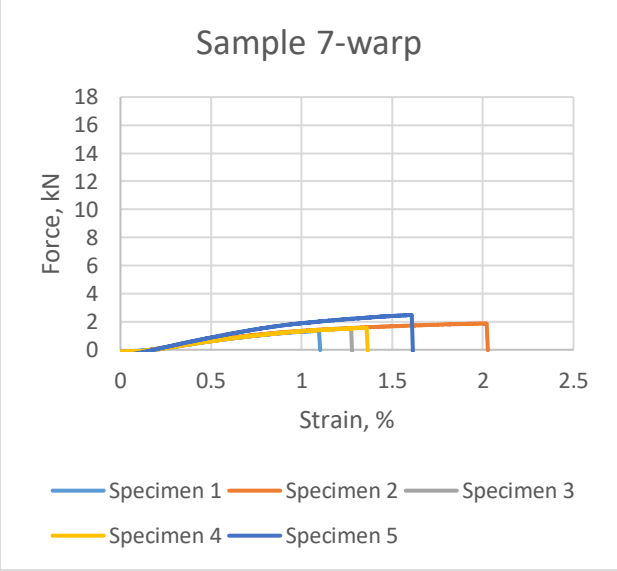
Sample 7-warp
Force, kN
Strain, %
Specimen 1
Specimen 2
Specimen 3
Specimen 4
Specimen 5

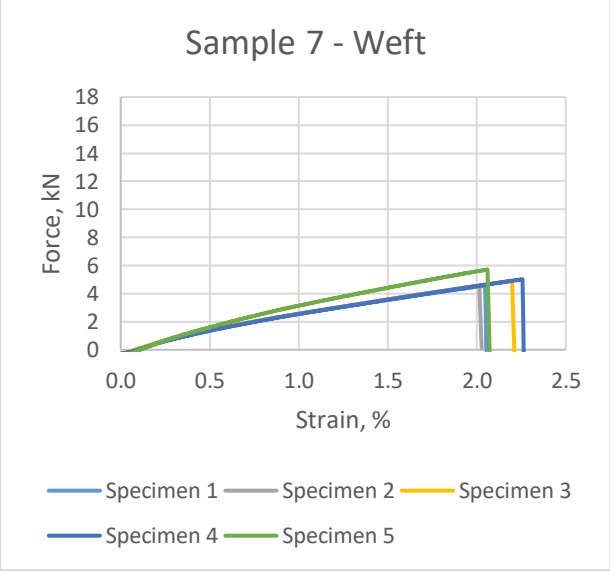
Sample 7 - Weft
Force, kN
Strain, %
Specimen 1
Specimen 2
Specimen 3
Specimen 4
Specimen 5

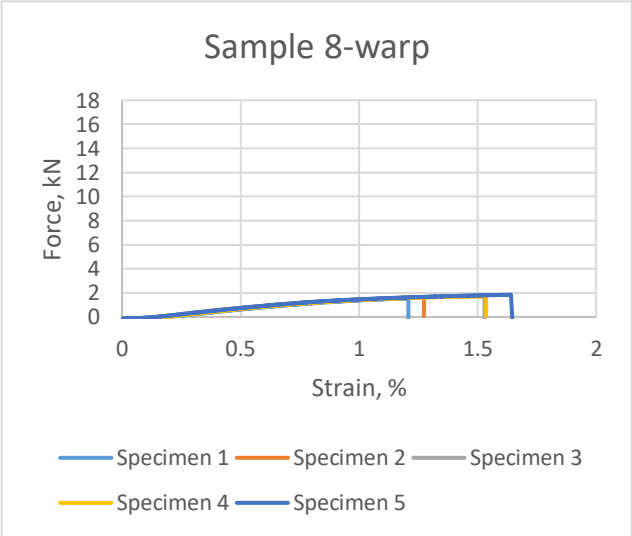
Sample 8-warp
Force, kN
Strain, %
Specimen 1
Specimen 2
Specimen 3
Specimen 4
Specimen 5

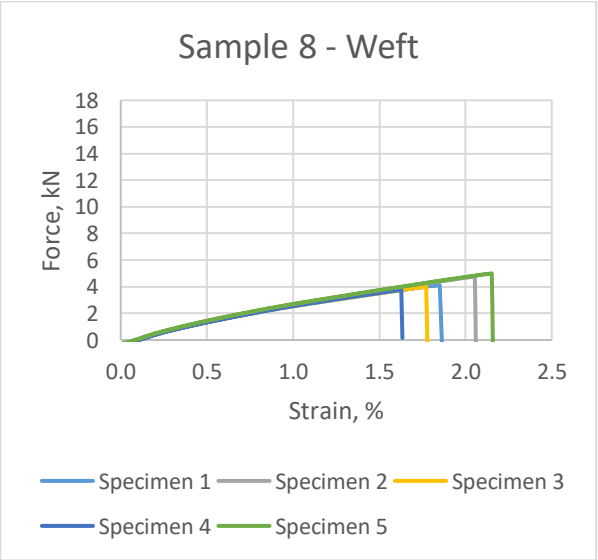
Sample 8 - Weft
Force, kN
Strain, %
Specimen 1
Specimen 2
Specimen 3
Specimen 4
Specimen 5

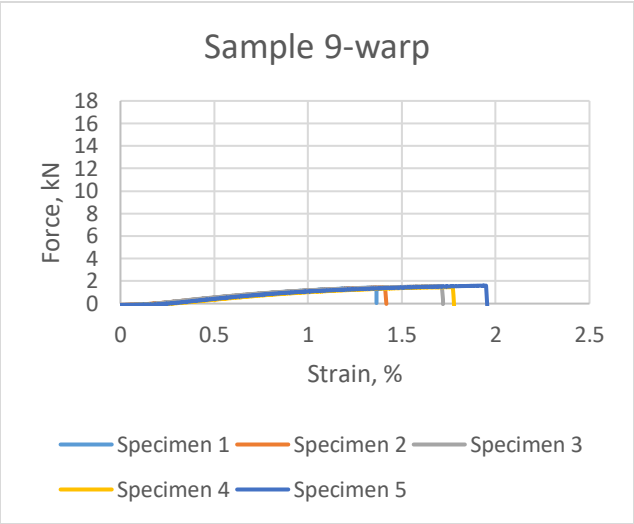
Sample 9-warp
Force, kN
Strain, %
Specimen 1
Specimen 2
Specimen 3
Specimen 4
Specimen 5

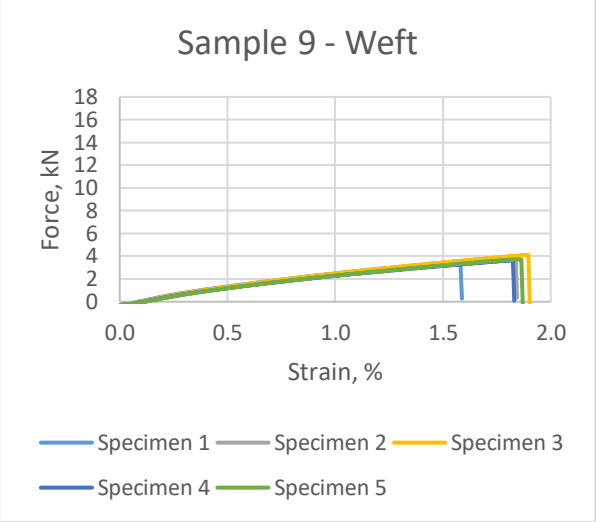
Sample 9 - Weft
Force, kN
Strain, %
Specimen 1
Specimen 2
Specimen 3
Specimen 4
Specimen 5

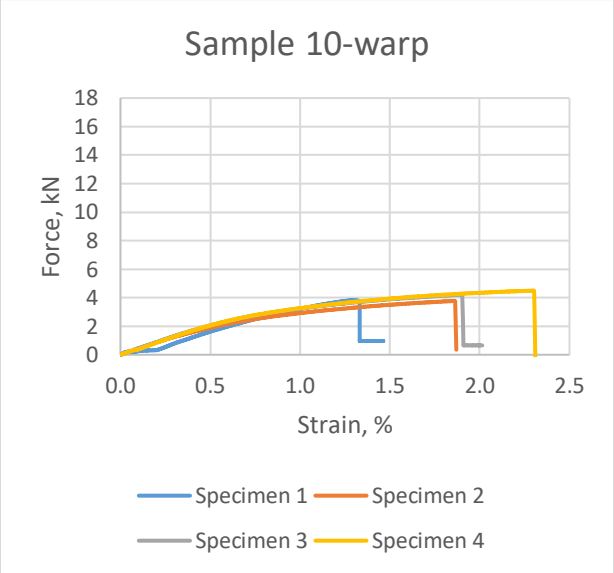
Sample 10-warp
Force, kN
Strain, %
Specimen 1
Specimen 2
Specimen 3
Specimen 4

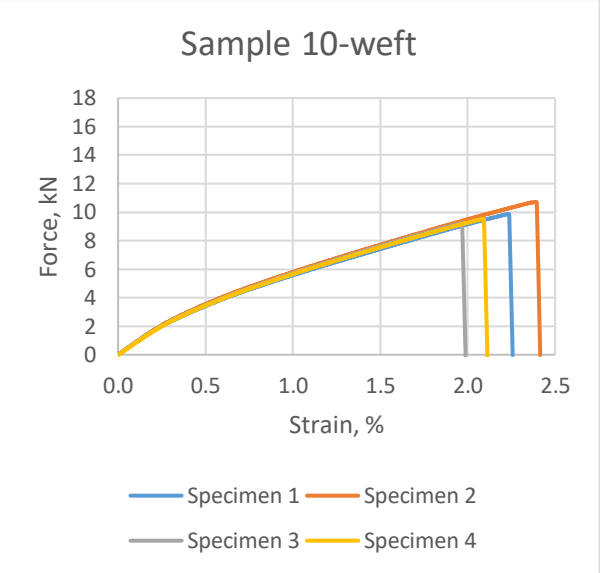
Sample 10-weft
Force, kN
Strain, %
Specimen 1
Specimen 2
Specimen 3
Specimen 4

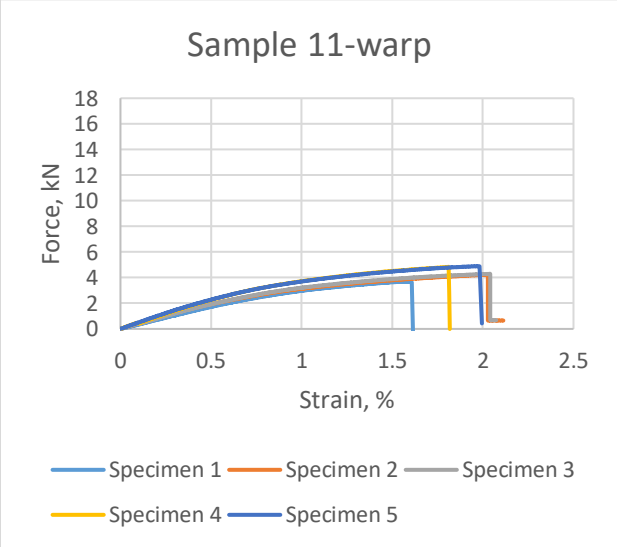
Sample 11-warp
Force, kN
Strain, %
Specimen 1
Specimen 2
Specimen 3
Specimen 4
Specimen 5

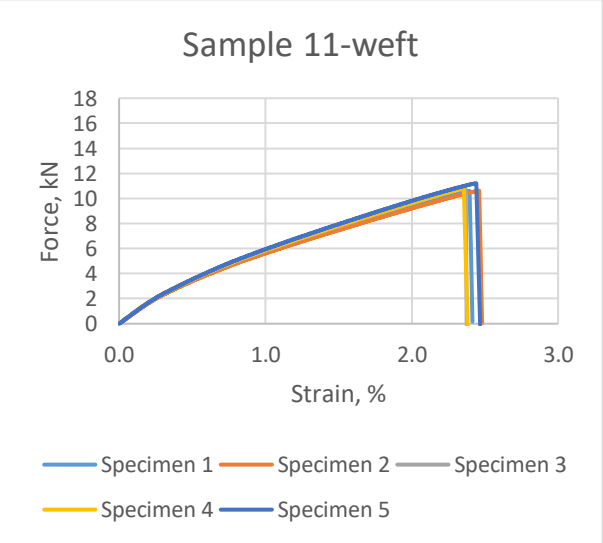
Sample 11-weft
Force, kN
Strain, %
Specimen 1
Specimen 2
Specimen 3
Specimen 4
Specimen 5

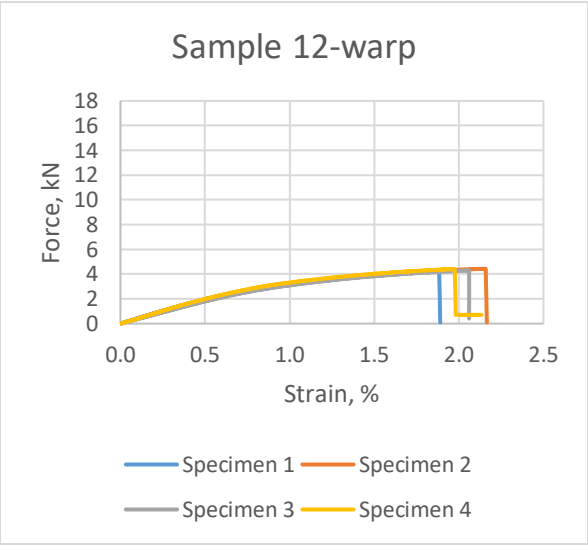
Sample 12-warp
Force, kN
Strain, %
Specimen 1
Specimen 2
Specimen 3
Specimen 4

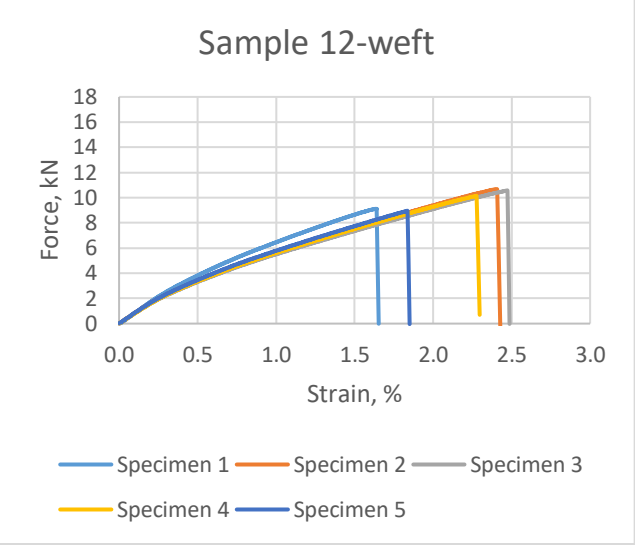
Sample 12-weft
Force, kN
Strain, %
Specimen 1
Specimen 2
Specimen 3
Specimen 4
Specimen 5

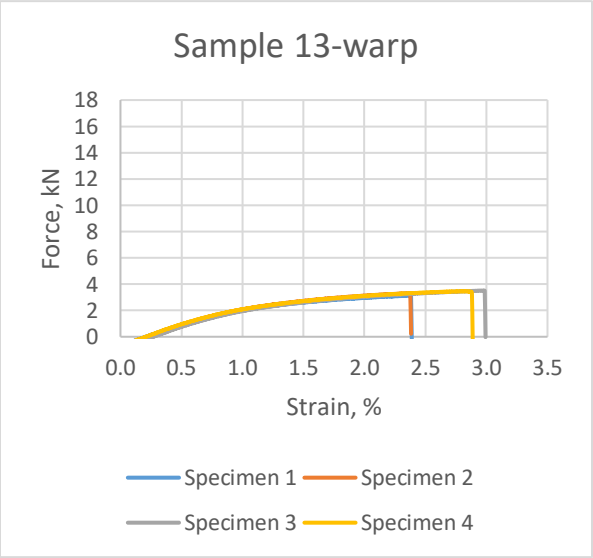
Sample 13-warp
Force, kN
Strain, %
Specimen 1
Specimen 2
Specimen 3
Specimen 4

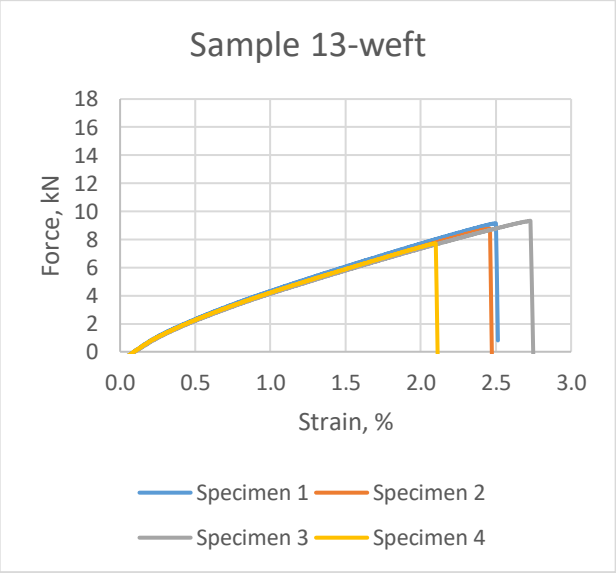
Sample 13-weft
Force, kN
Strain, %
Specimen 1
Specimen 2
Specimen 3
Specimen 4

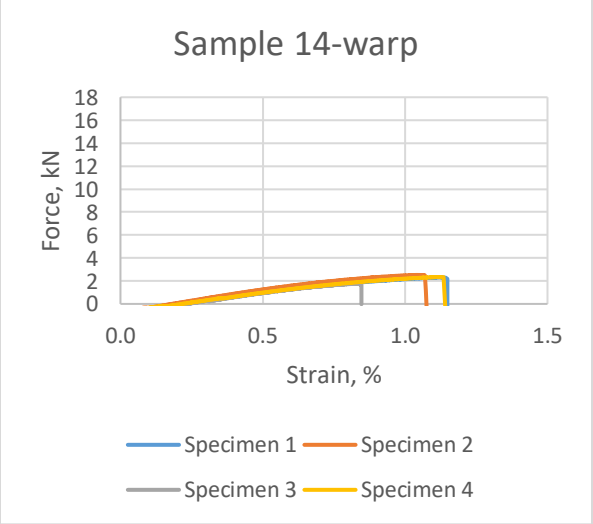
Sample 14-warp
Force, kN
Strain, %
Specimen 1
Specimen 2
Specimen 3
Specimen 4

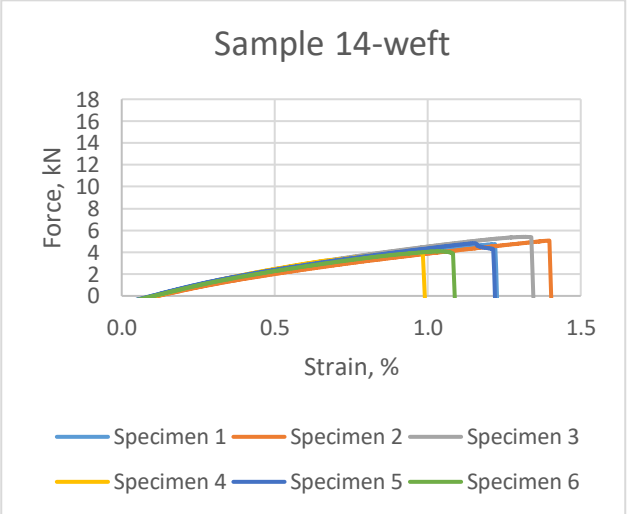
Sample 14-weft
Force, kN
Strain, %
Specimen 1
Specimen 2
Specimen 3
Specimen 4
Specimen 5
Specimen 6

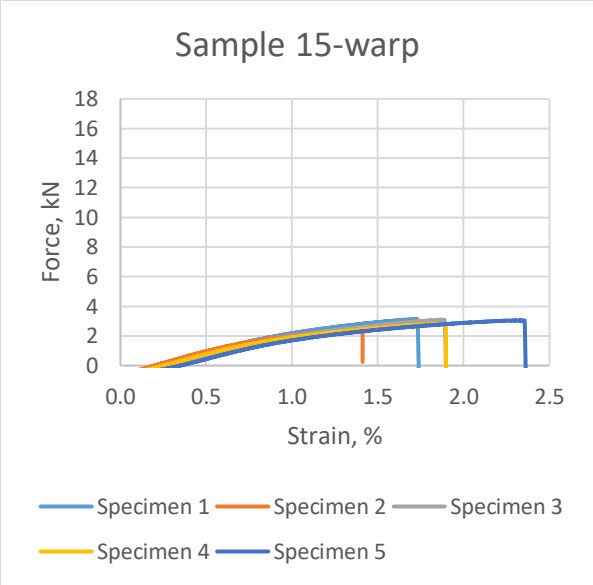
Sample 15-warp
Force, kN
Strain, %
Specimen 1
Specimen 2
Specimen 3
Specimen 4
Specimen 5

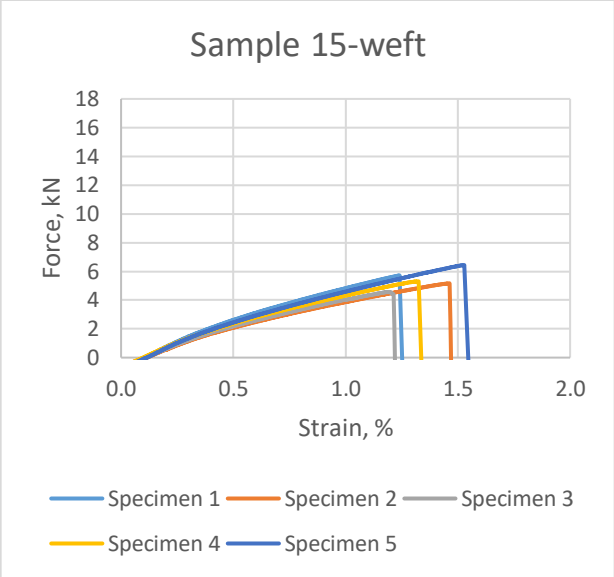
Sample 15-weft
Force, kN
Strain, %
Specimen 1
Specimen 2
Specimen 3
Specimen 4
Specimen 5

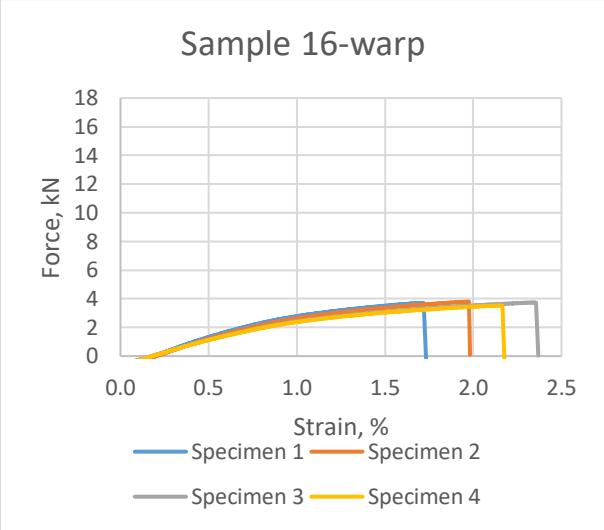
Sample 16-warp
Force, kN
Strain, %
Specimen 1
Specimen 2
Specimen 3
Specimen 4

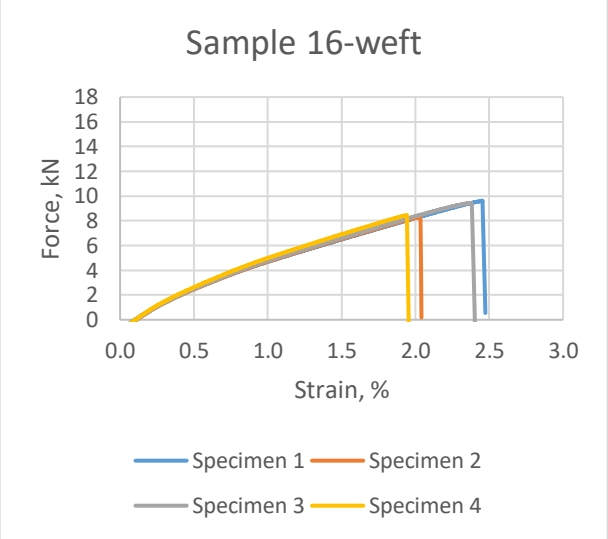
Sample 16-weft
Force, kN
Strain, %
Specimen 1
Specimen 2
Specimen 3
Specimen 4

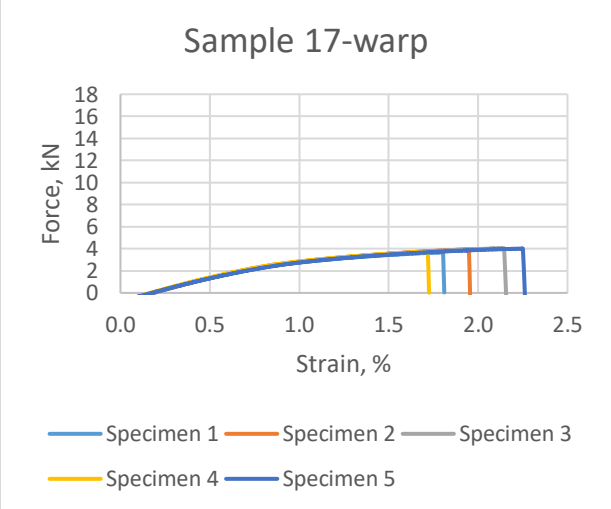
Sample 17-warp
Force, kN
Strain, %
Specimen 1
Specimen 2
Specimen 3
Specimen 4
Specimen 5

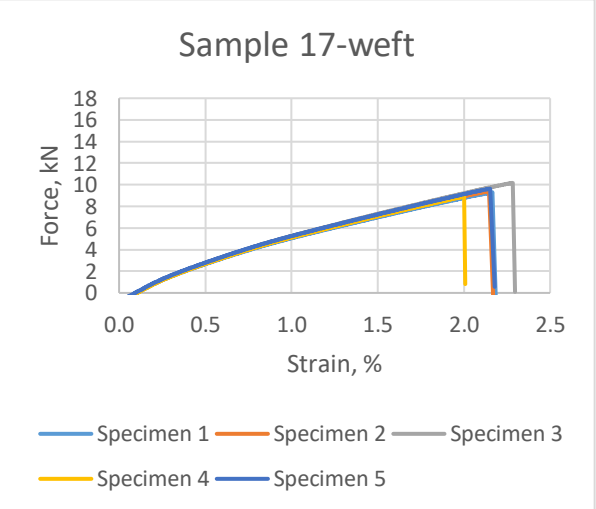
Sample 17-weft
Force, kN
Strain, %
Specimen 1
Specimen 2
Specimen 3
Specimen 4
Specimen 5

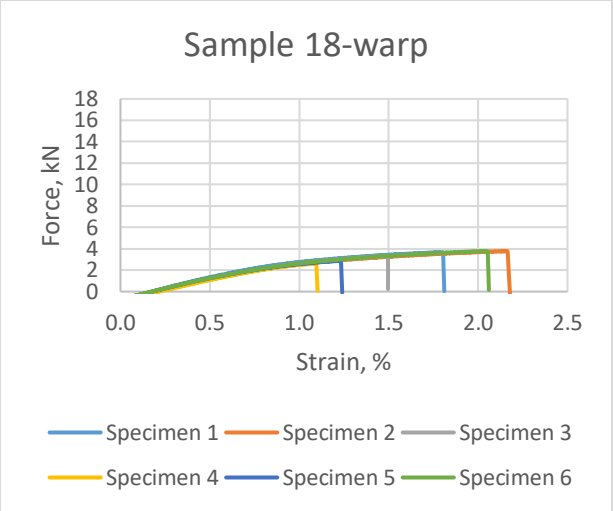
Sample 18-warp
Force, kN
Strain, %
Specimen 1
Specimen 2
Specimen 3
Specimen 4
Specimen 5
Specimen 6

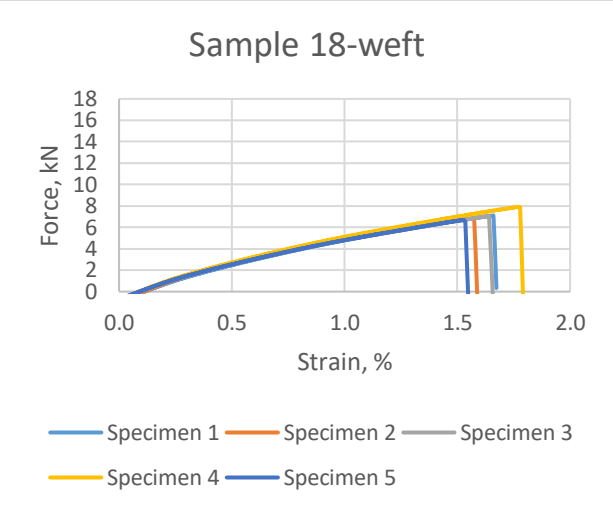
Sample 18-weft
Force, kN
Strain, %
Specimen 1
Specimen 2
Specimen 3
Specimen 4
Specimen 5

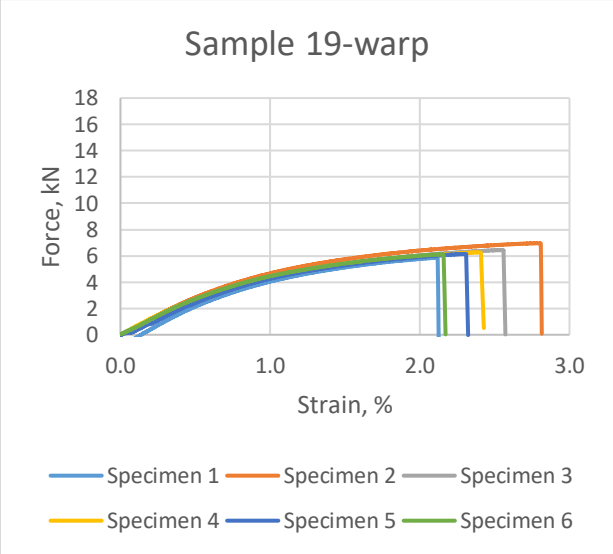
Sample 19-warp
Force, kN
Strain, %
Specimen 1
Specimen 2
Specimen 3
Specimen 4
Specimen 5
Specimen 6

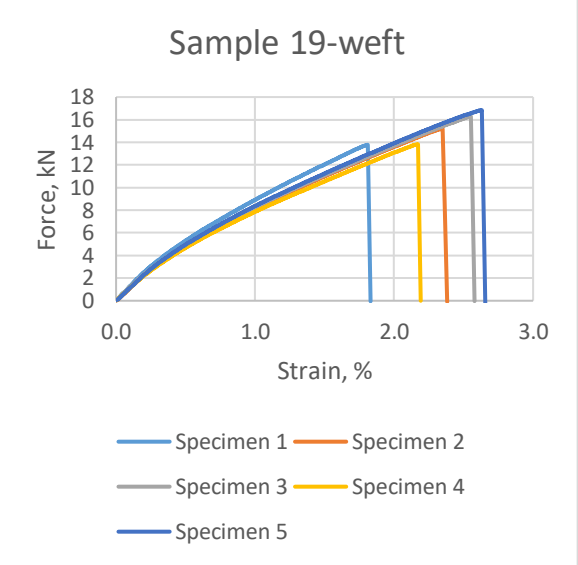
Sample 19-weft
Force, kN
Strain, %
Specimen 1
Specimen 2
Specimen 3
Specimen 4
Specimen 5

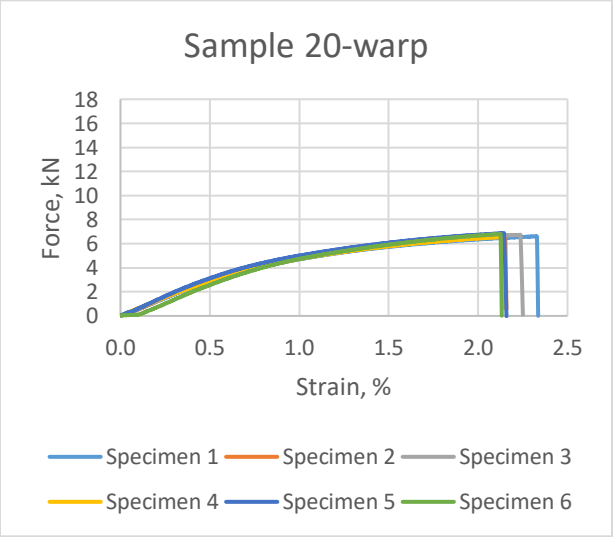
Sample 20-warp
Force, kN
Strain, %
Specimen 1
Specimen 2
Specimen 3
Specimen 4
Specimen 5
Specimen 6

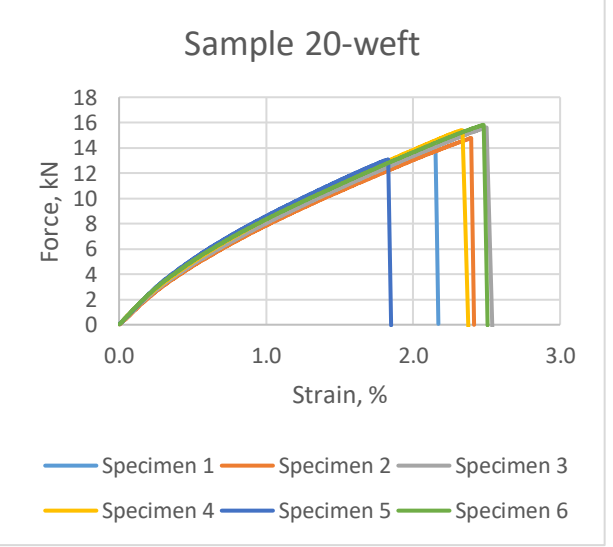
Sample 20-weft
Force, kN
Strain, %
Specimen 1
Specimen 2
Specimen 3
Specimen 4
Specimen 5
Specimen 6

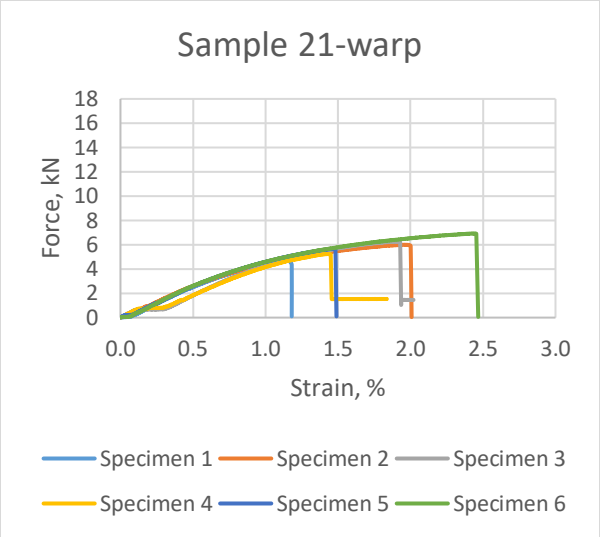
Sample 21-warp
Force, kN
Strain, %
Specimen 1
Specimen 2
Specimen 3
Specimen 4
Specimen 5
Specimen 6

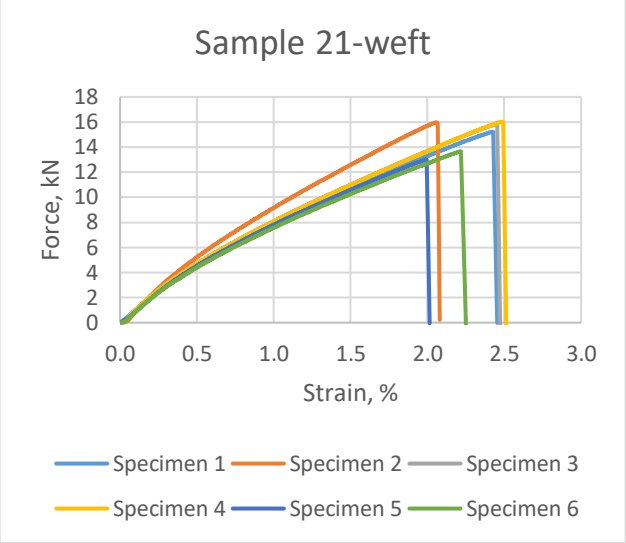
Sample 21-weft
Force, kN
Strain, %
Specimen 1
Specimen 2
Specimen 3
Specimen 4
Specimen 5
Specimen 6

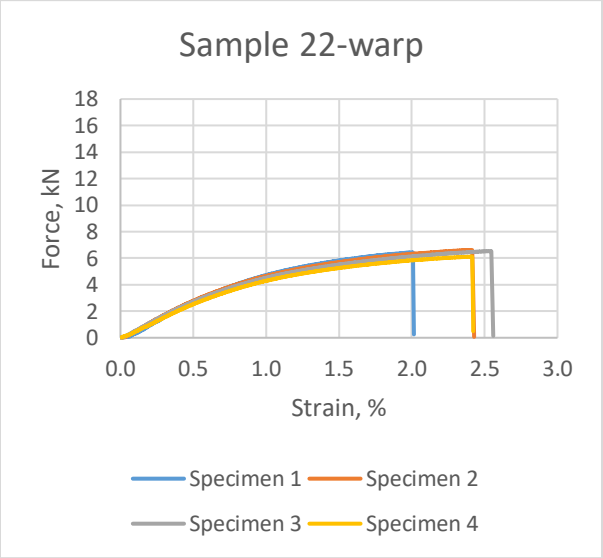
Sample 22-warp
Force, kN
Strain, %
Specimen 1
Specimen 2
Specimen 3
Specimen 4

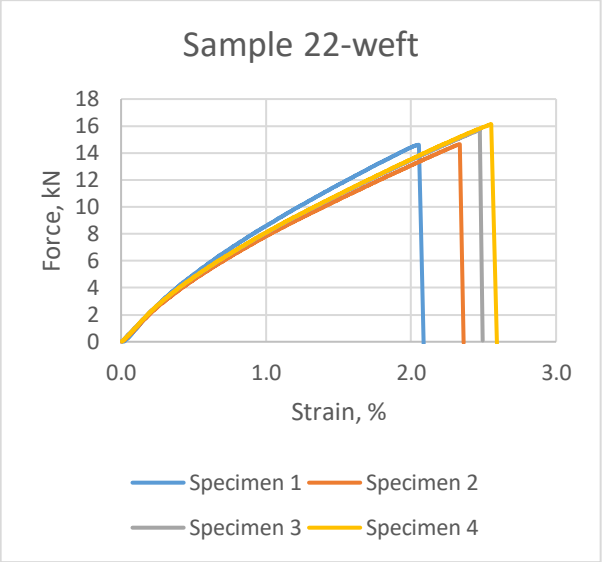
Sample 22-weft
Force, kN
Strain, %
Specimen 1
Specimen 2
Specimen 3
Specimen 4

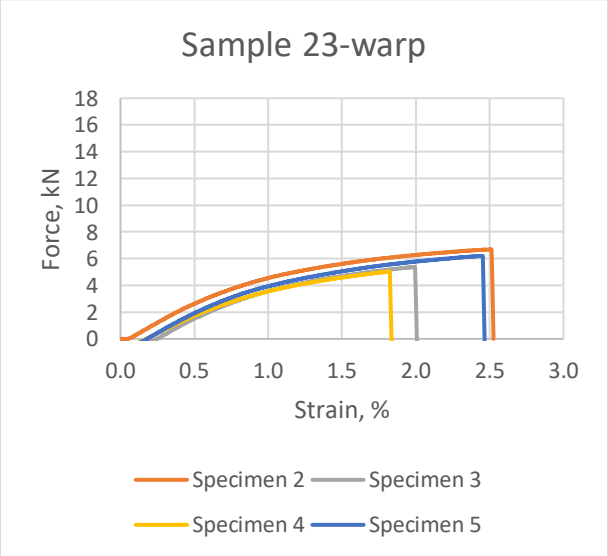
Sample 23-warp
Force, kN
Strain, %
Specimen 2
Specimen 3
Specimen 4
Specimen 5

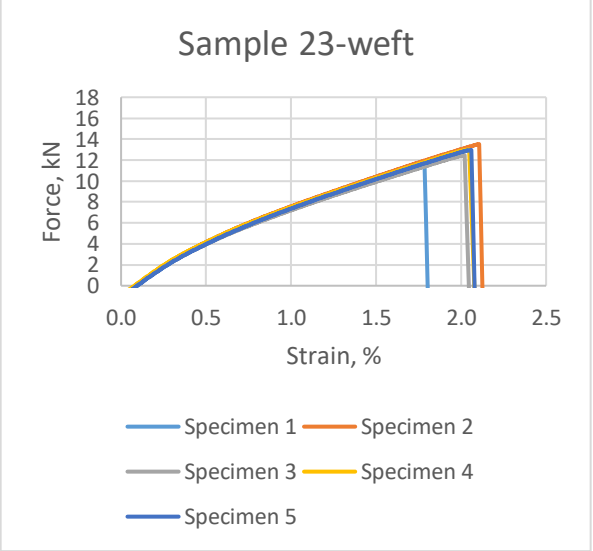
Sample 23-weft
Force, kN
Strain, %
Specimen 1
Specimen 2
Specimen 3
Specimen 4
Specimen 5

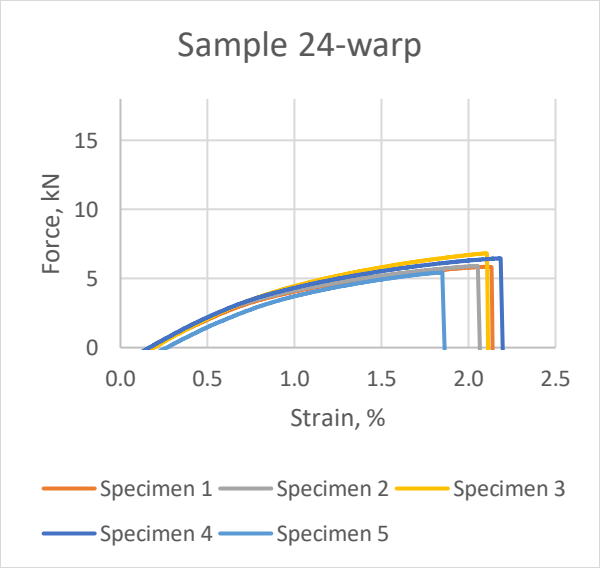
Sample 24-warp
Force, kN
Strain, %
Specimen 1
Specimen 2
Specimen 3
Specimen 4
Specimen 5

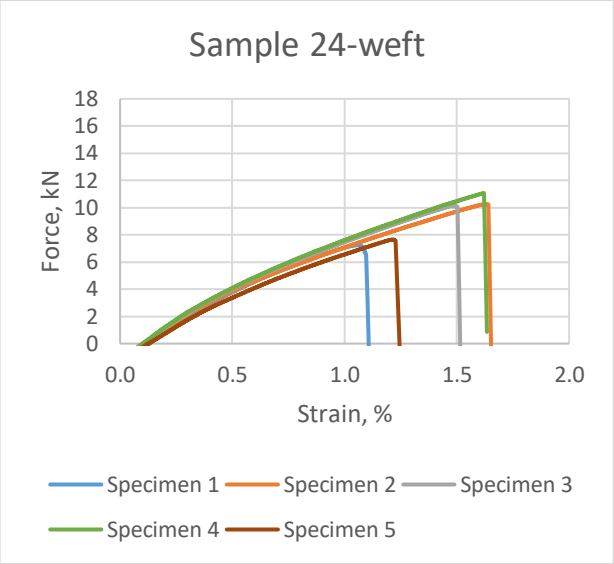
Sample 24-weft
Force, kN
Strain, %
Specimen 1
Specimen 2
Specimen 3
Specimen 4
Specimen 5

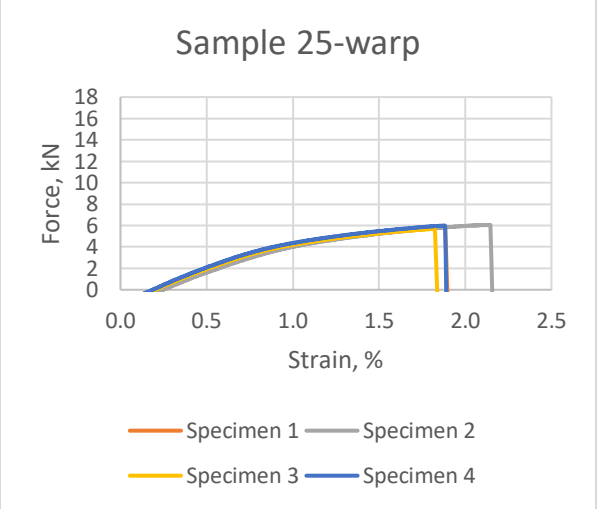
Sample 25-warp
Force, kN
Strain, %
Specimen 1
Specimen 2
Specimen 3
Specimen 4

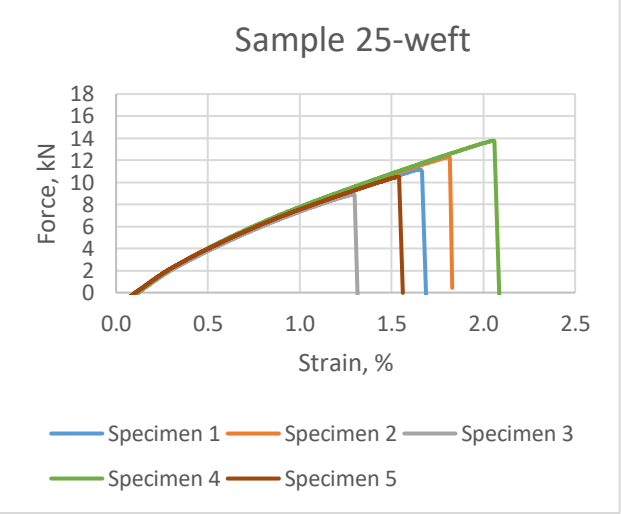
Sample 25-weft
Force, kN
Strain, %
Specimen 1
Specimen 2
Specimen 3
Specimen 4
Specimen 5

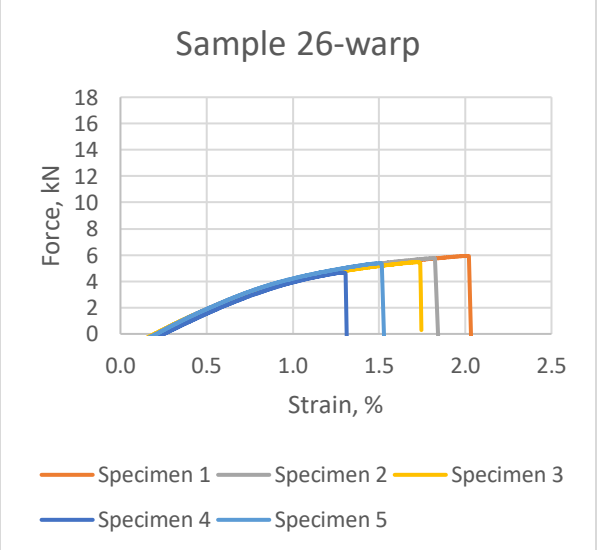
Sample 26-warp
Force, kN
Strain, %
Specimen 1
Specimen 2
Specimen 3
Specimen 4
Specimen 5

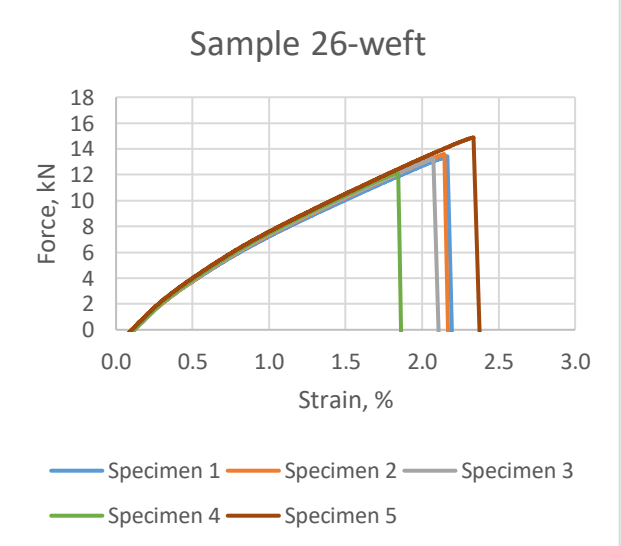
Sample 26-weft
Force, kN
Strain, %
Specimen 1
Specimen 2
Specimen 3
Specimen 4
Specimen 5

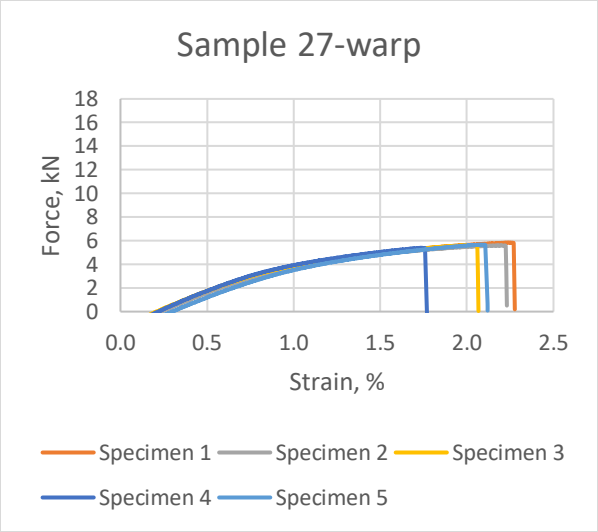
Sample 27-warp
Force, kN
Strain, %
Specimen 1
Specimen 2
Specimen 3
Specimen 4
Specimen 5

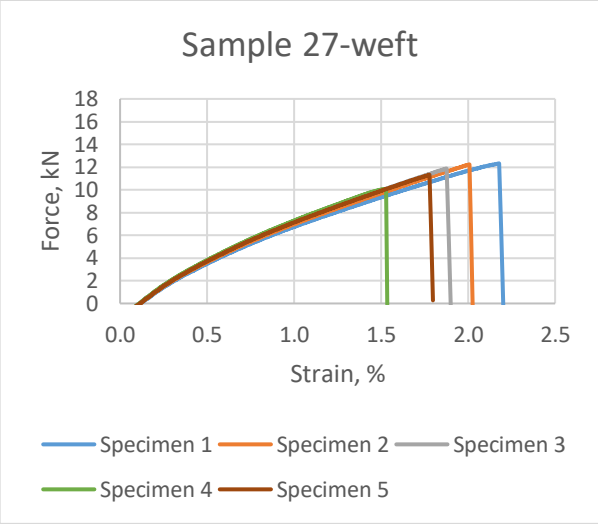
Sample 27-weft
Force, kN
Strain, %
Specimen 1
Specimen 2
Specimen 3
Specimen 4
Specimen 5

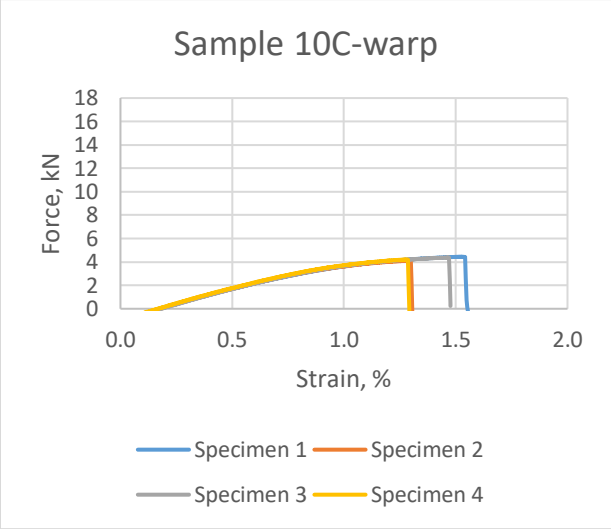
Sample 10C-warp
Force, kN
Strain, %
Specimen 1
Specimen 2
Specimen 3
Specimen 4

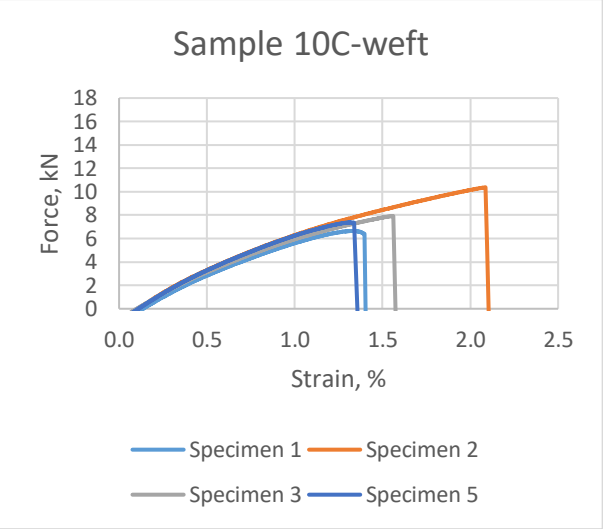
Sample 10C-weft
Force, kN
Strain, %
Specimen 1
Specimen 2
Specimen 3
Specimen 5

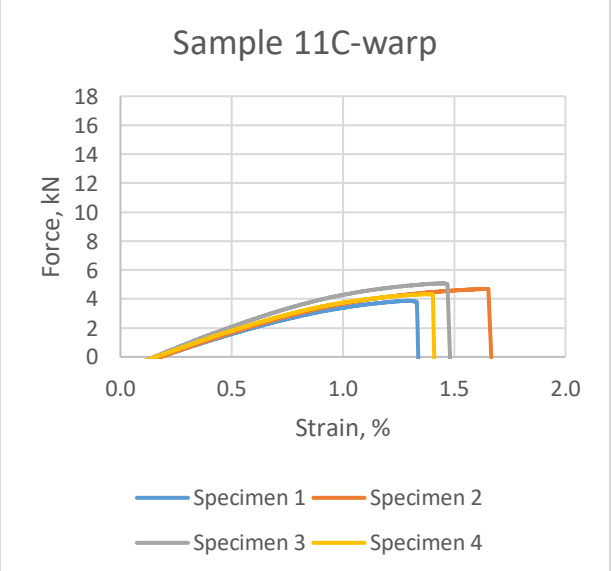
Sample 11C-warp
Force, kN
Strain, %
Specimen 1
Specimen 2
Specimen 3
Specimen 4

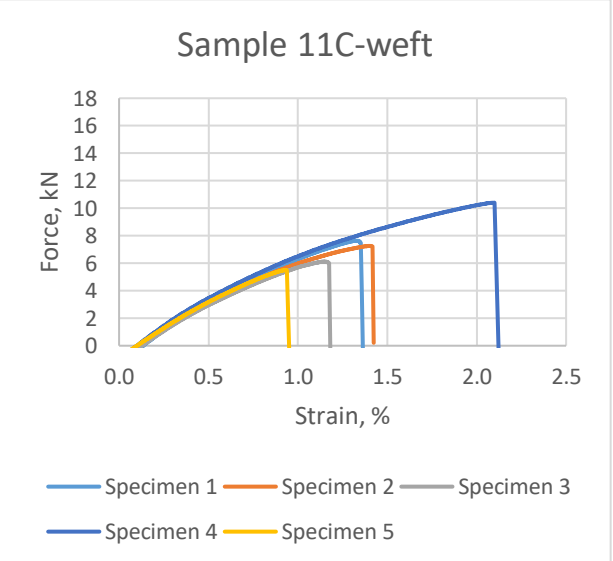
Sample 11C-weft
Force, kN
Strain, %
Specimen 1
Specimen 2
Specimen 3
Specimen 4
Specimen 5

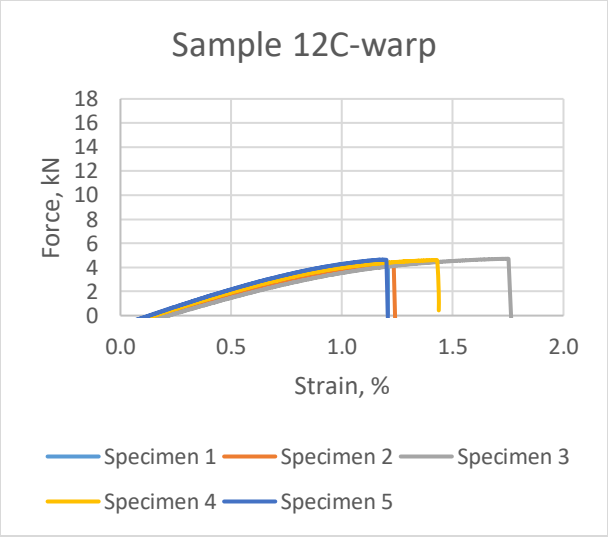
Sample 12C-warp
Force, kN
Strain, %
Specimen 1
Specimen 2
Specimen 3
Specimen 4
Specimen 5

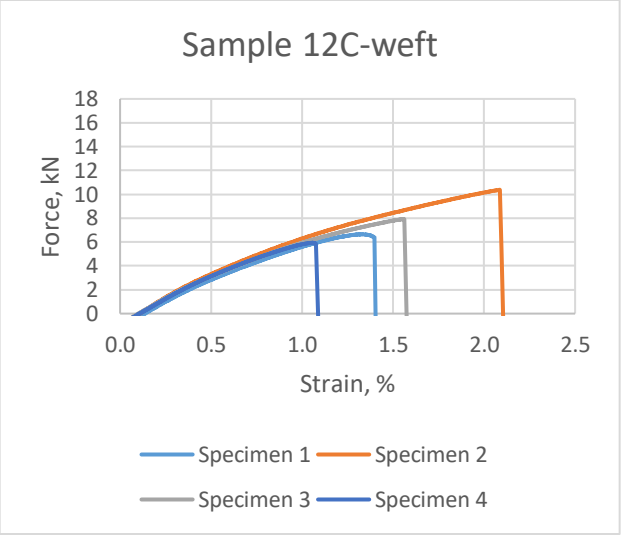
Sample 12C-weft
Force, kN
Strain, %
Specimen 1
Specimen 2
Specimen 3
Specimen 4

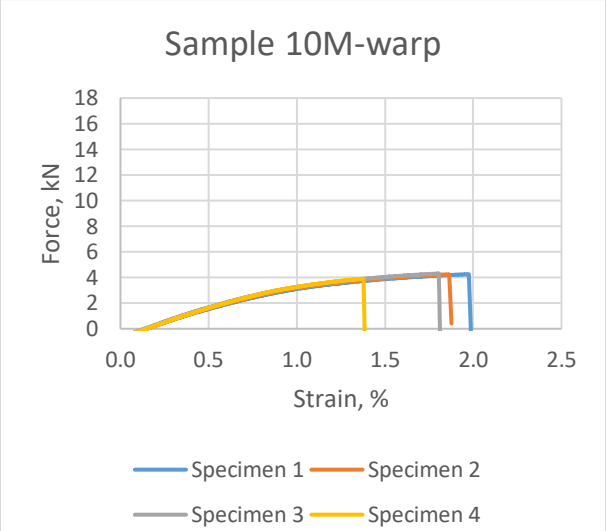
Sample 10M-warp
Force, kN
Strain, %
Specimen 1
Specimen 2
Specimen 3
Specimen 4

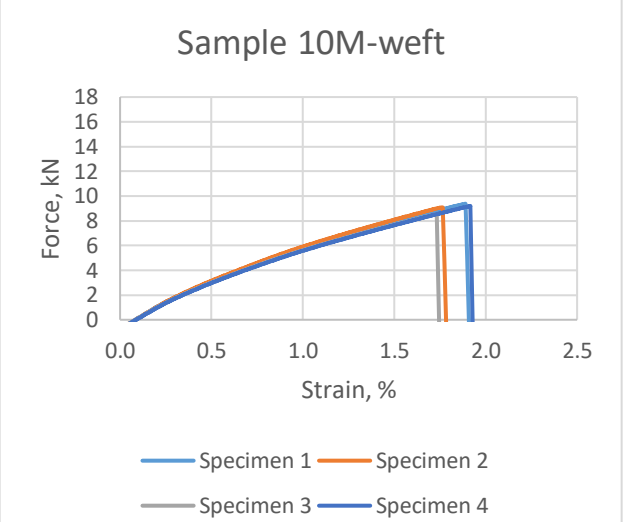
Sample 10M-weft
Force, kN
Strain, %
Specimen 1
Specimen 2
Specimen 3
Specimen 4

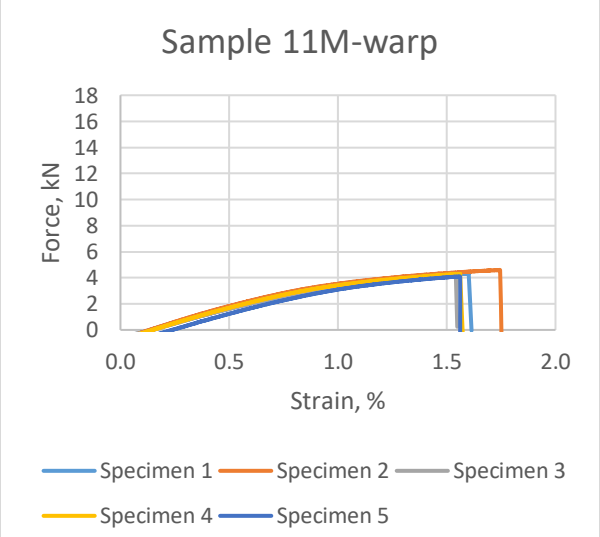
Sample 11M-warp
Force, kN
Strain, %
Specimen 1
Specimen 2
Specimen 3
Specimen 4
Specimen 5

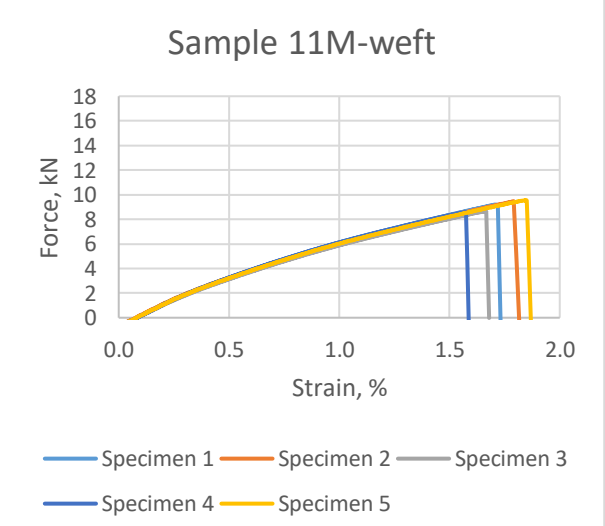
Sample 11M-weft
Force, kN
Strain, %
Specimen 1
Specimen 2
Specimen 3
Specimen 4
Specimen 5

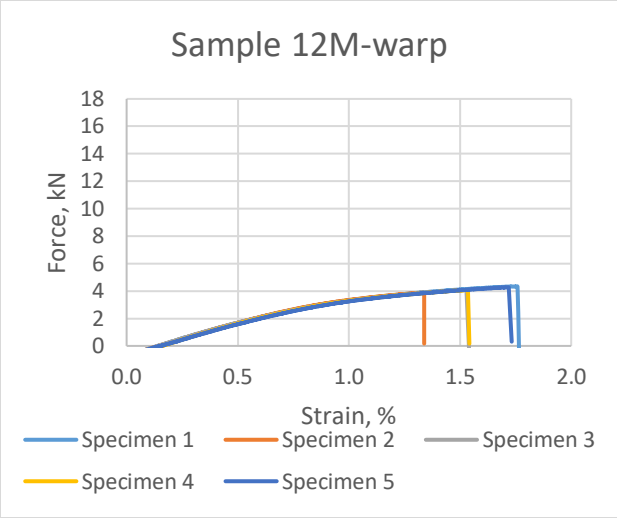
Sample 12M-warp
Force, kN
18
16
14
12
10
8
6
4
2
0
0.0
0.5
1.0
1.5
2.0
Strain, %
Specimen 1
Specimen 2
Specimen 3
Specimen 4
Specimen 5

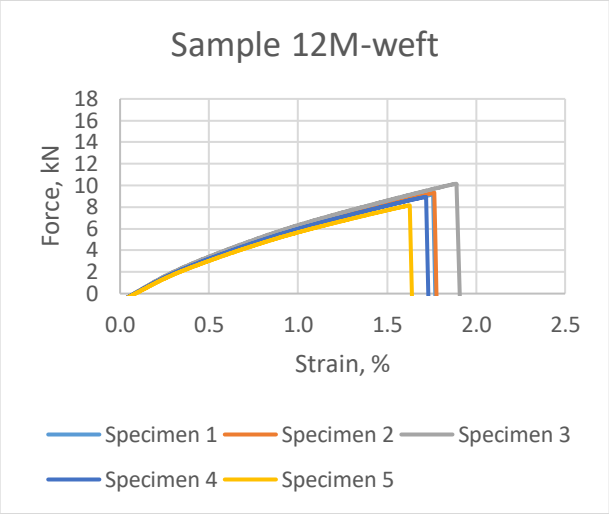
Sample 12M-weft
Force, kN
18
16
14
12
10
8
6
4
2
0
0.0
0.5
1.0
1.5
2.0
2.5
Strain, %
Specimen 1
Specimen 2
Specimen 3
Specimen 4
Specimen 5

Appendix 87. Test result from tup impact test

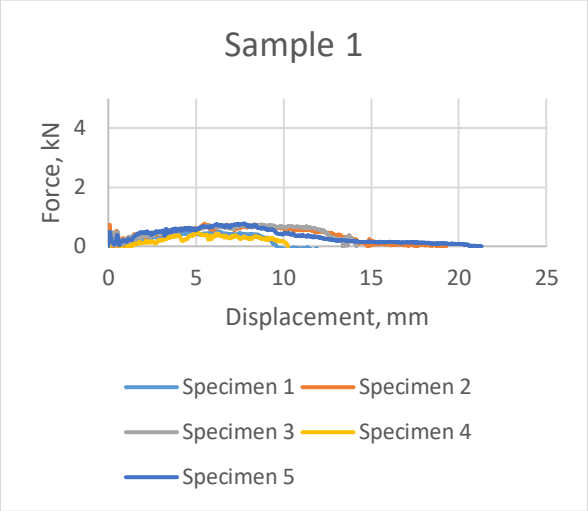

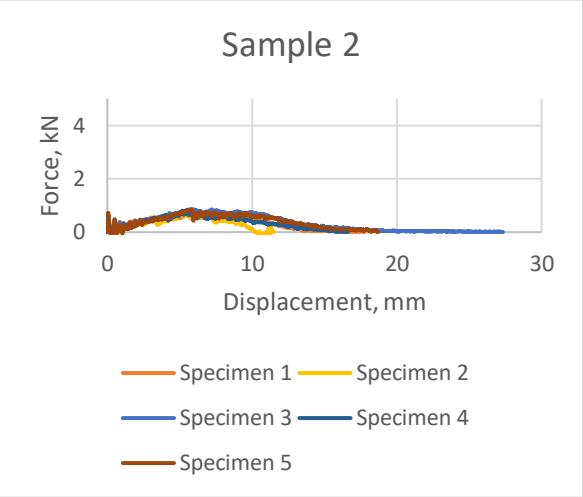

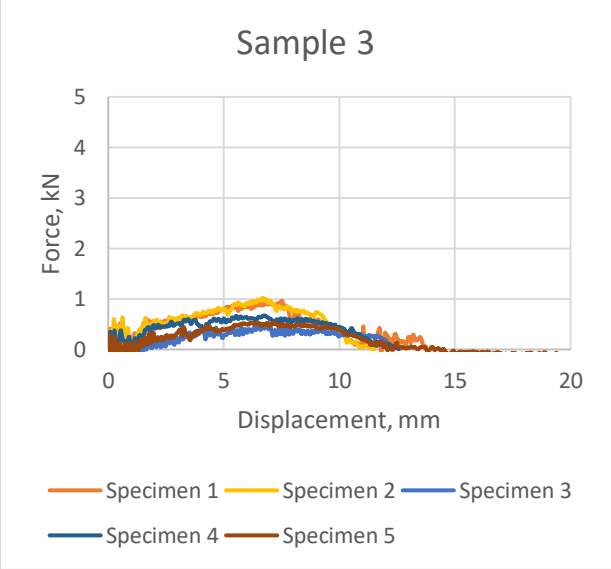

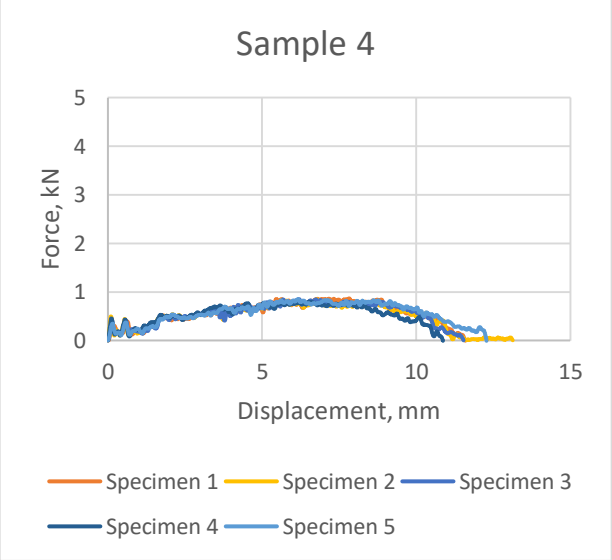

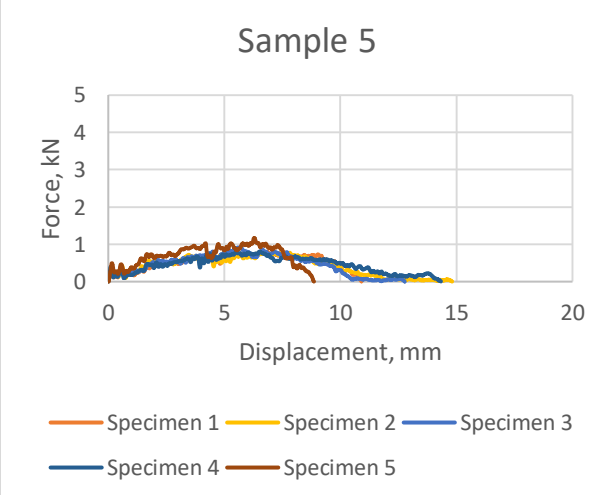

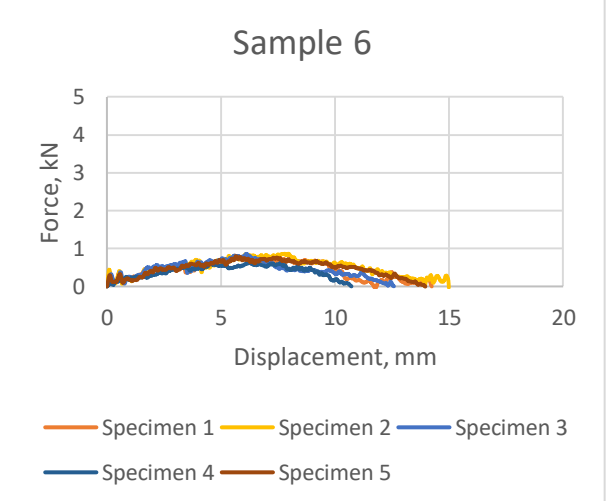

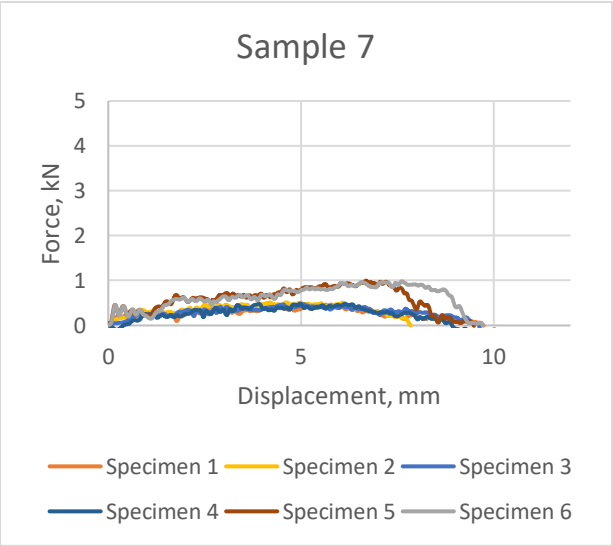
Sample 7
Force, kN
Displacement, mm
Specimen 1
Specimen 2
Specimen 3
Specimen 4
Specimen 5
Specimen 6

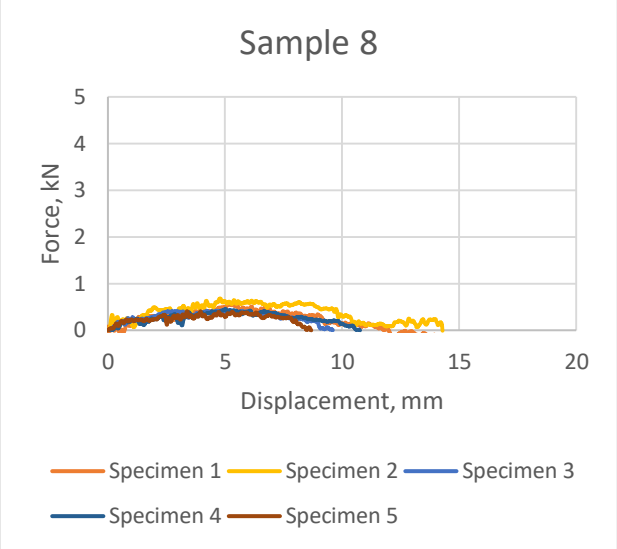
Sample 8
Force, kN
Displacement, mm
Specimen 1
Specimen 2
Specimen 3
Specimen 4
Specimen 5

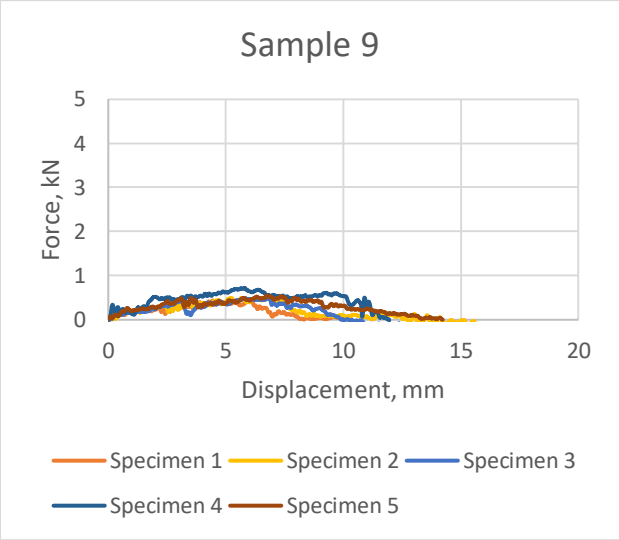
Sample 9
Force, kN
Displacement, mm
Specimen 1
Specimen 2
Specimen 3
Specimen 4
Specimen 5

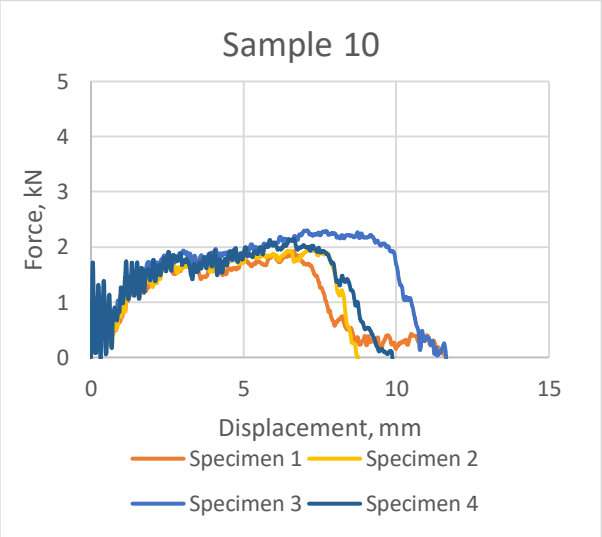
Sample 10
Force, kN
Displacement, mm
Specimen 1
Specimen 2
Specimen 3
Specimen 4

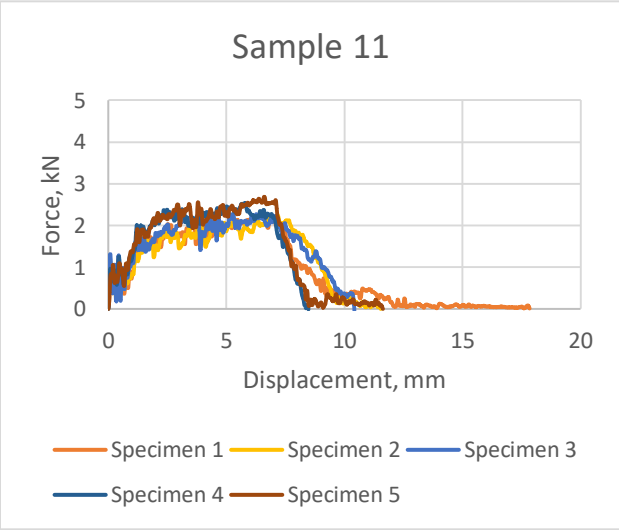
Sample 11
Force, kN
Displacement, mm
Specimen 1
Specimen 2
Specimen 3
Specimen 4
Specimen 5

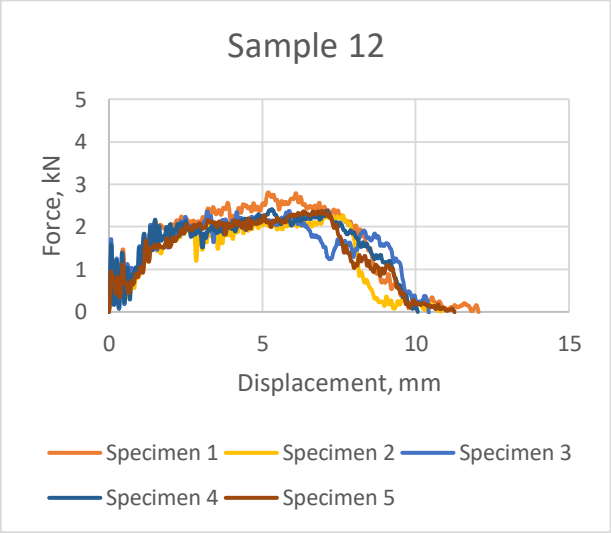
Sample 12
Force, kN
Displacement, mm
Specimen 1
Specimen 2
Specimen 3
Specimen 4
Specimen 5

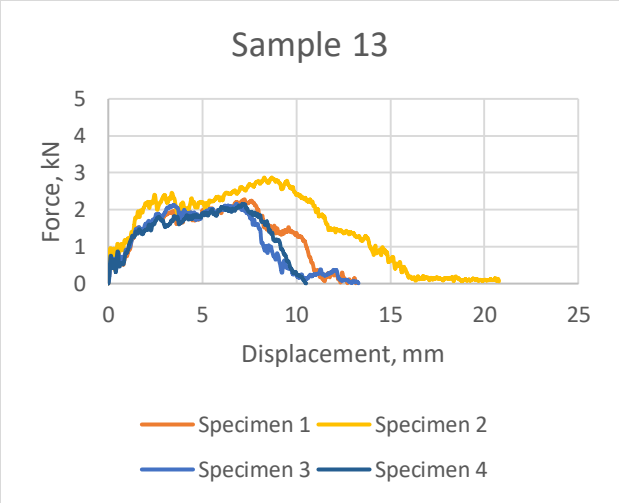
Sample 13
Force, kN
Displacement, mm
Specimen 1
Specimen 2
Specimen 3
Specimen 4

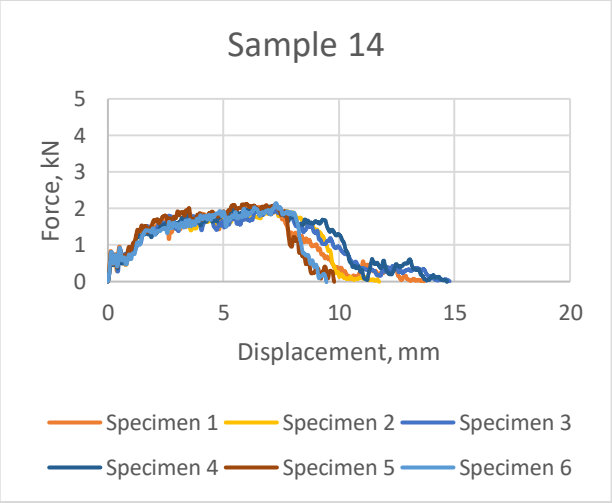
Sample 14
Force, kN
Displacement, mm
Specimen 1
Specimen 2
Specimen 3
Specimen 4
Specimen 5
Specimen 6

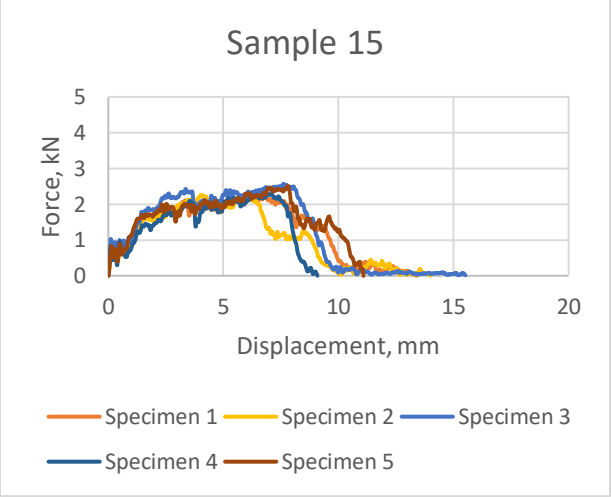
Sample 15
Force, kN
Displacement, mm
Specimen 1
Specimen 2
Specimen 3
Specimen 4
Specimen 5

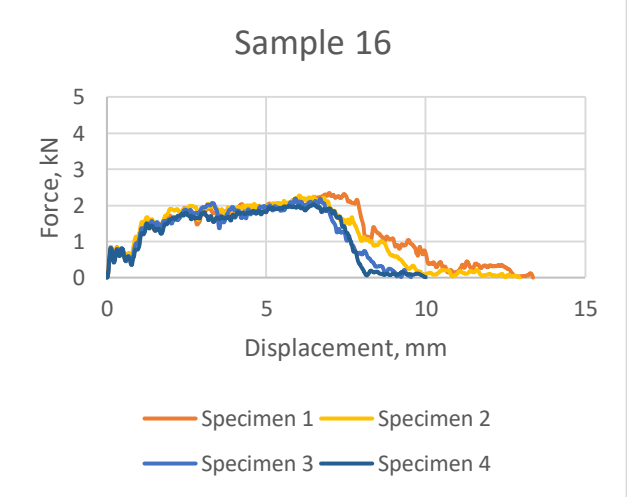
Sample 16
Force, kN
Displacement, mm
Specimen 1
Specimen 2
Specimen 3
Specimen 4

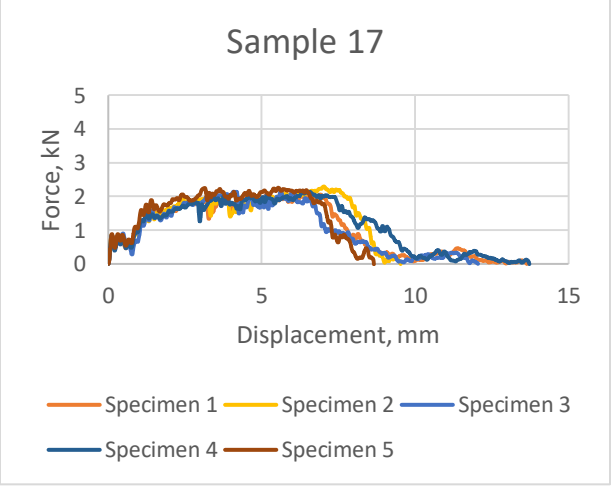
Sample 17
Force, kN
Displacement, mm
Specimen 1
Specimen 2
Specimen 3
Specimen 4
Specimen 5

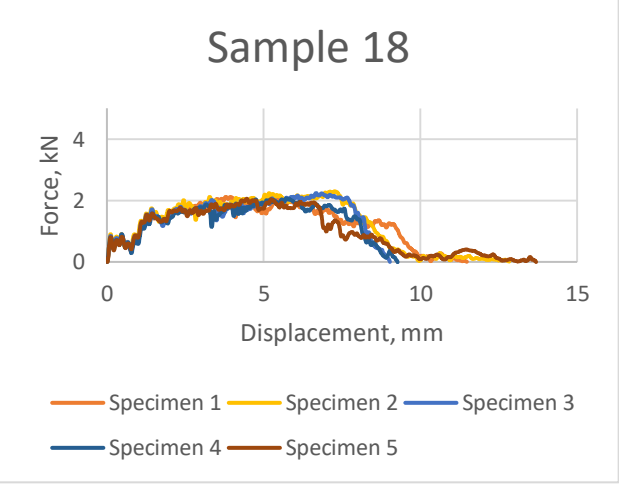
Sample 18
Force, kN
Displacement, mm
Specimen 1
Specimen 2
Specimen 3
Specimen 4
Specimen 5

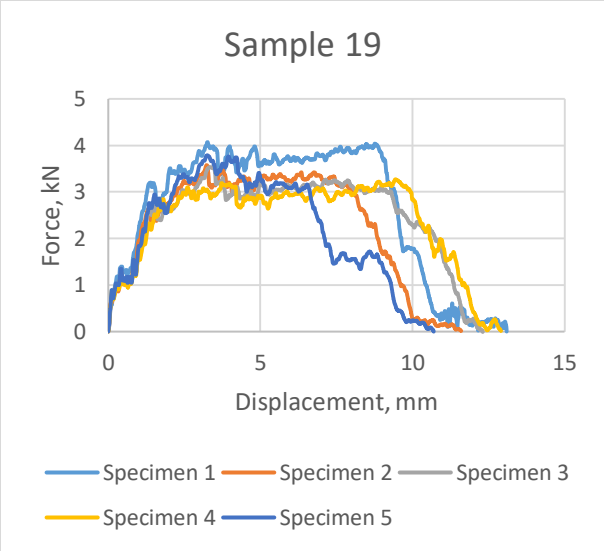
Sample 19
Force, kN
Displacement, mm
Specimen 1
Specimen 2
Specimen 3
Specimen 4
Specimen 5

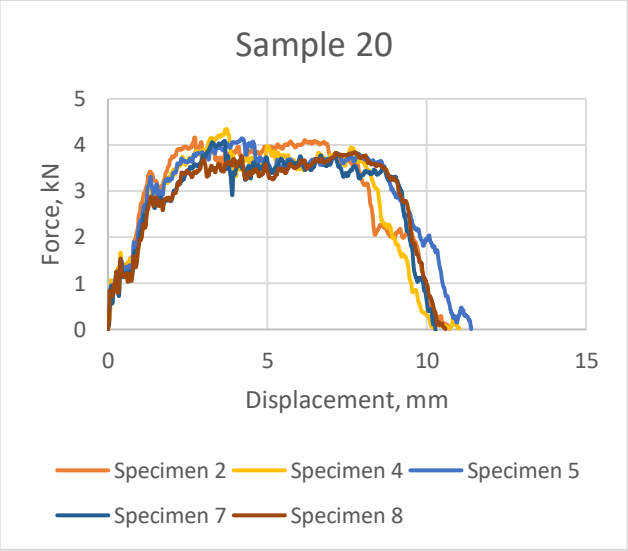
Sample 20
Force, kN
Displacement, mm
Specimen 2
Specimen 4
Specimen 5
Specimen 7
Specimen 8

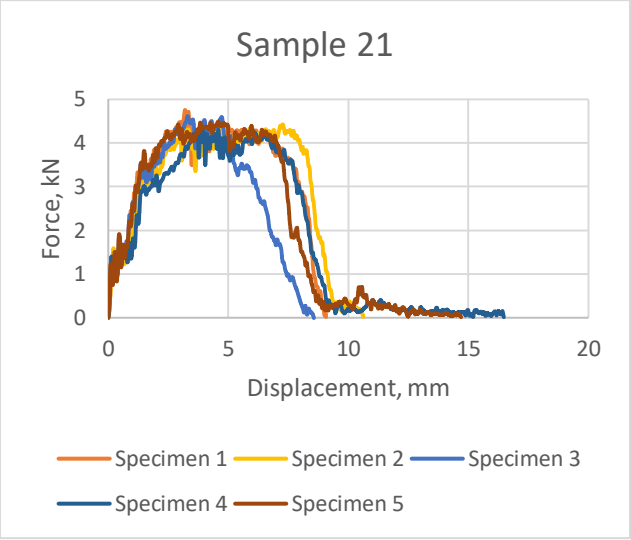
Sample 21
Force, kN
Displacement, mm
Specimen 1
Specimen 2
Specimen 3
Specimen 4
Specimen 5

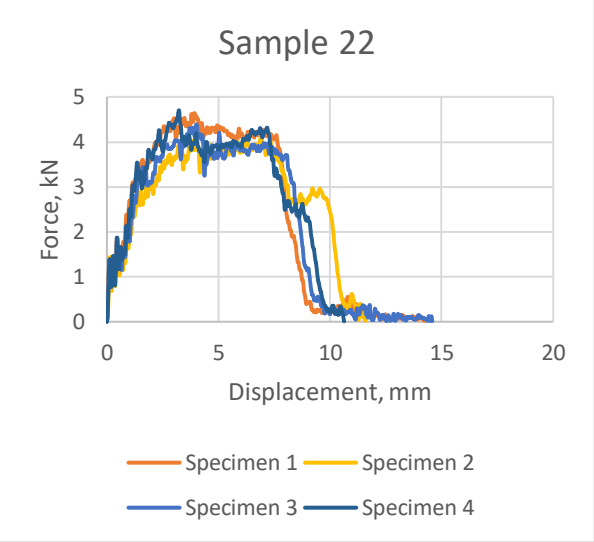
Sample 22
Force, kN
Displacement, mm
Specimen 1
Specimen 2
Specimen 3
Specimen 4

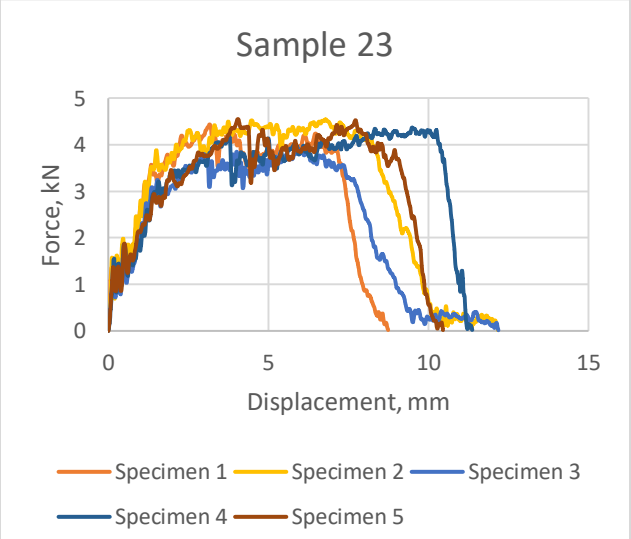
Sample 23
Force, kN
Displacement, mm
Specimen 1
Specimen 2
Specimen 3
Specimen 4
Specimen 5

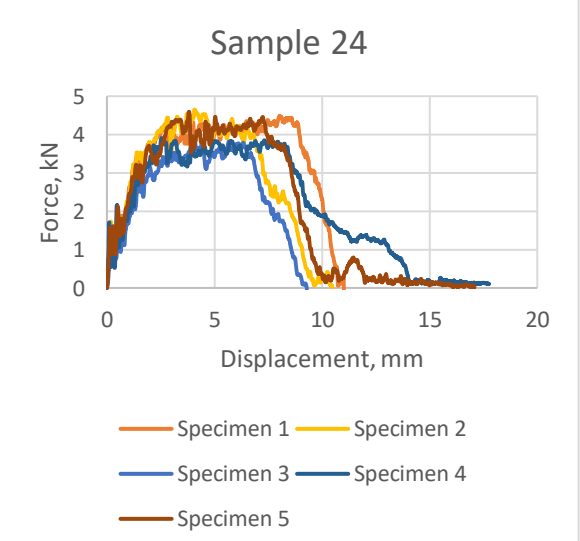
Sample 24
Force, kN
Displacement, mm
Specimen 1
Specimen 2
Specimen 3
Specimen 4
Specimen 5

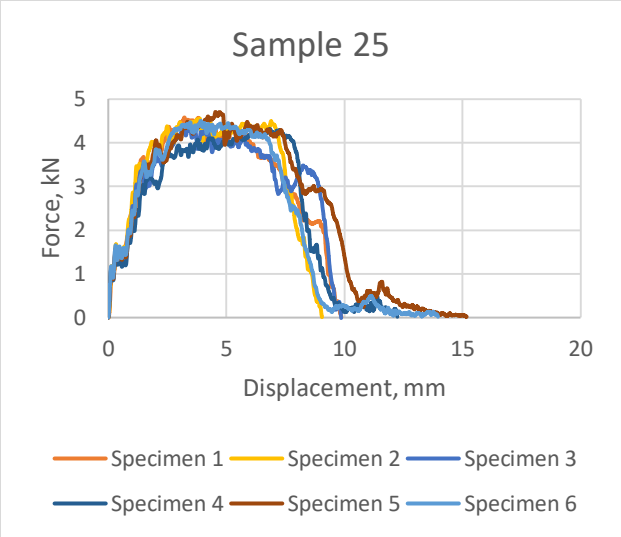
Sample 25
Force, kN
Displacement, mm
Specimen 1
Specimen 2
Specimen 3
Specimen 4
Specimen 5
Specimen 6

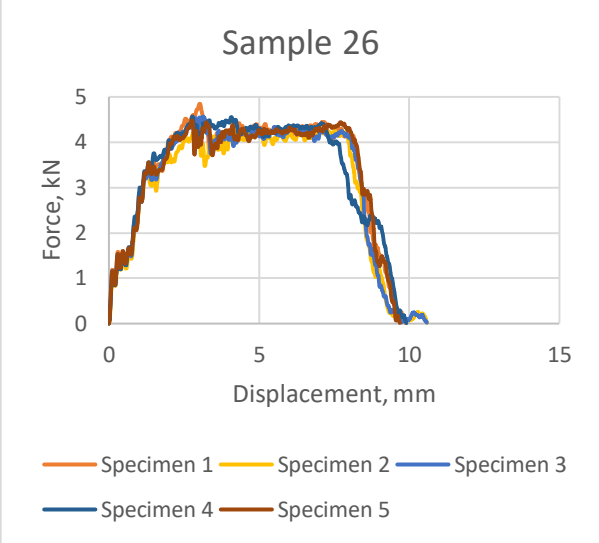
Sample 26
Force, kN
Displacement, mm
Specimen 1
Specimen 2
Specimen 3
Specimen 4
Specimen 5

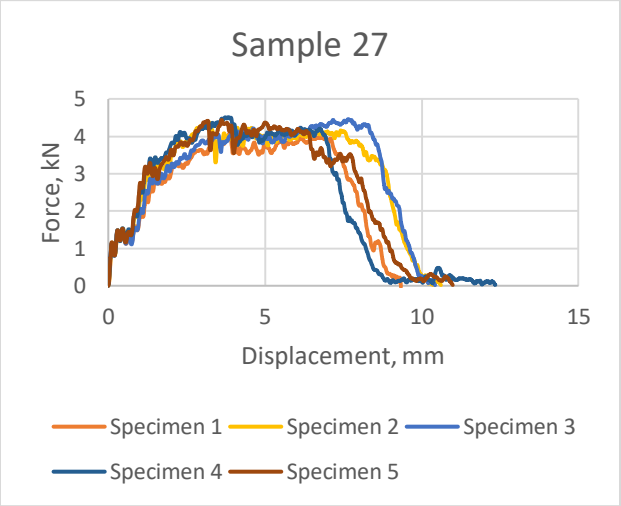
Sample 27
Force, kN
Displacement, mm
Specimen 1
Specimen 2
Specimen 3
Specimen 4
Specimen 5

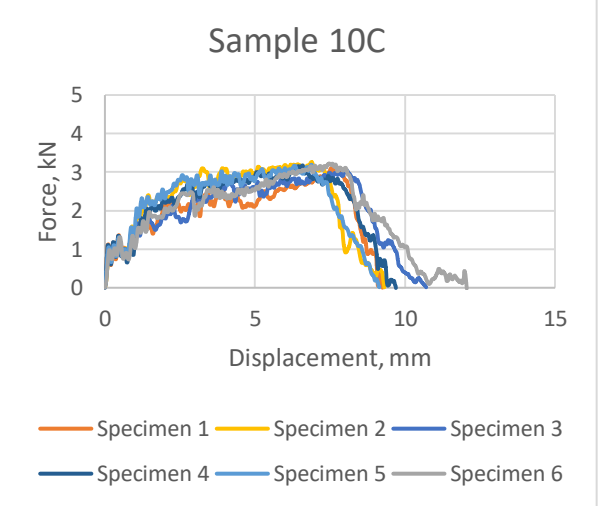
Sample 10C
Force, kN
Displacement, mm
Specimen 1
Specimen 2
Specimen 3
Specimen 4
Specimen 5
Specimen 6

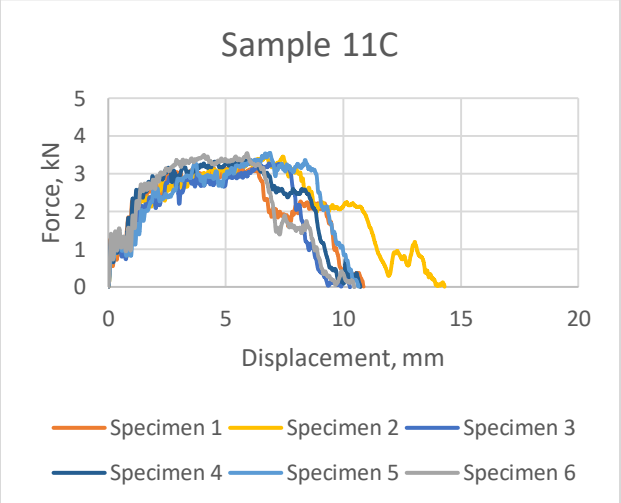
Sample 11C
Force, kN
Displacement, mm
Specimen 1
Specimen 2
Specimen 3
Specimen 4
Specimen 5
Specimen 6

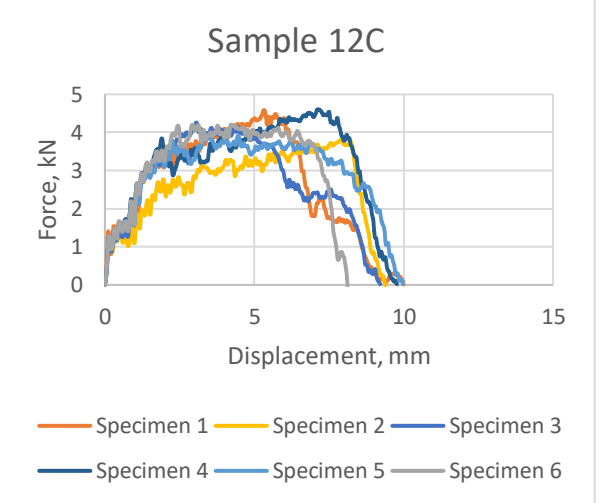
Sample 12C
Force, kN
Displacement, mm
Specimen 1
Specimen 2
Specimen 3
Specimen 4
Specimen 5
Specimen 6

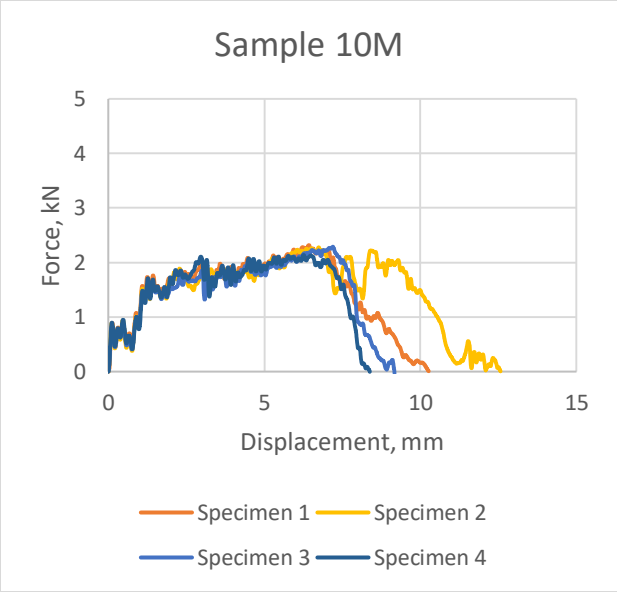
Sample 10M
Force, kN
Displacement, mm
Specimen 1
Specimen 2
Specimen 3
Specimen 4

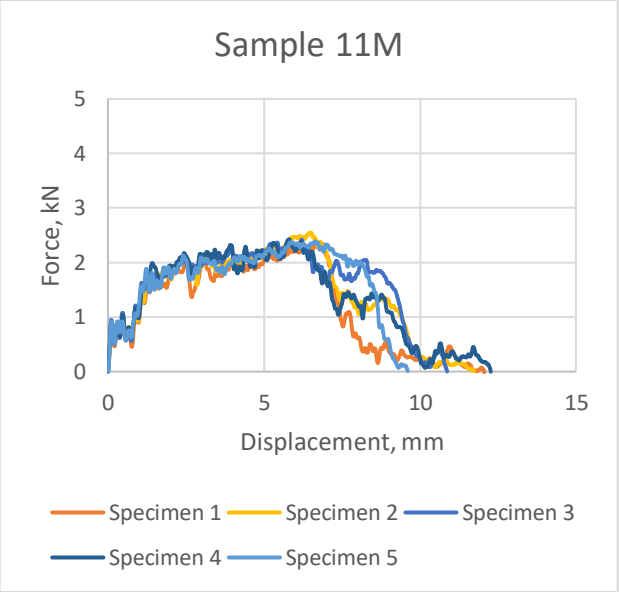
Sample 11M
Force, kN
Displacement, mm
Specimen 1
Specimen 2
Specimen 3
Specimen 4
Specimen 5

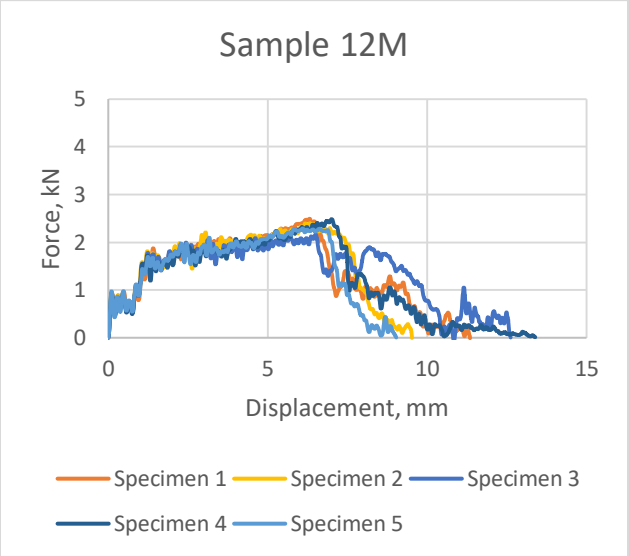
Sample 12M
Force, kN
Displacement, mm
Specimen 1
Specimen 2
Specimen 3
Specimen 4
Specimen 5

Appendix 88. Test result from compression (CLC) test

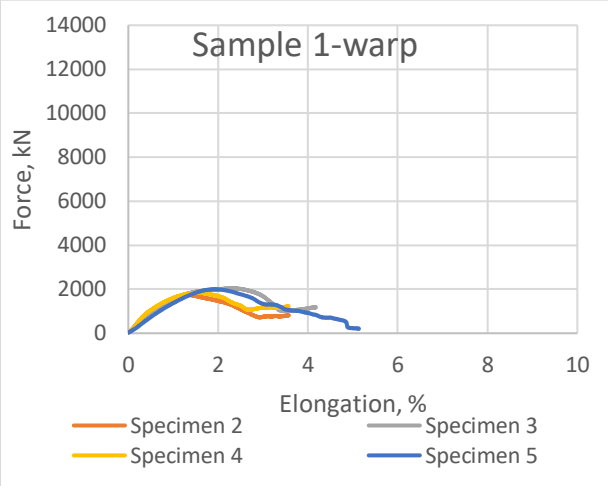

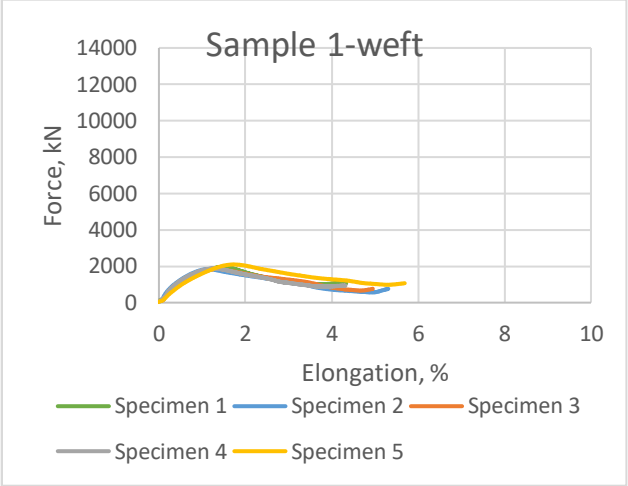

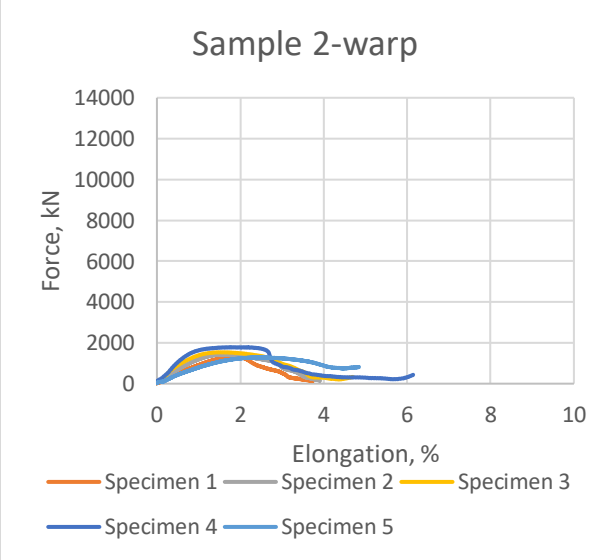

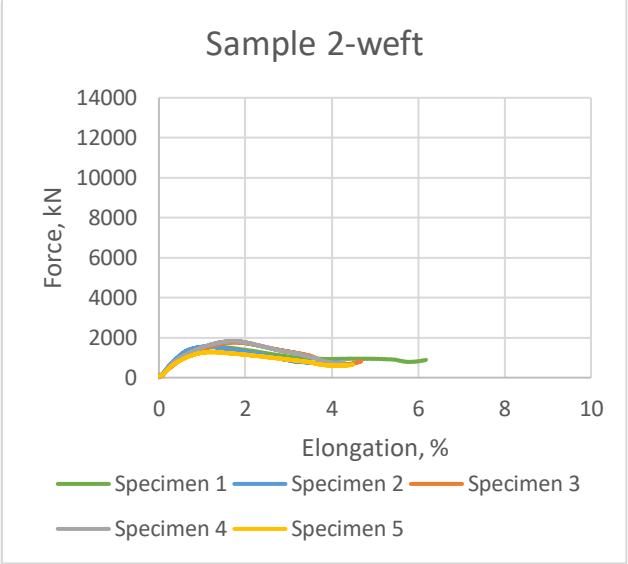

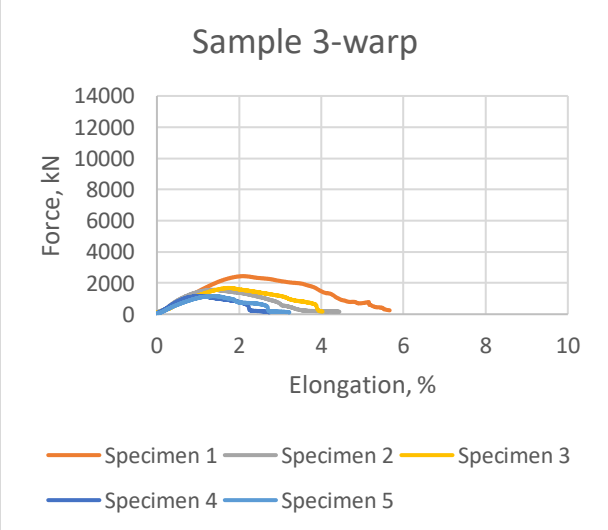

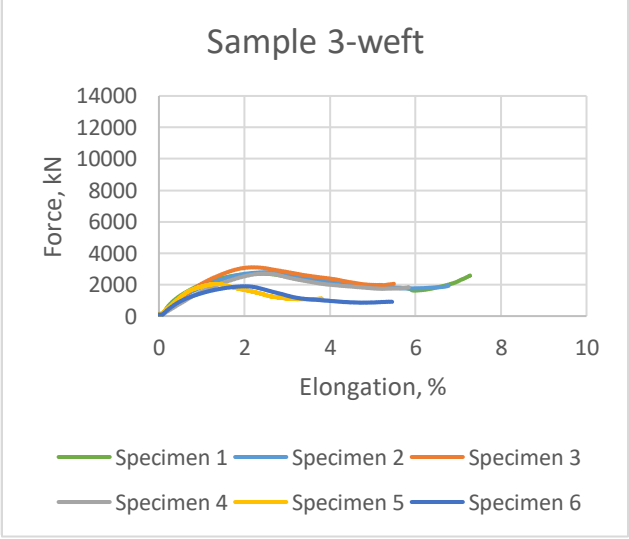

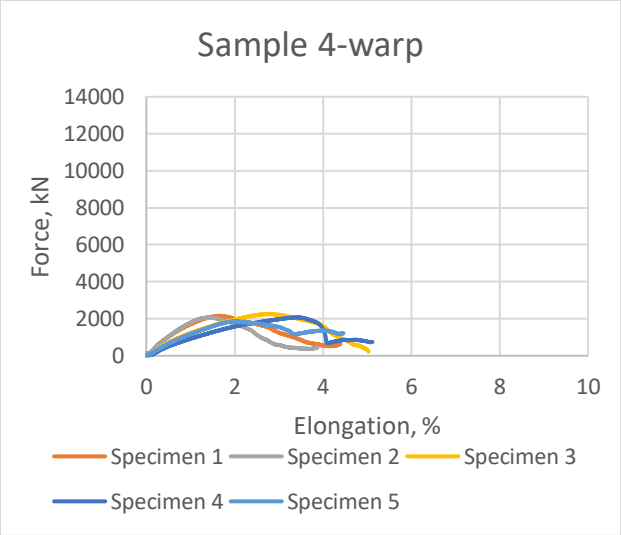
Sample 4-warp
Force, kN
14000
12000
10000
8000
6000
4000
2000
0
0
2
4
6
8
10
Elongation, %
Specimen 1
Specimen 2
Specimen 3
Specimen 4
Specimen 5

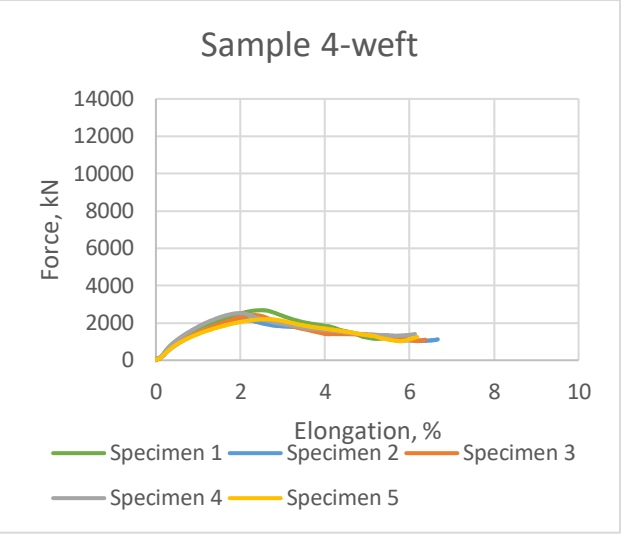
Sample 4-weft
Force, kN
14000
12000
10000
8000
6000
4000
2000
0
0
2
4
6
8
10
Elongation, %
Specimen 1
Specimen 2
Specimen 3
Specimen 4
Specimen 5

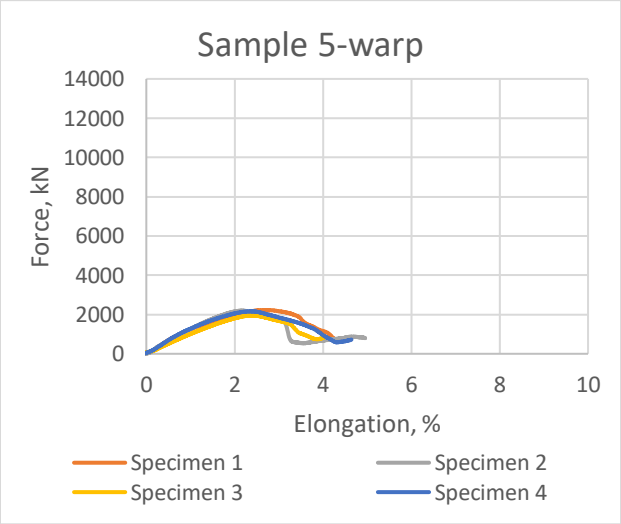
Sample 5-warp
Force, kN
14000
12000
10000
8000
6000
4000
2000
0
0
2
4
6
8
10
Elongation, %
Specimen 1
Specimen 2
Specimen 3
Specimen 4

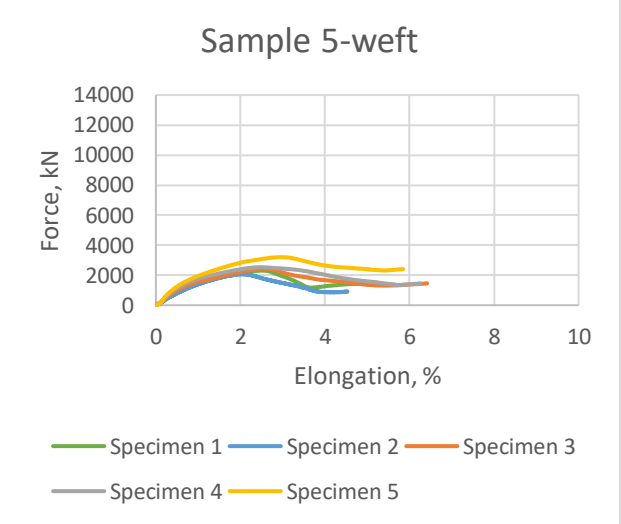
Sample 5-weft
Force, kN
14000
12000
10000
8000
6000
4000
2000
0
0
2
4
6
8
10
Elongation, %
Specimen 1
Specimen 2
Specimen 3
Specimen 4
Specimen 5

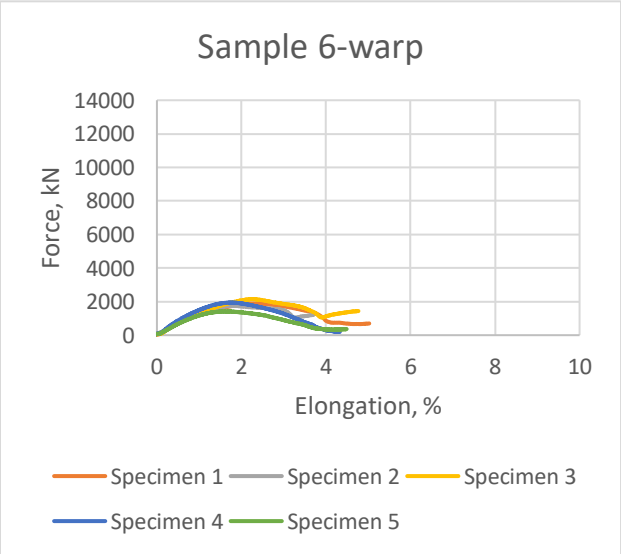
Sample 6-warp
Force, kN
14000
12000
10000
8000
6000
4000
2000
0
0
2
4
6
8
10
Elongation, %
Specimen 1
Specimen 2
Specimen 3
Specimen 4
Specimen 5

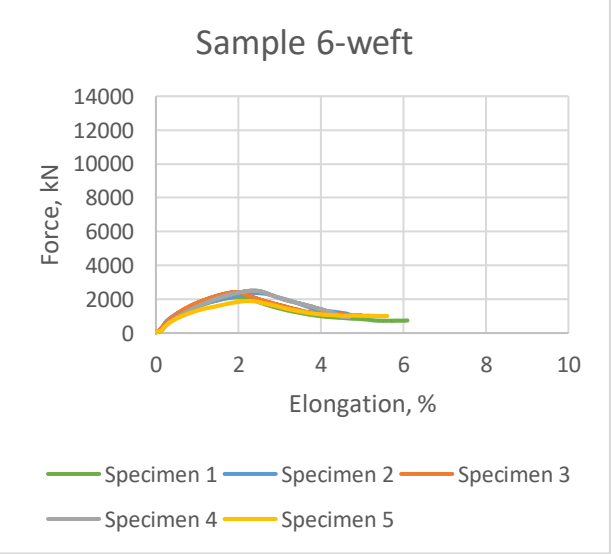
Sample 6-weft
Force, kN
14000
12000
10000
8000
6000
4000
2000
0
0
2
4
6
8
10
Elongation, %
Specimen 1
Specimen 2
Specimen 3
Specimen 4
Specimen 5

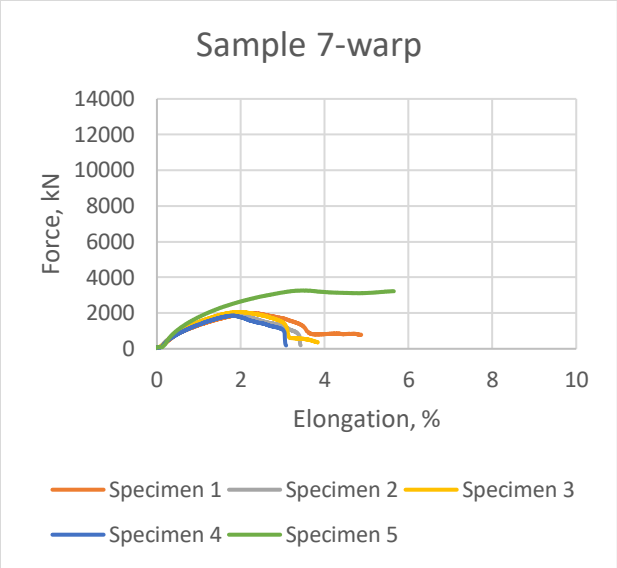
Sample 7-warp
Force, kN
14000
12000
10000
8000
6000
4000
2000
0
0
2
4
6
8
10
Elongation, %
Specimen 1
Specimen 2
Specimen 3
Specimen 4
Specimen 5

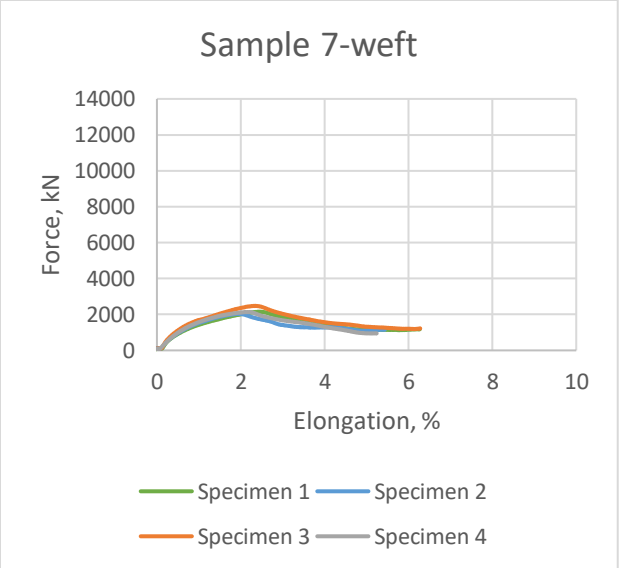
Sample 7-weft
Force, kN
14000
12000
10000
8000
6000
4000
2000
0
0
2
4
6
8
10
Elongation, %
Specimen 1
Specimen 2
Specimen 3
Specimen 4

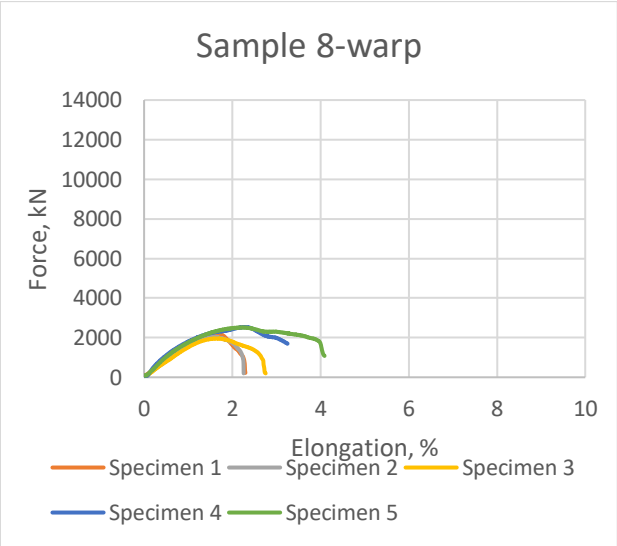
Sample 8-warp
Force, kN
14000
12000
10000
8000
6000
4000
2000
0
0
2
4
6
8
10
Elongation, %
Specimen 1
Specimen 2
Specimen 3
Specimen 4
Specimen 5

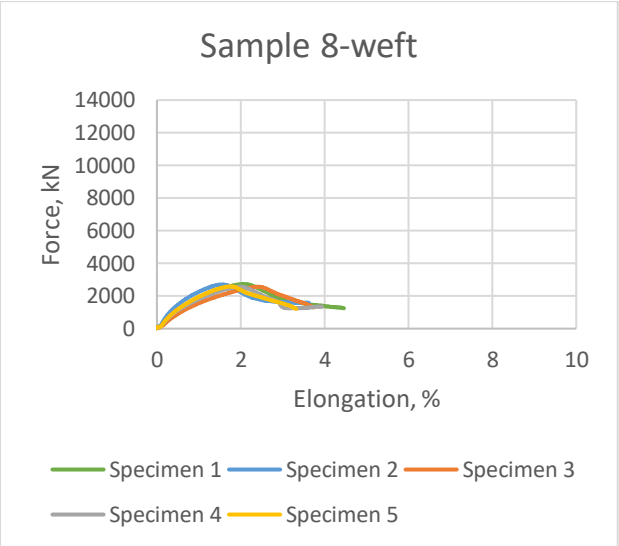
Sample 8-weft
Force, kN
14000
12000
10000
8000
6000
4000
2000
0
0
2
4
6
8
10
Elongation, %
Specimen 1
Specimen 2
Specimen 3
Specimen 4
Specimen 5

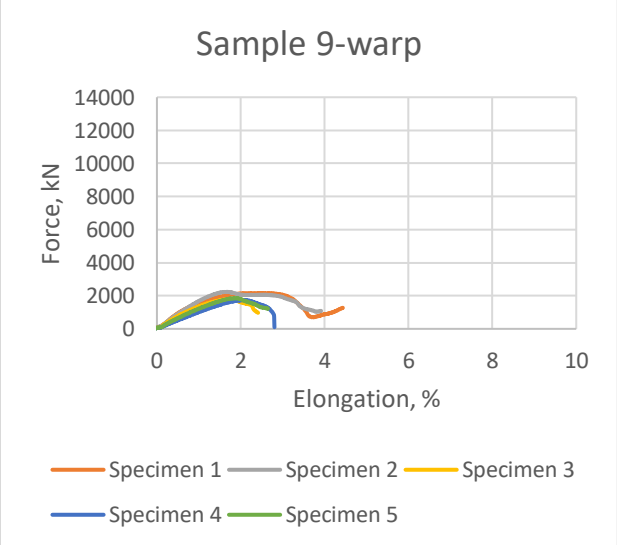
Sample 9-warp
Force, kN
14000
12000
10000
8000
6000
4000
2000
0
0
2
4
6
8
10
Elongation, %
Specimen 1
Specimen 2
Specimen 3
Specimen 4
Specimen 5

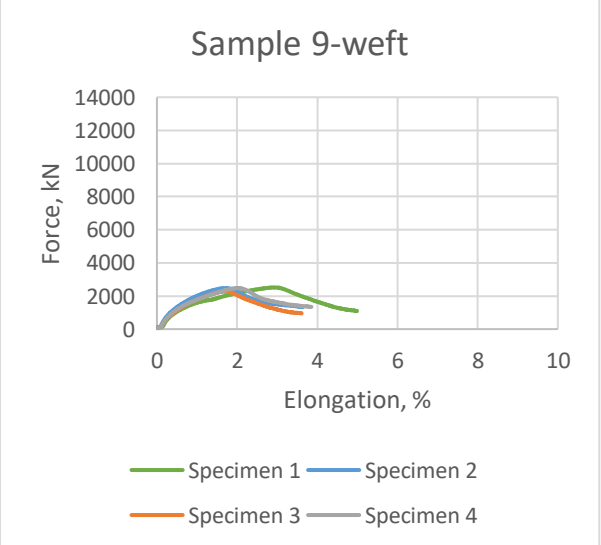
Sample 9-weft
Force, kN
14000
12000
10000
8000
6000
4000
2000
0
0
2
4
6
8
10
Elongation, %
Specimen 1
Specimen 2
Specimen 3
Specimen 4

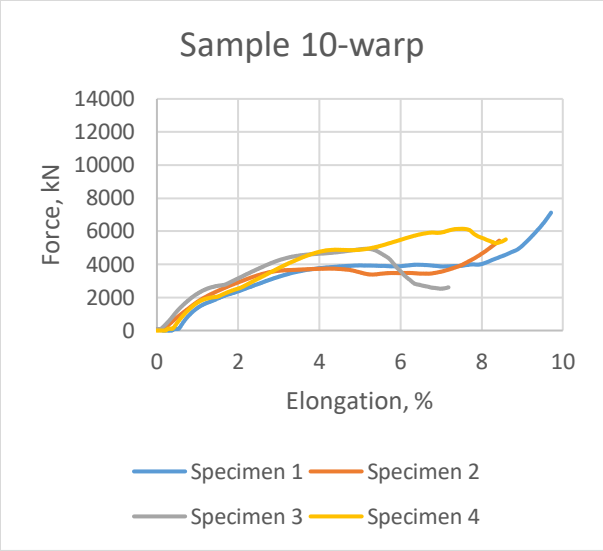
Sample 10-warp
Force, kN
14000
12000
10000
8000
6000
4000
2000
0
0
2
4
6
8
10
Elongation, %
Specimen 1
Specimen 2
Specimen 3
Specimen 4

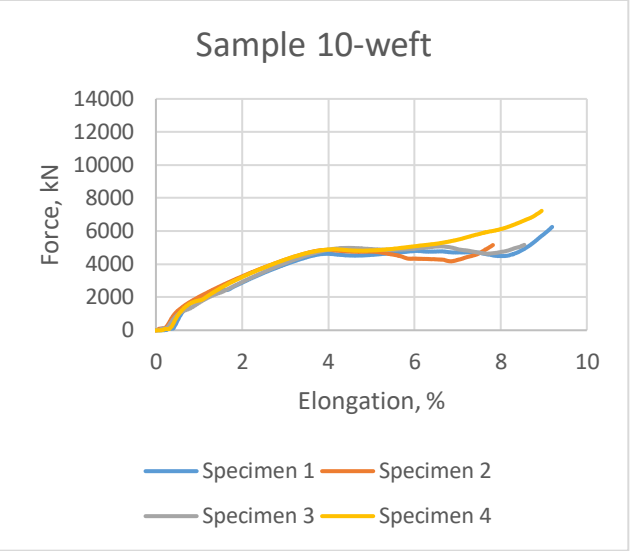
Sample 10-weft
Force, kN
14000
12000
10000
8000
6000
4000
2000
0
0
2
4
6
8
10
Elongation, %
Specimen 1
Specimen 2
Specimen 3
Specimen 4

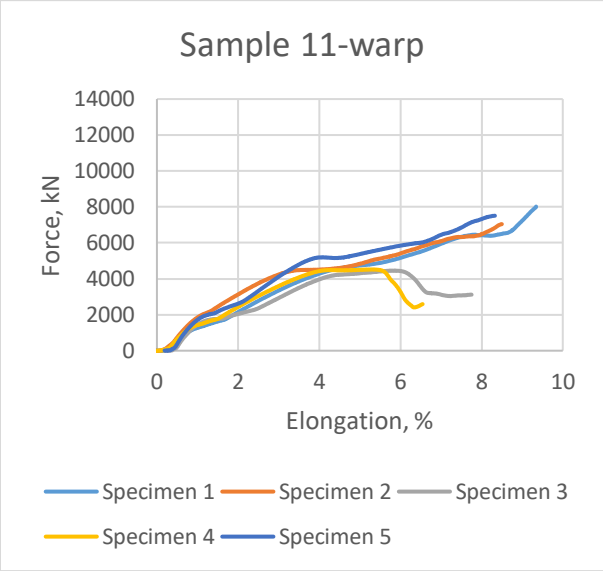
Sample 11-warp
Force, kN
14000
12000
10000
8000
6000
4000
2000
0
0
2
4
6
8
10
Elongation, %
Specimen 1
Specimen 2
Specimen 3
Specimen 4
Specimen 5

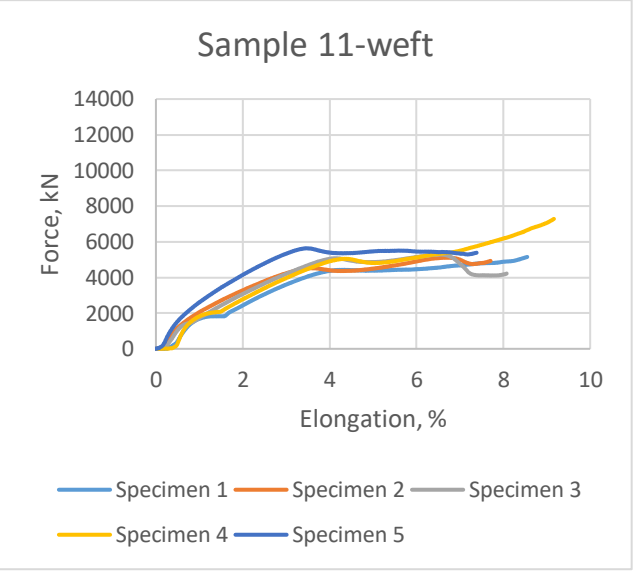
Sample 11-weft
Force, kN
14000
12000
10000
8000
6000
4000
2000
0
0
2
4
6
8
10
Elongation, %
Specimen 1
Specimen 2
Specimen 3
Specimen 4
Specimen 5

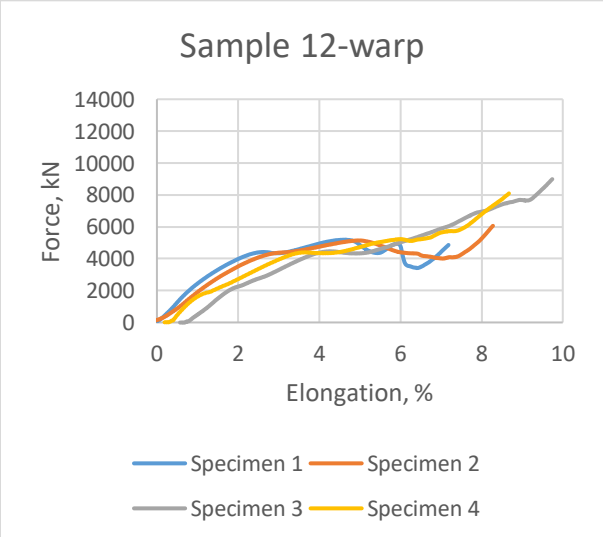
Sample 12-warp
Force, kN
14000
12000
10000
8000
6000
4000
2000
0
0
2
4
6
8
10
Elongation, %
Specimen 1
Specimen 2
Specimen 3
Specimen 4

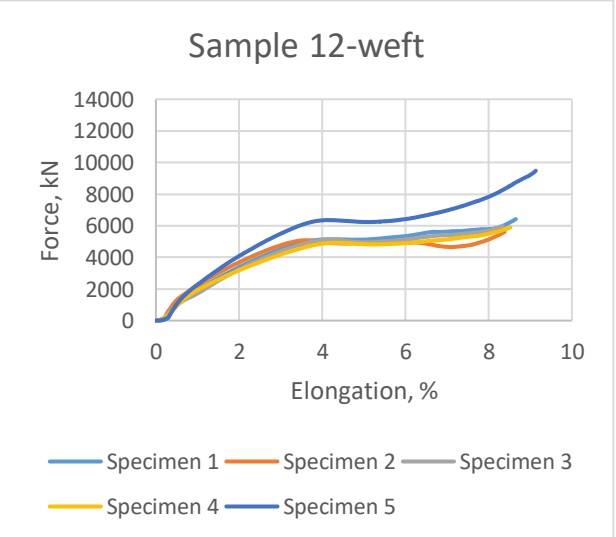
Sample 12-weft
Force, kN
14000
12000
10000
8000
6000
4000
2000
0
0
2
4
6
8
10
Elongation, %
Specimen 1
Specimen 2
Specimen 3
Specimen 4
Specimen 5

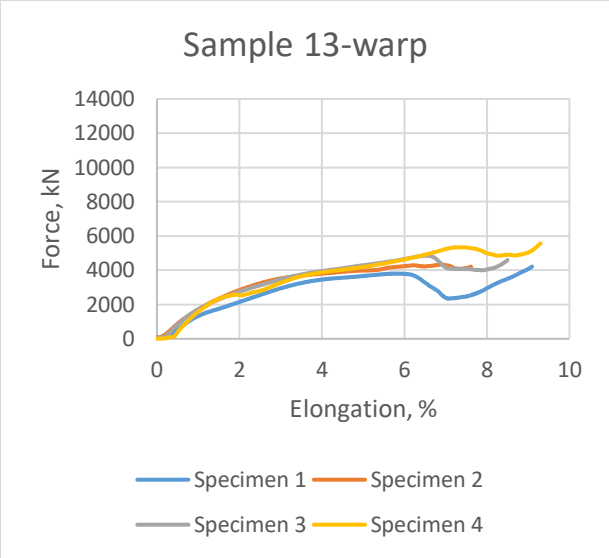
Sample 13-warp
Force, kN
14000
12000
10000
8000
6000
4000
2000
0
0
2
4
6
8
10
Elongation, %
Specimen 1
Specimen 2
Specimen 3
Specimen 4

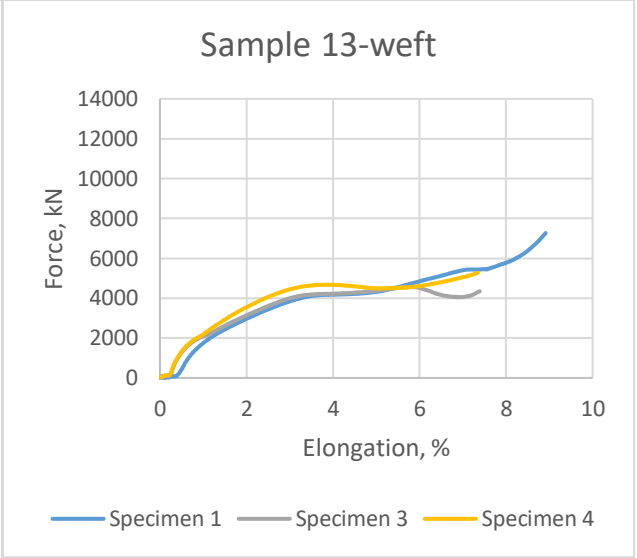
Sample 13-weft
Force, kN
14000
12000
10000
8000
6000
4000
2000
0
0
2
4
6
8
10
Elongation, %
Specimen 1
Specimen 3
Specimen 4

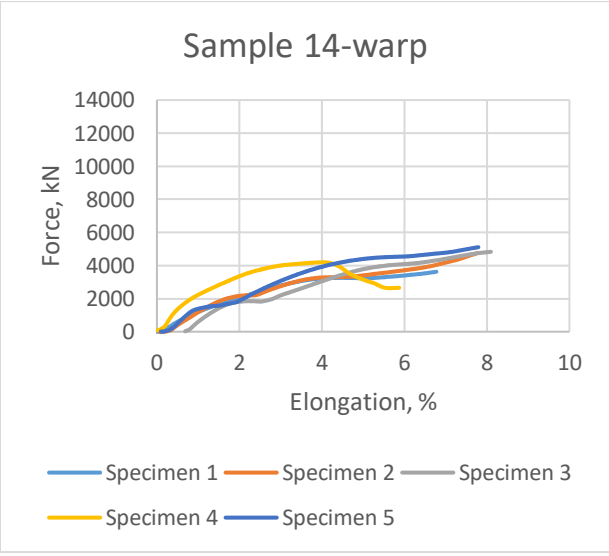
Sample 14-warp
Force, kN
14000
12000
10000
8000
6000
4000
2000
0
0
2
4
6
8
10
Elongation, %
Specimen 1
Specimen 2
Specimen 3
Specimen 4
Specimen 5

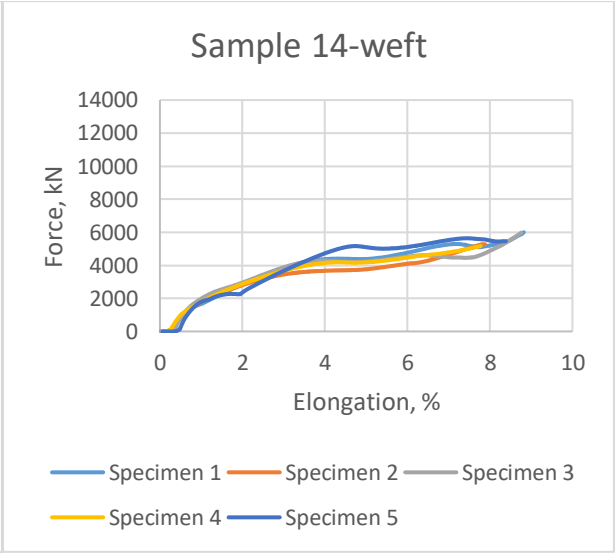
Sample 14-weft
Force, kN
14000
12000
10000
8000
6000
4000
2000
0
0
2
4
6
8
10
Elongation, %
Specimen 1
Specimen 2
Specimen 3
Specimen 4
Specimen 5

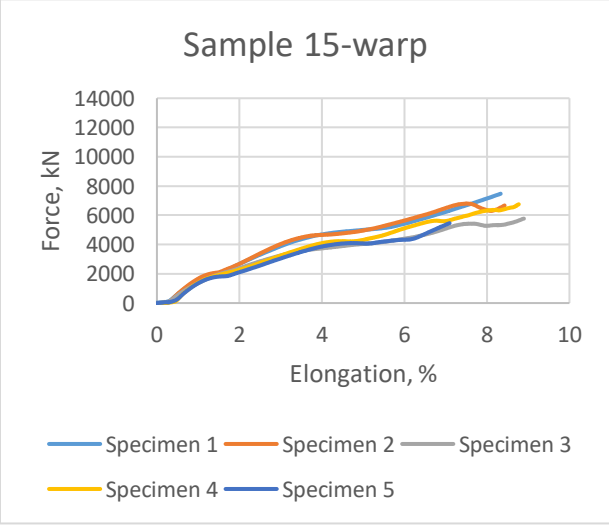
Sample 15-warp
Force, kN
14000
12000
10000
8000
6000
4000
2000
0
0
2
4
6
8
10
Elongation, %
Specimen 1
Specimen 2
Specimen 3
Specimen 4
Specimen 5

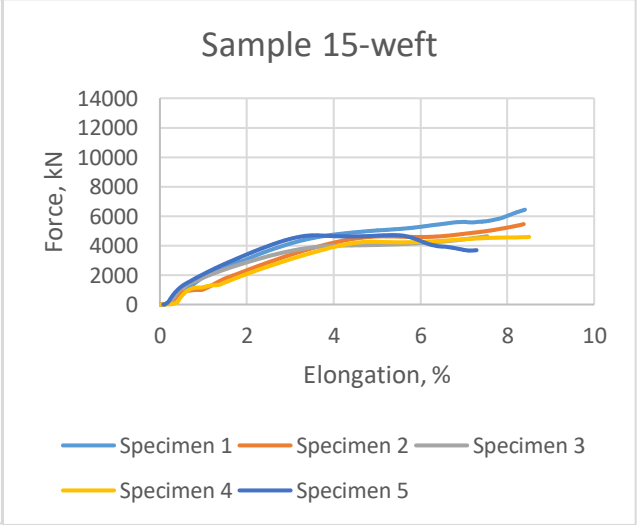
Sample 15-weft
Force, kN
14000
12000
10000
8000
6000
4000
2000
0
0
2
4
6
8
10
Elongation, %
Specimen 1
Specimen 2
Specimen 3
Specimen 4
Specimen 5

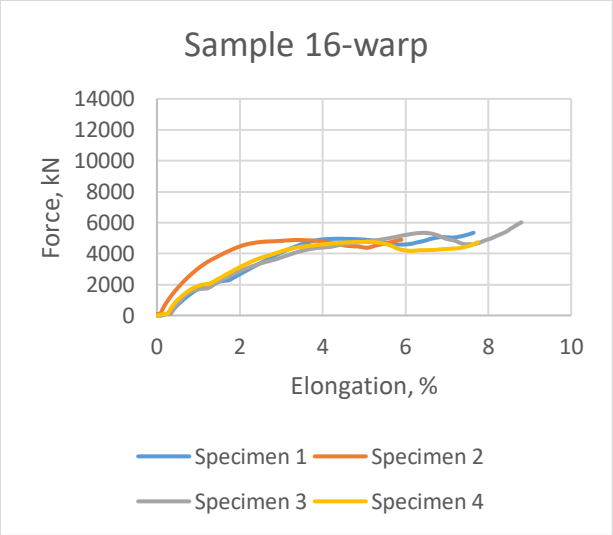
Sample 16-warp
Force, kN
14000
12000
10000
8000
6000
4000
2000
0
0
2
4
6
8
10
Elongation, %
Specimen 1
Specimen 2
Specimen 3
Specimen 4

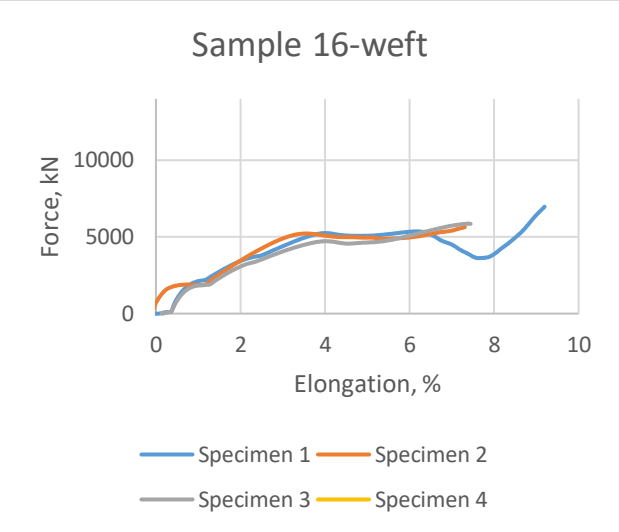
Sample 16-weft
Force, kN
10000
5000
0
0
2
4
6
8
10
Elongation, %
Specimen 1
Specimen 2
Specimen 3
Specimen 4

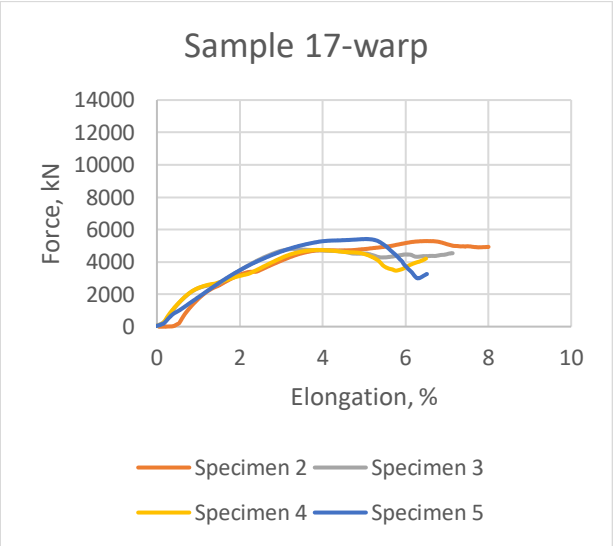
Sample 17-warp
Force, kN
14000
12000
10000
8000
6000
4000
2000
0
0
2
4
6
8
10
Elongation, %
Specimen 2
Specimen 3
Specimen 4
Specimen 5

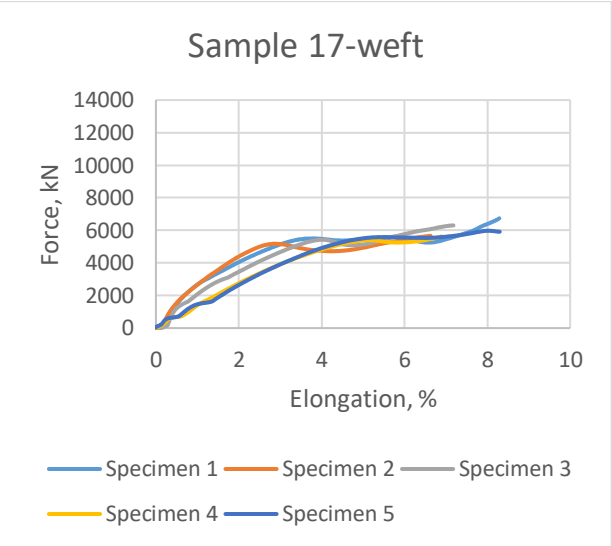
Sample 17-weft
Force, kN
14000
12000
10000
8000
6000
4000
2000
0
0
2
4
6
8
10
Elongation, %
Specimen 1
Specimen 2
Specimen 3
Specimen 4
Specimen 5

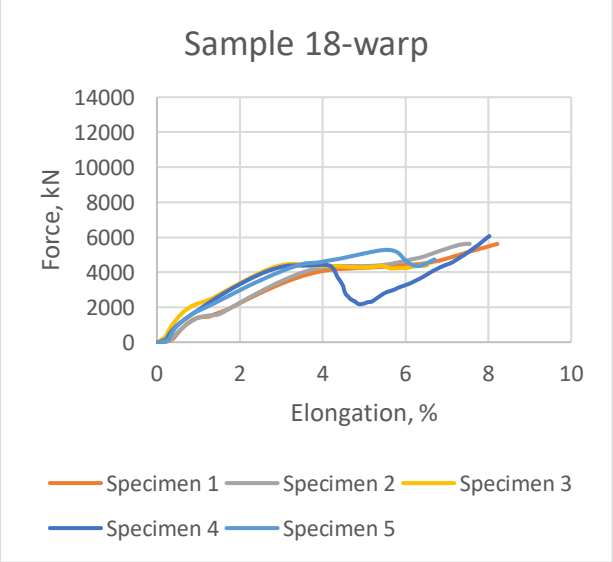
Sample 18-warp
Force, kN
14000
12000
10000
8000
6000
4000
2000
0
0
2
4
6
8
10
Elongation, %
Specimen 1
Specimen 2
Specimen 3
Specimen 4
Specimen 5

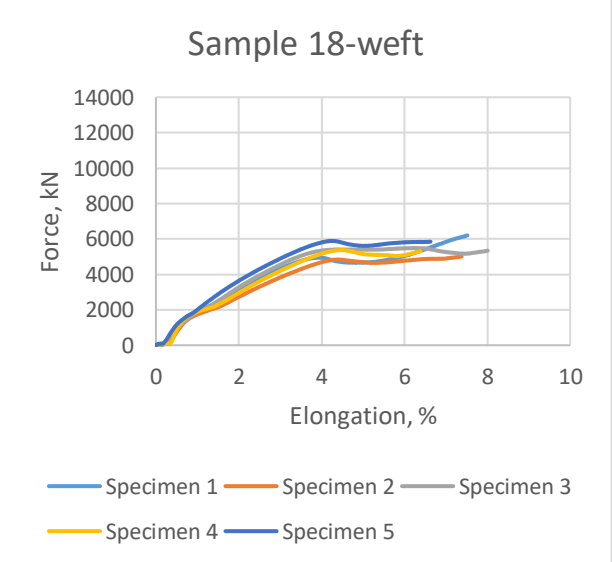
Sample 18-weft
Force, kN
14000
12000
10000
8000
6000
4000
2000
0
0
2
4
6
8
10
Elongation, %
Specimen 1
Specimen 2
Specimen 3
Specimen 4
Specimen 5

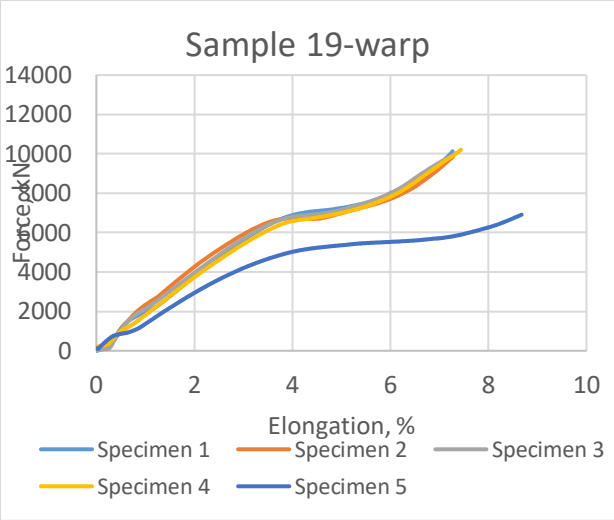
Sample 19-warp
Force, kN
Elongation, %
Specimen 1
Specimen 2
Specimen 3
Specimen 4
Specimen 5

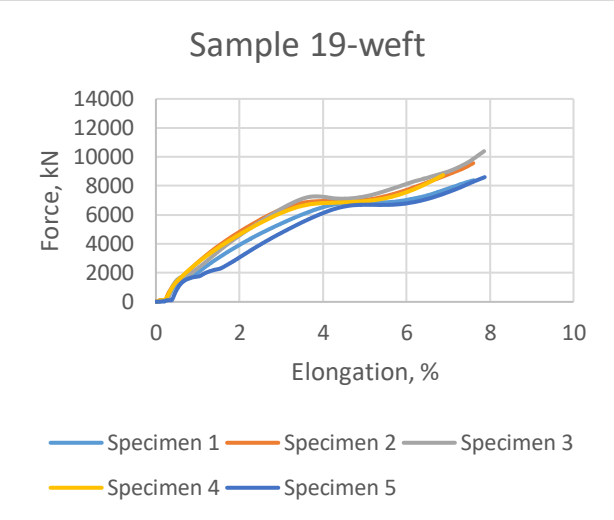
Sample 19-weft
Force, kN
Elongation, %
Specimen 1
Specimen 2
Specimen 3
Specimen 4
Specimen 5

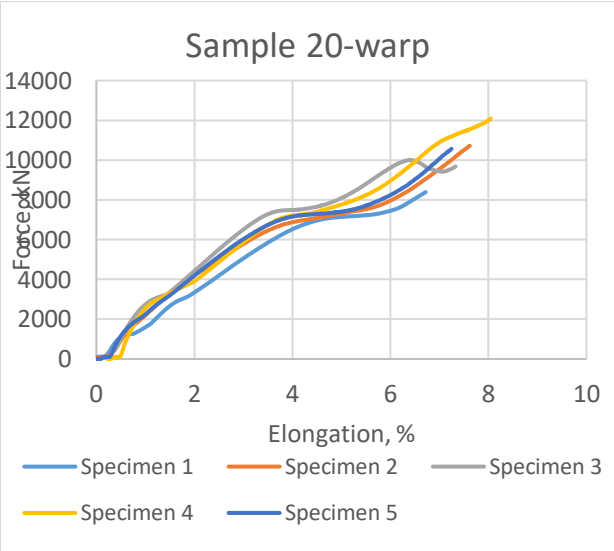
Sample 20-warp
Force, kN
Elongation, %
Specimen 1
Specimen 2
Specimen 3
Specimen 4
Specimen 5

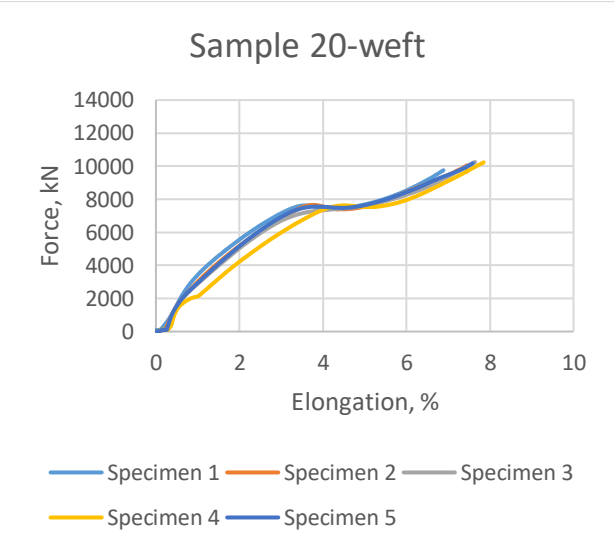
Sample 20-weft
Force, kN
Elongation, %
Specimen 1
Specimen 2
Specimen 3
Specimen 4
Specimen 5

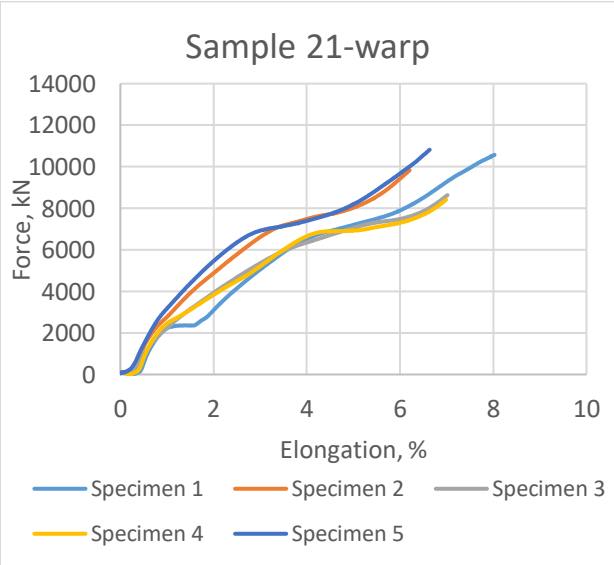
Sample 21-warp
Force, kN
Elongation, %
Specimen 1
Specimen 2
Specimen 3
Specimen 4
Specimen 5

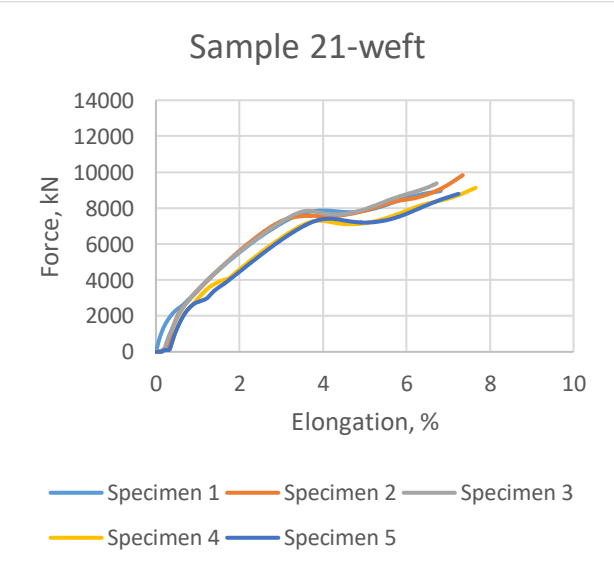
Sample 21-weft
Force, kN
Elongation, %
Specimen 1
Specimen 2
Specimen 3
Specimen 4
Specimen 5

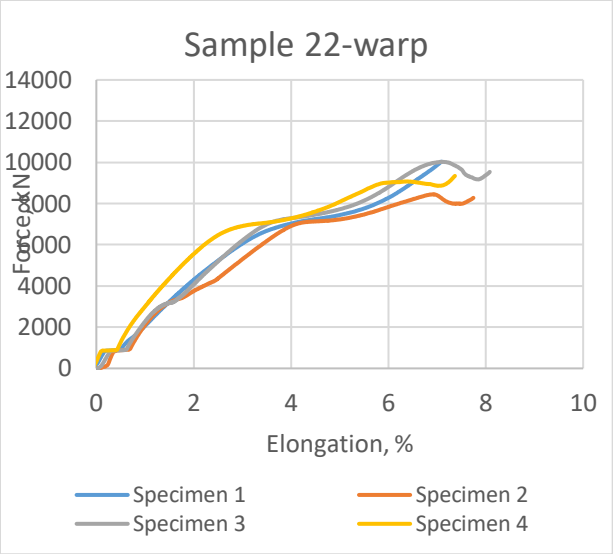
Sample 22-warp
Force, kN
Elongation, %
Specimen 1
Specimen 2
Specimen 3
Specimen 4

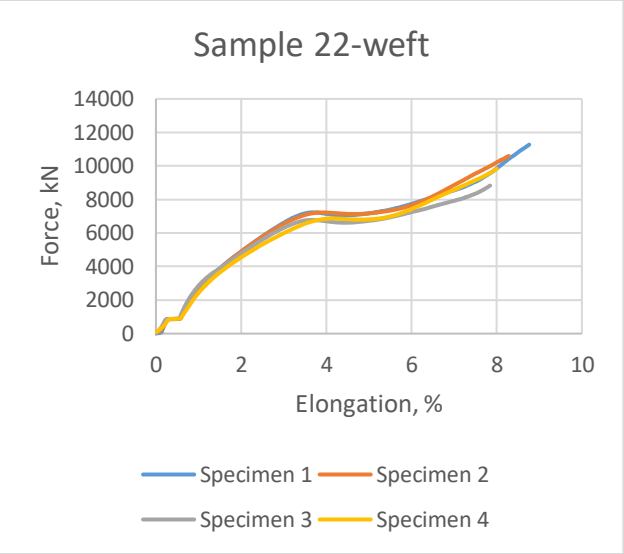
Sample 22-weft
Force, kN
Elongation, %
Specimen 1
Specimen 2
Specimen 3
Specimen 4

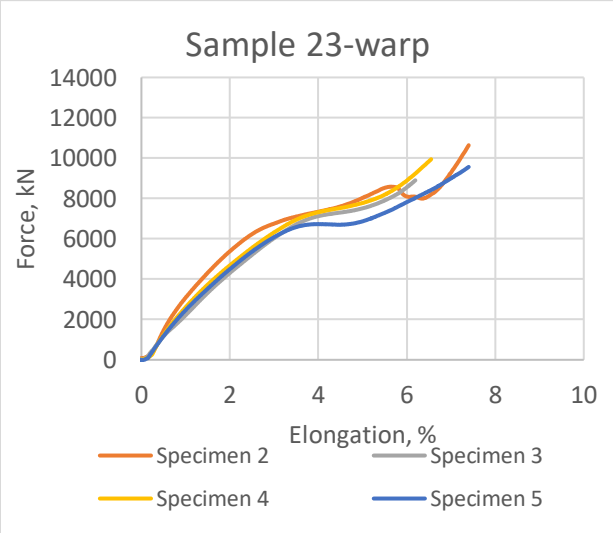
Sample 23-warp
Force, kN
Elongation, %
Specimen 2
Specimen 3
Specimen 4
Specimen 5

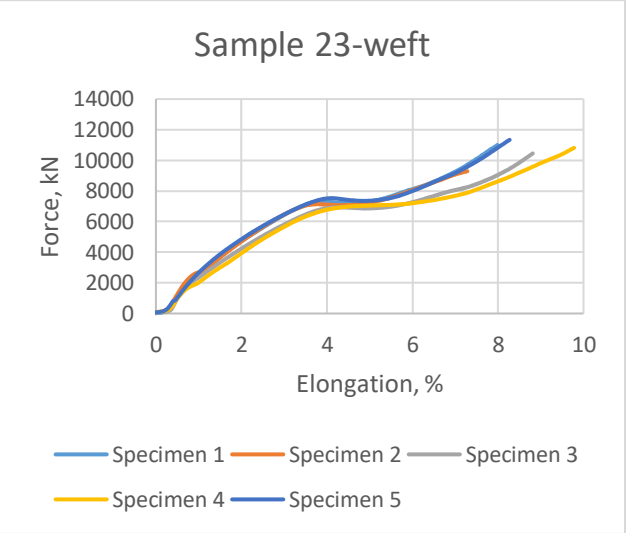
Sample 23-weft
Force, kN
Elongation, %
Specimen 1
Specimen 2
Specimen 3
Specimen 4
Specimen 5

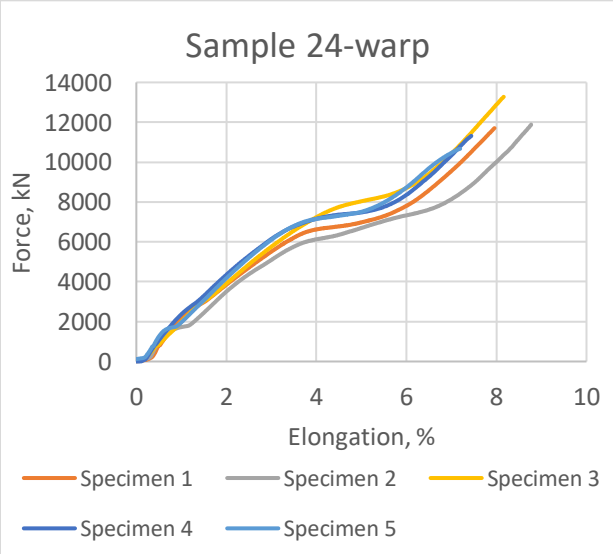
Sample 24-warp
Force, kN
Elongation, %
Specimen 1
Specimen 2
Specimen 3
Specimen 4
Specimen 5

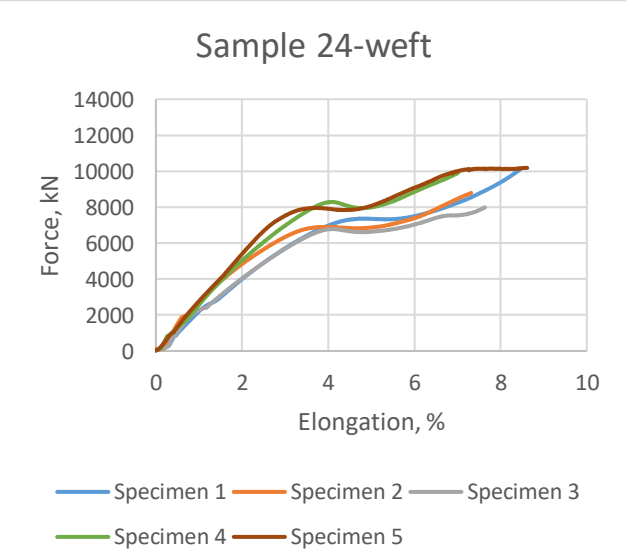
Sample 24-weft
Force, kN
Elongation, %
Specimen 1
Specimen 2
Specimen 3
Specimen 4
Specimen 5

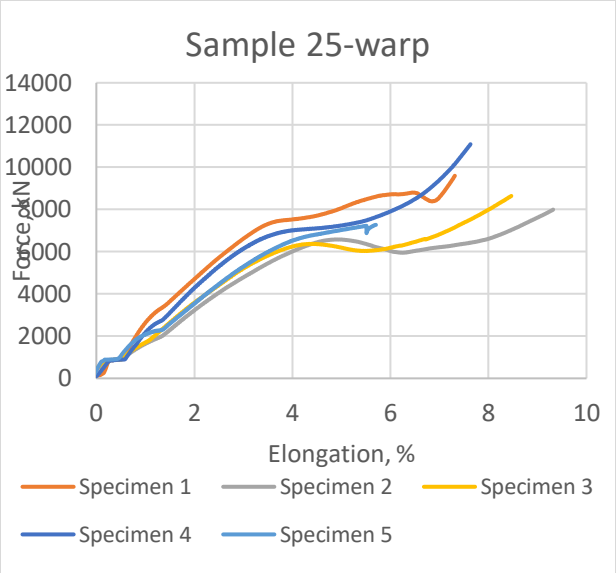
Sample 25-warp
Force, kN
Elongation, %
Specimen 1
Specimen 2
Specimen 3
Specimen 4
Specimen 5

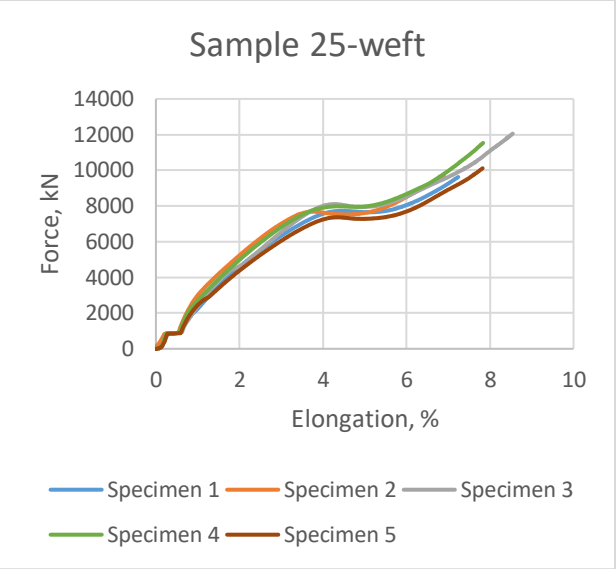
Sample 25-weft
Force, kN
Elongation, %
Specimen 1
Specimen 2
Specimen 3
Specimen 4
Specimen 5

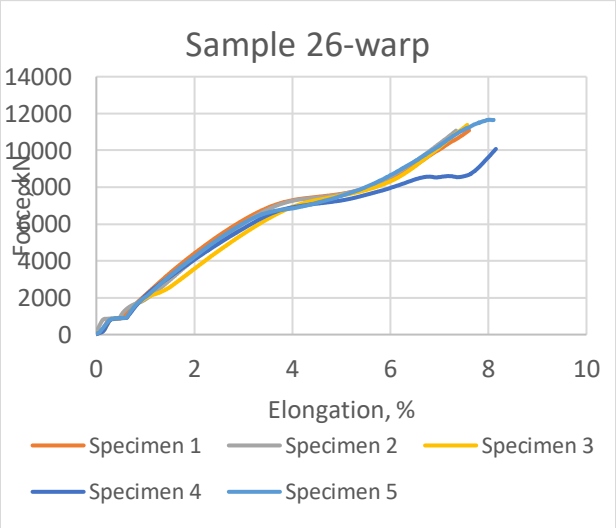
Sample 26-warp
Force, kN
Elongation, %
Specimen 1
Specimen 2
Specimen 3
Specimen 4
Specimen 5

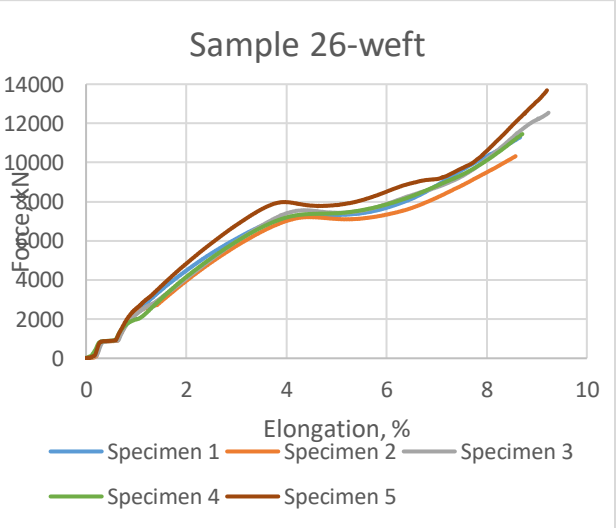
Sample 26-weft
Force, kN
Elongation, %
Specimen 1
Specimen 2
Specimen 3
Specimen 4
Specimen 5

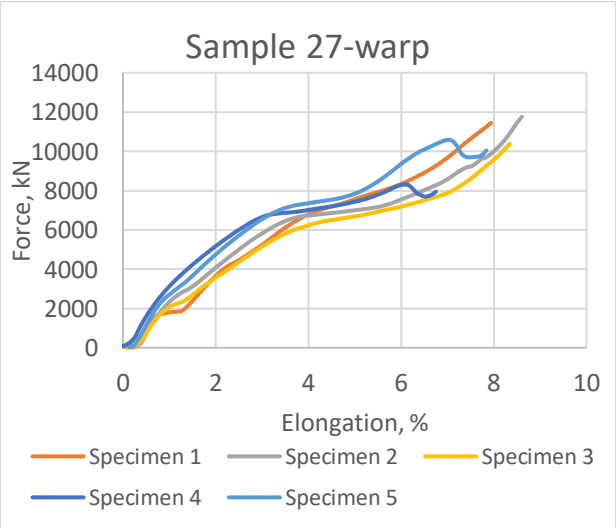
Sample 27-warp
Force, kN
Elongation, %
Specimen 1
Specimen 2
Specimen 3
Specimen 4
Specimen 5

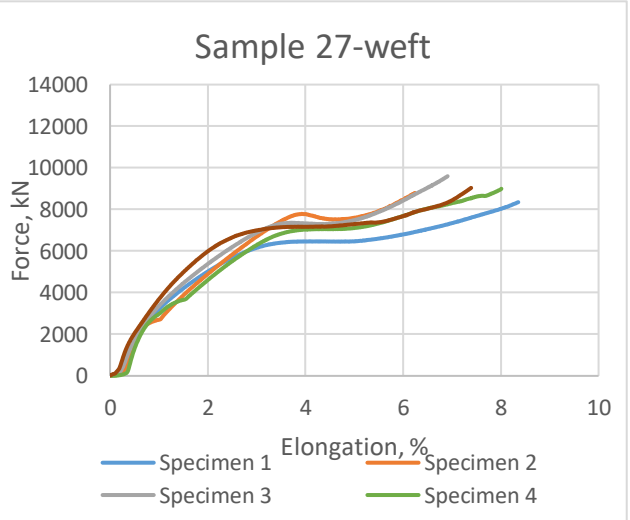
Sample 27-weft
Force, kN
Elongation, %
Specimen 1
Specimen 2
Specimen 3
Specimen 4

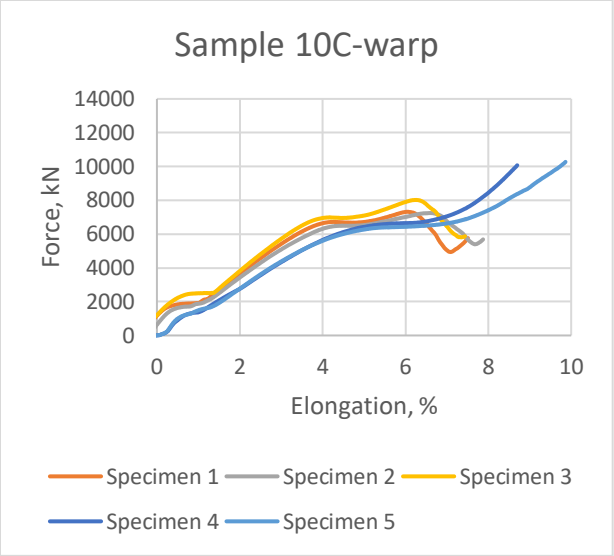
Sample 10C-warp
Force, kN
14000
12000
10000
8000
6000
4000
2000
0
0
2
4
6
8
10
Elongation, %
Specimen 1
Specimen 2
Specimen 3
Specimen 4
Specimen 5

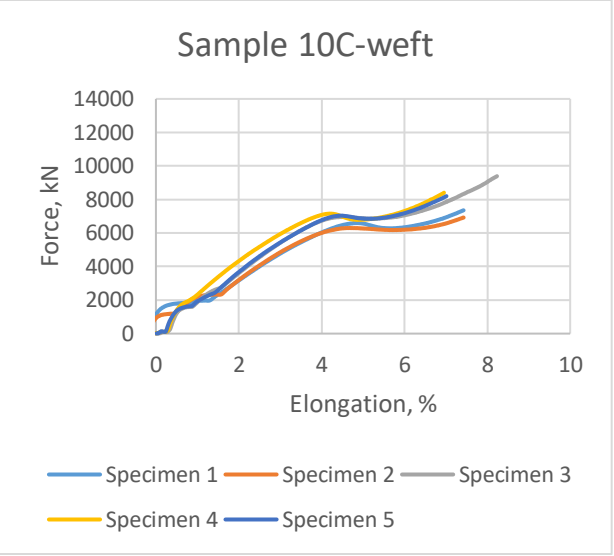
Sample 10C-weft
Force, kN
14000
12000
10000
8000
6000
4000
2000
0
0
2
4
6
8
10
Elongation, %
Specimen 1
Specimen 2
Specimen 3
Specimen 4
Specimen 5

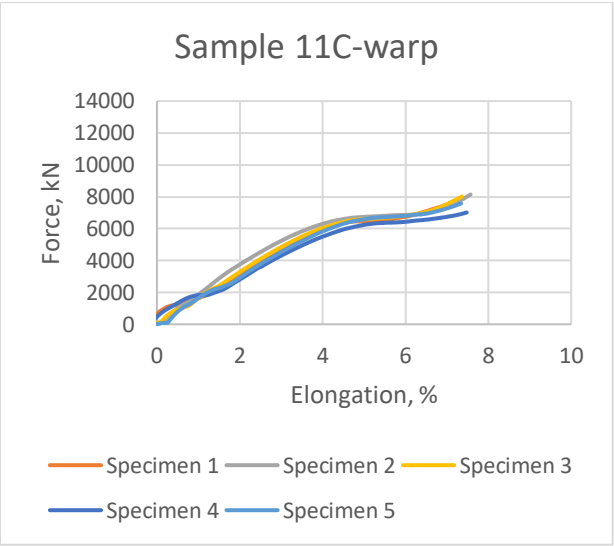
Sample 11C-warp
Force, kN
14000
12000
10000
8000
6000
4000
2000
0
0
2
4
6
8
10
Elongation, %
Specimen 1
Specimen 2
Specimen 3
Specimen 4
Specimen 5

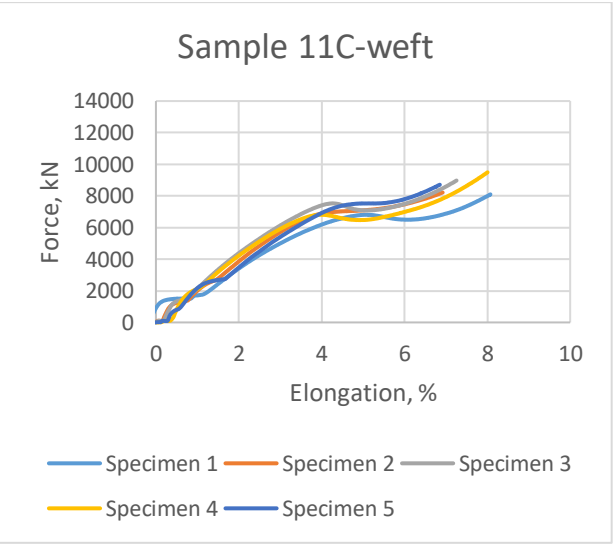
Sample 11C-weft
Force, kN
14000
12000
10000
8000
6000
4000
2000
0
0
2
4
6
8
10
Elongation, %
Specimen 1
Specimen 2
Specimen 3
Specimen 4
Specimen 5

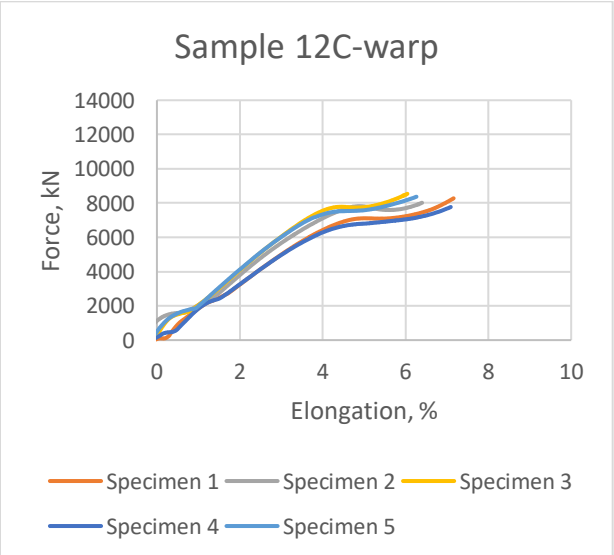
Sample 12C-warp
Force, kN
14000
12000
10000
8000
6000
4000
2000
0
0
2
4
6
8
10
Elongation, %
Specimen 1
Specimen 2
Specimen 3
Specimen 4
Specimen 5

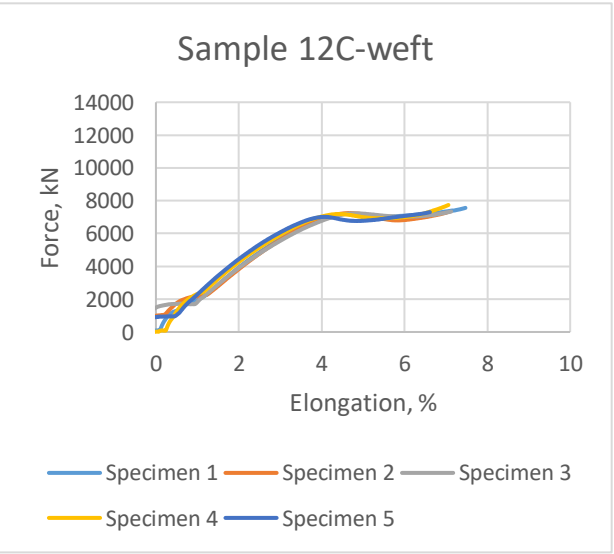
Sample 12C-weft
Force, kN
14000
12000
10000
8000
6000
4000
2000
0
0
2
4
6
8
10
Elongation, %
Specimen 1
Specimen 2
Specimen 3
Specimen 4
Specimen 5

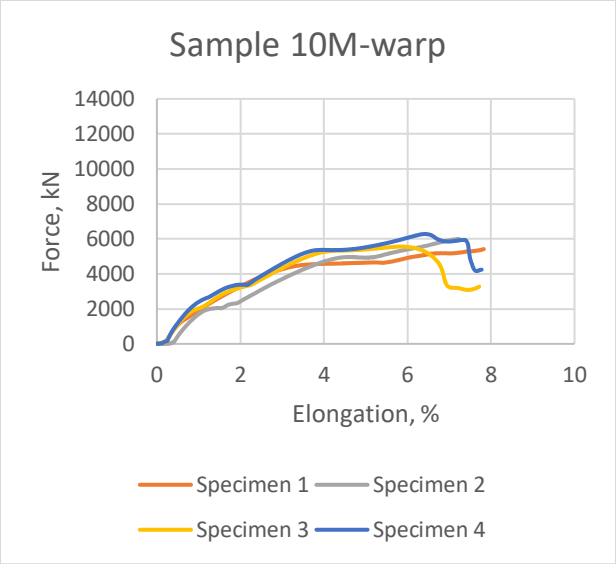
Sample 10M-warp
Force, kN
14000
12000
10000
8000
6000
4000
2000
0
0
2
4
6
8
10
Elongation, %
Specimen 1
Specimen 2
Specimen 3
Specimen 4

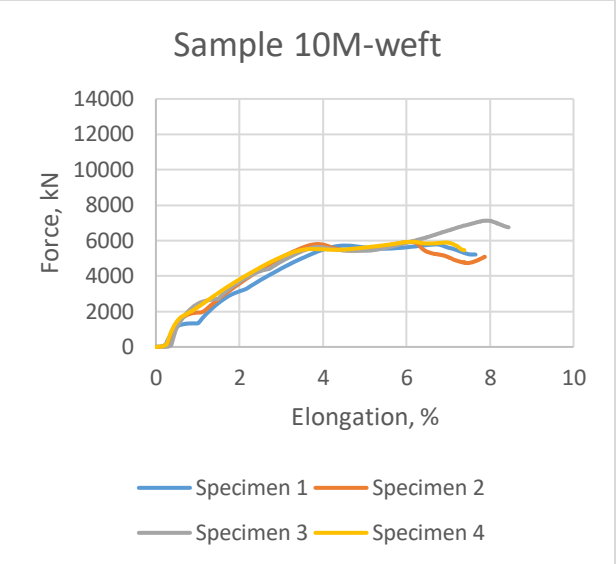
Sample 10M-weft
Force, kN
14000
12000
10000
8000
6000
4000
2000
0
0
2
4
6
8
10
Elongation, %
Specimen 1
Specimen 2
Specimen 3
Specimen 4

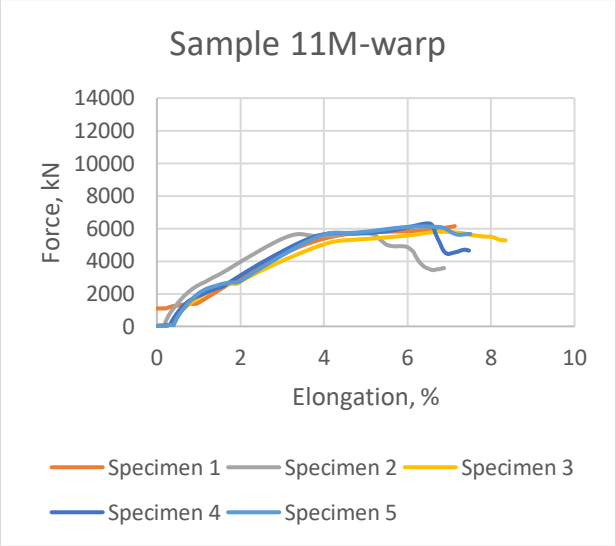
Sample 11M-warp
Force, kN
14000
12000
10000
8000
6000
4000
2000
0
0
2
4
6
8
10
Elongation, %
Specimen 1
Specimen 2
Specimen 3
Specimen 4
Specimen 5

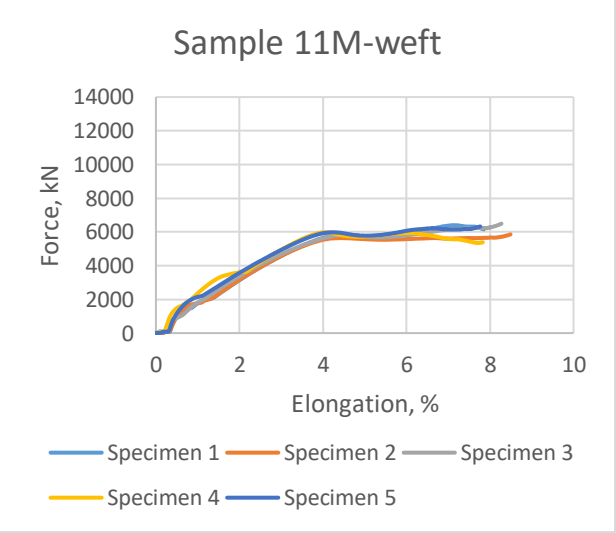
Sample 11M-weft
Force, kN
14000
12000
10000
8000
6000
4000
2000
0
0
2
4
6
8
10
Elongation, %
Specimen 1
Specimen 2
Specimen 3
Specimen 4
Specimen 5

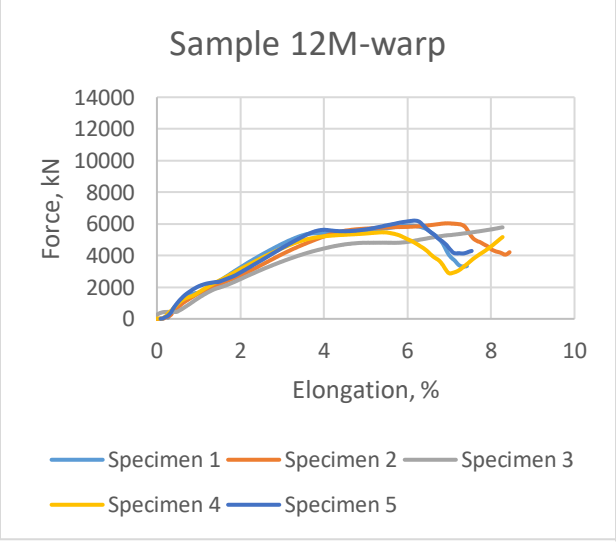
Sample 12M-warp
Force, kN
14000
12000
10000
8000
6000
4000
2000
0
0
2
4
6
8
10
Elongation, %
Specimen 1
Specimen 2
Specimen 3
Specimen 4
Specimen 5

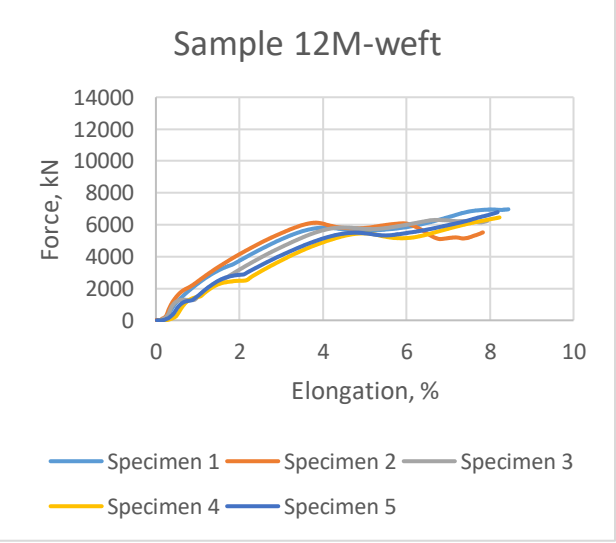
Sample 12M-weft
Force, kN
14000
12000
10000
8000
6000
4000
2000
0
0
2
4
6
8
10
Elongation, %
Specimen 1
Specimen 2
Specimen 3
Specimen 4
Specimen 5

Appendix 89. Design of experiment (Mohamad Midani, 2016).

Variable	**Levels**
Number of Y-yarn layers	2 ,3, 4
X-yarn density/layer, 1/cm	4.87, 5.48, 5.85
Weave	Plain, 2x2 Basket, 2x2 Twill
Total runs	27 samples (3x3x3)